

THE PHYSICO-CHEMICAL PROPERTIES OF SUPRAMOLECULAR SYSTEMS INVOLVING PHARMACEUTICALS AND ANIONS

By Maan Abdulrazzaq Suwiad Al-Nuaim



A Thesis is Submitted for the Degree of Doctor of Philosophy

Thermochemistry Laboratory

Department of Chemistry

Faculty of Engineering and Physical Sciences

University of Surrey, United Kingdom

January, 2016

© Maan Abdulrazzaq Suwiad Al-Nuaim

Abstract

Currently, the discharge of pollutants to the environment is considered one of the biggest problems challenging chemists and environmental scientists. These pollutants come from different sources and might be carcinogenic, toxic or radioactive compounds which can cause serious health hazards to humans, animals and plants. Intensive thermodynamic studies by Danil de Namor and co-workers in the Thermochemistry Laboratory indicated that functionalisation of calix[4]pyrroles, cyclodextrines and calix[n]arenes (n=4,6) leads to the production of selective macrocyclic receptors for the removal of anions, toxic heavy metals and other pollutants from water. The objective of this thesis is to design, synthesise and characterise macrocyclic receptors with suitable functional groups for the selective removal of drugs and anions from water. The drugs selected for this study are diclofenac, sodium diclofenac, clofibrac acid, carbamazepine, aspirin and ibuprofen. This selection is based on the fact that these drugs are extensively used and as a result these contaminate sewage, surface and ground water. Supramolecular chemistry is one of the most important areas of chemistry which offers many advantages due to the efficient, fast and economical way for removing pollutants from water. In this thesis a large number of macrocycles based on calix[4]arene, calix[4]pyrrole resorc[4]arene and pyrogallol[4]arene have been synthesised and characterised by ^1H NMR and microanalysis. From these receptors those based on cyclodextrin and calix[4]arene derivatives have been selected for sodium diclofenac while for drugs containing carboxylic acids in their structure, a partially substituted calix[4]arene amine was selected for further investigations involving these drugs. These interactions were assessed in solution by several techniques such as ^1H NMR titration, UV-Visible, conductivity, isothermal titration calorimetry. In the solid state, thermogravimetry and differential scanning calorimetry were explored. The extraction of these pharmaceuticals by some of these macrocycles under different conditions is reported. The importance of fundamental studies in searching for applications is demonstrated where the selectivity of the calix[4]arene amine for these drugs is shown in the extraction process. Modified silica with amino functional groups is explored for extracting aspirin from water. Preliminary research on the efficiency of pyrogallol[4]arene and resorcine[4]arene to work as molecular containers for selected drugs were tested by ^1H NMR. Two novel calix[4]pyrroles were investigated for complexation with halides and phosphates showing their selectivity for phosphates relative to halides. Final conclusions are given as well as suggestions for further work particularly with the new oligomeric material which has been characterised by various techniques which are FTIR, XRD, SEM, BET analysis

Acknowledgements

I am greatly indebted to my supervisor Professor Angela F. Danil de Namor for her supervision, guidance, dedication and patience in the writing of the present thesis and for her kind husband Dr. Melhem Namor for his encouragement.

I would like to thank my co-supervisor Prof. J. Varcoe for his help and support, Prof. B. Howlin for his help in the chemical modelling and interesting interpretations.

I would also like to thank Prof. I. Cunningham for his great advice given by me during the research period.

I wish to thank all academic staff in the Chemistry Department at the University of Surrey for their help and encouragement.

Also, I wish to say special thank you to all my colleagues in the Thermochemistry Laboratory, Oliver, Abdel, Weam, Adnan, Adhwa, Nawal and Rachida for their help and for sharing their scientific knowledge.

Also, I would like to thank the technical staff in the Chemistry Department at the University of Surrey, Judith, V. Dokova, Dave, Graham, Dan, Deryck, Nikki and Qinmin.

Also, I should to thank my colleagues in the College of Pharmacy in Basra University/ Iraq.

I would like to thank the Ministry of Higher Education & Scientific Research in Iraq for the financial support for this research through the College of Pharmacy in the University of Basra.

Finally, I have to say thank you for all the members of the Iraqi Cultural Attachee in London specially Prof. Mousa Al-Mousawi and Dr. Fadwaa Al-Saffar for their help and support

Dedication

To My Father & Mother with love

Table of Contents.....	Page
1. Chapter I Introduction.....	1
1.1 Supramolecular Chemistry.....	2
1.2 Pharmaceuticals, phosphate and halides in the environment.....	3
1.2.1 Occurrence of pharmaceuticals in the aquatic environment.....	3
1.2.2 Phosphate and halides in aquatic environment.....	5
1.3 Classification of macrocyclic receptors.....	6
1.3.1 Naturally occurring macrocycles.....	6
1.3.2 Synthetic macrocyclic receptors (crown ethers, cryptands, spherands and pillarenes).....	8
1.4 Calix[4]arenes.....	15
1.4.1 Properties and conformations of calix[4]arene.....	17
1.4.2 Lower Rim functionalisation of Calix[4]arenes.....	20
1.4.3 Upper rim functionalisation of calix[4]arene.....	25
1.4.4 Applications of Calixarenes and derivatives.....	29
1.5 Calix[4]pyrrole.....	30
1.5.1 Calix[4]pyrrole conformations.....	31
1.5.2 Functionalisation of calix[4]pyrrole.....	32
1.5.2.1 Functionalisation of C-rim (β -position).....	32
1.5.2.2 Functionalisation of N-rim.....	34
1.5.2.3 Functionalisation of <i>meso</i> position.....	34
1.5.3 Application of calix[4]pyrrole.....	39

1.6 Resorcin[4]arene.....	40
1.7 Pyrogallol[4]arene.....	45
1.8 The use of silica based compounds for extraction purposes.....	48
1.8.1 Click chemistry.....	51
1.9 BET theory.....	53
1.10 Aims of the thesis.....	53
2. Chapter two: Experimental Part.....	60
2.1 List of abbreviation.....	61
2.2 Chemicals.....	63
2.2.1 Solvents used in this work.....	63
2.2.2 Deuterated solvents used for the ¹ H NMR.....	64
2.2.3 Pharmaceuticals.....	64
2.2.4 Analytical reagents.....	65
2.2.5 Purification of solvents.....	66
2.2.6 Instruments used.....	67
2.3 Solubility measurements.....	68
2.3.1 Solubility of selected pharmaceuticals in different organic solvents at 298.15 K.....	68
2.3.2 Calibration curve for the determination of the solubility of pharmaceuticals.....	69
2.3.3 Solubility of selected pharmaceuticals.....	69
2.4 Determination of partition coefficients of selected drugs in water-1-octanol solvent system...69	
2.5 Synthesis of receptors.....	70

2.5.1 Synthesis and characterization of heptakis-(6-chloro-6-deoxy)- β -cyclodextrin.....	70
2.5.2 Synthesis of heptakis-(2, 3, 6-tri-O-benzoyl)- β -cyclodextrin.....	71
2.5.3 Synthesis of 5, 11, 17, 23- <i>tert</i> -butyl-25, 26, 27, 28-(oxy-ethylethanoate)calix[4]arene....	71
2.5.4 Synthesis of 5, 11, 17, 23-tetra- <i>p-tert</i> -butyl-25, 27-bis(2-cyanomethoxy)-26, 28- dihydrocalix[4]arene CA-(CN) ₂	73
2.5.5 Synthesis of 5, 11, 17, 23-tetra- <i>p-tert</i> -butyl-25, 27-bis(2-cyanomethoxy)-26, 28- dihydrocalix[4]arene CA-(NH ₂) ₂	73
2.5.6 Synthesis of 25, 26, 27, 28-tetrahydroxycalix[4]arene.....	74
2.5.7 Synthesis and characterisation of 5- <i>tert</i> -butyl-3-azidomethyl-2-hydroxybenzaldehyde.	75
2.5.8 Synthesis and characterisation of 5- <i>tert</i> -butyl-2-hydroxybenzaldehyde.....	75
2.5.9 Synthesis and characterisation of 5- <i>tert</i> -butyl-3-chloromethyl-2-hydroxybenzaldehyde.	76
2.5.10 Synthesis of 5- <i>tert</i> -butyl-3-azidomethyl-2-hydroxybenzaldehyde.....	76
2.5.11 Synthesis and characterisation of 25, 27-dihydroxy-26, 28-dioxypropargyl- <i>tert</i> - butylcalix[4]arene.....	76
2.5.12 Synthesis and Characterization of azido calix[4]arene	77
2.5.13 Preparation of 2-azidoacetamide.....	78
2.5.14 Synthesis of 25, 26, 27, 28-(diethylamino) ethoxy calix[4]arene.....	79
2.5.15 Synthesis of <i>meso</i> -tetramethyl-tetrakis-(4-hydroxyphenyl ethyl)calix[4]pyrrole.....	80
2.5.16 Synthesis of <i>meso</i> -tetramethyl-tetrakis-(4-ethylacetatophenoxyethyl)calix[4]pyrrole TTECP.....	81
2.5.17 Polymerisation of <i>meso</i> -tetramethyl-tetrakis-[2-(4- hydroxyphenyl)ethyl] calix	

[4]pyrrole (CPPOL).....	82
2.5.18 Synthesis of 2, 8, 14, 20-tetra-pentyl-resoc[4]arene(4,6, 10, 12, 16, 18, 22- octahydroxyl, 2, 8, 14, 20-tetrapentylcalix[4]arene.....	82
2.5.19 Esterfication of C-pentyl resorcin[4]arene.....	83
2.5.20 Synthesis of C-pentylpyrogallol[4]arene.....	85
2.5.21 Synthesis of C-decylpyrogallol[4]arene.....	86
2.5.22 Synthesis of C-4-aminophenyl pyrogallol[4]arene.....	87
2.6 Solubility measurements of the receptor.....	87
2.7 ¹ H NMR measurements.....	88
2.8 Conductometric measurements.....	88
2.8.1 Detrmination of the conductivity cell constant.....	89
2.8.2 Conductometric titrations at 298.15 K.....	90
2.9 Nano Isothermal Titration Calorimeter ITC.....	90
2.9.1 Calorimetric measurements.....	91
2.9.2 Calibration of the Nanocalorimeter.....	91
2.10 Determination of the stability constant and the composition of host-guest complex by UV- Vis, ¹ H NMR and calorimetric titrations.....	92
2.11 General procedure for the determination of optimum amount of the receptor for the uptake of targeted adsorbate from aqueous solution at 298.15 K.....	94
2.11.1 Effect of the amount of material on the extraction of pharmaceuticals.....	94

2.11.2 Effect of pH on the extraction.....	95
2.11.3 Kinetics of removal of pharmaceuticals by macrocycles and Sil-NH ₂	95
2.12 Thermal Properties measurements TGA and DSC.....	95
3. Chapter III	99
3.1 Solubility of drugs in different solvents.....	100
3.1.1 Solubility of sodium diclofenac in different solvents.....	100
3.1.2 Solubility of carbamazepine (CBZ) in different solvents.....	103
3.2 Determination of the partition coefficient for diclofenac, clofibric acid and carbamazepine in the water-1-octanol solvent system.....	104
3.3 Complex formation of sodium diclofenac NaDF and per-benzoylated- β -cyclodextrine.....	106
3.3.1 ¹ H NMR complexation studies.....	106
3.3.2 Photophysical properties of the host-guest complex.....	107
3.4 Conductometric measurements.....	110
3.4.1 Determination of the conductivity cell constant.....	110
3.4.2 Conductometric measurements of sodium diclofenac with <i>p-tert</i> -butylcalix[4]arene tetraester in acetonitrile at 298.15 K.....	110
3.5 Complexation studies of sodium diclofenac with per-benzoylated- β -cyclodextrin in 1-octanol using Nano-Isothermal titration calorimetry Nano-ITC.....	111
3.5.1 Calibration of the Nano-Isothermal Titration Calorimeter Nano-ITC.....	111
3.6 Determination of the thermodynamic parameters of complexation of sodium diclofenac with	

heptakis-(2, 3, 6-tri-O-benzoyl)- β -cyclodextrin in 1-Octanol at 298.15 K.....	115
3.7 Complexation studies of sodium diclofenac and 5, 11, 17, 27- <i>tert</i> -butyl-25, 26, 27, 28-(oxy ethylethanoate)calix[4]arene CAE.....	117
3.7.1 ^1H NMR complexation studies	117
3.7.2 Conductometric measurements of sodium diclofenac with 5, 11, 17, 27- <i>tert</i> -butyl-25, 26, 27, 28-(oxy-ethylacetate)calix[4]arene (CAE) in acetonitrile at 298.15 K.....	119
3.7.3 Investigation of the complexation between diclofenac sodium and 5, 11, 17, 27- <i>tert</i> -butyl -25, 26, 27, 28-(oxy-ethylacetato)calix[4]arene by thermogravimetric analysis TGA&DSC.	120
3.8 Removal of sodium diclofenac from water by using calix[4]arene tetraester from water.....	125
3.8.1 Determination of the optimum amount of calix[4]arene tetraester for the uptake of sodium diclofenac from aqueous solution at 298 K.....	125
3.8.2 Determination of the capacity of calix[4]arene tetraester to uptake NaDF from aqueous solution at 298.15 K.....	126
3.8.3 Determination of the effect of pH solution on the uptake of calix[4]arene ester to uptake sodium diclofenac NaDF from aqueous solution at 298 K.....	128
3.9 Complexation studies of CA-(NH ₂) ₂ and pharmaceuticals.....	129
3.9.1 ^1H NMR complexation studies of diclofenac, clofibric acid, aspirin and ibuprofen with the 5, 11, 17, 23-tetra- <i>tert</i> -butyl-25, 27-bis-(aminoethoxy)-26, 28-dihydroxycalix[4]arene in CD ₃ CN at 298 K.....	129
3.9.2 Investigation of the complexation of the pharmaceuticals with CA-(NH ₂) ₂ in acetonitrile by conductance measurements.....	134

3.9.2.1 Conductometric measurements for the pure receptor CA-(NH ₂) ₂ in acetonitrile at 298.15 K.....	134
3.9.2.2 Conductometric titration studies of diclofenac and CA-(NH ₂) ₂ in acetonitrile at 298.15 K.....	135
3.9.2.3 Conductometric titration studies of clofibric acid with CA-(NH ₂) ₂ in MeCN at 298.15 K.....	136
3.9.2.4 Conductometric titration of aspirin with CA-(NH ₂) ₂ in acetonitrile at 298.15 K...	137
3.10 Photophysical properties of the drug bindings.....	138
3.10.1 UV- Vis titration of diclofenac with calix[4]arene amine in acetonitrile at 298 K.....	138
3.10.2 UV-Vis titration of clofibric acid with calix[4]arene amine in MeCN at 298 K.....	140
3.10.3 UV-Vis titration of aspirin with calix[4]arene amine in acetonitrile at 298 K.....	142
3.11 Thermodynamic parameters of complexation of pharmaceuticals with CA-(NH ₂) ₂ receptor in acetonitrile at 298.15 K.....	143
3.12 Investigation of the interaction between diclofenac, clofibric acid and aspirin with CA-(NH ₂) ₂ by using thermogravimetric analysis TGA and differential scanning calorimetry DSC.....	150
3.13 Extraction of clofibric acid and diclofenac from water by CA-(NH ₂) ₂	152
3.13.1 The effect of mass on the extraction of clofibric acid from water.....	152
3.13.2 The effect of pH of the aqueous solution on the extraction of clofibric acid from water by CA-(NH ₂) ₂ at 298.15 K.....	154
3.13.3 Calculation of the capacity of the CA-(NH ₂) ₂ receptor to extract clofibric acid.....	154
3.14 Extraction of aspirin from water by CA-(NH ₂) ₂	155

3.15 Aspirin removal by 3-aminopropyl functionalized silica.....	156
3.15.1 Dose effect.....	157
3.15.2 Effect of pH of the aqueous solution on the removal of aspirin by Sil-NH ₂	158
3.15.3 Kinetic of removal.....	159
3.15.4 Determination of the capacity of Sil-NH ₂ for the removal of aspirin from water at 298 K.....	159
3.16 Complexation of C-decylpyrogallol[4]arene with carbamazepine.....	161
3.16.1 Investigation of the complexation of PG11 and CBZ by thermal analysis.....	161
4. Chapter IV	166
4.1 <i>Meso</i> -tetramethyl-tetrakis-[2-(4-hydroxyphenyl)ethyl]calix[4]pyrrole TTHCP and <i>meso</i> - tetramethyl-tetrakis-[2-(4-ethylacetatophenoxy)ethyl]calix[4]pyrrole TTCP.....	167
4.1.1 Characterization of <i>meso</i> -tetramethyl-tetrakis-[2-(4-hydroxyphenyl) ethyl] calix[4]pyrrole.....	168
4.1.2 Solubility of TTHCP in various solvents at 298.15 K.....	168
4.1.3 Complexation of TTHCP with anions, ¹ H NMR studies.....	170
4.2 Conductometric titrations of anion salts with TTHCP in acetonitrile at 298.15 K.....	172
4.2.1 Conductance measurements of <i>meso</i> -tetramethyl-tetrakis-[2-(4-hydroxyphenyl) ethyl] with TTHCP in acetonitrile at 298.15 K.....	172
4.2.2 Conductance measurements for the complexation of dihydrogen phosphate Bu ₄ NH ₂ PO ₄ with TTHCP in acetonitrile at 298.15 K.....	173
4.3 Thermodynamic parameters for the complexation of TTHCP with fluoride and phosphate	

anions (tetra- <i>n</i> -butylammonium counter ion) in acetonitrile at 298.15 K.....	174
4.4 Polymerisation of <i>meso</i> -tetramethyl-tetrakis-[2-(hydroxyphenyl)ethyl]calix[4]pyrrole.....	178
4.5 Characterisation of Novel <i>meso</i> -tetramethyl-tetrakis- <i>meso</i> -tetramethyl-tetrakis-(4-ethylacetatophenoxyethyl) calix[4]pyrrole TTECP.....	180
4.5.1 Solubility measurements of <i>meso</i> -tetramethyl-tetrakis-(4-ethylacetatophenoxyethyl) calix[4] pyrrole (TTECP).....	181
4.6 ¹ H NMR complexation studies.....	182
4.7 Conductance measurements for the complexation of <i>meso</i> -tetramethyl-tetrakis-(4-Ethylacetatophenoxyethyl) calix[4]pyrrole TTECP with the halides and phosphate anion (tetra- <i>n</i> -butylammonium counter-ion).....	183
4.7.1 Conductance measurements of TTECP and Bu ₄ NF in acetonitrile at 298.15 K.....	183
4.7.2 Conductometric titrations of chloride (Bu ₄ N ⁺ as counter-ion) with TTECP in acetonitrile at 298 K.....	184
4.7.3 Conductometric titration of tetra- <i>n</i> -butylammonium bromide (Bu ₄ NBr) with TTECP in acetonitrile at 298.15.....	185
4.7.4 Conductometric titration of tetra- <i>n</i> -butylammonium phosphate (Bu ₄ NH ₂ PO ₄) with TTEC in acetonitrile at 298.15 K.....	185
4.7.5 Thermodynamic parameters of complexation of <i>meso</i> -tetramethyl-tetrakis-[4-ethylacetatophenoxyethyl) calix[4]pyrrole TTECP with fluoride, bromide and phosphate anions (tetra- <i>n</i> -butylammonium as counter-ion) in acetonitrile at 298.15 K.....	186
5. Final conclusions.....	193

6. Suggestions for Further work.....	197
7. Referencess.....	198
8. Appendix.....	214

List of Figures.....	page
Chapter one	
Fig. 1.1 Dynamic elements of the host-guest complexation process.....	2
Fig. 1.2 Schematic representation of	4
Fig. 1.3 (a) Molecular structure of β -cyclodextrin (b) β -CD in a “Cone” shape.....	7
Fig. 1.4 Chemical structures of different macrocyclic crown ethers.....	9
Fig. 1.5 Structure of (a) 12-crown-4 (b) 1-benzyl-1-aza-12-crown-4 and 1-aza-12-crown-4.....	9
Fig. 1.6 Complexation reaction of guanidinium ion by 27-crown-9.....	11
Fig. 1.7 The structure of the receptor synthesised by Müllen and co-workers.....	13
Fig. 1.8 Chemical structure of the tri-aza-cryptand receptor containing a fluorophore.....	14
Fig. 1.9 Chemical structure of the spherands.....	14
Fig. 1.10 Images of (a) Greek Calyx Crater and (b) molecular modelling of <i>p</i> - <i>tert</i> -butyl calix[4]-arene showing the similarity between the Greek vase and the calix[4]arene.....	16
Fig. 1.11 ^1H NMR spectrum for <i>p</i> - <i>tert</i> -butylcalix[4]arene in CDCl_3 at 298 K (this work).....	17
Fig. 1.12 The upper and lower rim of <i>p</i> - <i>tert</i> -butyl calix[4]arene.....	18
Fig. 1.13 Possible conformations of <i>p</i> - <i>tert</i> -butylcalix[4]arene.....	19
Fig. 1.14 Patterns of signals expected in the (a) ^1H NMR and (b) ^{13}C NMR spectra of the four conformational isomers of calix[4]arene.....	20
Fig. 1.15 Lower rim functionalised <i>p</i> - <i>tert</i> -butylcalix[4]arene with ester and ketone groups.....	21
Fig. 1.16 Chemical structure of 5, 11, 17, 23-tetra- <i>tert</i> -butyl-25, 26, 27, 28-tetrakis (N, N-diethyl aminocarbonyl) methoxy calix[4]arene	23

Fig. 1.17 Chemical structure of <i>p-tert</i> -butylcalix[4]arene functionalised with phosphine oxide...	23
Fig. 1.18 Chemical structure of receptors used for the complexation of lanthanides cations	24
Fig. 1.19 Chemical structure of (a) bis-calix[4]arene and (b) methyl viologen	24
Fig. 1.120 Functionalisation of the upper rim of calix[4]arene by urea and the formation of dimeric structure when an appropriate guest is present	25
Fig. 1.21 Chemical structure of sulfonated calix[4]arene	26
Fig. 1.22 “Bis-Sulfonated” calix[4]arene as a molecular capsule.....	26
Fig. 1.23 Chemical structure of <i>p</i> -phosphonic acid calix[4]arene	27
Fig. 1.24 Lower and upper rim functionalized calix[4]arene	27
Fig. 1.25 Chemical structure of amphiphilic calix[4]arene and the aggregation to form vesicle ...	28
Fig. 1.26 The chemical structure of double cavity <i>p-tert</i> -butylcalix[4]arene	28
Fig. 1.27 Immobilizing calix[4]arene derivative on the gold nanoparticle surface	29
Fig. 1.28 Four different conformations adopted by calix[4]pyrrole	31
Fig. 1.29 Conformational changes of calix[4]pyrrole to a “cone” conformation up on anion complexation (A=F ⁻ , Cl ⁻ , Br ⁻)	31
Fig. 1.30 Different active positions for functionalization of calix[4]pyrrole	32
Fig. 1.31 Different products with different substituents at β-position on the pyrrole ring of the calix[4]pyrrole	33
Fig. 1.32 Functionalisation of <i>meso</i> -octamethylcalix[4]pyrrole through the N-rim	34
Fig. 1.33 Chemical structure of the synthesised receptor containing acetoxy group at <i>meso</i>	34

Fig. 1.34 Structure of <i>meso</i> -tetramethyl[N-(phenoxyethyl)-N-phenylurea]calix[4]pyrrole.....	35
Fig. 1.35 Chemical structure of the calix[4]pyrrole functionalised by sulphur	36
Fig. 1.36 Functionalised <i>meso</i> position of calix[4]pyrrole	36
Fig. 1.37 Calix[4]pyrrole as ion transporter across the membrane	38
Fig. 1.38 Formation supramolecular polymer during the addition of excess amount of caesium...	39
Fig. 1.39 General structure of resorcin[4]arene showing (a) the numbering of substituent and (b) hexameric aggregation in solution	41
Fig. 1.40 Possible conformations can adopted by resorcin[4]aren cyclic tetramer	42
Fig. 1.41 Structure of 4, 6, 10, 12, 16, 18, 22, 24-diethyl thiophosphate calix[4]resorcarene	43
Fig. 1.42 Showing bridging the hydroxyl groups of the resocin[4]arene by different groups	44
Fig. 1.43 2, 8, 14, 20-tetraalkyl-5, 11, 17, 23-tetrahydroxyresorc[4]arene showing the numbering of substituent positions	46
Fig. 1.44 Chemical structures of xanthan and C-alkyl pyrogallol[4]arene	47
Fig. 1.45 Molecular modelling of carceplex	47
Fig. 1.46 Chemical structure of 5, 11, 17, 23- <i>tetrakis</i> -[(diethylamine)ethoxy]calix[4]arene and its immobilisation	50
Fig. 1.47 The chemical structure of (a) the receptor used for the complexation and (b) 1-naphthyl methylcarbamate.....	50
Fig. 1.48 The chemical structures of synthesised receptors.....	58
Fig. 1.49 The chemical structures of synthesised receptor.....	59
Chapter III	99

Fig. 3.1 ^1H NMR spectrum for the complex resulted from the complexation of sodium diclofenac and per-benzoylated- β -cyclodextrin in DMSO- d_6 at 298 K.....	107
Fig. 3.2 UV-Vis spectra for the titration of sodium diclofenac solution in 1-octanol.....	108
Fig. 3.3 Plot of $[\text{Bz-}\beta\text{-CD}][\text{NaDF}]/A-A^\circ$ against the concentration of the receptor	109
Fig. 3.4 A plot of molar conductance of sodium diclofenac in 1-butanol against the ligand/ drug concentration ratio at 298.15 K.....	111
Fig. 3.5 Isothermal titration calorimetry for the complexation of 18-crown-6 (1×10^{-3} mol dm^{-3}) with BaCl_2 (1.5×10^{-2} mol dm^{-3}). The curve shows the change in enthalpy after each injection as a result of complexation.....	114
Fig. 3.6 Isothermal titration calorimetry for the complexation of sodium diclofenac and Bz- β -CD in 1-octanol at 298.15 K. Top: the heat evolved after each addition of sodium diclofenac to the receptor solution and bottom plotted against the molar ratio.....	116
Fig. 3.7 ^1H NMR spectrum for the complexation of <i>p-tert</i> -butylcalix[4]arene tetraester with NaDF in CD_3CN at 298 K. The lower spectrum for the receptor and the upper for the Complex..	118
Fig. 3.8 A plot of molar conductance against the receptor/ drug concentration ratio for the system involving <i>p-tert</i> -butylcalix[4]arene tetraester and sodium diclofenac in MeCN at 298 K.....	119
Fig. 3.9 TGA Thermogram for pure sodium diclofenac.....	121
Fig. 3.10 TGA Thermogram analysis curve as it is obtained for <i>p-tert</i> -butylcalix[4]arene ester	122
Fig. 3.11 TGA Thermogram for the complex formed between NaDF and the CAE receptor.....	122
Fig. 3.12 TGA curves for the sodium diclofenac NaDF, CAE and the complex formed.....	123
Fig. 3.13 DSC Thermogram of the sodium diclofenac.....	123

Fig. 3.14 DSC Thermogram for CAE receptor.....	124
Fig. 3.15 DSC analysis for the complex formed between NaDF and CAE.....	124
Fig. 3.16 The effect of mass on the uptake of NaDF from aqueous solution by CAE at 298 K.....	126
Fig. 3.17 Uptake isotherm for sodium diclofenac from aqueous solution by CAE at 298.15 K...	127
Fig. 3.18 The effect of pH on the on the diclofenac sodium uptake by 5, 11, 17, 27- <i>tert</i> -butyl- 25, 26, 27, 28-(oxy-ethylacetato) calix[4]arene (CAE).....	129
Fig. 3.19 Chemical structure of the receptor and diclofenac, clofibric acid, aspirin	130
Fig. 3.20 The chemical shift changes for the 5,11,17,23 tetra- <i>tert</i> -butyl, 25, 27-bis[aminoethoxy], 26, 28- dihydroxycalix[4]arene upon addition of diclofenac against the [drug]/ [receptor] concentration ratios in CD ₃ CN at 298 K.....	133
Fig. 3.21 Chemical shift changes for the 5, 11, 17, 23 tetra- <i>tert</i> -butyl, 25, 27-bis[aminoethoxy], 26, 28-dihydroxycalix[4]arene upon addition of clofibric acid against the [drug]/ [receptor] concentration ratios at 298 K.....	133
Fig. 3.22 Conductivity curve of the pure receptor in order to test it if it is undergoing to ionisation or not in acetonitrile at 298.15 K.....	134
Fig. 3.23 Change in molar conductance resulting from the addition of receptor against the [receptor]/ [drug] concentration ratio in acetonitrile at 298.15 K.....	136
Fig. 3.24 Change in molar conductance resulting from addition of the receptor against the [receptor]/ [clofibric acid] concentration ratio in acetonitrile at 298.15 K.....	137
Fig. 3.25 Conductance changes of aspirin solution in dry acetonitrile as a result from the gradual addition of calix[4]arene amine against the [receptor]/ [drug] concentration ratios at 298.15 K...	138

Fig. 3.26 UV- Vis titration of diclofenac in acetonitrile showing the increase in the absorbance bands intensity resulting from the addition of $\text{CA}(\text{NH}_2)_2$ at 298 K.....	139
Fig. 3.27 Plot of the absorbance of the diclofenac against the [receptor]/ [diclofenac] concentration ratios in acetonitrile at 298 K.....	140
Fig. 3.28 UV-Vis titration spectrum of clofibric acid in acetonitrile (3.35×10^{-4}) showing the increase in the absorbance bands resulting from the gradual addition of increasing concentration of $\text{CA}(\text{NH}_2)_2$ solution in acetonitrile at 298 K.....	141
Fig. 3.29 Plot of the absorbance of clofibric acid in acetonitrile against [receptor]/ [drug] concentration ratios at 298 K.....	141
Fig. 3.30 UV-Vis spectra of aspirin solution in acetonitrile (2.99×10^{-4}) resulting from gradual addition of $\text{CA}(\text{NH}_2)_2$ solution in acetonitrile at 298 K.....	142
Fig. 3.31 Variation in absorbance values of aspirin resulting from addition of increasing concentration of the receptor at 298 K.....	143
Fig. 3.32 Top is the base line editor; bottom is the titration curve resulted from the injection of the aspirin in acetonitrile into the cell containing 1mM of the receptor at 298.15 K.....	146
Fig. 3.33 Top is the base line; bottom is the titration curve for the interaction of clofibric acid with calix[4]amine in acetonitrile at 298.15 K.....	147
Fig. 3.34 Top is the base line, bottom is the titration curve for the interaction of diclofenac with calix[4]amine in acetonitrile at 298.15 K.....	148
Fig. 3.35 Molecular modelling of the interaction of diclofenac with calix[4]aren amine.....	149
Fig. 3.36 Molecular modelling of the interaction of clofibric acid and calix[4]arene amine.....	149

Fig. 3.37 Molecular modelling of the interaction of aspirin and calix[4]arene (CA-NH ₂) ₂	150
Fig. 3.38 TGA thermograms for diclofenac (DF), CA-(NH ₂) ₂ and the complex.....	151
Fig. 3.39 TGA thermogram for the complexation process between CA-(NH ₂) ₂ and the receptor.	151
Fig. 3.40 TGA thermogram for the complexation of aspirin with CA-(NH ₂) ₂	152
Fig. 3.41 The effect of receptor dose on the uptake of clofibrac acid from aqueous solution	153
Fig. 3.42 The effect of pH on the extraction of clofibrac acid by CA-(NH ₂) ₂ at 298 K.....	154
Fig. 3.43 The capacity of the calix[4]arene amine towards clofibrac acid.....	155
Fig. 3.44 Extraction of aspirin from water by CA-(NH ₂) ₂ at 298 K.....	156
Fig. 3.45 Effect of the mass of Sil-NH ₂ on the uptake of aspirin from aqueous solution at 298 K	158
Fig. 3.46 Effect of pH of the aqueous solution on the extraction of aspirin from water by Sil-NH ₂	159
Fig. 3.47 Capacity of Sil-NH ₂ to uptake aspirin from aqueous solution at 298 K.....	160
Fig. 3.48 TGA thermogram of C-decylpyrogallol[4]arene receptor.....	162
Fig. 3.49 TGA thermogram for the complex formed between C-decylpyrogallol[4] and CBZ...	163
Fig. 3.50 TGA thermogram for the complex of C-decylpyrogallol[4]arene and CBZ.....	163
Fig. 3.51 DSC thermogram of for the carbamazepine showing structural phase transition.....	164
Fig. 3.52 DSC thermogram for C-decylpyrogallol[4]arene.....	164
Fig. 3.53 DSC thermogram to the complex between C-decylpyrogallol[4]arene and CBZ.....	165
Chapter IV	166
Fig. 4.1 Chemical structure of novel calix[4]pyrrole derivatives (a) <i>meso</i> -tetramethyl- <i>tetrakis</i> -[2(4-hydroxyphenyl) ethyl]calix[4]pyrrole TTHCP and <i>meso</i> -tetramethyl- <i>tetrakis</i> -[2-(4	

ethylacetato-phenoxy) ethyl] calix[4]pyrrole TTECP.....	167
Fig. 4.2 ^1H NMR spectrum for <i>meso</i> -tetramethyl-tetrakis-(4-hydroxyphenyl ethyl) calix[4]pyrrole TTHCP in DMSO- d_6	168
Fig. 4.3 ^1H NMR spectrum of TTHCP and its fluoride complex (Bu_4N^+ as counter ion in DMSO- d_6 at 298 K.....	170
Fig. 4.4 ^1H NMR spectrum for the complex formed between <i>meso</i> -tetramethyl-tetrakis-(4-hydroxy phenyl ethyl) calix[4]pyrrole TTHCP and tetra- <i>n</i> -butylammonium phosphate ($\text{Bu}_4\text{NH}_2\text{PO}_4$) at 298 K in DMSO- d_6	171
Fig. 4.5 Conductometric titrations of TTHCP against $\text{Bu}_4\text{NH}_2\text{PO}_4$ in acetonitrile at 298.15 K...	173
Fig. 4.6 Conductivity titration between TTHCP and tetrabutylammonium phosphate $\text{Bu}_4\text{NH}_2\text{PO}_4$ in acetonitrile at 298.15 K, $[\text{TTHCP}] = 9.99 \times 10^{-4}$, $[\text{Bu}_4\text{NH}_2\text{PO}_4] = 9.4 \times 10^{-5} \text{ mol dm}^{-3}$	174
Fig. 4.7 Isothermal titration calorimetry for the complexation of TTHCP with fluoride (tetra- <i>n</i> -butylammonium counter ion) in acetonitrile at 298.15 K.....	175
Fig. 4.8 Isothermal titration calorimetry for the complexation of phosphate (tetra- <i>n</i> -butyl-ammonium counter in acetonitrile at 298.15 K.....	176
Fig. 4.9 SEM analysis for the polymer showing the porosity in the structure in different region..	178
Fig. 4.10 Shows the X-ray diffractogram of the polymer. It is characteristic of an amorphous compound with little or, no crystal structure.....	179
Fig. 4.11 EDS spectrum of the polymer formed.....	179
Fig. 4.12 ^1H NMR spectrum of <i>meso</i> -tetramethyl-tetrakis-[4-(oxy-ethylethanoato)-phenyl]ethyl calix[4]pyrrole TTHCP in DMSO- d_6 at 298 K.....	180

Fig. 4.13 Conductometric titrations of fluoride (Bu_4N^+ as counter-ion) with TTECP in acetonitrile at 298.15 K.....	183
Fig. 4.14 Conductometric titration curve of TTECP [$9 \times 10^{-4} \text{ mol dm}^{-3}$] against tetra-n-butylammonium chloride Bu_4NCl in [$1.09 \times 10^{-4} \text{ mol dm}^{-3}$] in acetonitrile at 298.15 K.....	184
Fig. 4.15 Conductometric titration of tetra-n-butylammonium bromide (Bu_4NBr) with TTECP in acetonitrile at 298.15 K.....	185
Fig. 4.16 Molar conductance of $\text{Bu}_4\text{NH}_2\text{PO}_4$ against the $[\text{TTECP}]/[\text{H}_2\text{PO}_4]^-$ concentration ratios in acetonitrile at 298.15.....	186
Fig. 4.17 Nano-isothermal titration calorimetry of the interaction of fluoride (Bu_4NF as counter ion and CP-tetraester in acetonitrile at 298.15 K.....	188
Fig. 4.18 Nano-isothermal titration calorimetry of the Interaction of CP-tetraester with Bu_4NCl in acetonitrile at 298.15 K.....	189
Fig. 4.19 Nano isothermal titration calorimetry for the interaction of the calix[4]pyrrole ester CP-tetraester and Bu_4NB in acetonitrile at 298.15 K, top, is the baseline editor, and bottom is the titration curve.....	190
Fig.4.20 Nano isothermal titration calorimetry for the complexation of Bu_4NPO_4 with TTECP in acetonitrile at 298.15 K.....	191

List of Scheme.....	Page
Scheme 1.1 Synthetic pathway of cryptand 222.....	8
Scheme 1.2 Synthetic pathway of pillar[5]arene receptor.....	10
Scheme 1.3 Synthesis of <i>p-tert</i> -butylcalix[4]arene.....	16
Scheme 1.4 De-alkylation and upper rim functionalization of <i>p-tert</i> -butylcalix[4]arene.....	25
Scheme 1.5 Synthesis of <i>meso</i> -octamethylcalix[4]pyrrole.....	30
Scheme 1.6 Complexation of ions in different sites of calix[4]pyrrole.....	38
Scheme 1.7 Synthesis pathway of resorcin[4]arene.....	40
Scheme 1.8 Synthetic rout for the cavitands.....	43
Scheme 1.9 Synthesis of the carcerands and the encapsulation of guest to form carceplex.....	44
Scheme 1.10 Synthesis of hemicarcerand and showing the formation of hemicarceplex and the possibility of the guest to leave the cavity.....	45
Scheme 1.11 Synthesis of pyrogallol[4]arene macrocycle.....	45
Scheme 1.12 Polymerisation of Silicic acid.....	48
Scheme 1.13 Modification of silica by (a) organic functional group, (b) inorganic groups.....	49
Scheme 1.14 Using of Silica as solid support for functionalised <i>p-tert</i> -butylcalix[4]arene.....	51
Scheme 1.15 Uncatalysed and catalysed azide-alkyne cycloaddition reaction.....	52
Scheme 1.16 Proposed mechanism for catalysed azide-alkyne cycloaddition reaction.....	52
Scheme 1.17 Main strategy for this research.....	55
Chapter two	61

Scheme 2.1 Synthesis of heptakis-(6-chloro-6deoxy)- β -cyclodextrin.....	70
Scheme 2.2 Synthesis of heptakis-(2, 3 , 6-tri-O-benzoyl)- β -cyclodextrin.....	71
Scheme 2.3 Synthesis of 5, 11, 17, 27- <i>tert</i> -butyl-25, 26, 27, 28-(ethylacetoxy)calix[4]arene	72
Scheme 2.4 Synthesis of 5, 11, 17, 23 tetra- <i>tert</i> -butyl, 25, 27 bis[2-cyanomethox] methoxy, 26, 28- dihydroxycalix[4]arene.....	73
Scheme 2.5 Synthesis of 5, 11, 17, 23 tetra- <i>tert</i> -butyl, 25, 27-bis[aminoethoxy],26, 28 dihydroxycalix[4]arene.....	74
Scheme 2.6 Synthesis 25, 26, 27, 28-tetrahydroxycalix[4]arene.....	74
Scheme 2.7 Synthesis and characterization of 5- <i>tert</i> -butyl-3-azidomethyl-2-hydrox-benzaldehyde	75
Scheme 2.8 Preparation of 25, 27-dihydroxy-26, 28-(dioxypropargyl) <i>tert</i> -butylcalix[4]arene....	77
Scheme 2.9 preparation of 4- <i>tert</i> -butyl-azidocalix[4]arene.....	78
Scheme 2.10 Preparation of 2-azidoacetamide.....	78
Scheme 2.11 Synthesis of 25, 26, 27, 28-(diethylamino)ethoxy calix[4]arene.....	79
Scheme 2.12 Synthesis of <i>meso</i> -tetramethyl-tetrakis-(4-hydroxyphenylethyl)calix[4]pyrrole....	80
Scheme 2.13 Synthesis of <i>meso</i> -tetramethyl-tetrakis-(4-ethylacetato-oxyphenylethyl) calix[4]pyrrole....	81
Scheme 2.14 Synthesise of calix[4]pyrrole polymer.....	82
Scheme 2.15 Synthesis of C-pentyl-resorcin[4]arene.....	83
Scheme 2.16 Synthesis of C-pentylresorci[4]arene ester.....	84
Scheme 2.17 Synthesis of C-pentylpyrogallol[4]arene.....	85
Scheme 2.18 Synthesis of C-decylpyrogallol[4]arene PG11.....	86

Scheme 2.19 Synthesis of C-4-aminophenyl pyrogallol arene.....87

Scheme 3.1 The standard reaction between BaCl₂ and 18-crown-6 ether in aqueous media.....112

Scheme 3.2 The oxidation of the sodium diclofenac causes cyclisation to sodium diclofenac....121

List of Tables.....	Page
Table 1.1 Physicochemical properties of α , β , γ -cyclodextrine.....	7
Table 1.2 Stability constants expressed as $\log K_s$ and derived standard Gibbs energies ($\Delta_c G^\circ$) enthalpies ($\Delta_c H^\circ$), and entropies ($\Delta_c S^\circ$) of complexation of crown ethers (12-crown-4 (12-C-4) and 1-Benzyl-1-aza-12-crown-4 (1-BA-12-C4) and lithium (using salts containing different anions)in MeCN and in propylene carbonate at 298.15 K.....	10
Table 1.3 Thermodynamic parameters of complexation of amino acids with 18-crown-6 in methanol at 298.15.....	12
Table 1.4 Thermodynamic parameters for the complexation of (a) <i>p-tert</i> -butylcalix[4]arene tetraester and (b) <i>p-tert</i> -butylcalix[4]arene ketone with bivalent cations in acetonitrile using different techniques obtained by Danil de Namor and co-workers.....	22
Table 1.5 Thermodynamic parameters and stoichiometric ratios for the complexation of calix[4]-pyrrole and functionalized calix[4]pyrrole at <i>meso</i> position with anions synthesized by Danil de Namor and co-workers.....	37
Table 1.6 The chemical structure of pharmaceuticals with commercial and IUPAC names.....	56
Chapter two.....	60
Table 2.1 Different conditions used during TGA analysis.....	97
Table 2.2 The conditions applied for DSC analysis.....	98
Chapter III.....	99
Table 3.1 Solubility and standard Gibbs energies of solution of sodium diclofenac in different solvent at 298.15 K.....	101

Table 3.2 Solubility of carbamazepine CBZ in different solvents at 298.15 K and derived standard Gibbs energies of solution and from water.....	103
Table 3.3 Partition coefficients of drugs in the water-1-octanol system at 298.15 K.....	105
Table 3.4 Chemical shift changes for the NH proton of sodium diclofenac resulting from complexation with per-benzoylated- β -cyclodextrin in DMSO- d_6 at 298 K.....	107
Table 3.5 Molar conductance of an aqueous solution of potassium chloride KCl at 298.15 K for the calculation of the cell constant, θ	110
Table 3.6 Thermodynamic parameters of complexation of barium with 18-crown-6 measured by Nano-ITC in aqueous medium at 298.15 K.....	113
Table 3.7 Thermodynamic parameters of complexation of the cyclodextrin derivative with sodium diclofenac at 298.15 K in 1-octanol.....	115
Table 3.8 Chemical shift changes for the receptor protons as a result from the addition of sodium diclofenac in CD_3CN at 298 K.....	118
Table 3.9 Effect of the amount of calix[4]arene tetraester on the extraction of sodium diclofenac from aqueous solution at 298 K.....	125
Table 3.10 Illustrate the initial equilibrium and removed concentration of NaDF by CAE.....	126
Table 3.11 Effect of pH on the extraction of sodium diclofenac at 298 K.....	128
Table 3.12 1H NMR complexation study to check the affinity of the receptor to complex with the Pharmaceuticals in CD_3CN at 298 K.....	132
Table 3.13 Thermodynamic parameters of the binding between the drugs and calix[4]arene	

aminereceptor in acetonitrile at 298 K.....	145
Table 3.14 Drug concentration before and after the extraction, adsorbent used and extraction Percentages.....	153
Table 3.15 Initial and equilibrium concentration of aspirin before and after the extraction and the percentages of extraction by CA-(NH ₂) ₂	155
Table 3.16 Percentage of extraction of aspirin as a function of the dose of Sil-NH ₂ at 298 K...	157
Table 3.17 Initial, equilibrium and the capacity of silica to remove aspirin from water at 298 K	160
Chapter IV	166
Table 4.1 Solubility data and derived standard Gibbs energies of solution of TTHCP in different solvents at 298.15 K. Transfer Gibbs energies from acetonitrile to other solvents is ($\Delta_t G^\circ_{\text{MeCN} \rightarrow \text{S}_2}$) at 298.15 K.....	169
Table 4.2 ¹ H NMR chemical shifts (δ) and chemical shift changes ($\Delta\delta$) of CPD protons upon addition of fluoride, phosphate and bromide as tetra-n-butylammonium salts in DMSO-d ₆	171
Table 4.3 The thermodynamic parameters for the interaction of <i>meso</i> -tetramethyl-tetrakis-(4-hydroxyphenyl ethyl)calix[4]pyrrole TTHCP and phosphate, fluorid, chloride, as tetrabutylammonium counter ion in acetonitrile at 298.15 K.....	177

Chapter I

Introduction

1.1 Supramolecular chemistry

Supramolecular Chemistry^{1,2} is a branch of chemistry which was made up from early ideas resulting from the contributions on receptors by Ehrlich and Silverstein³, the coordination chemistry introduced by Werner⁴ and the lock-key mechanism suggested by Fischer⁵. Great interest has been focused on Supramolecular Chemistry since three scientists; Pederson^{6,7}, Lehn^{8,9} and Cram^{10,11} were awarded the Nobel Prize in Chemistry in 1987 for their work on crown ethers, cryptands and spherands respectively. Supramolecular Chemistry is concerned with the reversible interactions between the receptor molecule (host) bearing multiple recognition sites consisting of holes and cavities in their structures for binding ions, radicals or neutral species (guests) leading to molecular aggregates with supermolecular structures¹²⁻¹⁴. These aggregation processes are attributed to the combination of non-covalent forces which are ion-dipole, ion-ion, dipole-dipole, cation- π , anion- π , van der Waals, π - π interactions, and hydrogen bonding¹⁵⁻¹⁸. The perfect encapsulation of the guest in the cavity leads to excellent complexation with high stability constant values. Thus the re-organization of the conformation of the receptor molecule commonly leads to maximum strength of complexation¹⁹. Also the external environment surrounding host-guest complexes can play a major role in complexation processes because of the weakness of the non-covalent forces, for example hydrogen bonded host-guest complexes are very sensitive to the polarity of the solvent surrounding supermolecule structures (Fig. 1.1). Danil de Namor and co-workers²⁰⁻²⁷ have made extensive thermodynamic studies on the effect of the medium on host-guest complexes. There are many applications of Supramolecular Chemistry in separation science, drug-delivery systems and molecular sensing and recognition²⁸⁻³³.

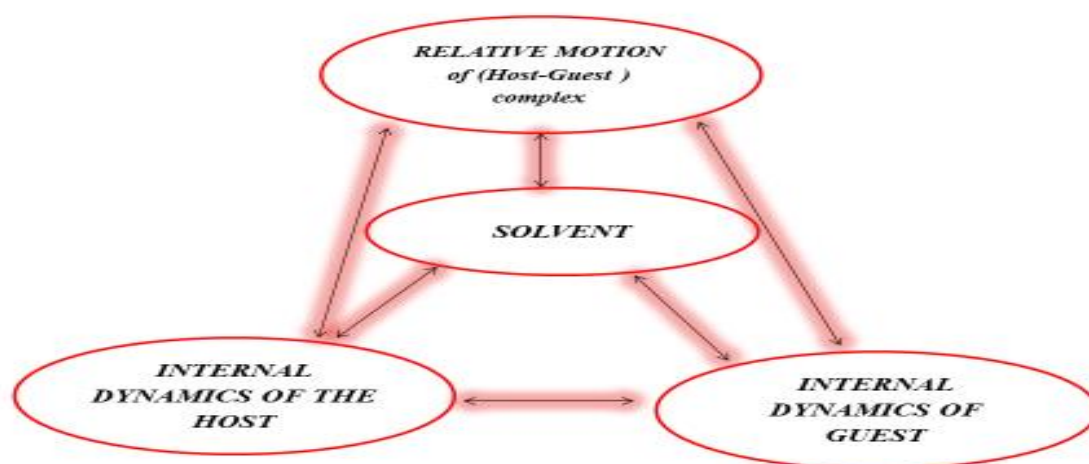


Fig. 1.1 Dynamic elements of the host-guest complexation process

1.2 Pharmaceuticals, phosphate and halides in the environment

1.2.1 Occurrence of pharmaceuticals in the aquatic environment

In the last few years, contamination of water by a variety of pharmaceuticals has been gaining serious concern by environmental scientists³⁴⁻³⁶. There are many sources for the pharmaceuticals to enter the aquatic environment. These are as follows: (i) the use of various pharmaceuticals for treatment of human and animals which are excreted as unchanged compounds or as metabolites entering the aquatic environment as a result of inadequate treatment of wastewater in sewage treatment plants (STPs); (ii) the discarding of unused pharmaceuticals *via* toilet; (iii) the discharge of residuals of drugs manufacturers³⁷⁻³⁹. As a consequence of globally different regulations applied of drugs marketing and manufacturing, different concentrations levels in different countries have been diagnosed for many types of drugs in the analysed water samples and this come from that these samples were collected from different regions in different countries. Some of these samples were taken from the sewage treatment plants or from the water streams which are located near the effluents of the hospitals or near the drug manufactories which have the higher risk to the environment.⁴⁰

Up to date, few studies concerning the removal of these pollutants from water have been carried out. Currently a number of techniques are used to treat wastewater such as powdered activated carbon, ozonation, ultraviolet photolysis, zeolites, and reverse osmosis. However, powdered activated carbon is not effective to remove many organic pollutants at low concentration level and also cannot be recycled when the saturated point is reached. Oxidation by ozone is effective to remove most pharmaceuticals from water but the toxicity of ozone and by-products resulting from this process has implications on human health and the environment. Ultraviolet photolysis is not effective to remove most pharmaceuticals from water. Zeolites also show low efficiency to remove organic pollutants. Reverse osmosis is effective to remove most pharmaceuticals from water but this technology is economically undesirable⁴¹⁻⁴³.

As in oxidation by ozone, less promising experimental work has been reported by Jiang and co-workers⁴⁴⁻⁴⁶ using ferrate (VI) as oxidizing agent for the removal of ciprofloxacin, ibuprofen, sulfamethoxazole, diclofenac, carbamazepine and benzaifibrate from water. The authors have revealed that ferrate (VI) effectively degrades ciprofloxacin, diclofenac and carbamazepine, but it is not effective to remove ibuprofen and benzaifibrate. The limitations of this process were the doses of ferrate (VI) required to complete the oxidation process, the large number of pharmaceuticals that can resist the oxidation by ferrate (VI) and the undesirable oxidation products formed which can

cause high impact on the environment. For example, more than half a dozen of oxidation products were identified from the oxidation of ciprofloxacin by ferrate (VI) FeO_4^{2-} .

Molecularly imprinted techniques⁴⁷ were also used in the production of molecularly imprinted polymers, MIPs, which are used for the removal of pharmaceuticals from water. MIPs are activated synthetic polymers obtained from the introduction of a number of specific functional groups into a polymer matrix which can enhance the specificity towards a template. These MIPs have gained much interest due to their usage in many applications involving solid phase extraction, sensing, drug delivery systems and chromatography. The implantation process of functional groups can be made by applying one of two subsequent strategies depending on the nature of the chemical interaction between the functional monomer and the template. Firstly, the non-covalently aggregation process resulting from the interaction between an analyte (template) and a functional monomer is to be fixed in a polymeric matrix containing a cross-linking material and an initiator in the appropriate solvent. In this method, non-covalent bonds drive the polymerization procedure and the template must be removed after polymerization while the monomer will remain bound covalently into the polymer structure. Secondly⁴⁸, the covalently complex of a functional monomer with a template is co-polymerised with a cross linker, an initiator and an appropriate solvent. The release of the template from the cross-linking polymer in both procedures leads to the formation of a polymer with cavities and specific recognition sites homogeneous in shape, size and functionality to those of the imprinted template (Fig. 1.2)⁴⁹.

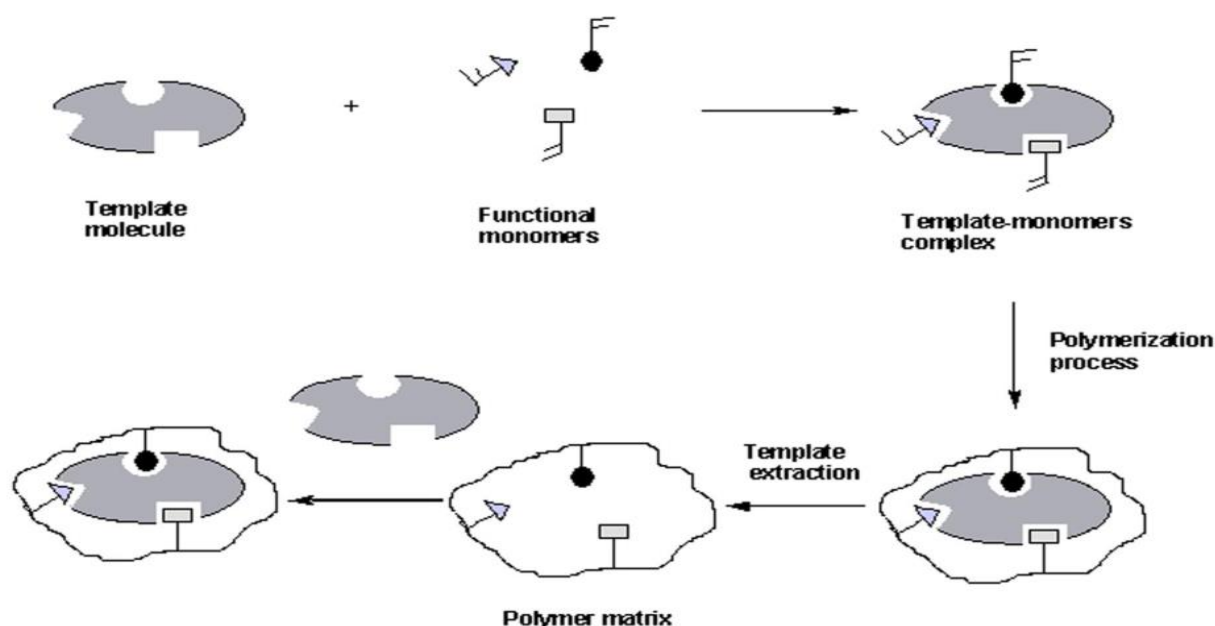


Fig. 1.2 Schematic representation of molecularly imprinted polymer⁴⁹

Geissen *et al*⁵⁰ have demonstrated that the MIP synthesised by polymerisation of 2-vinylpyridine monomer, ethylene glycol dimethacrylate as cross linker and azo-bis-isobutyronitrile as initiator in the presence of diclofenac as template in toluene removes selectively diclofenac from water in the 3-8 pH range

It has been emphasized that the use of a number of templates in the polymerization process can lead to produce molecularly imprinted polymers with multiple active sites with different and effective reactivity for the simultaneous removal of a number of materials without any reduction in their efficiency.

C. Dai *et al*⁵¹ have reported the use of the precipitation polymerisation process for the synthesis of multi-templates MIP using ketoprofen, naproxen, clofibric acid, diclofenac and ibuprofen as templates and demonstrated that these polymers are able to remove acidic pharmaceuticals effectively in the 3-7 pH range and the removal process was found to be kinetically fast.

Many drawbacks still remain in the removal of drugs by MIPs including the incarceration of targeted materials in cavities which can make the long term clean-up process unrealistic or even economically disappointing due to the large quantity of organic solvents utilised. Also, the use of an excess amount of the monomer in the polymerisation process can lead to the presence of non-selective sites in the polymeric matrix and can increase the density of monoliths which can also decrease the selective interaction between the MIP and the targeted material. In addition to these drawbacks, the synthesis of MIPs is considered to be rather tedious^{52,53}.

Therefore, there is serious concern about the need to find an effective and economical method to remove these organic pollutants from water. Supramolecular Chemistry can therefore be a suitable strategy to overcome this problem. The reversible complexation of macrocyclic receptors with different types of anions, cations and neutral species *via* cooperative interactions through non-covalent bonds may be a fast and an economical way for the removal of these pollutants from water due to the possibility of recycling the host.

1.2.2 Phosphate and halides in the environment

The phosphate anion is a fundamental constituent in all living systems and plays crucial role in the production of energy required to drive the biological reactions. It is also presents in fertilizers, product metabolism, and traditional detergents. The presence of phosphates in a high concentration levels in the environment leads to growing algae and can cause negative impact on the environment whereas the variation of the concentration levels of phosphate in living cell reflects the biological activity and

healthiness of these systems. For example, it is difficult to control phosphate levels in blood for patients with kidney failure⁵⁴. Another issue of considerable environmental concern is that related to the presence of fluorides in water. Long-term exposure to high concentration levels of fluoride leads to a number of health problems such as skeletal fluorosis, which is a health disorder related to the building up of fluoride in the bones. This disease can cause joint stiffness and pain, and may result in weak bones or fractures in older adults. Over the years, many studies have looked at the possible link between fluoride and cancer. Most of the concern about cancer seems to be around osteosarcoma. One theory on how fluoridation might affect the risk of the osteosarcoma is based on the fact that fluoride is localised on the bones and can lead to cancer⁵⁵⁻⁵⁷. Probing and trapping these anions by artificial supramolecular receptors is still challenging and therefore, it will be one of the main targets in this project.

1.3 Classification of Macrocyclic receptors

Macrocyclic receptors can be divided into two classes; naturally occurring and synthetic macrocycles⁵⁸

1.3.1 Naturally occurring macrocycles

Some of the macrocycles can be considered as naturally occurring receptors. Representative examples are valinomycin, chlorophyll, nigericin and cyclodextrin (CDs). Cyclodextrins (CDs) are biosynthetic cyclic oligosaccharides first obtained by Villers through the enzymatic degradation of starch¹³. CDs consist of six (α -cyclodextrin), seven (β -cyclodextrin), eight (γ -cyclodextrin) or more anhydrous glucopyranosyl units connected together through α -(1, 4)-D-glycosidic bonds with a truncated “cone” structure having a lipophilic internal cavity and a polar outer surface. The primary hydroxyl groups which involve C-6 (Fig. 1.3 a & b) are located on the narrow rim of the “cone” but the secondary hydroxyl group on C-2 and C-3 are located on the wider rim. These unique properties enabled CDs to embedding a variety of hydrophobic molecules with an appropriate size in their hydrophobic cavities leading to inclusion complexes in equilibrium processes⁵⁹⁻⁶¹. The inclusion complexes formed are used in a number of applications such as agriculture, food, separation sciences and the pharmaceutical industry. For example, CDs enhance the water solubility of low soluble drugs to increasing their bioavailability and stabilise drugs towards light and thermal decomposition⁶²⁻⁶⁶. The numerical values of the stoichiometry and the stability constants of these inclusion complexes can be determined by observing the changes in their physicochemical properties like solubility, chemical reactivity, UV-Vis absorbance, drug retention and chemical stability⁶⁷.

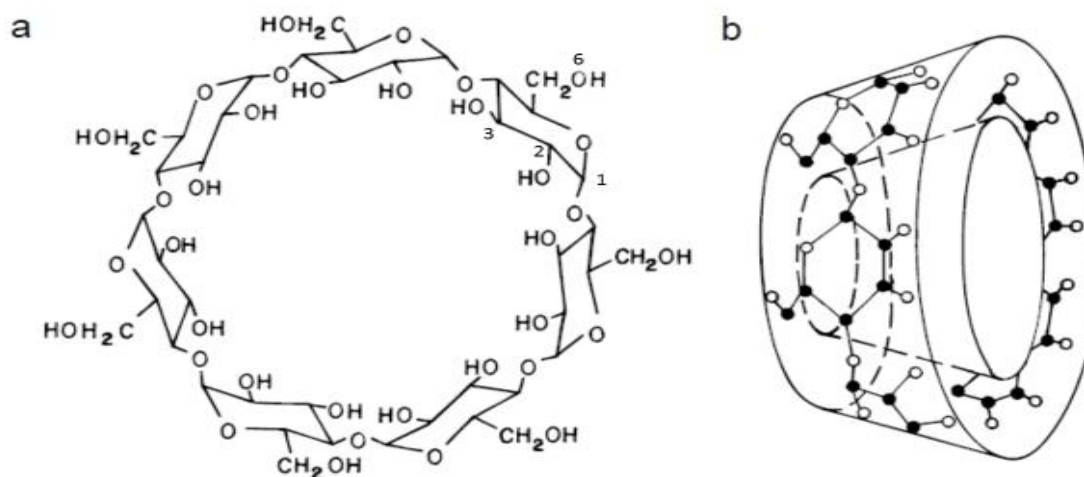


Fig. 1.3 (a) Molecular structure of β - cyclodextrin (b) β -CD in a “cone” conformation⁵⁹

The difference of the number of glucose units and the size of cavities between the isolated CDs leads to differences in their chemical and physical properties (Table 1.1)⁶⁸. There are a large number of cyclodextrin derivatives due to the possibility of introducing functional groups through the hydroxyl groups (18-OH in α -CD, 21-OH in β -CD and 24-OH in γ -CD) with different reactivities which can be modified by different methods. Substitution on the CDs rims can give a high degree of binding properties towards many lipophilic guest compounds⁶⁹⁻⁷².

Danil de Namor and coworkers^{73,74} have carried out a series of thermodynamic studies for cyclodextrins as hosts with different guests. CDs with different functional groups have shown to have a strong effect on the receptor properties⁷⁵⁻⁷⁸.

Table 1.1 Physicochemical properties of α , β and γ -cyclodextrins⁶⁸

Physico-chemical Properties	α -Cyclodextrin	β -Cyclodextrin	γ -Cyclodextrin
Number of glucopyranose units	6	7	8
Molecular weight (g mol ⁻¹)	972	1135	1297
Solubility in water at 25 °C (% , w/v)	14.5	1.85	23.2
Outer diameter (Å)	14.6	15.4	17.5
Cavity diameter (Å)	4.7–5.3	6.0–6.5	7.5–8.3
Height of torus (Å)	7.9	7.9	7.9
Cavity volume (Å ³)	174	262	427

1.3.2 Synthetic macrocyclic receptors (crown ethers, cryptands, spherands, calixarenes, calixpyroles and pillarenes)

Due to the importance of the field of Supramolecular Chemistry, a huge number of synthetic macrocycles has been synthesised such as crown ethers, cryptands, spherands, *p*-*tert*-butylcalix[n]arene (n=4, 5, 6, 8), calix[n]pyrroles and pillarenes^{1,2,29}.

Pederson^{4,5} in the early seventies reported the first synthesis of the macrocyclic known as Dibenzo-18-crown-6 consisting of oxyethylene repeating units (-O-CH₂CH₂) containing a hole in its structure, large enough, to interact with alkali and alkaline-earth metal cations to form host-guest complexes driven by ion-dipole interactions between the cation and the negative charge of the oxygen donor atoms of the receptor. He concluded that dibenzo macrocyclic crown ethers are good complexing agents for these metal cations, particularly those containing five to ten oxygen atoms, thus a strong binding affinity of dibenzo crown-5 towards the sodium cation was observed. The enhancement of the interaction behaviour of these macrocycles towards targeted guests can be achieved by controlling the size of the macrocyclic hole or by introducing other donor atoms like sulphur or nitrogen to generate crown ethers which have affinity to interact strongly and selectively with the targeted guest (Fig. 1.4).

Pederson *et al*⁷⁹ reported the synthesis of crown thio-ethers and demonstrated that the binding affinity of these receptors was raised towards the silver cation but decreased towards the potassium cation which means that the introduction of a soft donor atom such as sulphur makes them selective for soft metal cations such as silver.

Thermodynamic studies by Izzat *et al*⁸⁰ related to thio-crown ethers revealed that complexation processes between thio-crown ethers with silver and mercury cations are enthalpically driven. This means that the energy required to drive the complexation process are provided as a heat (exothermic) from the interaction of the reactants leading to produce the most favourable stable state of the targeted complex. Also, significant contribution by the sulfur moiety in the complexation process was detected.

Table 1.2 Stability constants expressed as $\log K_s$ and derived standard Gibbs energies ($\Delta_c G^\circ$), enthalpies ($\Delta_c H^\circ$), and entropies ($\Delta_c S^\circ$) of complexation of crown ethers (12-crown-4 (12-C-4) and 1-Benzyl-1-aza-12-crown-4 (1-BA-12-C4)) and lithium (using salts containing different anions) in acetonitrile (MeCN) and in propylene carbonate at 298.15 K

In MeCN

Electrolyte	Receptor	$\log K_s$	$\Delta_c G^\circ/\text{kJ mol}^{-1}$	$\Delta_c H^\circ/\text{kJ mol}^{-1}$	$\Delta_c S^\circ/\text{Jmol}^{-1}\text{K}^{-1}$
$\text{Li}^+\text{AsF}_6^-$	12-C-4	3.23	- 18.4	- 22.78	- 14.7
Li^+BF_4^-	12-C-4	3.46	- 19.8	- 21.66	- 6.20
$\text{Li}^+\text{CF}_3\text{SO}_3^-$	12-C-4	3.52	- 20.1	- 21.35	- 4.60
$\text{Li}^+\text{ClO}_4^-$	12-C-4	3.31	- 18.9	- 21.87	10.0
$\text{Li}^+\text{AsF}_6^-$	1-A-12-C4	4.23	- 24.2	- 18.84	18.0
Li^+BF_4^-	1-A-12-C4	4.24	- 24.2	- 19.91	14.4
$\text{Li}^+\text{CF}_3\text{SO}_3^-$	1-A-12-C4	4.23	- 24.2	- 18.69	18.5
$\text{Li}^+\text{AsF}_6^-$	1-BA-12-C4	4.25	- 24.3	- 27.14	- 9.50
Li^+BF_4^-	1-BA-12-C4	4.30	- 24.6	- 27.54	- 9.90
$\text{Li}^+\text{CF}_3\text{SO}_3^-$	1-BA-12-C4	4.31	- 24.6	- 27.44	- 9.30
$\text{Li}^+\text{ClO}_4^-$	1-BA-12-C4	4.31	- 24.6	- 28.50	- 13.1
Propylene Carbonate					
$\text{Li}^+\text{AsF}_6^-$	12-C4	2.81	- 16.0	-15.9	- 5.70
Li^+BF_4^-	12-C4	2.79	- 15.9	-17.71	- 6.10
$\text{Li}^+\text{CF}_3\text{SO}_3^-$	12-C4	2.84	- 16.2	-17.05	- 2.80
$\text{Li}^+\text{ClO}_4^-$	12-C4	2.81	- 21.0	-15.29	2.40
$\text{Li}^+\text{AsF}_6^-$	1A-12-C4	3.67	-21.1	-14.78	20.9
Li^+BF_4^-	1A-12-C4	3.69	-22.1	-14.63	21.7
$\text{Li}^+\text{CF}_3\text{SO}_3^-$	1A-12-C4	3.87	-23.3	-15.08	23.5
$\text{Li}^+\text{AsF}_6^-$	1-BA-12-C4	4.08	-25.1	-24.59	- 4.30
Li^+BF_4^-	1-BA-12-C4	4.39	-25.1	-24.98	0.40
$\text{Li}^+\text{CF}_3\text{SO}_3^-$	1-BA-12-C4	4.59	-26.2	-24.70	5.00
$\text{Li}^+\text{ClO}_4^-$	1-BA-12-C4	4.32	-24.7	-23.30	4.70

Crown ethers have been mainly used as receptors to complex with metal cations. However Cram and coworkers⁸² have reported the complexation of 27-crown-9 with organic cations such as *tert*-butyl ammonium, guanidinium and arenediazonium salt and demonstrated that the complexation process was governed by hydrogen bond formation (Fig. 1.6)

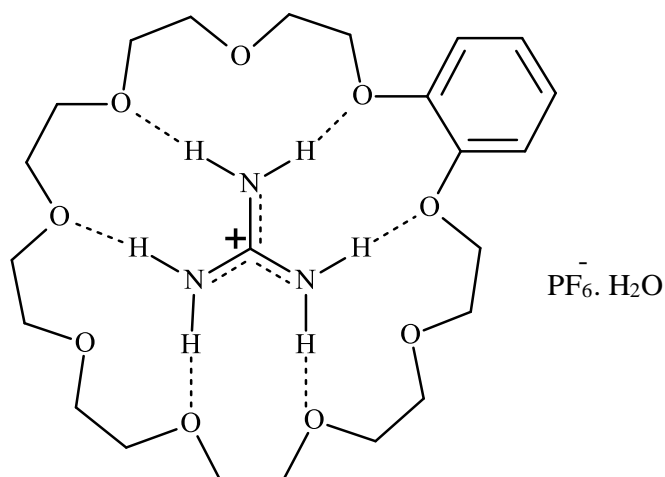


Fig. 1.6 Complexation reaction of guanidinium ion by 27-crown-9

Reinhoudt and co-workers⁸³ have carried out thermodynamic studies on the complexation of 18-crown-6 with nitromethane, acetonitrile and malonitrile as neutral guests by using ¹H NMR in deuterated benzene and concluded that 18-crown-6 hosted these guests in solution with stoichiometric ratios of 1: 1 and 1: 2 [receptor: guest].

Daniil de Namor and co-workers⁸⁴ have reported interesting solution thermodynamic studies of complexation processes involving 18-crown-6 with different types of amino acids in methanol and demonstrated that 18-crown-6 is complexed with these amino acids and the complexation was enthalpically driven and controlled by hydrogen bond formation and electrostatic interactions. The stability constants expressed as log K_s, standard Gibbs energies Δ_cG°, enthalpies Δ_cH° and entropies Δ_cS° are given in Table 1. 3

Table 1. 3 Thermodynamic parameters of complexation of amino acids with 18-crown-6 in methanol at 298.15 K

Amino acid	Log K_s	$\Delta_c G^\circ / \text{kJ mol}^{-1}$	$\Delta_c H^\circ / \text{kJ mol}^{-1}$	$\Delta_c S^\circ / \text{J mol}^{-1}\text{K}$
DL-Alanine	3.59	- 20.49	- 45.94	- 85.4
DL-Arginine	3.42	- 19.52	- 40.11	- 69.1
DL-Asparagine	3.14	- 17.92	- 40.24	- 74.9
DL-Aspartic acid	2.99	- 17.07	- 38.55	- 72.0
DL-Cysteine	3.28	- 18.72	- 30.67	- 40.1
DL-Glutamic acid	3.34	- 19.07	- 35.78	- 56.0
Glycine	3.98	- 22.72	- 53.83	- 104.3
DL-Histidine	3.03	- 17.29	- 39.26	- 73.7
DL-Isoleucine	3.17	- 18.10	- 36.42	- 61.4
DL-Leucine	3.35	- 19.12	- 42.47	- 78.7
DL-Methionine	3.66	- 20.89	- 37.85	- 56.9
DL-Phenylalanine	3.15	- 17.98	- 39.38	- 71.7
DL-Proline	2.6	- 15.07	- 11.38	12.4
DL-Serotonin	3.37	- 19.24	- 38.80	- 65.6
DL-Thyronine	3.02	- 17.24	- 35.36	- 60.8
DL-Tryptophan	3.06	- 17.74	- 41.36	- 81.0
DL-Tyrosine	2.93	- 16.72	- 45.39	- 96.0
DL-Valine	3.19	- 18.72	- 34.49	- 54.6

Recently various crown ethers with different functional groups have been synthesised to enhance the complexation properties of these macrocyclic receptors⁸⁵⁻⁸⁷. Müllen and co-workers⁸⁵ have synthesised benzo-21-crown-7 including dibenzocoronene tetracarboxdiimide chromophore (Fig. 1.7) and the receptor has shown selectivity towards lead and potassium cations in acetonitrile.

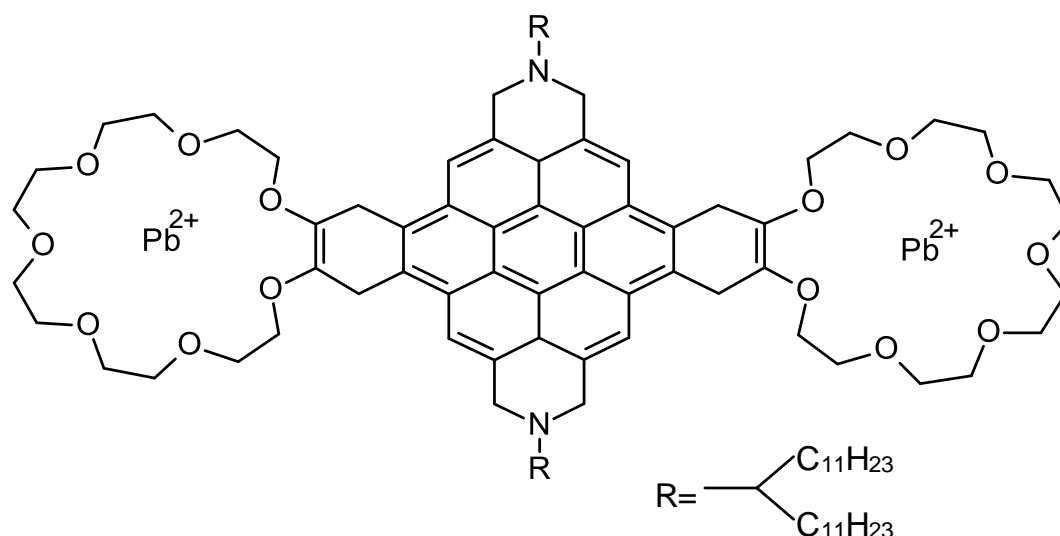
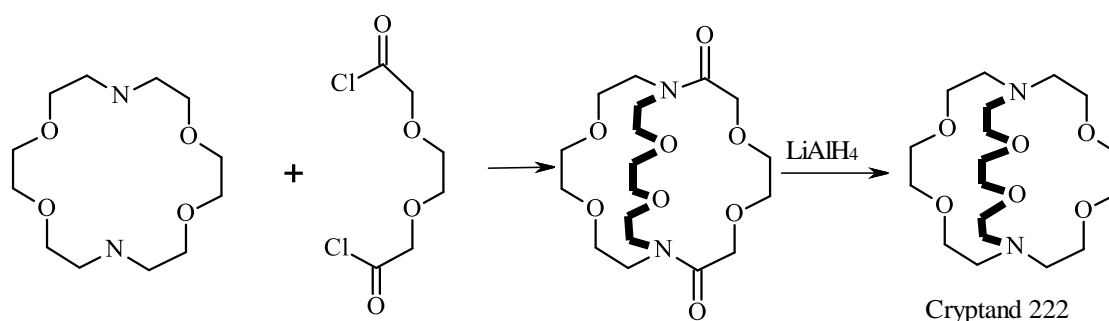


Fig. 1.7 The structure of the receptor synthesised by Müllen and coworkers⁷⁵.

J-M. Lehn^{8,9} and co-workers have reported the first synthesis of macrocyclic receptors known as “**cryptands**” described as more rigid and selective for alkali metal cations than crown ethers. These receptors contain a three dimensional cavity with mixed donor atoms such as oxygen and nitrogen in their molecular structure (Scheme 1.1). The authors concluded that the direction of the nitrogen atom to the interior of the cavity may facilitate the complexation with cations. Also complexation with anions occurs when these macrocycles receptors are protonated⁸⁸. The supermolecular structure of the complex resulting from the interaction between cryptand with the metal cation described initially by Lehn as “**cryptate**” but the term was extended to include all the cationic or anionic species imprisoned in the cage- like structure of this receptor



Scheme 1.1 Synthetic pathway of cryptands 222

Daniil de Namor and co-workers^{22,89} have extensively reported thermodynamic studies of the complexation of cryptand 222 with silver and alkali metal cations in a variety of solvents. These authors concluded that the cations are fully desolvated after complexation by showing a linear relationship between the complexation of cryptand 222 and univalent cations in dipolar aprotic

solvents and the solvation of these cations in these solvents in terms of Gibbs energies, enthalpies and entropies. Recently Sui and co-workers⁹⁰ have reported the synthesis of a tri-aza-cryptand modified by boron-dipyrromethene fluorophore and they concluded that the receptor has a high binding affinity towards potassium over other metal cations. The efficiency of the receptor to complex with the potassium cation was studied by following the variation in the fluorescence emission spectrum of the receptor as a result of the addition of potassium to the receptor solution in acetonitrile (Fig. 1.8)

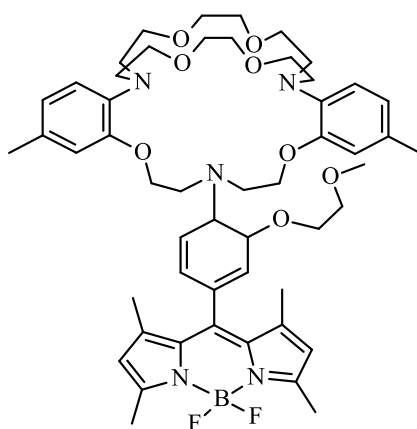


Fig. 1.8 Chemical structure of the tri-aza-cryptand receptor containing a fluorophore

Other interesting receptors are those synthesised by Cram⁹¹⁻⁹³ known as “**spherands**” (Fig. 1.9). These are pre-organised macrocycles with rigid cavities which can interact strongly with lithium but to a lesser extent with sodium. Due to their rigidity, these must be pre-organised for complexation during the synthesis. The host-guest complexes resulting from the complexation of spherands with guests are called “**spheraplex**”.

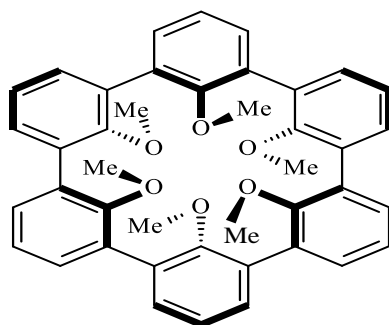
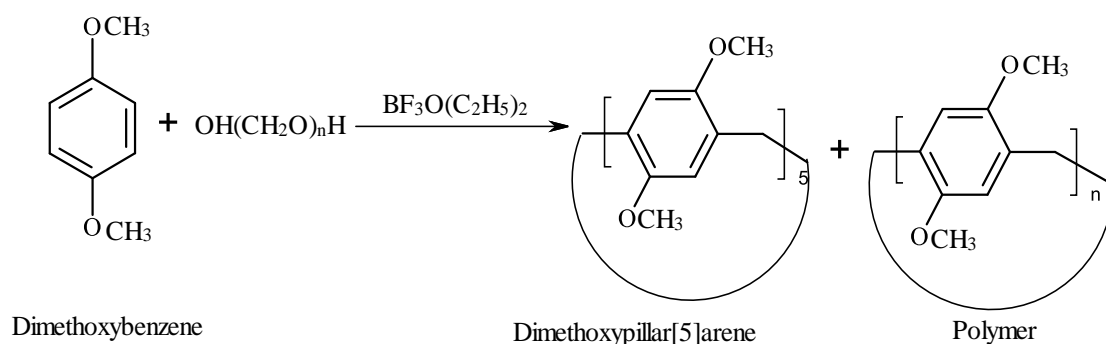


Fig. 1.9 Chemical structure of the spherands

Ogoshi *et al*⁹⁴ have reported in 2008 the synthesis and classification of a new class of macrocycles called “pillarenes”. These were obtained by the Lewis acid catalysed condensation reaction of 1,4-dimethoxybenzene with paraformaldehyde and consist of hydroquinone units connected together by methylene bridges at the 2 and 5 positions (Scheme 1.2). Pillarenes macrocycles have become very attractive due to their ease of preparation and modification, are rigid with a π -rich cavity and superior host-guest complexing properties. This type of macrocycles have been synthesised with different shapes, different functional groups with attractive chelating behavior. The deprotection of alkoxy groups and the introduction of hydroxyl groups enabled the macrocyclic structure to have ten reactive hydroxyl groups which can be modified by the introduction of different functional groups. Therefore this modification has led to the production of receptors with a large number of active sites which enhance the selectivity towards guests⁹⁵⁻⁹⁹.

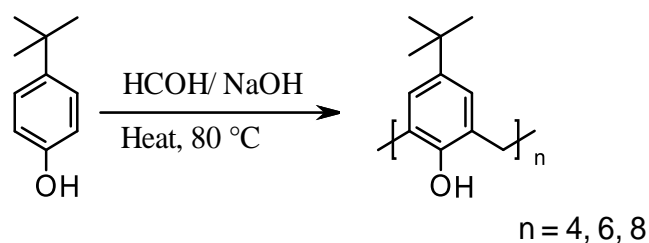


Scheme 1.2 Synthetic pathway of pillar[5]arene receptor

Given that the research carried out in this thesis involves the use of calix[4]arenes, calix[4]pyrrole, resorcin[4]arene and pyrogallol[4]arene derivatives, an account on the two former receptors is now described.

1.4 Calix[4]arenes

These belong to a class of macrocyclic receptors containing repeating phenolic units linked together by methylene bridges with rigid cone-like structures that can hold ionic and neutral species in their cavities. Calix[n]arenes were synthesised by Zinke in 1940 from the condensation of *p-tert*-butyl phenol with formaldehyde in basic medium (Scheme 1.3)



p-tert-butyl phenol

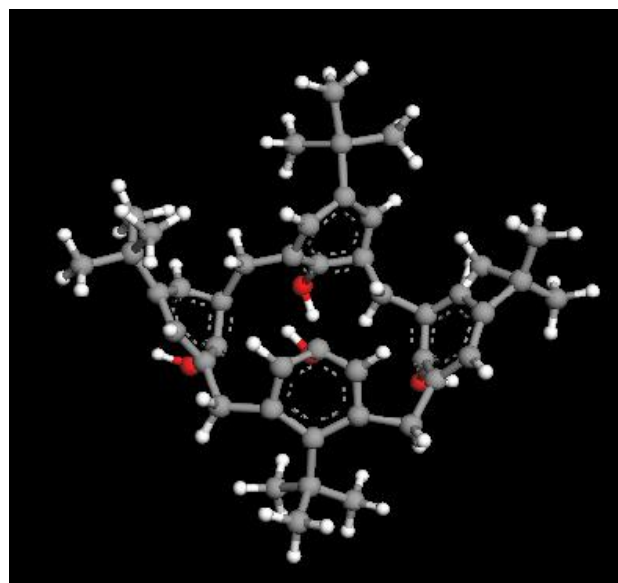
p-tert-butyl calix[n]arene ($n=4, 6, 8$)

Scheme 1.3 Synthesis of *p*-tert-butylcalix[4]arene.

The term calix[n]arene was given by Gutsche in 1987 to macrocyclic compounds which have a cup body structure similar to the Greek vase known as calyx crater (Fig. 1.10); calix means cup-like structure, crater is applicable due to the cavity arising from the connectivity between phenyl (arene) rings included in the structure and n between two brackets indicates the number of phenol groups in the macrocyclic structure¹⁰⁰⁻¹⁰⁶.



(a)



(b)

Fig. 1.10 Images of (a) Greek Calyx Crater and (b) molecular modelling of *p*-tert-butyl calix[4]arene showing the similarity between the Greek vase and the calix[4]arene.

The ¹H NMR technique has been used to characterise and to recognise *p*-tert-butylcalix[4]arene from *p*-tert-butylcalix[6]arene and *p*-tert-butylcalix[8]arene. For *p*-tert-butylcalix[4]arene, there were five different resonances in the ¹H NMR spectrum at room temperature as noticed for the first time by

Kammerer and co-workers¹⁰⁷. The resonance of the hydroxyl, aryl and *tert*-butyl protons are observed as singlets whereas the resonances of the methylene bridge protons are observed as a pair of doublets (Fig. 1.11). Ungaro and co-workers¹⁰⁸ have identified these two doublets for the methylene bridge protons and demonstrated precisely that the higher field doublet resonance corresponds to the equatorial protons (close to the aryl group) and the downfield doublet arises from the axial protons (close to the hydroxyl groups). Gutsche and co-workers¹⁰⁹ have revealed that the ¹H NMR spectrum for the methylene bridge protons of *p-tert*-butylcalix[4]arene in a nonpolar solvents like CDCl₃ and bromobenzene-*d*₅ are in a similar pattern with *p-tert*-butylcalix[8]arene and were observed as a pair of doublets but there were no doublet resonance noticed for the *p-tert*-butylcalix[6]arene which showed only a singlet at room temperature. The distinction between the *p-tert*-butylcalix[4]arene and *p-tert*-butylcalix[8]arene was illustrated by using pyridine-*d*₅ as solvent, *p-tert*-butylcalix[4]arene is able to maintain its occurrence as a pair of doublets even at 0 °C whereas only one singlet peak was observed for the *p-tert*-butylcalix[8]arene even at -90 °C.

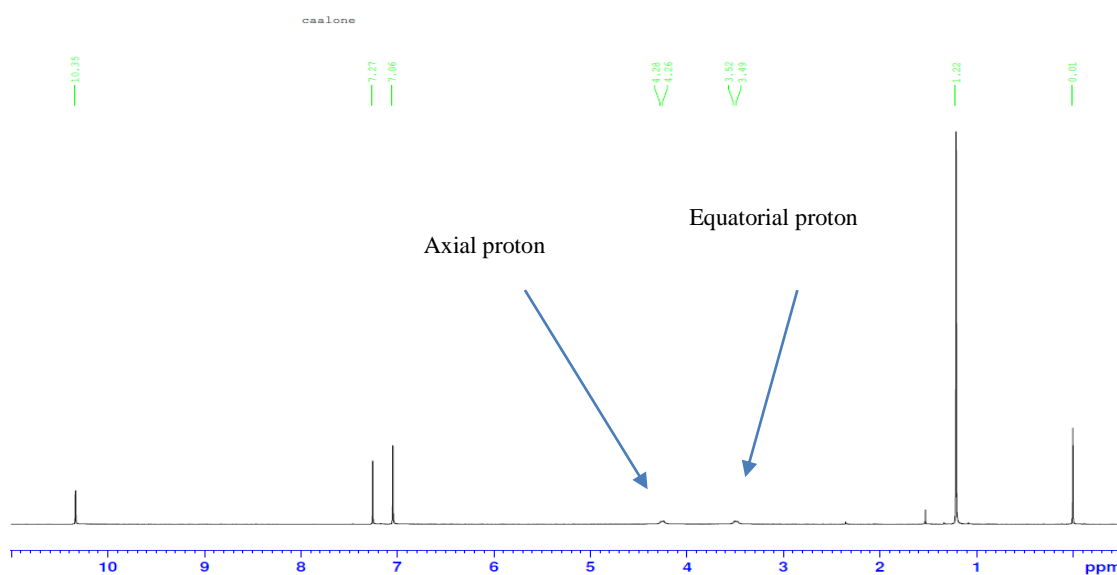


Fig. 1.11 ¹H NMR spectrum for *p-tert*-butylcalix[4]arene in CDCl₃ at 298 K (this work)

1.4.1 Properties and conformations of *p-tert*-butylcalix[4]arene

Due to the presence of intramolecular hydrogen bonding between the four phenolic hydroxyl groups the structure of calix[4]arene is described as rigid with two cavities (Fig. 1.12) which are the upper hydrophobic cavity found between the aromatic rings which is considered as a container for

electron deficient species and the lower hydrophilic cavity or semi-cavity which is formed through the substitution of the phenolic hydrogens by different functional groups^{109,110}.

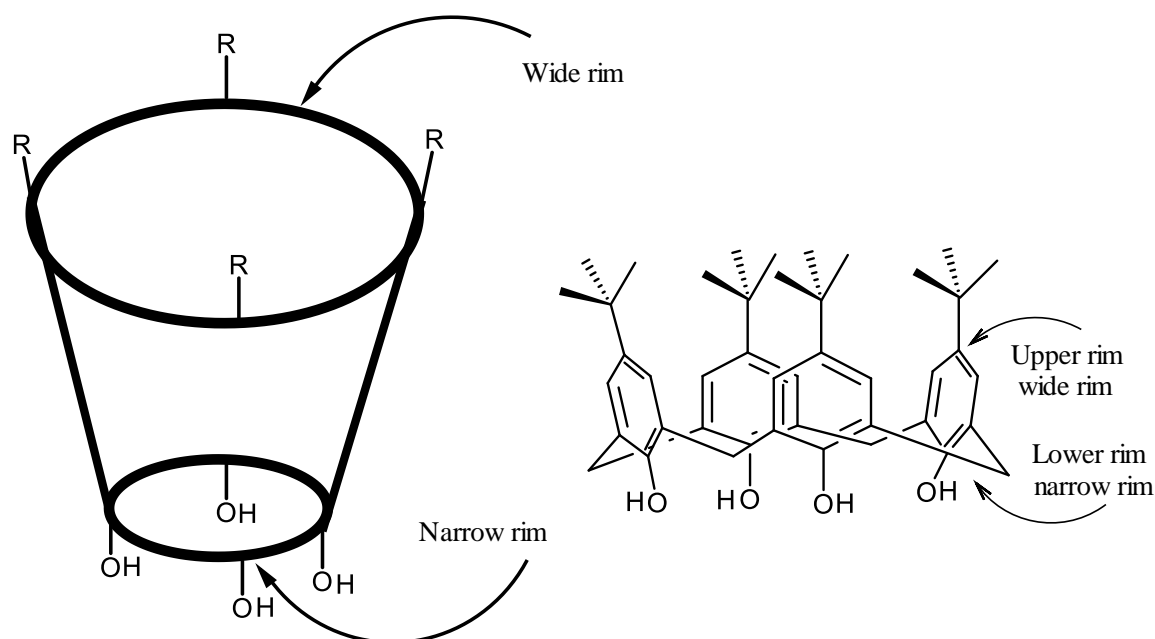


Fig. 1.12 The upper and lower rim of *p-tert*-butylcalix[4]arene

Due to the presence of four separated phenol rings by methylene bridges, these rings are flexible to rotate *via* the methylene bridges leading the calix[4]arene to adopt four different conformations recognised first by Cornforth¹¹¹ and later coined by Gutsche as *cone*, *partial cone*, *1,2-alternate* and *1,3-alternate* conformations resulting from different orientations of the phenolic rings in the space. In a “*cone*” conformation all phenol rings are oriented in one direction (up or down) (Fig. 1.13(a)) and this is considered the more favourable conformation due to the formation of intramolecular hydrogen bonds between the hydroxyl groups. In a partial ‘*cone*’ conformation three of the phenol rings are oriented in the same direction (up or down) except one ring which is oriented in the opposite direction (Fig. 1.13 (b)), The *1,2-alternate* conformation contains two adjacent phenolic rings oriented in the same direction while the others are oriented in the opposite direction (Fig. 1.13 (c)). The *1, 3-alternate* conformation involves phenol neighbouring rings in the opposite direction up or down (Fig. 1.13 (d)). The parent *p-tert*-butylcalix[4]arene adopts a “*cone*” conformation in solution and in the solid state and the inter-conversion between these conformers can take place because of the possibility for the phenolic groups to rotate *via* the methylene bridges¹⁰⁵.

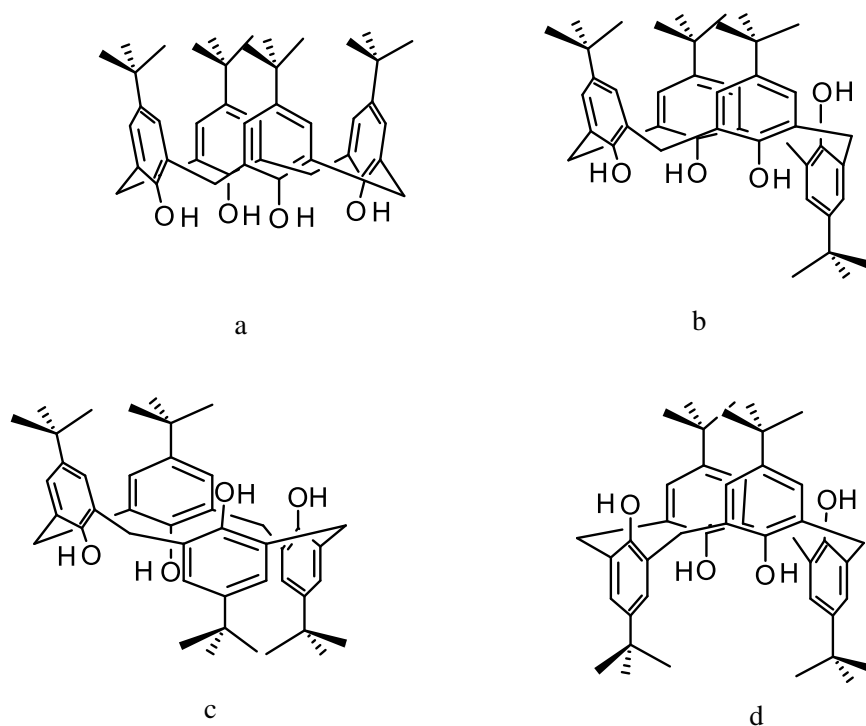


Fig. 1.13 Possible conformations of *p*-*tert*-butylcalix[4]arene: (a) *Cone*, (b) *Partial cone*, (c) *1,2-alternate*, (d) *1,3-alternate*.

^1H and ^{13}C NMR spectra are used to distinguish between these stereoisomers especially ^1H and ^{13}C NMR patterns for the bridging methylene groups which are different for three out of four conformations. In a “*cone*” conformation the methylene bridge protons appear as a pair of doublets. The *1, 2-alternate* conformation and the “*partial cone*” have similar patterns and appear as a pair of doublets and one singlet, it can be recognised in the aromatic part of the spectrum whereas a *1, 3-alternate* conformation appears as one singlet¹¹⁰. The ^{13}C NMR spectrum for the bridge methylene carbon have been used by De Mendoza and co-workers¹¹² to identify the possible conformations adopted by *p*-*tert*-butylcalix[4]arene and they demonstrated that the resonance near $\delta = 31$ ppm is related to the bridge methylene carbon when the connected phenyl groups are in the “*syn*” direction (both phenyl groups up or both phenyl groups down) and near $\delta = 37$ ppm when they are in opposite orientation (Fig. 1.14)

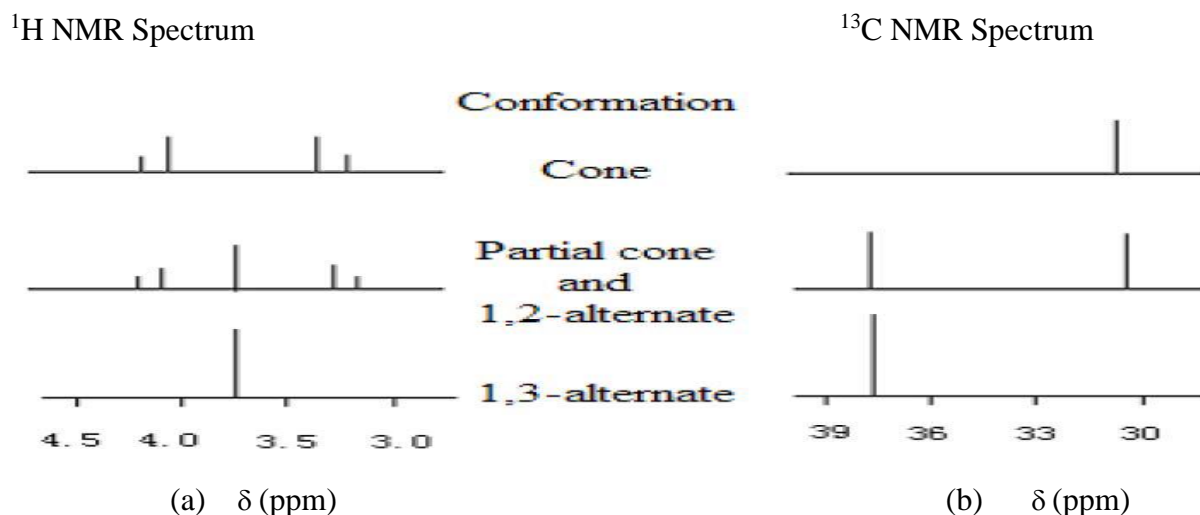


Fig. 1.14 Patterns of signals expected in the (a) ^1H NMR and (b) ^{13}C NMR spectra of the four conformational isomers of calix[4]arene¹¹⁰

1.4.2 Lower Rim Functionalisation of calix[4]arenes

There is a diverse number of calix[4]arene derivatives due to the flexibility of the upper (*p-tert-butyl*) and lower rim (phenolic hydroxyl groups) to be functionalised by different functional groups. This modification with additional functional groups increases the binding ability of parent calix[*n*]arenes to form complexes with cations, anions and neutral species. There are a variety of functionalised calix[4]arenes which have been synthesised either by functionalisation of the phenolic rim or the upper rim. As far as functionalisation of the lower rim is concerned, alkylation of the phenolic groups is one of the easiest reactions which can occur at the lower rim. This involves functional groups such as esters, ketones, amines and amides which can be introduced into the phenolic hydrogens of calixarenes¹¹³⁻¹¹⁹.

McKervey *et al*¹¹³ have carried out the synthesis of functionalised *p-tert-butyl-calix*[*n*]arene [*n*=4, 5, 6] by ester groups and they reported the complexation processes of these receptors with alkali metal cations in non-aqueous media. These authors concluded that *p-tert-butylcalix*[4]arene containing ester groups showed high selectivity towards the sodium cation over other metal cations. It was aimed that the “cone” conformation of the receptor and the presence of *tert-butyl* group at the upper rim drive the ester group at the lower rim to form a cavity for coordination. Also, it was emphasised that the complexation of *p-tert-butylcalix*[6]arene was less towards sodium and have shown selectivity towards the potassium ion which means that the formation of a larger cavity leads to alter the ability of the receptor to interact with larger cations¹¹³⁻¹¹⁶. Arnaud-Neu *et al*¹¹⁴ have reported the synthesis of a series of new receptors containing esters and ketones functionalities at the

lower rim of *p-tert*-butyl-calix[n]arenes [n=4, 5, 6] and found that these derivatives exhibited affinity to interact with alkali metal cations. The effect of the cavity size on the complexation process was demonstrated.

Danil de Namor and co-workers^{117,118} have carried out novel studies about the synthesis and characterisation of lower rim calix[4]arene derivatives (Fig. 1.15 a and b) and the effect of these functional groups on cation and anion complexation processes. This was carefully followed by the change in the electrical behaviour of ionic solutions as a result of complexation using conductometric and potentiometric titrations. In fact they reported the effect of ester and ketone hydrophilic groups on the complexation behaviour of these functionalised receptors towards alkali, alkaline earth-metal, transition and heavy metal cations and they found that the calix[4]arene functionalised by ketone groups in acetonitrile was more selective for these cations than the ester derivatives especially towards Ca^{2+} ($\log K_s = 12.16$, Table 1.4)

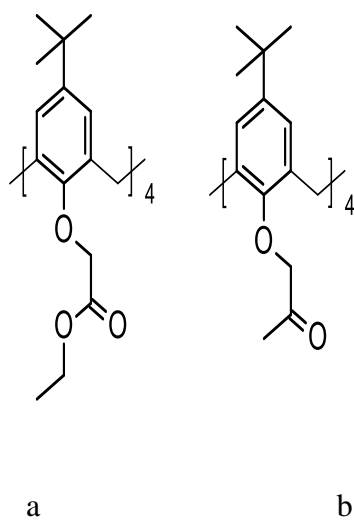


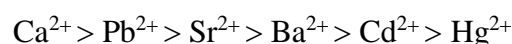
Fig. 1.15 Lower rim functionalised *p-tert*-butylcalix[4]arene with (a) ester and (b) ketone groups

Table 1.4 Thermodynamic parameters for the complexation of (a) *p-tert*-butylcalix[4]arene tetraester and (b) *p-tert*-butylcalix[4]arene ketone with bivalent cations in acetonitrile using different techniques obtained by Danil de Namor and co-workers¹¹⁷

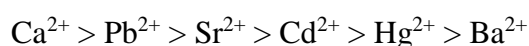
Receptor (a)	log K _s	ΔcG° (kJ mol ⁻¹)	ΔcH° (kJ mol ⁻¹)	ΔcS° (JK ⁻¹ mol ⁻¹)
Ca ²⁺	8.15 ^b	-46.23	-53.8 ^a	-25
Sr ²⁺	5.35 ^a	-30.48	-37.6 ^a	-24
Ba ²⁺	4.34 ^a	-24.80	-29.6 ^a	-16
Pb ²⁺	7.39 ^a	-42.18	-59.7 ^a	-59
Cd ²⁺	4.08 ^c	-23.29	-22.4 ^c	3
Hg ²⁺	3.69 ^c	-21.01	-21.1 ^c	-0.3
Receptor (b)	log K _s	ΔcG° (kJ mol ⁻¹)	ΔcH° (kJ mol ⁻¹)	ΔcS° (J K ⁻¹ mol ⁻¹)
Mg ²⁺	3.33 ^c	-19.01	48.1 ^c	225
Ca ²⁺	12.16 ^b	-69.41	-65.3 ^b	14
Sr ²⁺	7.90 ^d	-45.10	-49.8 ^d	-16
Ba ²⁺	5.14 ^a	-29.34	-36.9 ^a	-25
Pb ²⁺	9.30 ^b	-53.09	-62.7 ^a	-32
Cd ²⁺	6.60 ^c	-37.67	-22.7 ^c	50
Hg ²⁺	5.90 ^d	-33.68	-32.3 ^d	5

(a) Direct calorimetry, (b) competitive macrocalorimetry, (c) direct microcalorimetry, (d) competitive microcalorimetry titrations

Stability constant values shown in Table 1.3 indicate that the selectivity of the ester derivative followed the sequence,



While the ketone derivative showed different trend and followed the sequence



Considerable enhancement in the binding affinity towards alkali-metal cations were noticed when tetra-diethylamide functionalities were introduced in the lower rim of *p-tert*-butylcalix[4]arene (Fig. 1.16) and have exhibited strong affinity to complex with alkali metal cations especially with sodium and potassium cations. The X-ray crystal structure indicated that the cation is properly accommodated in the polar cavity while a “cone” conformation is adopted by the receptor. Also, the receptor has affinity to complex with alkaline-earth metal cations and the highest affinity was found for calcium over other alkaline-earth metal cations. The addition of the amide functionality leads to increasing the basicity of the receptor and has made it more basic than ester and ketone derivatives¹¹⁹.

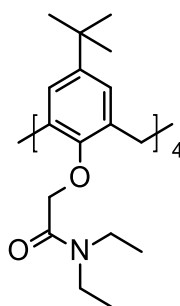


Fig. 1.16 Chemical structure of 5, 11, 17, 23-tetra-*tert*-butyl-25, 26, 27, 28-tetrakis(N, N-diethylaminocarbonyl) methoxy calix[4]arene

The functionalisation of the calix[4]arene with phosphine oxide at the lower rim (Fig. 1.17) has led to increase the affinity of the receptor to bind with lanthanide metal cations and this modification was used to remove radioactive elements such as europium, Eu (III), thorium, Th (IV), plutonium, Pu (IV) and americium, Am (IV) from nuclear waste¹²⁰

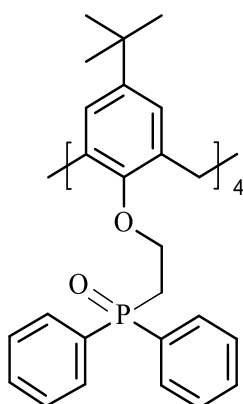


Fig. 1.17 Chemical structure of *p-tert*-calix[4]arene functionalised with phosphine oxide

Calixarine derivatives containing mixed functionalities like amide-bipyridine or amide phenantroline (Fig. 1.18) have also shown affinity to interact with lanthanide cations¹¹⁹.

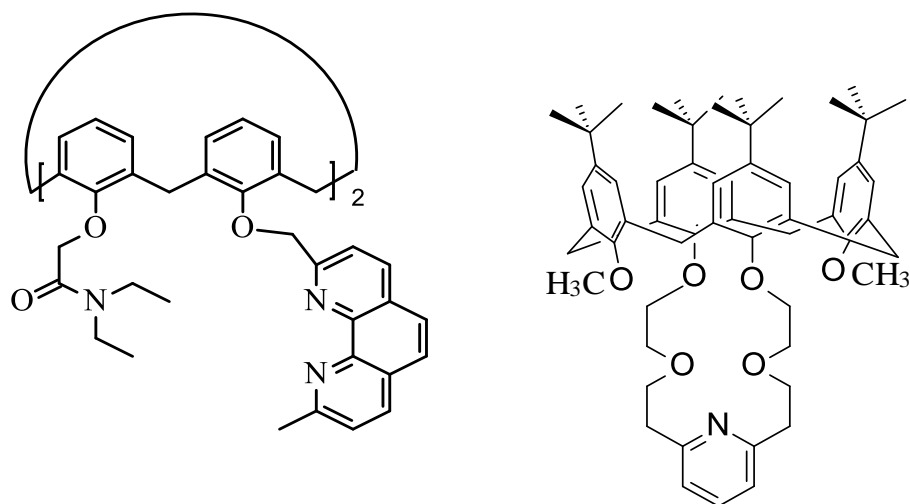
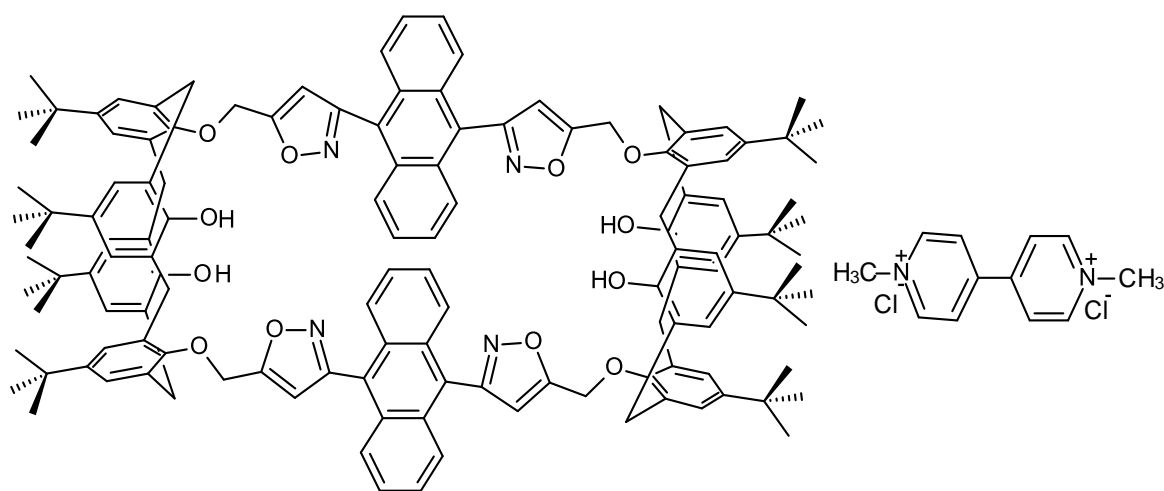


Fig. 1.18 Chemical structure of receptors used for the complexation of lanthanides cations

It has been demonstrated that bis-calix[4]arene (Fig. 1.19 a) has affinity to bind with methyl viologen (N-N-dimethyl-4,4-bipyridinium dichloride) (Fig. 1.19 b) which is commonly utilised as a herbicide and it is well known for its negative impact to human health and the environment. The complexation process revealed that the herbicide is completely incarcerated in the π -rich rectangular cavity and the complexation process is promoted by cation- π interaction between the positive charge of the hosted herbicide with the π -system zoomed by two parallel anthracenes and the calix[4]arene skeleton. The receptor has the ability to act as a fluorescent chemosensor to this toxic material due to the presence of anthryl group in the receptor skeleton¹²¹.



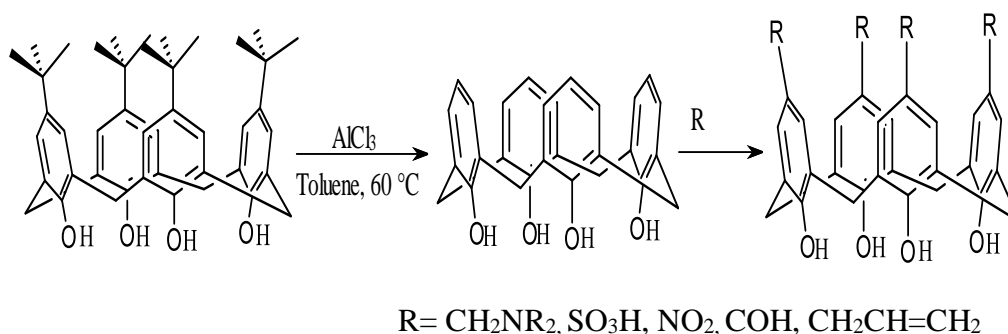
(a)

(b)

Fig. 1.19 Chemical structure of (a) bis-calix[4]arene and (b) methyl viologen

1.4.3 Upper rim functionalisation

As previously stated the upper rim of calixarenes can be functionalised through the removal of the *p*-*tert*-butyl groups which makes the *p*-positions of the phenolic groups as a target for electrophilic substitution reactions^{122,123}.



Scheme 1.4 De-alkylation and upper rim functionalization of *p*-*tert*-butylcalix[4]arene

Rebek¹²⁴ has reported remarkable research on the functionalization of the upper rim of calix[4]arene by urea and found that the functionalised compound tends to form a dimeric capsule facilitated by hydrogen bonding through the urea groups (Fig. 1.20). Thus the substituent works as a linker between two molecules of calix[4]arene. This work has been expanded and exploited by chemists to produce molecular capsules with unique behaviour¹²⁵

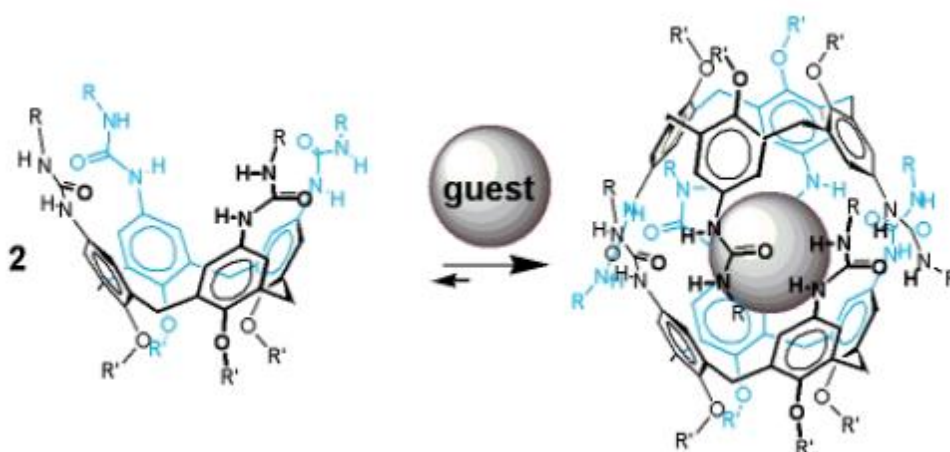


Fig. 1.20 Functionalization of the upper rim of calix[4]arene by urea and the formation of dimeric structure when an appropriate guest is present¹²⁴

Sulfonation of calix[4]arene and calix[5]arene (Fig. 1.21) has led to the formation of non-toxic molecules which were found soluble in aqueous media. As such these findings gained much attention for biological and environmental applications due to their binding properties with different guests and their application as molecular capsules in the solid state governed by guest size^{125,126}

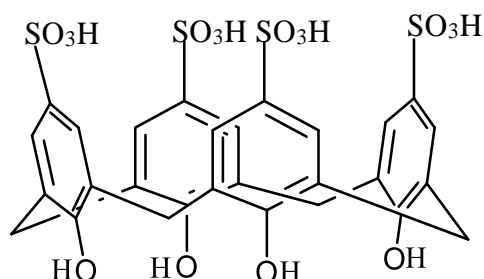


Fig. 1.21 Chemical structure of sulfonated calix[4]arene

Wang *et al*¹²⁶ reported the formation of bis molecular capsules resulting from the complexation of *p*-sulphonatocalix[4] arene (SC4A), *p*-sulphonatocalix[5]arene (SC5A) and *p*-sulphonatocalix[4]arene (STC4A) with 5, 6- dihydropyrazin[1, 2, 3, 4- lmn] [1,10] phenanthroline-4, 7-dium (DP²⁺) in aqueous media at a pH range of 2-3 and they demonstrated that the guest molecule is encapsulated between two molecules of the host and thermodynamically stable complexes were formed stabilised by π - π interaction between the hosted phenanthroline rings with the hydrophobic cavity of calix[n]arene n=4, 5 (Fig. 1.22)

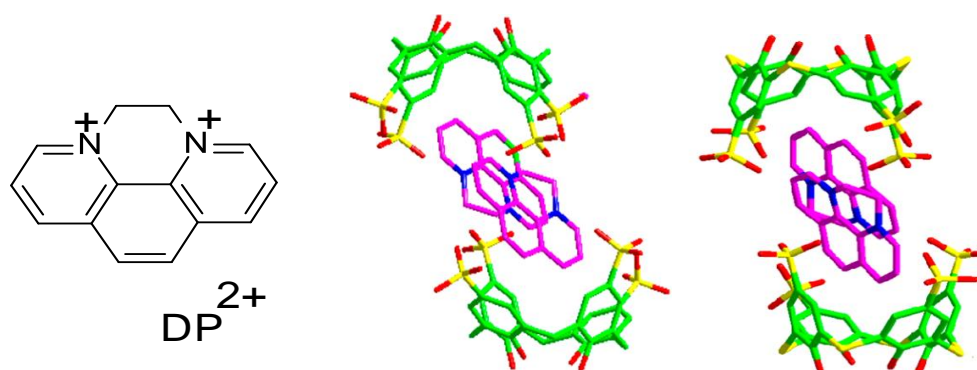


Fig. 1.22 “Bis-Sulfonated” calix[4]arene as a molecular capsule¹²⁶

Water soluble *p*-phosphonic acid calix[4]arene (Fig.1.23) tends to self-assembled in the presence of acetonitrile into a bilayer and a nanorrafts structure is formed driven by multiple hydrogen bonds associated with π stacking and C-H... π bonding¹²⁷.

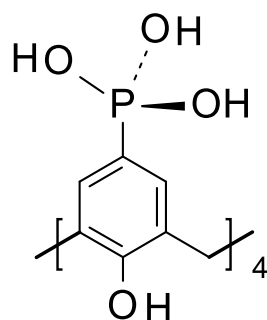


Fig. 1.23 Chemical structure of *p*-phosphonic acid calix[4]arene

Functionalization of both, the lower and the upper rim of calix[4]arene by different functional groups led to enhance their ability towards radioactive elements. Lu *et al*¹²⁸ have used *p*-phosphorylated calix[4]arene to extract thorium from aqueous media (nitrate as counter-ion) and have shown a good selectivity for thorium over other radioactive species (Fig. 1.24)

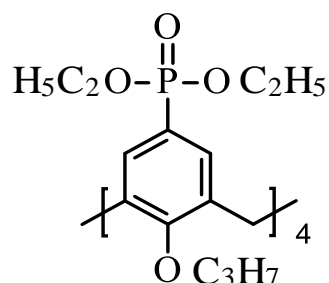


Fig. 1.24 Lower and upper rim functionalized calix[4]arene.

Functionalisation of the upper rim by hydrophilic groups such as sodium sulfonate Na^+SO_3^- and hexyl hydrophobic substituents at the lower rim leads to the formation of amphiphilic macrocycles which can be self-assembled to generate spherical nano vesicles in aqueous solution (Fig. 1.25). This aggregation has gained much attention in the field of nanomedicine due to their application as a chaperone in drug delivery¹²⁹⁻¹³⁰. The drug non-covalently loaded inside the nanocup of the amphiphilic macrocycle generates supramolecular amphiphiles driving the drug directly to targeting the infected cells. The aggregation process is not continuous and the releasing of the drug from the vesicle is induced by a specific enzyme. The usefulness of this approach is to concentrate the drug at the disease site in order to maximise the therapeutic activity by increasing the drug uptake by the cells and also to minimise the metabolic pathway of the drug in order to minimise the undesired side effects which exist by using other technologies. This approach was utilised successfully to drive and localise the cationic anticancer drug at the cancerous tissues¹²⁹.

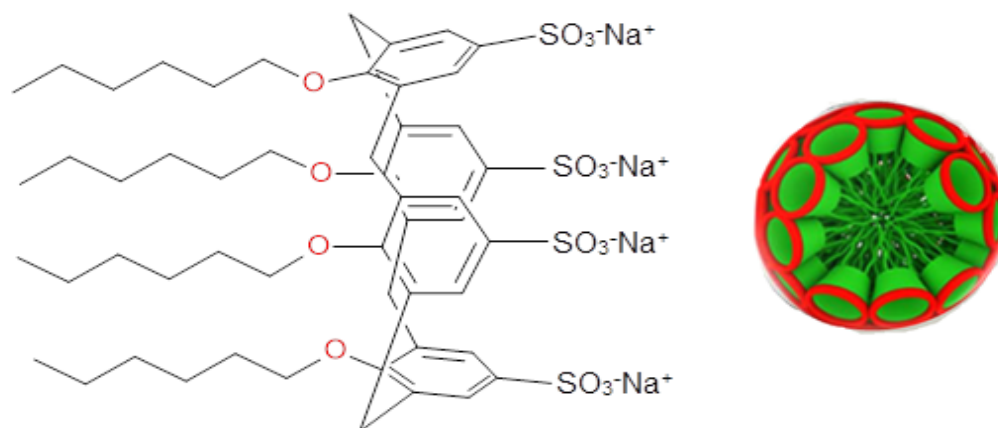
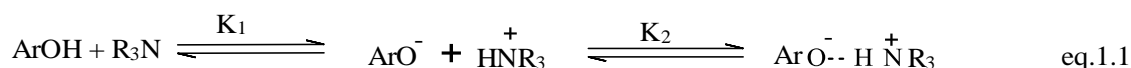


Fig. 1.25 Chemical structure of amphiphilic calix[4]arene and the aggregation to form vesicle¹²⁹

Gutsche *et al*¹³¹ have reported the interaction of *p-tert*-butylcalix[4]arene and *p*-tetraallylcalix[4]arene with *tert*-butyl amine in acetonitrile and they concluded that the complexation process is promoted by a proton transfer reaction from the *p-tert*-butylcalix[4]arene to the amino compound. They suggested that the complexation process occurred in two steps, the first step includes the proton transfer to form ions and the second step includes the association of these ions to form a host-guest complex (eq.1.1)



Gutsche and See¹³² demonstrated that the double-cavity calix[4]arene (Fig. 1.26) has a weak affinity to complex with neutral guests such as phenols, aldehydes, carboxylic acids, pyridines, imidazoles and aliphatic amines and they reported stability constants in the order of 5 to 55.

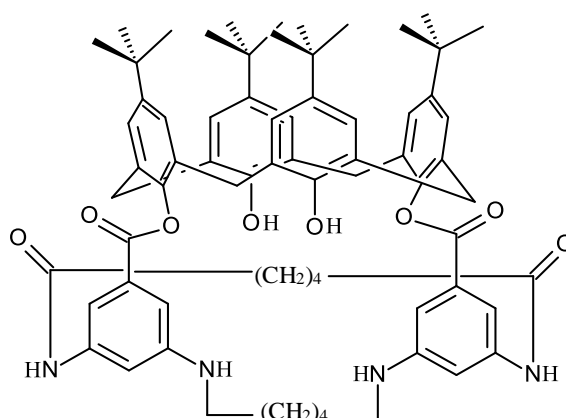


Fig. 1.26 The chemical structure of a double cavity *p-tert*-butylcalix[4]arene

Immobilisation of a functionalised calix[4]arene containing di-substituted dithiocarbamate (Fig. 1.27) on the surface of gold nanoparticles surface led to enhance the colorimetric and quantitative response of the receptor towards the cobalt (II) metal cation over other metal cations. The anchoring process has led to produce a rigid macrocycle compared with the non-immobilized calix[4]arene moiety that has affinity to interact strongly with cobalt (II). The advantage of this process is to induce changes in the physico-chemical properties of the gold nanoparticles which could lead to increase this sensitivity. The changes include red shift in the SPR (surface plasmon resonance) absorption band as a result of complexation with Co^{2+} compared with the free form of the receptor¹³³.

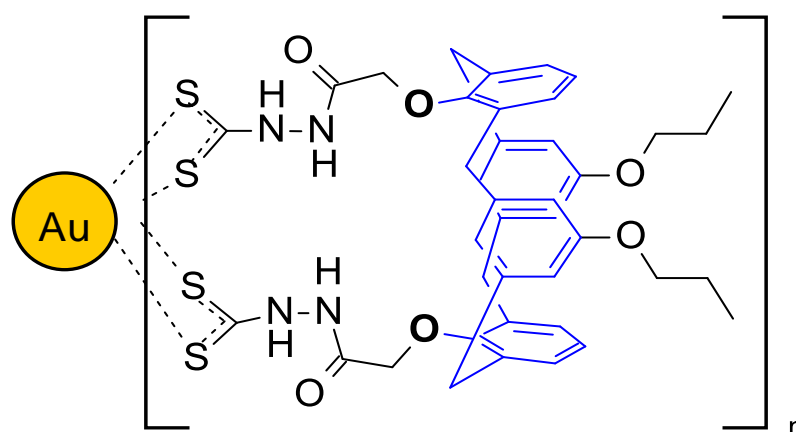


Fig. 1.27 Immobilizing calix[4]arene derivative on the surface of gold nanoparticles

1.4.4 Applications of calixarenes and derivatives

The potential industrial applications of calixarenes have been discussed by Perrin and co-workers¹³⁴ Applications included i) the recovery of high concentrations of caesium from nuclear waste using a calixarene derivative ii) the selective transport of cations using calixarenes, iii) the removal of lanthanides, iv) their use as antioxidants for polymers, iv) separation of organic molecules making use of the hydrophobic cavity of these receptors v) Extracting agents mainly for cations, vi) environmental control and vi) the production of the electronic devices such as calixarene based ion selective electrodes. In addition, new materials have been produced in which calixarenes were anchored to silica through the upper rim, prior removal of the *p-tert butyl* groups so the complexing properties of the functionalised lower rim for cations are not disturbed as a result of this modification.

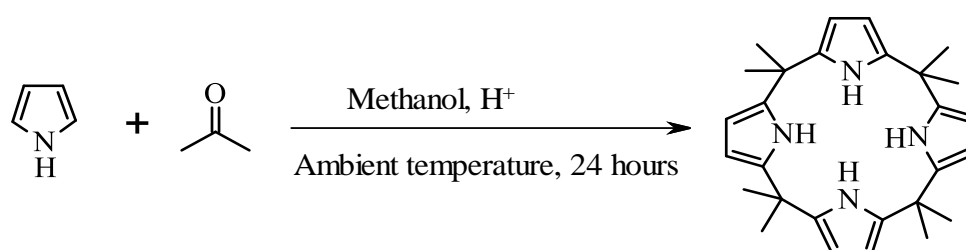
Since then this area of applied research has expanded significantly to an extent that the role of calixarenes in Nanosciences has been the subject of a book (*Calixarenes in the Nanoworld*)¹³⁵

The complexing ability of calixarenes for actinides has been emphasised in several review articles related to the nuclear industry¹³⁶. A recent review by Kiegel and co-workers¹³⁷ contains a comprehensive account on the efficient use of calix[6]arenes for uranium separation processes and their involvement in liquid-liquid extraction, liquid-membrane separation and ion exchange processes. Among them, the advantage of the ion exchange process was highlighted in that the use of environmentally unfriendly organic solvents is eliminated

In recent years the use of unsupported calixarenes and derivatives have been considered as an efficient approach for the removal of pollutants from water due to the lack of solubility of these receptors in aqueous medium and the advantages with respect to liquid-liquid extraction processes which involve the use of non-aqueous solvents particularly chlorinated ones such as dichloromethane. Within this context Toumi and co-workers¹³⁸ used unsupported *p-tert*-butyl calix[4] arene and lower rim functionalised calix[4] arenes for the removal of polluting cations such as Cu(II), Cd(II) and Pb(II) from water with satisfactory results. The recycling of the material, an important issue for commercial applications, was also considered by these authors. This point is addressed here because extraction processes investigated in this thesis make use of unsupported calix[4]arene derivatives.

1.5 Calix[4]pyrrole (CP)

The calix[4]pyrrole, a tetrapyrrolic macrocyclic receptor synthesised over a century ago by Baeyer¹³⁹ from the acidic catalysed condensation reaction of pyrrole with acetone (Scheme 1.5), was given the name of *meso*-octamethyl porphyrinogen. In the last three decades, calix[4]pyrrole has been used as a receptor by Sessler and co-workers^{140,141} for hosting anionic and electron rich neutral moieties through the formation of four intermolecular hydrogen bonding aided by the current effect of the four pyrrole rings.



Scheme 1.5 Synthesis of *meso*-octamethylcalix[4]pyrrole

1.5.1 Calix[4]pyrrole conformations

Due to the presence of four pyrrole rings in the structure of calix[4]pyrrole, separated from each other by methylene bridges, these rings are flexible to rotate *via* the methylene bridges leading to four different conformations (*cone*, *partial cone*, *1,2-alternate* and *1,3-alternate*) for this receptor. The conversion from one conformation into another is very fast. In a *cone* conformation all pyrrole rings are oriented in one direction (up or down) while in a *partial cone* conformation, three pyrrole rings are oriented in the same direction (either up or down) with the remaining one in the opposite direction. As far as the *1,2-alternate* conformation is concerned, two neighbouring pyrrole rings are oriented in the same direction while the remaining two in the opposite direction. The *1,3-alternate* conformation pyrrole rings are up or down in an alternate fashion as shown in Fig. 1.28. The “*cone*” conformation was found to be the less stable due to the electrostatic repulsion between the pyrrole rings¹⁴²⁻¹⁴⁵.

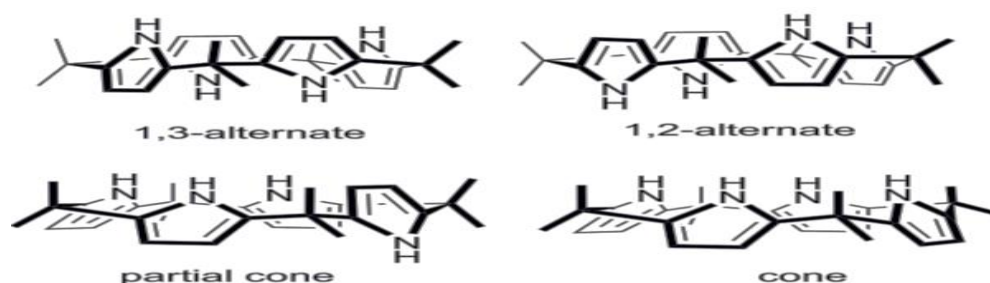


Fig. 1.28 Four different conformations adopted by calix[4]pyrrole¹⁴⁴

Therefore the free calix[4]pyrrole receptor adopts in the solid state and in solution the *1,3-alternate* conformation to minimise the electrostatic repulsion between the pyrrole rings which then re-organised to a “*cone*” conformation upon complexation with the anion through hydrogen bond formation (Fig. 1.29)

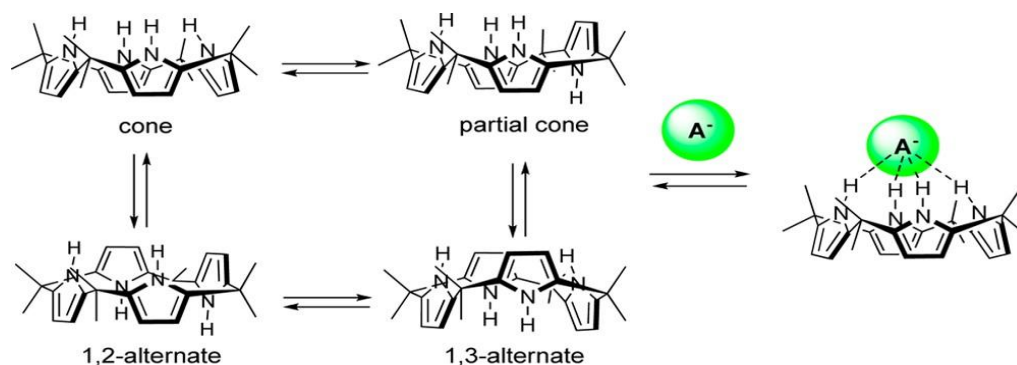


Fig. 1.29 Conformational changes of calix[4]pyrrole to a “*cone*” conformation upon anion complexation ($A^- = F^-, Cl^-, Br^-$)¹⁴¹.

1.5.2 Functionalisation of calix[4]pyrrole

Calix[4]pyrrole derivatives can be obtained by introducing different functional groups in three active positions in order to enhance their chelating behaviour. These positions are the C-rim or β -position, the *meso* position and the N-rim (Fig. 1.30)

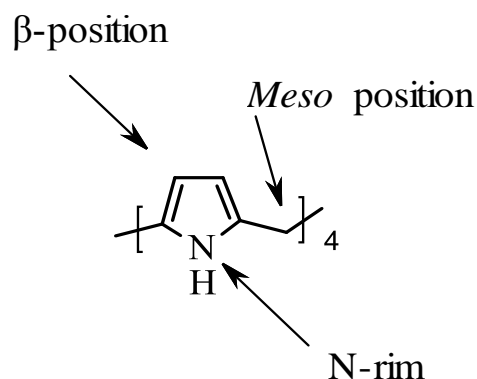


Fig. 1.30 Different active positions for functionalization of calix[4]pyrrole

1.5.2.1 Functionalisation of the C-rim (β -position) of calix[4]pyrrole

In order to study the effect of the substituents at β -position on the chelating behaviour of calix[4]pyrrole, Gale and co-workers¹⁴⁶ reported that the functionalised calix[4]pyrrole at the β -rim can alter the chelating behaviour of this macrocycle towards guests. This modification can be achieved by applying two subsequent strategies; firstly by condensation of 2, 3-disubstituted pyrrole with ketones, and secondly by the introduction of substituents directly into the pre-synthesised calix[4]pyrrole.

By applying the first strategy they reported the synthesis of β -octamethoxy-*meso*-tetra-spiro-cyclohexylcalix[4]pyrrole by the condensation reaction of the 3,4-dimethoxypyrrole with cyclohexanone catalysed by glacial acetic acid.(Fig. 1.31 (a)). The condensation reaction between 3, 4-di-fluoropyrrole-1H- pyrrole with acetone catalysed by methanesulfonic acid has led to the formation of the octamethyl-octafluorocalix[4]pyrrole (Fig. 1.31 (b)) It should be emphasised that this macrocycle showed a higher affinity towards fluoride and chloride anions in solution than the non-fluorinated calix[4]pyrrole due to the formation of stronger hydrogen bonds. It also led to an increasing affinity for neutral guests in the solid state as a result of the higher acidity of N-H groups. Following the second strategy described above, Gale and co-workers¹⁴⁶ have reported the first esterification of *meso*-octamethylcalix[4]pyrrole at the β -position (Fig. 131 (c)) through the electrophilic substitution by ethylbromacetate in the presence of *tert*-butyl lithium as the base. The

product was partially and fully substituted at the β -position. The de-esterification of the compound facilitated the reaction with the solid support. The resulting material was used as an extracting agent for the removal of halides anions from water.

Anzenbacher *et al*¹⁴⁷ have demonstrated that the direct formylation of the pre-synthesised *meso*-octamethylcalix[4] pyrrole by the Vilsmeier reagent led to produce optical sensors for anionic species (Fig. 1.31 (d)) which were further modified by Farinha and co-workers¹⁴⁸ to produce receptors containing the C-N group (Fig. 1.31 (e)). These exhibited a strong affinity to complex with fluoride, chloride and dihydrogen phosphate anions.

According to the second strategy, Gale and co-worker¹⁴⁶ have reported the fully brominated calix[4]pyrrole(Fig. 1.31 (f)) from the reaction of *meso*-octamethylcalix[4] pyrrole with N-bromo-succinimide by using methanol as solvent and methansulfonic acid as catalyst. By doing these modifications these authors concluded that the functionallisation of the β -position by electron withdrawing groups led to increase the strength of the hydrogen bond between the N-H functionality of the pyrrole ring and the targeted guest.

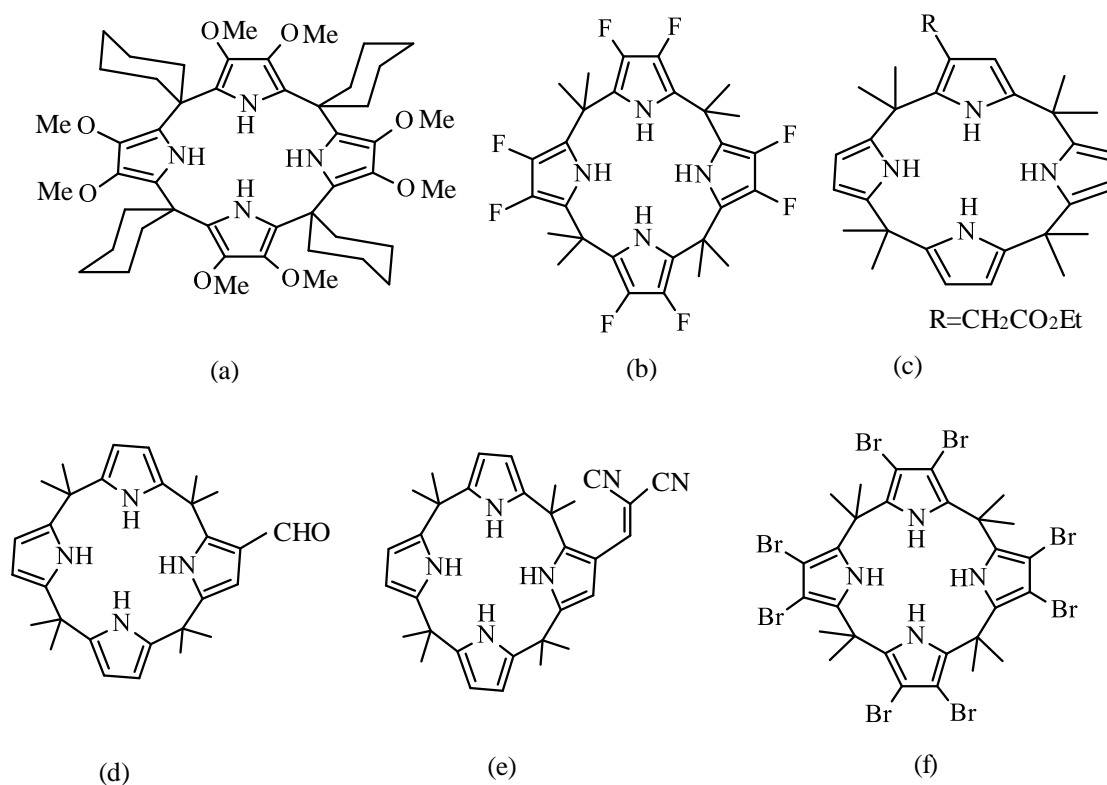
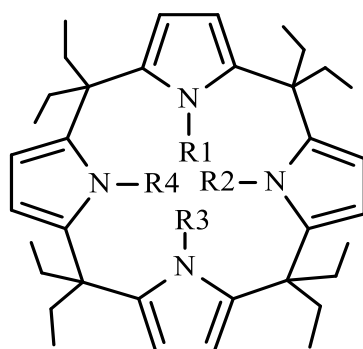


Fig. 1.31 Different products with different substituents at the β -position on the pyrrole rings of calix[4]pyrrole.

1.5.2.2 Functionalisation of the N-rim of calix[4]pyrrole

The functionalization of the N-rim of calix[4]pyrroles has been carried out by Furusho *et al*¹⁴⁹ to introduce alkyl groups to the N-rim of *meso*-octaethylcalix[4]pyrrole by using alkyl iodide in the presence of n-butyllithium as a base. The author has demonstrated that five possible N-methylated and N-monomethylated *meso*-octaethylporphyrinogens were obtained (Fig. 1.32)



$R_1 = \text{Methyl}, R_2 = R_3, R_4 = \text{H}$

$R_1 = R_2 = \text{Methyl}, R_3 = \text{H}, R_4 = \text{H}$

$R_1 = R_3 = \text{Methyl}, R_2 = R_4 = \text{H}$

$R_1 = R_2 = R_3 = \text{Methyl}, R_4 = \text{H}$

$R_1 = R_2 = R_3 = R_4 = \text{Methyl}$

$R_1 = \text{Ethyl}, R_2 = R_3 = R_4 = \text{H}$

Fig. 1.32 Functionalisation of *meso*-octaethylcalix[4]pyrrole through the N-rim

1.5.2.3 Functionalisation of the *meso* position

Woods *et al*¹⁴³ reported the synthesis and complexation studies for an extended calix[4]pyrrole (Fig. 1.33) with halides and hydrogen phosphate anions (as tetrabutylammonium salts) in DMSO and they concluded that the receptor exhibited selectivity towards fluoride over other anions

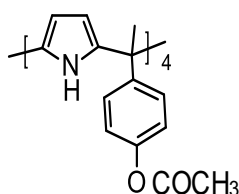


Fig. 1.33 Structure of the receptor synthesised containing acetoxy group at the *meso* position

Danil de Namor and Shehab¹⁵⁰ have carried out complexation of *meso*-octamethylcalix[4]pyrrole with halides and dihydrogen phosphate in acetonitrile and DMF and they demonstrated that the receptor exhibited preferences towards the fluoride over the chloride anion with stoichiometric ratio 1: 1 and the thermodynamic parameters for the complexation was derived from calorimetry.

Thermodynamic studies by Danil de Namor and Shehab³² revealed that the extended calix[4]pyrrole derivative containing a double cavity (Fig. 1.34) has significant effect on the binding properties of the receptor towards halide anions and complexation studies were confirmed by ¹H NMR and conductivity measurements in addition to calorimetric studies to derive the thermodynamic parameters of the complexation process. They identified that the ability of the receptor to complex with the fluoride anion dramatically increases as compared with other halides and dihydrogen phosphate anions

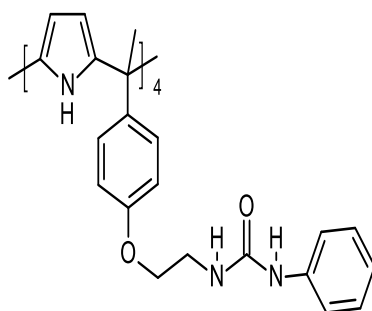


Fig. 1.34 Structure of *meso*-tetramethyl[N-(phenoxyethyl)-N-phenylurea]calix[4]pyrrole

Danil de Namor and co-workers¹⁵¹ reported thermodynamic studies of the interaction of the *meso*-tetramethyl-tetrakis{4-[2-(thio) ethoxy] phenyl}calix[4]pyrrole (Fig. 1.35) as a ditopic receptor with fluoride and mercury ions in acetonitrile. The receptor exhibited affinity to complex with Hg²⁺ and Ag⁺ cations as well as the fluoride anion. The composition of the complexes formed was investigated by conductance measurements. Titration calorimetry was used to calculate the thermodynamic parameters of complexation. They concluded that the addition of sulphur moieties has played an important role in the complexation with the cations whereas the NH interacts with the fluoride anion.

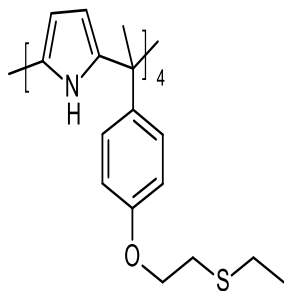


Fig. 1.35 Chemical structure of the calix[4]pyrrole functionalised by groups containing sulphur

Danil de Namor and co-worker¹⁵² reported detailed thermodynamic studies for a new ditopic receptor by modification of the *meso* position (Fig. 1.36) and they found that increasing the depth of the calix[4]pyrrole cavity led to increasing the binding strength towards halide anions especially towards the fluoride anion. Thermodynamic parameters and stoichiometric ratios for the complexation of calix[4]pyrrole and derivatives functionalised at the *meso* position reported by Danil de Namor and co-workers with anions are included in Table 1.5¹⁵⁰⁻¹⁵²

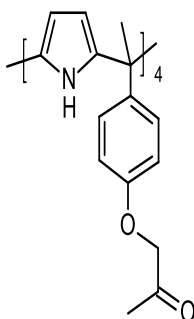
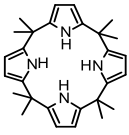
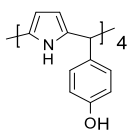
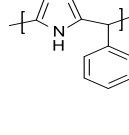
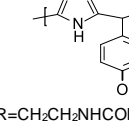
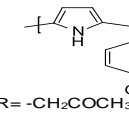
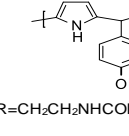
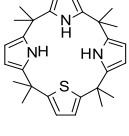


Figure 1.36 Functionalised *meso* position of calix[4]pyrrole synthesised by Danil de Namor *et al*

Table 1.5 Thermodynamic parameters and stoichiometric ratios for the complexation of calix[4]pyrrole and functionalised calix[4]pyrrole at the *meso* position with anions synthesised by Danil de Namor and co-workers¹⁵⁰⁻¹⁵².

Receptor	Anion	L: X ⁻	log K _s	Δ _c G° kJ mol ⁻¹	Δ _c H° kJ mol ⁻¹	Δ _c S° J mol ⁻¹ K ⁻¹
	F ⁻	1: 1	6.21	-35.4	-43.5	-27
	Cl ⁻	1: 1	4.70	-26.8	-44.7	-60
	Br ⁻	1: 1	3.65	-20.8	-30.7	-33
	I ⁻	1: 1	1.55	-8.8	-4.0	15
	H ₂ PO ₄ ⁻	1: 1	5.00	-28.5	-48.1	-66
	F ⁻	1: 1	5.44	-31.1	-32.4	-5
	Cl ⁻	1: 1	3.82	-21.8	-20.5	5
	Br ⁻	1: 1	3.20	-18.2	-15.4	9
	H ₂ PO ₄ ⁻	1: 1	4.82	-27.5	-32.1	-15
	F ⁻	1: 1	3.08	-17.6	-97.1	-267
	Cl ⁻	1: 1	2.36	-13.5	-55.9	-142
	Br ⁻	1: 1	1.61	-9.2	-58.6	-166
	H ₂ PO ₄ ⁻	1: 1	4.80	-27.4	20.2	25
		1:2	4.66	-15.2	-29.9	-50
 R=CH ₂ CH ₂ NHCONHC ₆ H ₅	F ⁻	1: 1	5.00	-28.5	-31.4	-10
		1:2	4.72	-27	-61.5	-116
	Cl ⁻	1: 1	2.43	-13.9	-86.4	-244
	H ₂ PO ₄ ⁻	1: 1	4.8	-27.4	-61.5	-116
	1:2	4.66	-27.4	-29.9	-50	
 R= -CH ₂ COCH ₃	F ⁻	1: 1	4.3	-24.6	-21.1	12
		1:2	2.8	-15.7	-6.4	32
	H ₂ PO ₄ ⁻	1: 1	4.11	-23.4	-22.74	03
 R=CH ₂ CH ₂ NHCONHC ₆ H ₅	F ⁻	1: 1	5.00	-28.7	-20.2	29
	Cl ⁻	1: 1	3.3	-18.7	-3.1	52
	Br ⁻	1: 1	2.2	-12.7	-1.8	36
	F ⁻	1: 2	5.25	-29.9	-31.5	-05
	Cl ⁻	1: 1	4.15	-23.7	-51.7	-95
	Br ⁻	1: 1	3.46	-19.7	-34.6	-49
	H ₂ PO ₄ ⁻	1: 1	4	-22.7	-43.7	-70
	1:2	3.7	-21.2	-17.8	11	

Introduction of different functional groups to the parent calix[4]pyrrole at the *meso* position enabled these macrocycles to interact with anionic and cationic guests and have gained considerable attention due to their application in biological processes. These receptors can be used as ion transporter through biological membranes (Fig. 1.37)¹⁵³

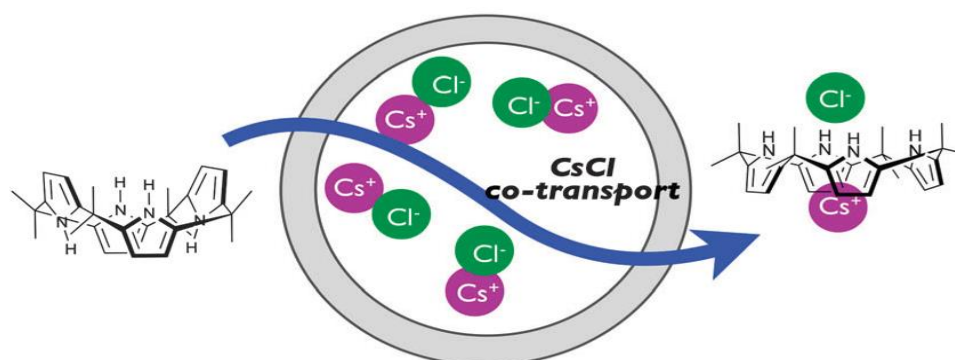
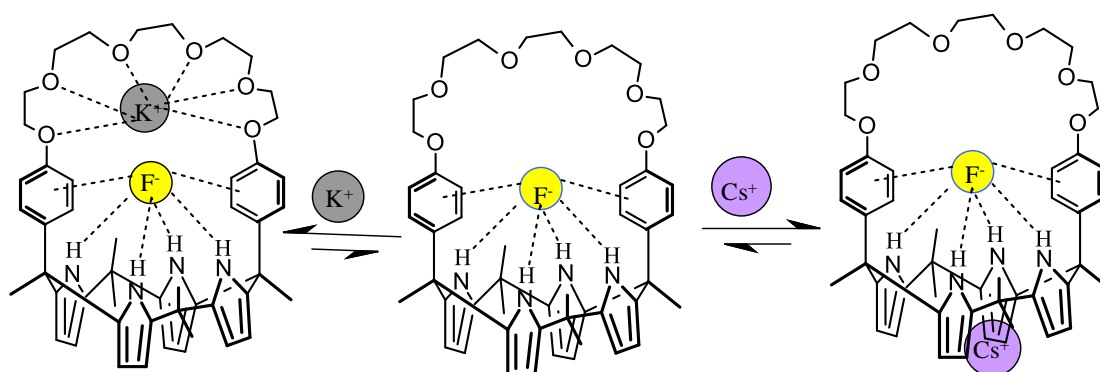


Fig. 1.37 Calix[4]pyrrole as ion transporter across the biological membrane¹⁵³

Sessler *et al*^{154-a} concluded that the addition of caesium perchlorate to the fluoride complex with functionalised calix[4]pyrrole in an acetonitrile: methanol (9: 1) mixture led to fasten the complexation with the fluoride anion and the caesium cation nested in the cup-like portion of the calix[4]pyrrole whereas the addition of potassium perchlorate led to complex with the potassium in the crown ether part. They demonstrated that this type of complexation led to increase the electrostatic interaction between the receptor and the ion-pair and can be act as a ion-pair transporter through the cell membrane (Scheme 1.6)



Scheme 1.6 Complexation of ions in different sites of calix[4]pyrrole

Also Sessler *et al*^{154-b} reported the synthesis of strapped calix[4]pyrrole with calix[4]arene at the *meso* position as an ion pair receptor which has affinity to interact with anionic and cationic moieties.

They demonstrated that the receptor has affinity to complex with Cs^+ and F^- ions in a mixture of methanol and chloroform ($\text{MeOD}:\text{CDCl}_3$) and found that the addition of an excess of CsF led to the formation of a supramolecular polymer (Scheme 1.7)

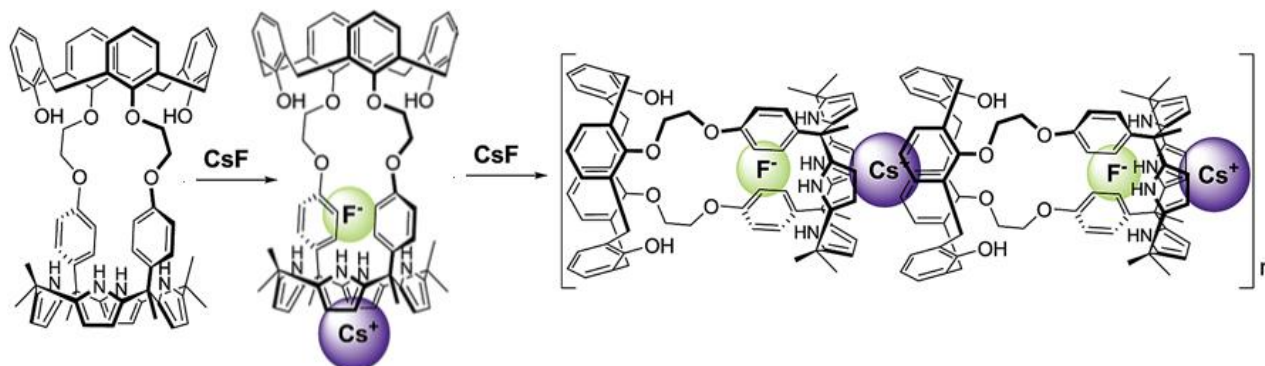


Fig. 1.38 Schematic representation for the formation of a supramolecular polymer during the addition of an excess amount of caesium fluoride.^{154-b}

1.5.3. Applications of calix[4]pyrroles

Calix[4]pyrrole Ion Selective Electrodes ISEs

Producing electrical devices used to determine the activity of specific ion in electrolyte solutions in the presence of others remains a huge challenge¹⁵⁵. Supramolecular chemistry enabled chemists to produce selective and sensitive hosts that can be used as sensors for anions, electron deficient cations and neutral molecules even in very diluted solutions^{156,157}. Calix[4]pyrroles possess relatively large cavity for hosting anions supported by four hydrogen bonds between the anions and the NH groups and electron rich cavity that can be reorganised when this is essential. Calix[4]pyrroles are easily to synthesise and functionalise to make them useful receptors for different guests especially for electron rich guests with appropriate size and the cooperative effect of solvents. This unique behaviour has been explored to construct potentiometric sensors through the formation of supermolecular host-guest complexes reflected in the potentiometric signals. ISEs based on polyvinyl chloride (PVC) containing calix[4]pyrrole (Fig. 1.27) produced by Kra'1¹⁵⁷ and co-workers showed much higher responses at low pH ($\text{pH} = 3.5-5.5$) towards Br^- , Cl^- and H_2PO_4^- than F^- . This was attributed to the anionic propensity for the macrocycle and to the size fitting effect in the coordination processes. At high pH ($\text{pH} = 9$) the membrane displayed non-Hofmeister selectivities ($\text{Br}^- < \text{Cl}^- < \text{OH}^- \approx \text{F}^- < \text{HPO}_4^-$) as a

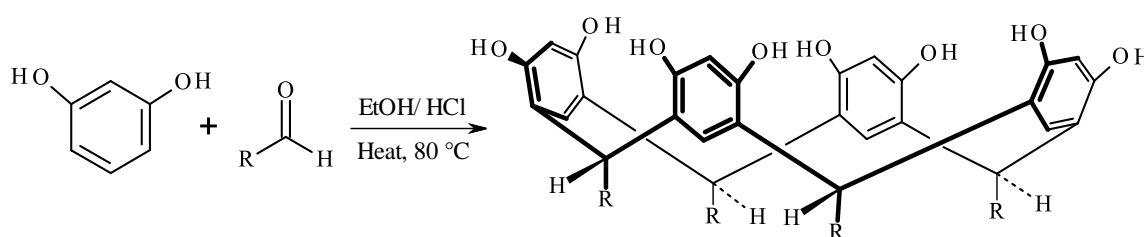
result of the coordination of the receptor with the OH^- anion^{157,158}. Steinle *et al*¹⁵⁹ have studied the enhancement of anion selectivity of octaethyl (OEP) and tetraphenyl porphyrines derivatives drugged with trivalent gallium, indium and thallium into the polymeric ISEs membrane. These authors have concluded that the ISEs based on PVC doped indium (III) has a significant effect on the selectivity enhancement of the membrane towards the chloride anion. In the same way the membrane containing gallium (III) showed remarkable sensing properties toward the fluoride anion whereas general selectivity enhancement was obtained in the sensitivity by the membrane doped with thallium (III) towards the chloride over other anions. Park *et al*¹⁶⁰ have studied the efficiency of calix[4]pyrrole based ISEs and its derivative to respond to monovalent thallium and they found that the receptor was more efficient than others as a result of the presence of four cyclohexyl groups which led to increasing the rigidity and the geometry of the receptor towards monovalent thallium.

Recently Danil de Namor and co-workers¹⁶¹ have demonstrated that the functionalised calix[4]pyrrole containing amide groups showed high selectivity towards mercury cation (II).

Resorcinarenes are receptors involved in this thesis, therefore a brief introduction on the synthesis and properties of these ligands with reference to the cyclic tetramer is now given

1.6 Resorcin[4]arenes

A new class of molecular capsules synthesised by the acid catalysed condensation reaction of aliphatic or aromatic aldehydes with resorcinol in 1940 by Niederl and Vogel¹⁶² are currently known as resorcin[4]arenes (Scheme 1.8)



Scheme 1.7 Synthetic pathway of resorcin[4]arene

The cyclic tetramer structure was confirmed by X-ray crystallography by Erdtman *et al*¹⁶³ in 1968. Gutsche and Böhmer⁹¹ have proposed that the compound was similar to calix[4]arenes and classified these cyclic tetramers as calix[4]resorcinarenes. Due to the presence of more hydroxyl groups on the phenyl rings with respect to calix[4]arenes which enhances hydrogen bond formation, these receptors are more rigid than calix[4]arenes and hexameric aggregation¹⁶⁴ for these macrocycles in

the solid state and in solution have been reported. The connectivity between the aryl groups *via* the methylene bridges allows the formation of hydrophobic cavities able to encapsulate guests with the appropriate size.

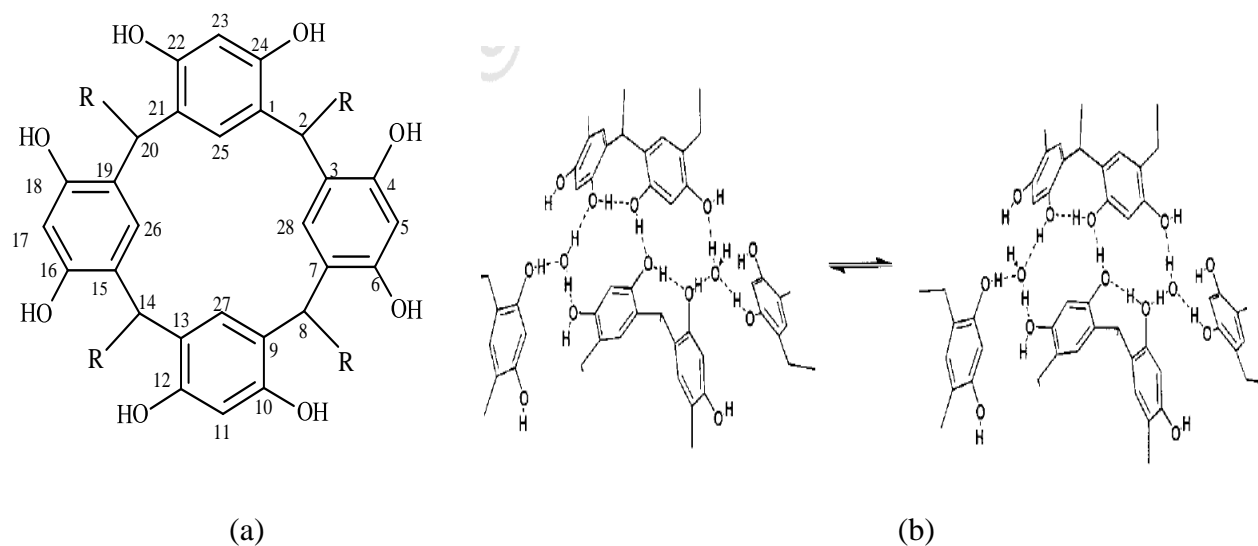


Fig. 1.39 General structure of resorcin[4]arene showing (a) 2, 8, 14, 20-tetramethyl, the numbering of substituent positions and (b) Hexameric aggregation in solution¹⁶⁴

Högberg¹⁶⁵ has reported the condensation of resorcinol with different aldehydes. The resorcin[4]arene formed can adopt four different conformations; “*crown*”, “*boat*”, “*chair*”, and “*saddle*” conformation (Fig.1.40) but he demonstrated that the cyclic tetramer is formed in only two isomers namely “*chair*” and “*crown*” conformers. Although the “*chair*” conformation is energetically more favoured than the “*crown*” to reduce the repulsion between the aryl groups, the ratio between these isomers depends on the reaction conditions. Atwood *et al*¹⁶⁶ have synthesised a series of resorcin[4]arene derivatives containing phenyl groups as pendant arms and they concluded that the isolated products was only in a chair conformation.

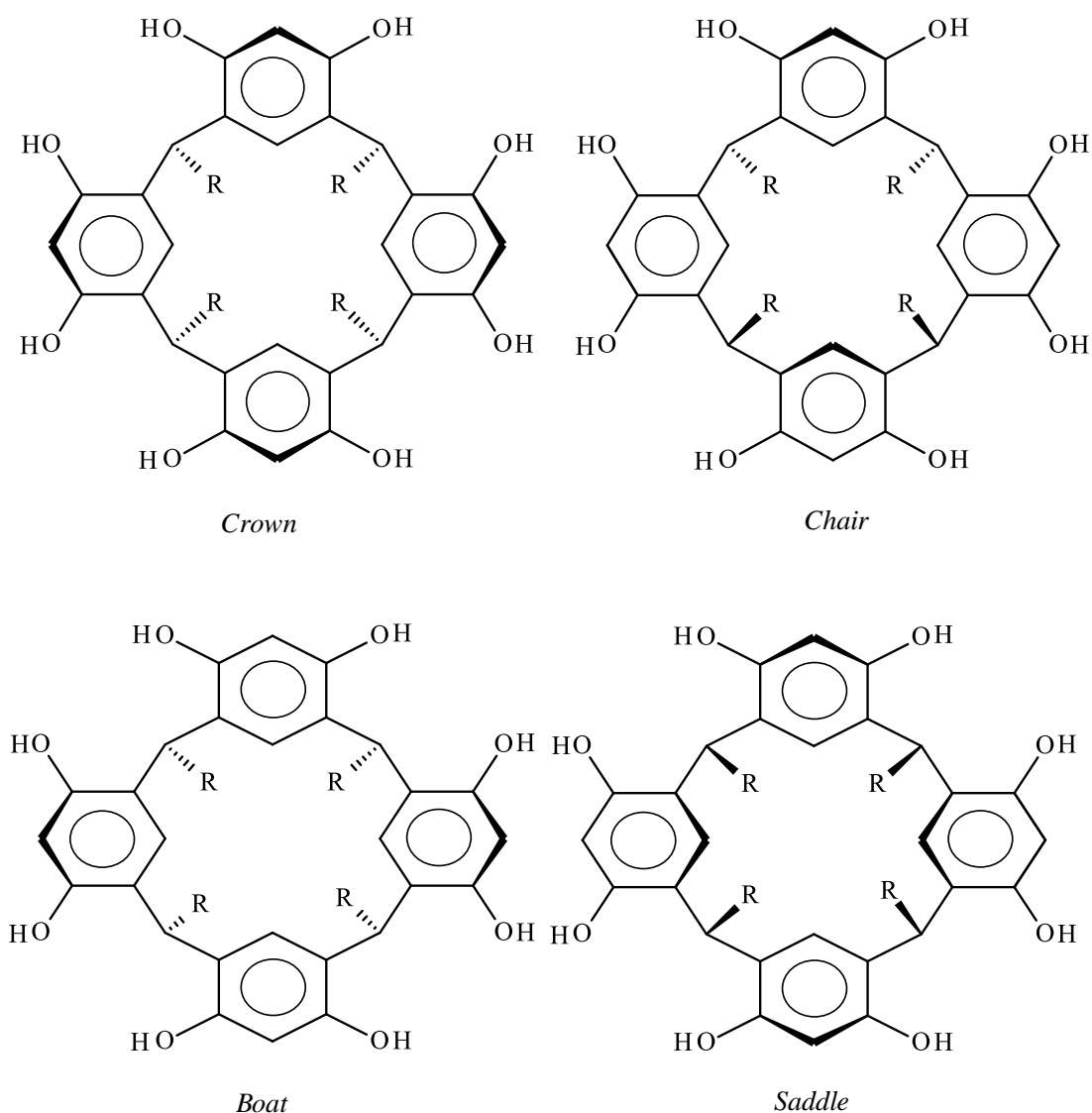


Fig. 1.40 Possible conformations can be adopted by the resorcin[4]arene cyclic tetramer.

Atwood and co-workers¹⁶⁷ in their pioneering work on C-methyl resorcin[4]arene in wetted chloroform proved that the compound tends to form a hexameric capsule in the solid state aided by eight water molecules. Rebek and Shivanyuk¹⁶⁸ reported that the resorcin[4]arene containing dodecyl pendant arms in moisturized chloroform tends to form a stable hexameric capsule driven by the appropriate guest. Modification of these molecular capsules through the hydroxyl groups prevents self-aggregation and leads to enhance their electrostatic attraction towards the guests. Steric factors as well as the size of the guests play a crucial role in the formation of molecular capsules. Danil de Namor and co-workers have synthesised and characterised a resorcin[4]arene derivative containing

P, O and S donor atoms (Fig. 1.41) and found that the receptor exhibited selectivity towards mercury¹⁶⁹.

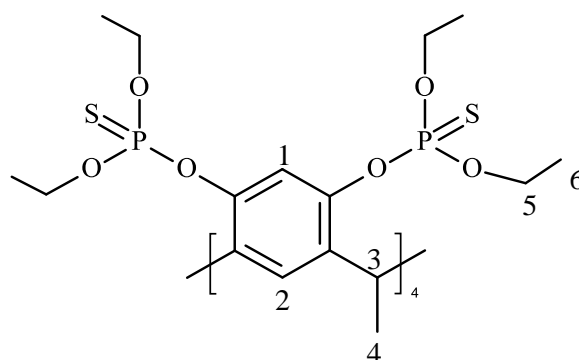
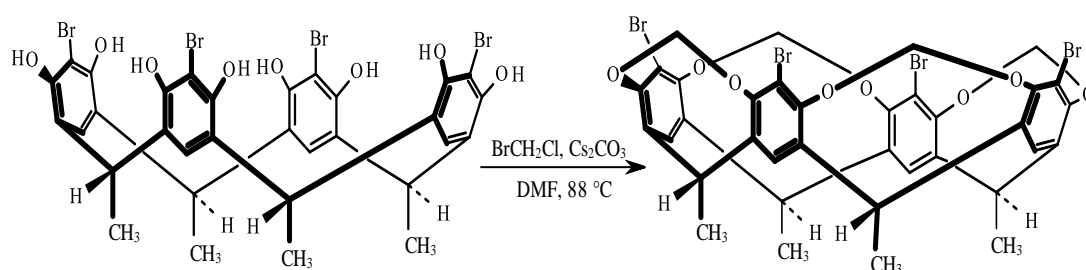


Fig. 1.41 Structure of 4, 6, 10, 12, 16, 18, 22, 24-diethyl thiophosphate calix[4]resorcarene

Cram and co-workers^{170,172} have reported the synthesis of new rigid macrocyclic containers created by the modification of resorcin[4]arene called “**cavitands**” (Scheme 1.9). The fully bridging of the adjacent aryl rings through the hydroxyl groups leads to the production of these cavitands with a deep cavity, rigid enough to encapsulate strongly appropriate guests. Their complexes are known as “**caviplex**”, Cram derived the concept “molecule within molecule” according to his research on these molecular containers. These cavitands have gained much attention in host-guest, coordination and material chemistry



Scheme 1.8 Synthetic route for the cavitands

The bridging of the neighbouring hydroxyl groups can be achieved by different groups which can expand the size of the container and also to assist in the production of different bridges with different functional and consequently different reactivities (Fig. 1.42). Danil de Namor and co-workers¹⁷³ have demonstrated that the selectivity of functionalised resorcin[4]arene towards the silver cation has been dominated when the adjacent hydroxyl moieties are bridged by sulphur and phosphorous groups (Fig. 1.42-c)

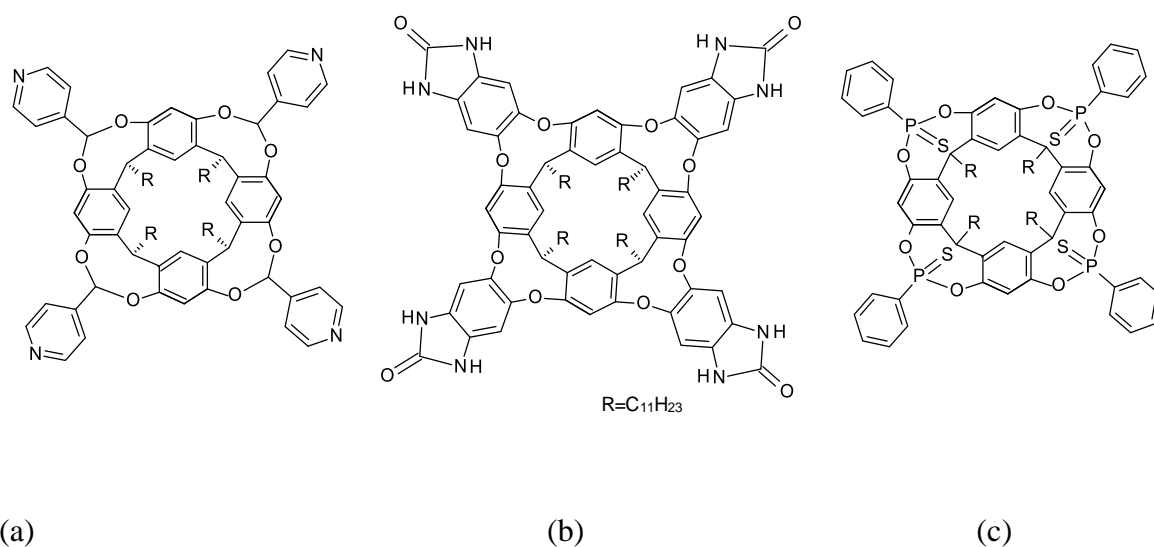
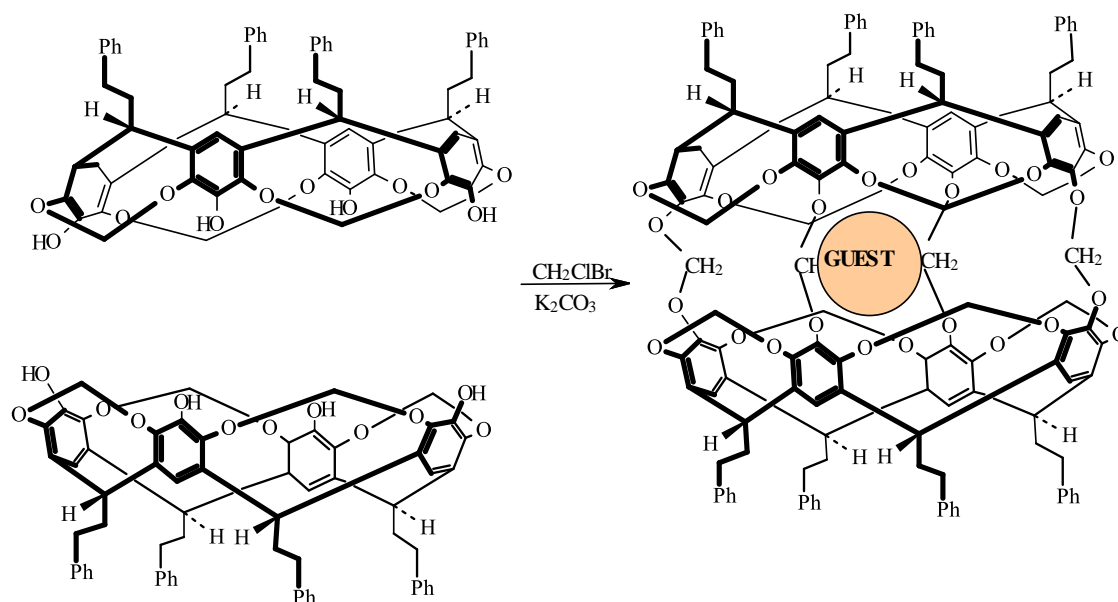


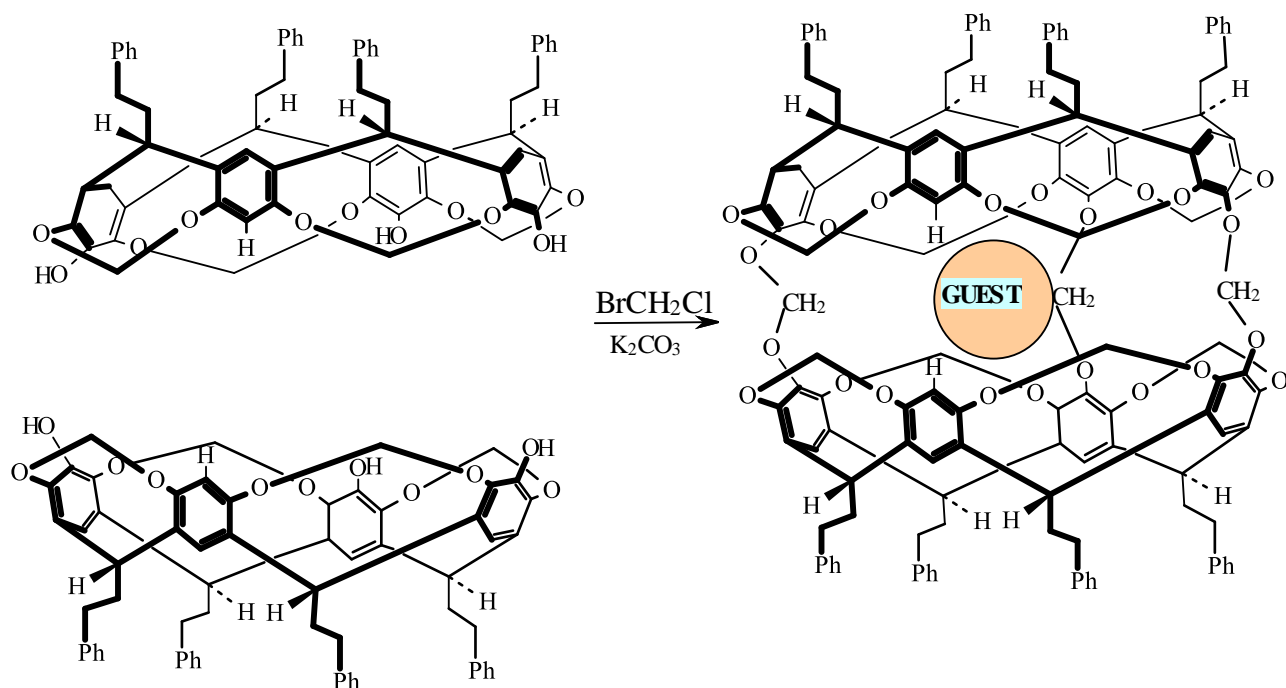
Fig. 1.42 Showing the bridging of the hydroxyl groups of the resorcin[4]arene by different groups

The bridging of two cavitands leads to produce more complicated and spherical closed capsules named by Cram as “**carcerands**”. In these receptors the guest is imprisoned permanently in the closed structure which means that the guest must be introduced before the encapsulation process takes place (Scheme 1.10). The carcerand complexes are known as “**carciplex**” and there is no possibility for the guest to leave the cavity without disruption of the bridges bonds.



Scheme 1.9 Synthesis of carcerand capsules and encapsulation of the guest to form the “**carciplex**”

The partially bridging of the hydroxyl groups of cavitands has led to produce “**hemicarcerands**” in which the guest can leave the cavity without any disruption to the host bonds (Scheme 1.11)¹⁷¹

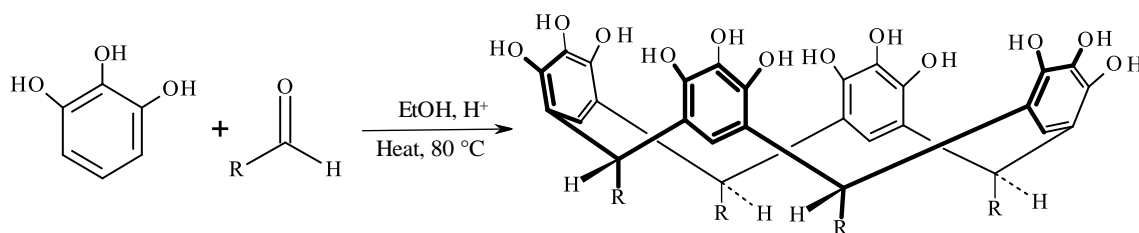


Scheme 1.10 Synthesis of an hemicarcerand and showing the formation of hemicarceplex and the possibility of the guest to leave the cavity.

Given that in this thesis preliminary studies were carried out with pyrogallol[4]arenes, a brief introduction on these macrocycles is now reported

1.7 Pyrogallol[4]arenes

These macrocyclic tetramers were first synthesised in 1990 from the condensation reaction between pyrogallol and an aldehyde in acidic conditions (Scheme 1.12)



Scheme 1.11 Synthesis of the pyrogallol[4]arene macrocycle

A general structure of this macrocycle is shown in Fig. 1.43. Theoretically there is a possibility of producing receptors containing an increased number of aryl groups in their structure to form pyrogallol[n]arenes but all the work reported in the literature is referred to the cyclic tetramer.

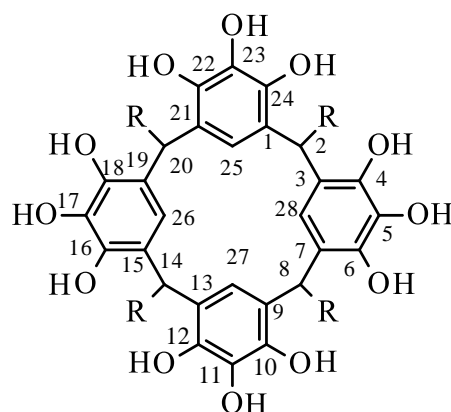


Fig. 1.43 2, 8, 14, 20-tetra-alkyl-5, 11, 17, 23-tetrahydroxyresorc[4]arene showing the numbering of substituent positions

Studies carried out by Atwood and co-workers¹⁷⁴ in 2002 on *p-tert*-butyl-calix[4]arene have revealed that the macrocycle does not contain pores in its chemical structure but it can be used as a molecular container for the solid guests to form thermodynamically stable supermolecular structure, the hosted solid can be dynamically transported through the host structure as a result of a reversible phase transition of the crystal structure to another form with significant change in the size and dimensions until the system reaches the stable state. Crystal phase transfer leads to defect the properties of the structure and may lead to enhance its packing capacity^{175,176}. Based on these results, pyrogallol[4]arene containing C-pentyl pendant arms was exploited as a container for gas storage and the effects of chain length of the pendant arms and the solvent on the storage capacity of these receptors have been investigated¹⁷⁷. They conclude that the C-pentylpyrogallol[4]arene is able to frusturate CO₂ gas at ambient temperature and they emphasised the important contribution for the C-pentyl pendant arm in the storage efficiency as compared with the pyrogallol[4]arene containing propyl as pendant arm.

Atwood *et al*¹⁷⁸ reported the use of pyrogallol[4]arene with different pendant arms (R= methyl, ethyl, propyl) as molecular containers for xanthone as solid guest to form co-crystal host-guest complexes in different solvents. They demonstrated the role of the solvent and the length of the bendant arm on the cavity size which leads to increase the number of guest molecules encapsulated in the cavity, which consequently resulted in the production of complexes of different composition.

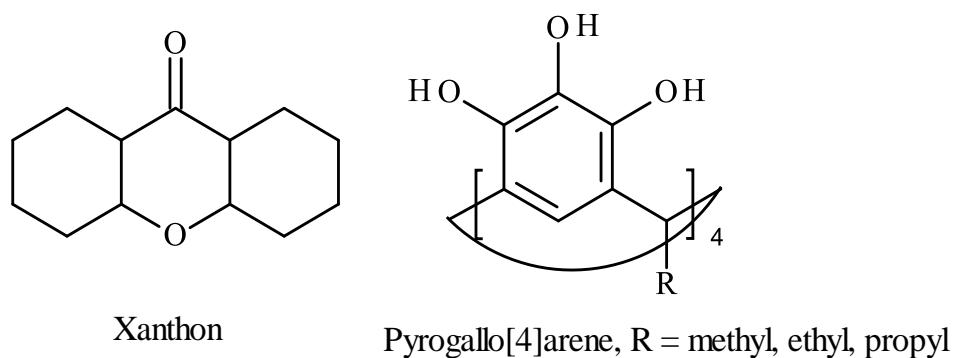


Fig. 1.44 Chemical structure of xanthon and C-alkyl pyrogallol[4]arene

Avram and Cohen¹⁷⁹ studies on resorcin[4]arene and pyrogallol[4]arene capsules proved that the capsules formed by pyrogallol[4]arene are more stable than those formed by resorcin[4]arene. Water molecules were not included in the complexation processes involving the former capsules. It was therefore concluded that no hetero molecular capsules were obtained by mixing pyrogallol[4]arene and resorcin[4]arene solutions, and these capsules disrupted in both cases by adding a protic polar solvent like methanol. Recently Danil de Namor and O. Webb have been carried out the synthesis of cavitand, carceplex (Fig. 1.45), carcerands and hemicarcerands arising from resorcin[4]arene and pyrogallol[4]arene and were tested as promising capsules to remove unwanted amines from the fuel (petrol or diesel) to enhance the quality of fuel¹⁸⁰.

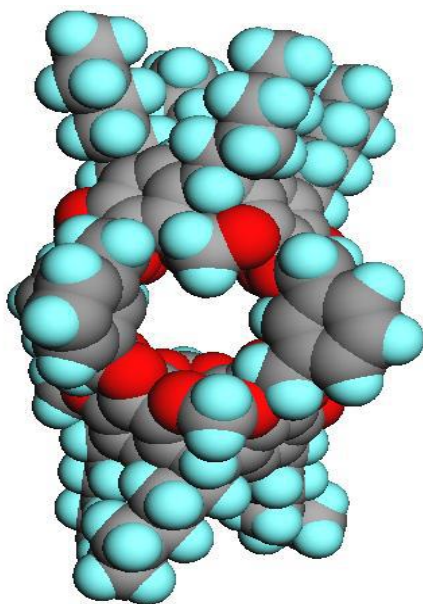
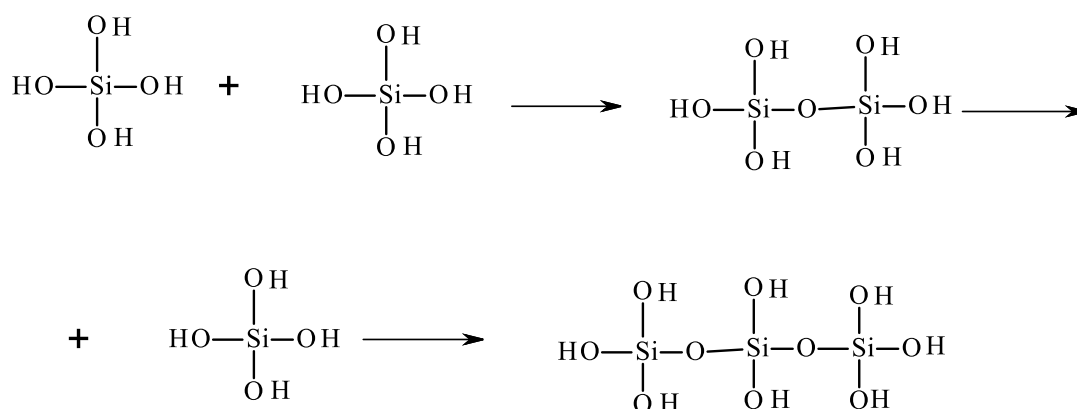


Fig. 1.45 Molecular modelling of carceplex¹⁸⁰

1.8 The use of silica based compounds for extraction purposes

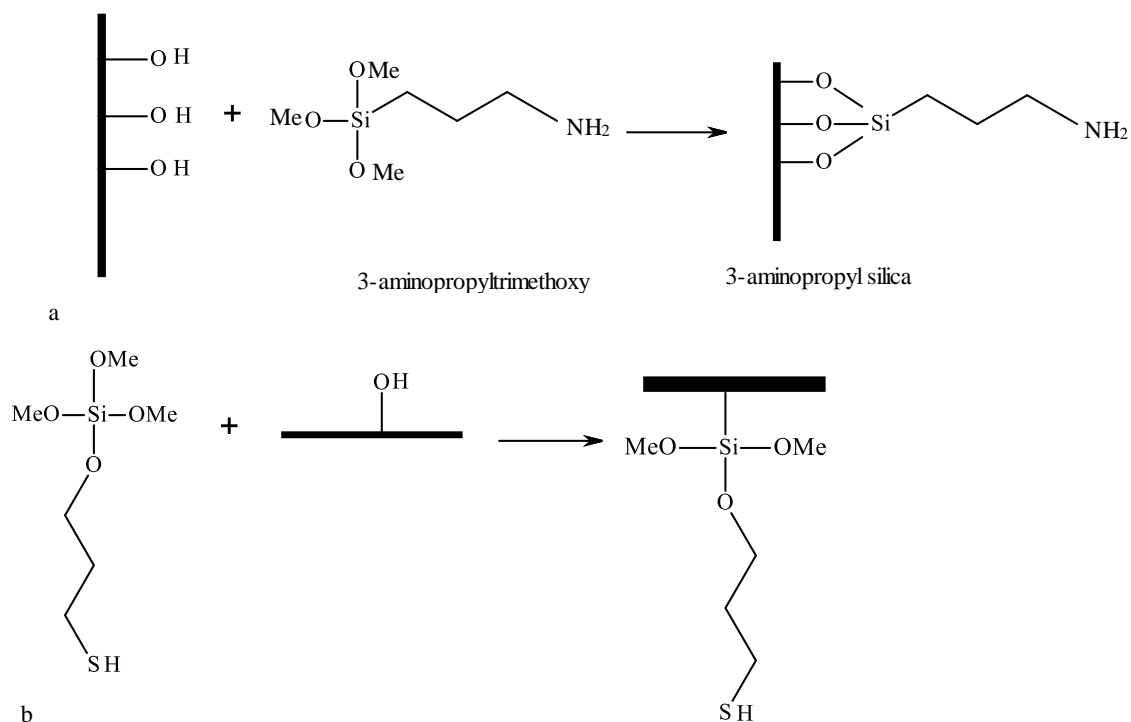
Silica gel was first synthesized by Thomas Graham in 1861 from reacting an aqueous solution of hydrochloric acid on sodium silicate¹⁸¹. Nowadays silica gel is produced by the Patrick's process in a similar manner which includes releasing silicic acid by hydrochloric acid from an aqueous solution of sodium silicate (eq.1.2). This is prepared by heating sand at a high temperature in the presence of sodium hydroxide or sodium carbonate followed by self-polymerisation of the silicic acid with the removal of water (Scheme 1.13)



Scheme 1.12 Polymerisation of Silicic acid

The polymer continues to grow to form aggregates followed by the conversion to polymeric spheres. The simplicity, stability over a wide range of pH and the low cost of silica make this material as one of the most important materials for solid phase extraction processes which also shows good extraction efficiency as compared with liquid-liquid extraction processes. Although the silica has advantages but it is considered to be time and energy consuming due to the time and energy required for sonication processes in order to disperse it well and to prevent its aggregation in solution. In order to overcome these problems, the surface of silica can be modified by different functional groups to enhance the uptake efficiency towards targeted species. This modification can be achieved by the introduction of appropriate organic (Scheme 1.14 a) or inorganic functional groups (Scheme 1.14 b). Also the modification of the surface of silica can make the surface more hydrophylic with higher energy which can lead to reduce the affinity of silica to interact with materials which are considered hydrophobic in nature. From the health view point silica is considered harmful, the too fine dust of silica called respirable crystalline silica (RCS) which is not easily shown in the normal light but its

inhalation can cause silicosis, bronchitis or cancer and reduces the capacity of lungs towards oxygen¹⁸²⁻¹⁸⁴.



Scheme 1.13 Modification of silica by (a) organic functional group, (b) inorganic groups

Danil de Namor and co-workers¹⁸⁵ have reported the use of silica as a solid support for the functionalised *p-tert-butylcalix[4]arene* containing amino groups (Fig. 1.46) and they demonstrated the ability of this material to remove the acidic herbicides from water. These authors revealed that the silica used interacted with water and the heat of interaction was determined calorimetrically. Also, the removal of *tert-butyl* group can reduce the hydrophobicity of the macrocycle which means this modification is also useful for the removal of hydrophilic species.

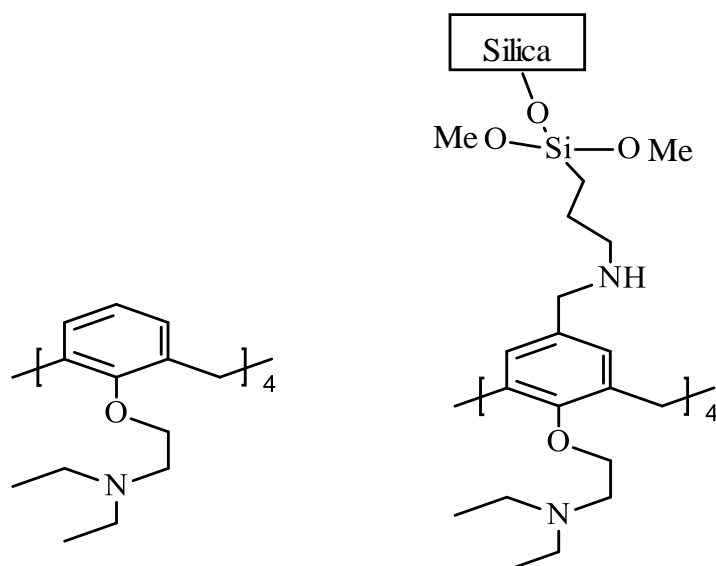


Fig. 1.46 Chemical structure of 5, 11, 17, 23-*tetrakis*-[(diethylamine)ethoxy]calix[4]arene legend and its immobilization to silica

Recently Li and co-workers¹⁸⁶ reported the complexation of *p-tert*-butylcalix[4]arene containing crown-5 ether (Fig. 1.47 a) with 1-naphthyl methylcarbamate (Fig. 1.47 b) which is used as an insecticide and they demonstrated that the crown ether pendant arm of the receptor exhibited excellent efficiency to bind the insecticide.

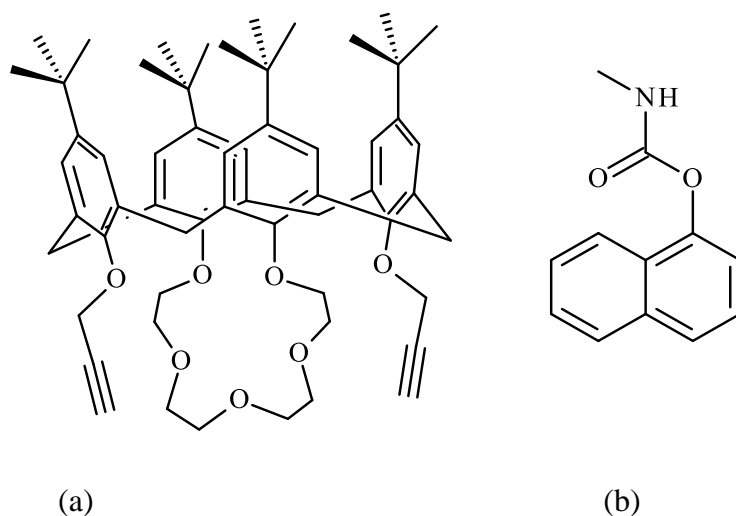
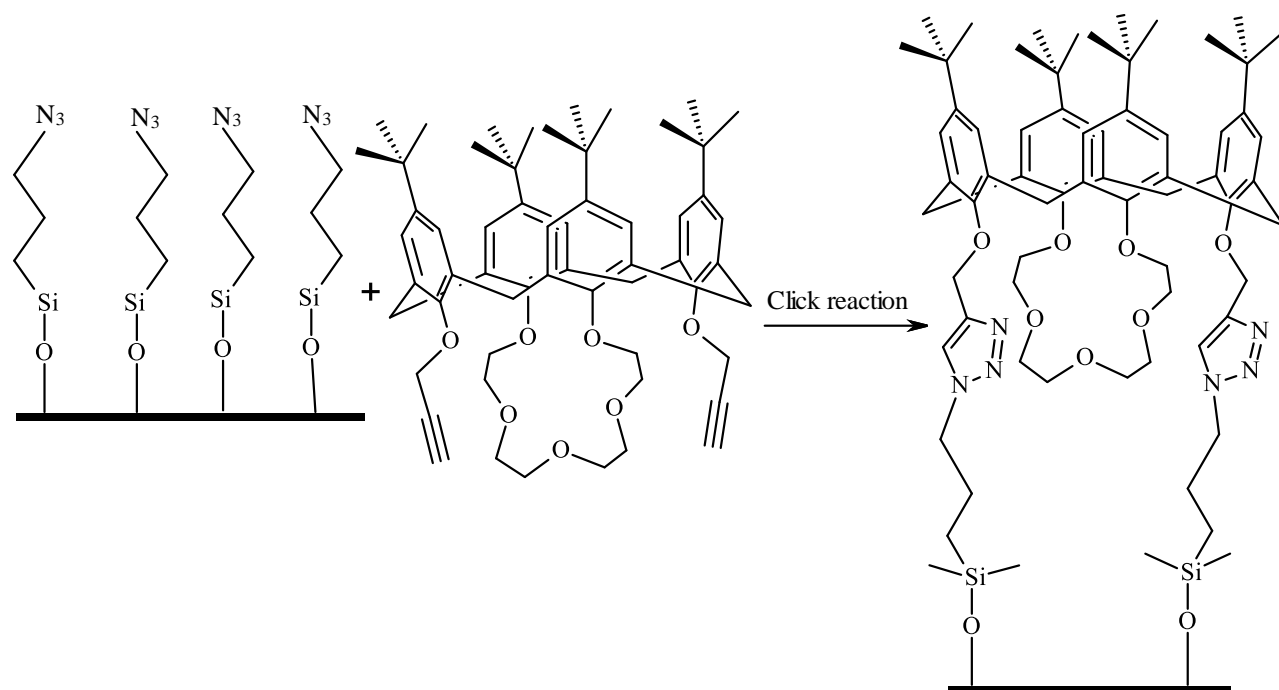


Fig. 1.47 The chemical structure of (a) the receptor used for the complexation and (b) the 1-naphthyl methylcarbamate

The propargylated pendant arm was used to link the receptor with a solid support like silica *via* click reaction (Scheme 1.15). The binding selectivity of the crown ether towards the potassium cation was exploited to switch off the complexation between the receptor and the insecticide for recycling the receptor.

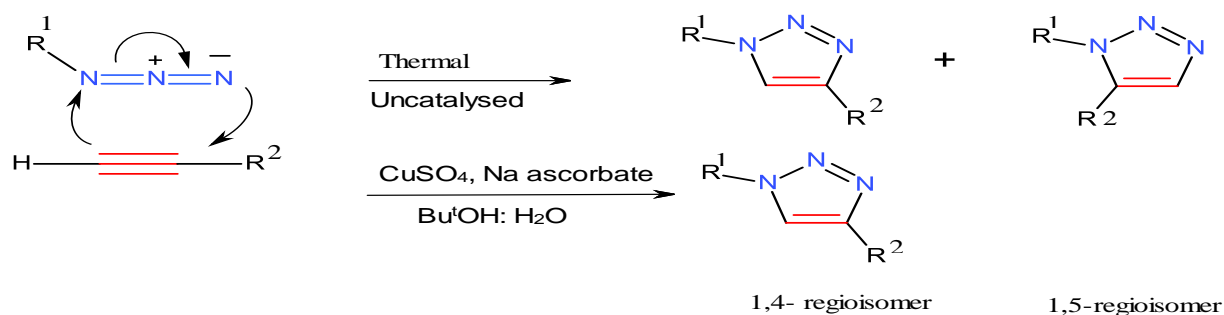


Scheme 1.14 Using of Silica as solid support for functionalised *p-tert*-butylcalix[4]arene

1.8.1 Click Chemistry

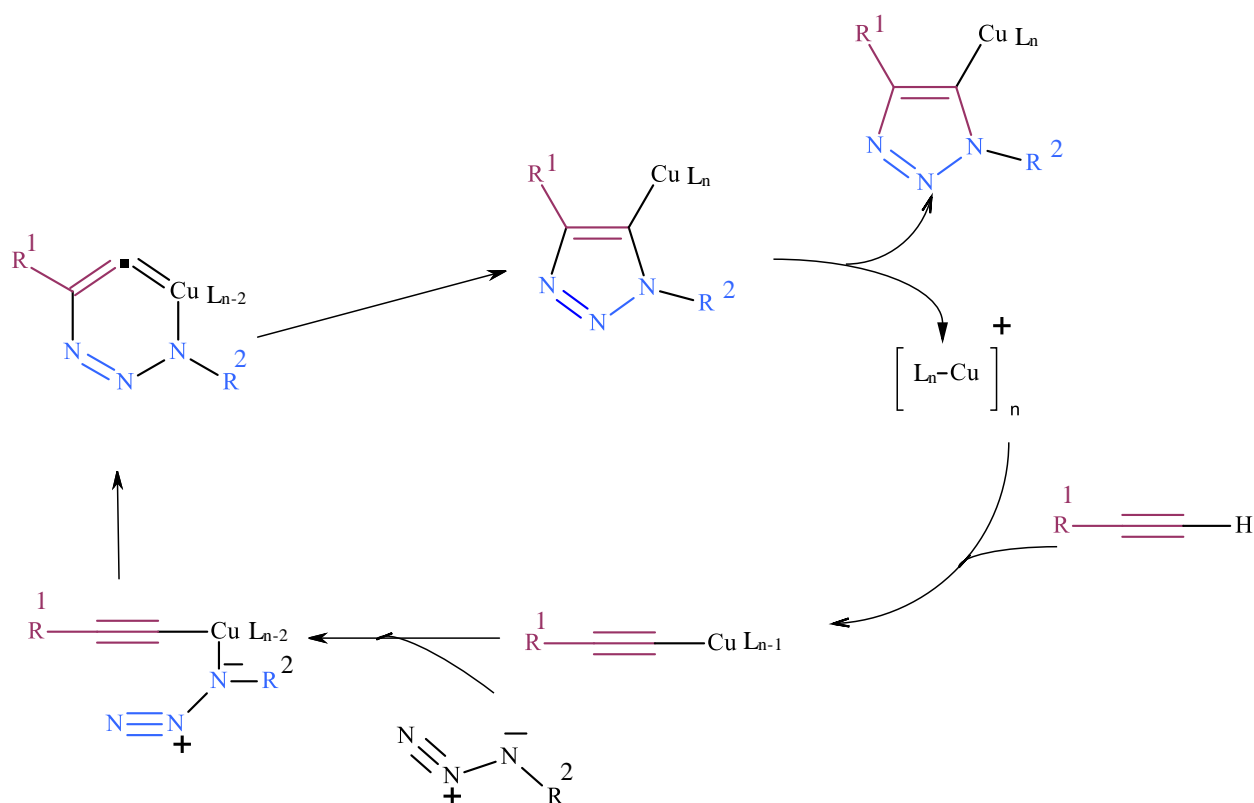
The Click chemistry term was introduced by Sharpless *et al* in 2001¹⁸⁷. According to these authors for this terminology to be applied, reactions “*must be fast, modular, wide in scope, give very high yields, generate only inoffensive by-products that can be removed by non-chromatographic methods, and be stereospecific (but not necessarily enantioselective)*”¹. The characteristics of the process involve simple reaction conditions, starting materials and reagents readily available, the use of environmentally friendly solvents such as water or those easily removed and a straight forward methodology of isolation. The azide-alkyne cycloaddition to form five-membered heterocyclic compounds is the most prominent click reaction and has gained much attention due to its use in the synthesis of a wide variety of compounds with important applications such as drugs, biomarkers, nano-carriers polymeric materials and many others. In the absence of heat and catalyst, the reaction is slow and when reactants are used in small concentration levels, a mixture of products are formed.

Meldal *et al* in Denmark and Sharpless *et al*^{188,189} in US independently discovered that the reaction is kinetically fast and has an increase in specificity for a target compound when Cu (I) is used as catalyst (Scheme 1.15)



Scheme 1.15 Uncatalysed and catalysed azide-alkyne cycloaddition reaction

The following mechanism was proposed (Scheme 1.16)



Scheme 1.16 Proposed mechanism for catalysed azide-alkyne cycloaddition reaction

1.9 BET Theory

BET is the abbreviation of three names of three scientists; Brunauer, Emmett and Teller (**BET**), BET theory was suggested by the above scientists to describe the ability of porous materials to adsorb gases such as nitrogen gas by specific surface area and this ability can be expressed by the following BET equation (eq.1.3)

$$1/(W((P/P^\circ) - 1)) = 1/W_m C + (C - 1)/W_m C \{P/P^\circ\} \quad \text{eq.1.3}$$

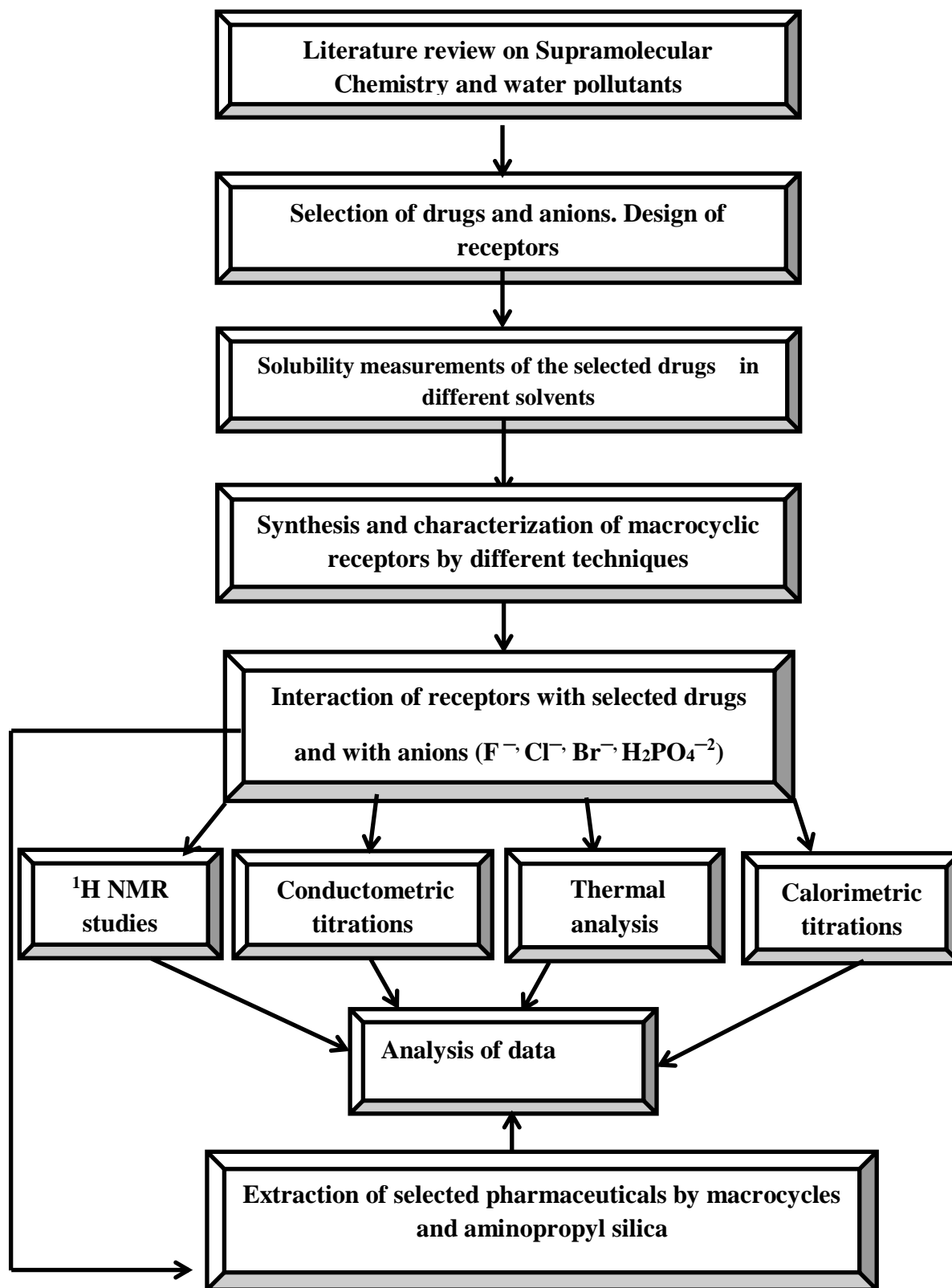
In this equation, W is the weight of gas adsorbed, P/P° is the relative pressure in torr unit applied on the solid sample, W_m is the weight of the solid as a monolayer and C is the BET constant. Plotting the relation of $1/[W(P/P^\circ) - 1]$ against P/P° gives a straight line for most solids, using nitrogen as adsorbent. The porosity of the material under study can be predicted from the plot^{190,191}

1.10 Aims of the Thesis

This thesis is concerned with the design, synthesis and characterisation of a number of macrocyclic receptors (host) with the ability to bind biologically active species (guest). In addition, a functionalised silica will be tested for the same purpose. Pharmaceuticals are targeted in this thesis due to lack of thermodynamic studies concerning the interaction of macrocyclic receptors with pharmaceuticals. Supramolecular hosts are selected due to their selective behaviour for a particular guest, provided suitable functionalities are incorporated in their structure. The pharmaceuticals selected are diclofenac, sodium diclofenac (NaDF), chlofibric acid, ibuprofen, aspirin and carbamazepine (CBZ) due to their common usage (Table 1.6). Diclofenac belongs to the group of non-steroidal anti-inflammatory drugs (NSAIDs) used in human medical care to treat painful conditions such as arthritis, sprains and strains, gout, migraine, dental and pain after surgical operations. It is a pain-killer which also reduces inflammation. Ibuprofen (also belongs to NSAIDs) is used as an analgesic and antipyretic. Aspirin (NSAIDs) is used as an analgesic, antipyretic, anti-inflammatory and anti-coagulant, carbamazepine is an anti-epileptically drug used worldwide. Clorofibric acid is used as a lipid regulator in blood to lower the risk of atherosclerosis^{192,193}.

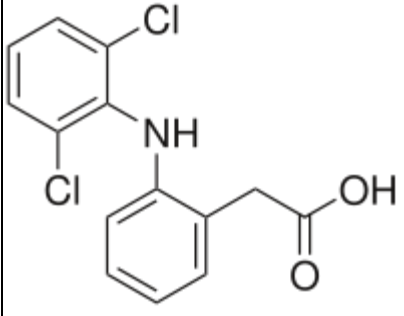
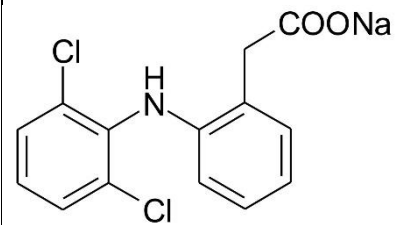
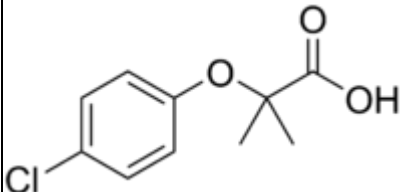
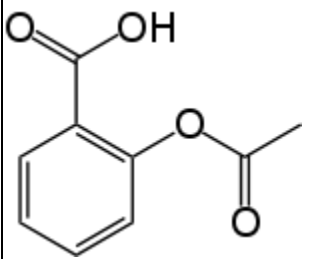
The design and synthesis of macrocyclic receptors able to interact with the selected drugs requires information about the guest such as its solubility in water and common organic solvents as well as knowledge of the partition coefficients for these drugs in water-membrane-like solvent systems. Receptors to be synthesised and characterised are cyclodextrins (heptakis-(6-chloro-6-deoxy)- β -cyclodextrin and heptakis-(2, 3, 6-tri-O-benzoyl)- β -cyclodextrin) and synthetic macrocycles such

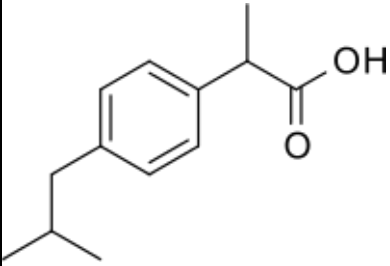
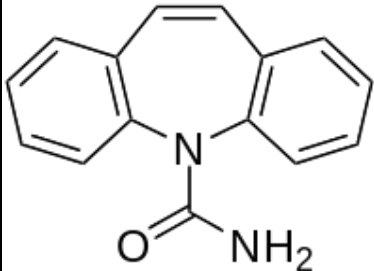
as calix[4]arenes (5, 11, 17, 23- *tert*-butyl-25, 26, 27, 28-(*O*-ethylethanoate)calix[4]arene, 5, 11, 17, 23- tetra-*tert*-butyl, 25, 27-bis (2-cyanomethoxy)-26, 28-dihydroxycalix[4]arene , 25, 27-dihydroxy-26-28-(dioxypargyl) *tert*-butylcalix[4]arene , 4-*tert*-butyl-azidocalix[4]arene, 25, 26, 27, 28-(diethylamino) ethoxycalix[4]arene), calix[4]pyrroles (*meso*-tetramethyl-tetrakis-(4-hydroxyphenyl ethyl) calix[4]pyrrole, *meso*-tetramethyl-tetrakis-(4-ethylacetatophenoxyethyl) calix[4]pyrrole), resorc[4]arene (C-pentyl-resorcin[4]arene ,C-pentylresorci[4]arene ester) and pyrogallol[4]arene (C-decyl pyrogallol[4]arene and C-4-aminophenyl pyrogallol[4]arene) Fig. 1.48 and Fig. 49. This is to be followed by ^1H NMR studies to obtain information whether or not interaction between receptor and drug takes place and if so the identification of the active sites of the receptor. From all receptors synthesised, the ones selected for further studies involving drugs (aspirin, clofibric acid, diclofenac, sodium diclofenac, ibuprofen and carbamazepine) were the calix[4]arene ester, (5, 11, 17, 27- *tert*-butyl-25, 26, 27, 28-(ethylacetatoethoxy)calix[4]arene) CAE, the *per*-benzoylated cyclodextrin (BzBCD), the partially functionalised calix[4]arene amine derivative (5, 11, 17, 23 tetra-*p-tert*-butyl, 25, 27- bis[aminoethoxy], 26, 28 dihydroxycalix[4]arene) (CA-(NH₂)₂), C-decylpyrogallol[4]arene (PG11), calix[4]pyrrole derivatives which are *meso*-tetramethyl-tetrakis-(4-hydroxyphenyl ethyl)calix[4]pyrrole (TTHCP) and *meso*-tetramethyl-tetrakis-(4-ethylacetatophenoxyethyl) calix[4]pyrrole (TTECP) . The 3 -aminopropyl functionalised silica gel was used for the removal of aspirin from water. When ionic species are present or occur as a result of complexation, conductivity measurements will be performed to establish the composition of the complex and obtain qualitative information on the strength of host-guest binding and also the stoichiometry of the complexation. UV measurements will be explored to further corroborate the composition of the complex. Whenever possible the complexation process will be thermodynamically characterised to obtain the stability constant ($\log K_s$) and the standard Gibbs energy $\Delta_c G^\circ$, enthalpy $\Delta_c H^\circ$ and entropy $\Delta_c S^\circ$ associated with this process. Aminopropyl silica will be also tested to remove the selected drugs from water. Following previous work on calix[4]ester derivatives and their complexation with metal cations in a variety of solvents, calix[4]pyrrole esters will be for the first time synthesised and characterised and their binding properties will be investigated. The aim of this part of the work is to assess the effect of i) the calix structure on the selective complexation of cations and ii) the ester functionality on the recognition of anions by calix[4]pyrrole. The strategy of this research is shown in Scheme 1.18



Scheme 1.18 Main strategy for this research

Table 1.6 The chemical structure of pharmaceuticals with commercial and IUPAC names

PHARMACEUTICALS	IUPAC NAME
 <p>Diclofenac [DF]</p>	2-[2-(2,6-Dichloroanilino)phenyl]ethanoic acid
 <p>Sodium diclofenac [NaDF]</p>	Sodium {2-[(2,6-dichlorophenyl)amino]phenyl}ethanoate
 <p>Clofibric acid [CLF]</p>	2-(4-Chlorophenoxy)-2-methylpropanoic acid
 <p>Aspirin</p>	2-(Acetoxy)benzoic acid

PHARMACEUTICAL	IUPAC NAME
 <p data-bbox="188 562 411 600">Ibuprofen [Ibu]</p>	<p data-bbox="810 376 1374 450">(R,S)-2-(4-(methylpropyl)phenyl)propanoic acid</p>
 <p data-bbox="188 981 643 1019">Carbamazepine (tegretol) [CBZ]</p>	<p data-bbox="810 674 1326 712">5H-dibenzo[b,f]azapine-5-carboxamide</p>

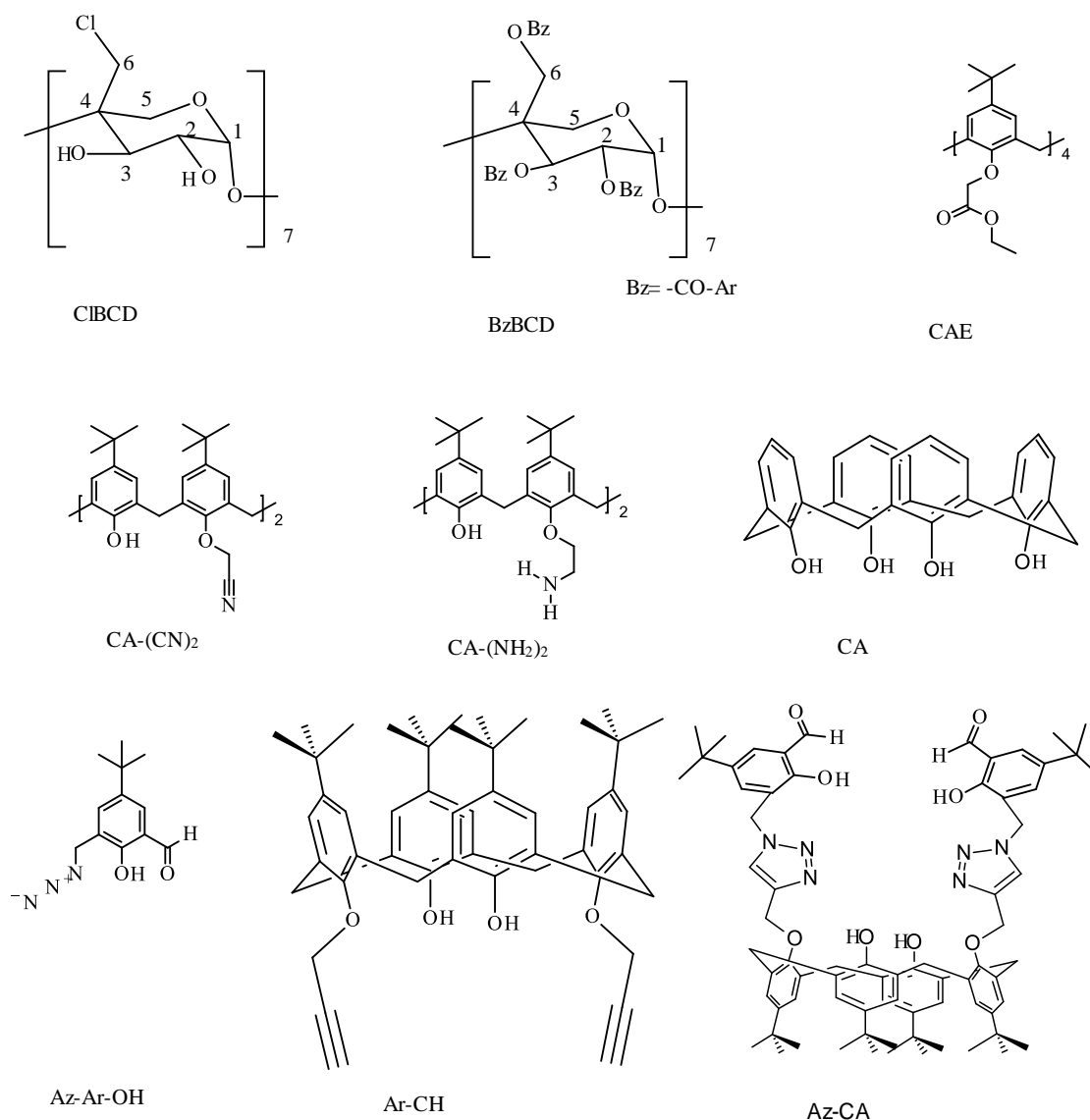


Fig. 1.48 Chemical structures of heptakis-(6-chloro-6-deoxy)- β -cyclodextrin, (CIBCD), heptakis-(2, 3, 6-tri-O-benzoyl)- β -cyclodextrin (BzBCD), 5, 11, 17, 27-*tert*-butyl-25, 26, 27, 28-(ethylacetoxycalix[4]arene(CAE) , 5, 11, 17, 23 tetra- *tert* -butyl, 25, 27 bis[2-cyanomethox] methoxy, 26, 28 dihydroxycalix[4]arene (CA-(CN)₂) , 5, 11, 17, 23 tetra-*tert*-butyl, 25, 27-bis[aminoethoxy]-26, 28 dihydroxycalix[4]arene [CA-(NH₂)₂], Synthesis 25, 26, 27, 28-tetrahydroxycalix[4]arene (CA), 5-*tert*-butyl-3-azidomethyl-2-hydroxybenzaldehyde (AzArOH) , 25, 27-dihydroxy-26, 28-(dioxypargyl)*tert*-butylcalix[4]arene (Ar-CH) , *tert*-butyl-azidocalix[4]arene (AzCA)

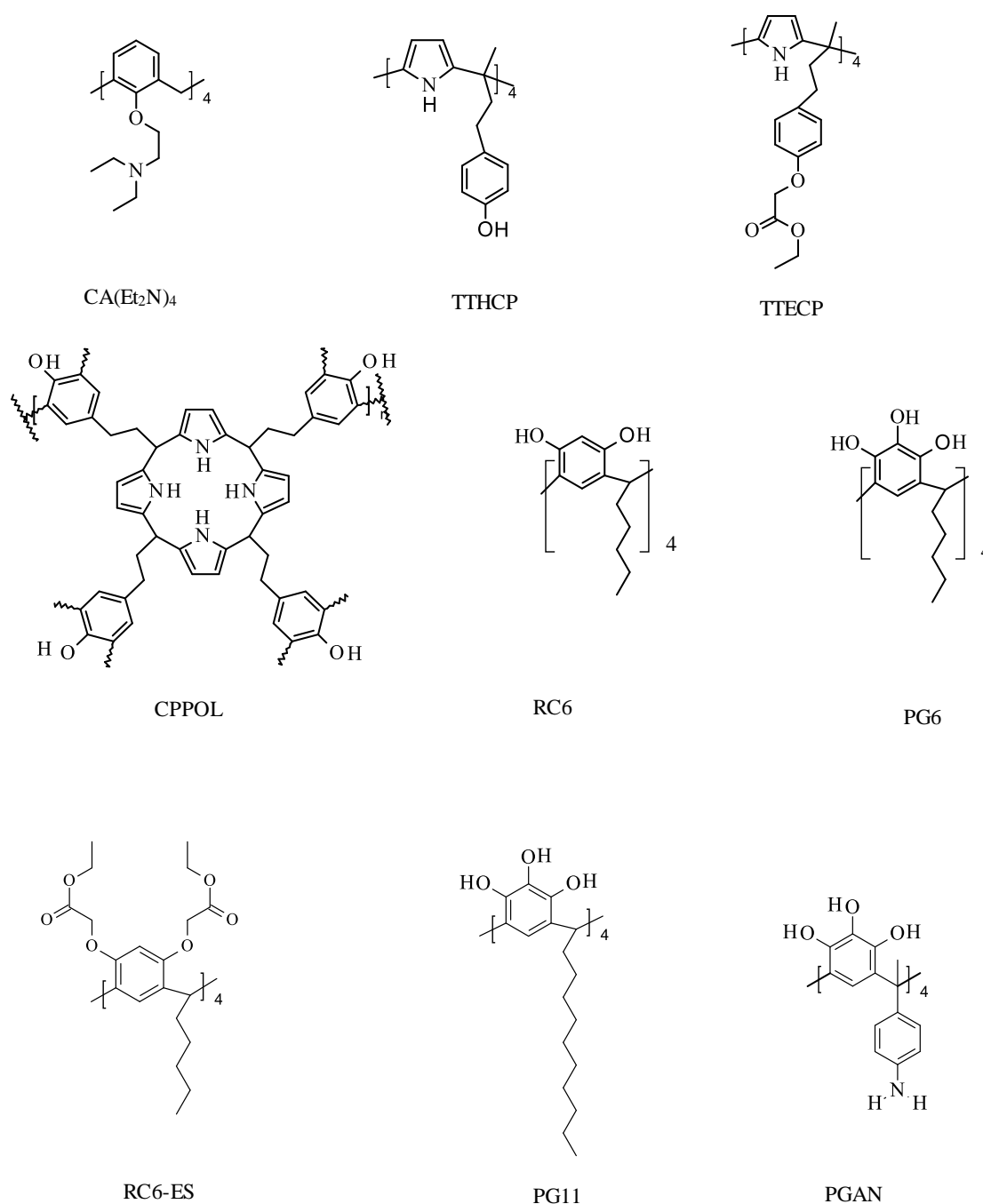


Fig. 1.49 Chemical structures of 25, 26, 27, 28-(diethylamino) ethoxy calix[4]arene [CA(Et₂N)₄], *meso*-tetramethyl-tetrakis-(4-hydroxyphenylethyl) calix[4]pyrrole (TTHCP), *meso*-tetramethyl-tetrakis-(4-ethylacetato-oxyphenylethyl) calix[4]pyrrole (TTECP), calix[4]pyrrole polymer (CPPOL), 2, 8, 14, 20-tetra-pentyl-1-resoc[4]arene (RC6), 4, 6, 10, 12, 16, 18, 22-octahydroxyl, (PG6), [4, 6, 10, 12, 16, 18, 22, 24-octa-oxy-ethylacetato-2, 8, 14, 20-tetrapentylresorc[4]arene (RC6-Es), 2, 8, 14, 20-tetraphenylpyrogallol[4]arene, 4, 5, 6, 10, 11, 12, 16, 17, 18, 22, 23, 24-dodecahydroxyl-2, 8, 14, 20-tetrapentylcalix[4]arene (PG6), C-decyl pyrogallol[4]arene (PG11)

Chapter II

Experimental Part

2.1 List of abbreviation

BCD	β -Cyclodextrin
BrCH ₂ Cl	Bromochloromethane
CA	Calix[4]arene
CA-(NH ₂) ₂	5,11, 17, 23-tetra- <i>p-tert-butyl</i> , 25, 27-bis[aminoethoxy], 26, 28-dihydroxycalix[4]arene
CA(CN) ₂	5, 11, 17, 23-tetra- <i>tert-butyl</i> , 25, 27-bis(2-cyanomethoxy)-26, 28-dihydroxycalix[4]arene
CD	Cyclodextrin
CD ₃ OD	Methanol-d ₄
CDCl ₃	Chloroform-d
CP	Calix[4]pyrrole
TTHCP	<i>meso</i> -tetramethyl-tetrakis-[2-(4-hydroxyphenyl)ethyl]calix[4]pyrrole
TTECP	Meso-tetramethyl-tetrakis-[2(4-ethylacetatophenoxy)ethyl]calix[4]pyrrole
$\Delta\delta$	Change in chemical shift
δ	Chemical shift (ppm)
DCM	Dichloromethane
DEPT	Distortionless Enhancement by Polarisation Transfer
DMF	<i>N,N</i> -Dimethylformamide
DMSO	Dimethyl sulfoxide
EtOAc	Ethyl acetate
H ₂ O ₂	Hydrogen peroxide

HCl	Hydrochloric acid
MHz	MegaHertz
LiAlH ₄	Lithium aluminum hydride
MeCN	Acetonitrile
MeOH	Methanol
MgSO ₄	Magnesium sulphate
NaOH	Sodium hydroxide
Na ₂ SO ₄	Sodium sulphate
NMR	Nuclear Magnetic Resonance
NMP	<i>N</i> -methyl-2-pyrrolidone
PG11	C-decyl pyrogallol[4]arene
P ₄ O ₁₀	Phosphorous pentoxide
ppm	Parts per million
Pyrogallol	1, 2, 3-Trihydroxybenzen
RC6	C-pentylresorc[4]arene
Resorcinol	1,3-Benzenediol
RC6-Es	4, 6, 10, 12, 16, 18, 22, 24-octa-oxy-ethylacetato-2, 8, 14, 20-tetrapentyl-resorcin[4]arene
Sol.	Solid
TEA	Triethylamine
THF	Tetrahydrofuran

TLC	Thin Layer chromatography
TMS	Tetramethylsilane
UV-vis	Ultraviolet-visible
Nano-ITC	Nano-Isothermal Titration Calorimetry
FTIR	Fourier transform infrared Spectroscopy
BET	Brunauer-Emmett-Teller
DSC	Differential Scanning Calorimetry
TGA	Thermogravimetric analysis
EDS	Energy Dispersive X-ray Spectroscopy
XRD	X-Ray Powder Diffraction

2.2 Chemicals

Chemicals used during the course of this research, abbreviations and sources are given as follows:

2.2.1 Solvents

Acetonitrile (MeCN), Fisher Scientific, HPLC grade, 99.99 %

Acetone (Me)₂CO, Sigma-Aldrich, 99 %

Chloroform (CHCl₃), Fisher Scientific, Reagent grade, 99 %

Dichloromethane (DCM), Sigma-Aldrich, ≥ 99 % (GC)

Diethylether, (Sigma-Aldrich), 99 %

Dimethyl sulfoxide (DMSO), Fisher Scientific, 99 %, E/0850/1

Ethanol (EtOH) Fisher Scientific, Reagent grade, 99.98 % v/v.

Ethyl acetate (EtAc), Sigma-Aldrich ≥ 99.5 %.

Hexanal, Sigma-Aldrich, 98 %

Hydrochloric acid, Fisher Scientific, 35-38 %, H/1150/PB17

Hexane (Hex), Fisher Scientific, Laboratory reagent grade, 95 %

Methanol (MeOH), Sigma-Aldrich, HPLC grade, 99.7 %.

N, N- Dimethylformamide (DMF), Sigma- Aldrich, anhydrous 99.8 %, 22705-6

1-Octanol, Acros organics, 99 %

Pyrogallol, Sigma-Aldrich, ≥ 99 %

Resorcinol, Sigma-Aldrich, 99 %

Silica 60 A, Fisher Scientific, 40-63 μm , S/0698/53

3-Aminopropyl- functionalised silica gel, 40-63 μm

Sulfuric acid, Sigma-Aldrich, 95-98 %

Tetrahydrofuran, (THF) Scientific, HPLC grade, 99.99

1-Methyl-2-pyrrolidone (NMP), Acros organics, 97 %

2.2.2 Deuterated solvents used in ^1H NMR experiments

Deuterated acetonitrile, CD_3CN , Cambridge Isotope Laboratories, Inc, (D, 99.8 %).

Deuterated chloroform, CDCl_3 , Cambridge Isotope Laboratories, Inc, (D, 99.8 %) + 0.05 % v/v TMS.

Deuterated methanol, CD_3OD , Cambridge Isotope Laboratories, Inc, (D, 99.8 %).

Deuterated dimethyl sulfoxide, $(\text{CD}_3)_2\text{SO}$, Cambridge Isotope Laboratories, Inc (D, 99.9 %)

2.2.3 Pharmaceuticals

1. Sodium diclofenac, Sodium {2-[(2,6-dichlorophenyl)amino]phenyl} ethanoate $\text{C}_{14}\text{H}_{10}\text{Cl}_2\text{NNaO}_2$

2. Clofibric acid, 2-(4-Chlorophenoxy)-2-methylpropanoic acid $\text{C}_{10}\text{H}_{11}\text{ClO}_3$, 97 %, Aldrich

3. Carbamazepine, 5H-Dibenz[b, f]azepine-5-carboxamide, $\text{C}_{15}\text{H}_{12}\text{N}_2\text{O}$, Sigma-Aldrich

4. Aspirin (Acetylsalicylic acid), Sigma-Aldrich
5. Ibuprofen (RS)-2-(4-(2-methyl propyl) phenyl) propanoic acid; $C_{13}H_{18}O_2$, $\geq 98\%$ Sigma-Aldrich.

2.2.4 Analytical Reagents

Reagents used in the synthesis (without further purification).

β -Cyclodextrin, Sigma-Aldrich, $\geq 97\%$

P-tert-butyl calix[4]arene, $C_{44}H_{56}O_4$ $\geq 97\%$ HPLC, Sigma- Aldrich

18-Crown-6, 18-C-6, $C_{12}H_{24}O_6$, Fluka, 99 %.

Pyrrrole reagent grade, Sigma-Aldrich, 98 %

4-[4-hydroxyphenyl]-2-butanone $C_{10}H_{12}O_2$, Sigma-Aldrich $\geq 98\%$)

Magnesium sulphate anhydrous $MgSO_4$, Fisher Scientific

Potassium carbonate anhydrous, K_2CO_3 , Fisher Scientific, 99.99 %

Sodium hydride, NaH, Sigma-Aldrich, 95 %

Sodium azide, NaN_3 , Sigma-Aldrich, $\geq 99.99\%$

Lithium aluminium hydride, $LiAlH_4$, Sigma-Aldrich, 95 %

Acetic acid, CH_3COOH , Fisher Scientific, glacial analytical reagent grade 99.7 %.

Bromoacetonitrile, $BrCH_2CN$, Aldrich, 97 %.

Phenol, C_6H_5OH , Sigma-Aldrich, $> 99\%$

Ethyl bromoacetate, $BrCH_2COOC_2H_5$, Sigma-Aldrich, $> 98\%$

4-*tert*-Butylphenol, $(CH_3)_3CC_6H_4OH$ Fluka, $\geq 97\%$

Triethylamine, $(C_2H_5)_3N$ Sigma-Aldrich, $\geq 99.5\%$

Tin (IV) chloride $SnCl_4$, Sigma- Aldrich, 98 %

(2-Diethylamino) ethylchloride hydrochloride, $(C_2H_5)_2N(CH_2)_2Cl \cdot HCl$, Aldrich-Sigma.

(+)-Sodium L-ascorbate, $C_6H_7NaO_6$, Sigma-Aldrich $\geq 98\%$

Lead (II) perchlorate trihydrate, $Pb(ClO_4)_2 \cdot 3H_2O$, Aldrich –Sigma.

Lithium perchlorate, $LiClO_4$, Aldrich –Sigma.

Mercury (II) perchlorate hydrate, $Hg(ClO_4)_2 \cdot xH_2O$, Aldrich –Sigma, 99.99 %

Methanesulfonyl chloride, CH_3CO_2Cl , Sigma-Aldrich, 99.7 %

Potassium chloride, KCl , Fisher Scientific, 99%

Sodium chloride, $NaCl$, Fisher Scientific 99 %

pH buffer tablets from Fisher Scientific

Magnesium (II) perchlorate hexahydrate, $Mg(ClO_4)_2 \cdot 6H_2O$, Aldrich –Sigma.

Sodium perchlorate monohydrate, $NaClO_4$, Sigma-Aldrich

Strontium (II) perchlorate, $Sr(ClO_4)_2$, Sigma-Aldrich

Zinc (II) perchlorate hexahydrate, $Zn(ClO_4)_2 \cdot 6H_2O$, Aldrich –Sigma.

2.2.5 Purification of Solvents ^[194]

1. Acetonitrile, MeCN, was refluxed under a nitrogen atmosphere and distilled over calcium hydride. The middle fraction of the distilled solvent was collected
2. Tetrahydrofuran, THF, was stored over a sodium metal wire for 24 hours. Then it was distilled under nitrogen, using benzophenone as an indicator
3. Toluene was treated with anhydrous calcium chloride, filtered and then placed over metallic sodium in a round-bottomed flask fitted with a reflux condenser protected by a drying tube containing calcium chloride. Then it was refluxed for two hours. The middle fraction of the distilled solvent was collected and used.
4. N, N-Dimethylformamide, DMF, was dried using molecular sieves for 24 hours and then it was refluxed under reduced pressure. Only the middle fraction of the purified solvent was collected.

2.2.6 Instruments used

1. ^1H -NMR spectra were taken on a Bruker AC-500 NMR spectrometer.
2. ^1H NMR spectra Bruker AC-300 MHz
3. UV-visible spectrophotometry measurements were taken on a Cecil CE7200 spectrophotometer.
4. Conductance measurements were carried out by Wyne Keer LCR Meter 4300
5. The isothermal Titration Calorimeter ITC type TA Nano-calorimeter
6. Differential scanning calorimeter DSC, Instrument DSC Q1000 V9.9 Build 303
7. Thermogravimetric analysis, Instrument TGA Q 500, V6.7 Build 203
8. FTIR Spectrometer type Agilent technologies, Cary 600 series
9. Scanning electron microscope, SEM analysis, Mechanical Engineering Sciences, FEPS
10. AB 15 pH meter Fisher Scientific (AB 15 pH Meter Fisher Scientific)
11. BET analysis by Gemini model V2.00

2.3 Solubility measurements

2.3.1 Solubility of selected pharmaceuticals in different organic solvents at 298.15 K

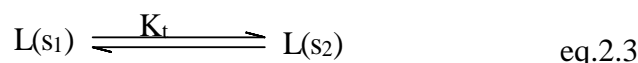
The solubility of a solid is defined as an equilibrium state between the solid and its saturated solution at constant pressure and temperature (eq.2.1). Addition to the temperature and the pressure, the solubility correlates with the lattice energy holding the crystals together in the crystal structure and the polarity of solvents. The solubility of a substance has significant importance in a number of scientific fields like medical applications and pollutants transportations. The determination of the solubility of a substance leads to the calculation a number of parameters such as the solution Gibbs energy $\Delta_s G$, the enthalpy $\Delta_s H$ and therefore the entropy $\Delta_s S$. In general, the equilibrium state between a ligand L as solid (sol.) and its saturated solution (s) can be expressed in the following equation (eq.2.1)



This enabled to calculate the solubility s (mol dm^{-3}) of the solid in different solvents. For a non-electrolyte, L, the standard Gibbs energy of solution, $\Delta_s G^\circ$, can be calculated from the following equation (eq.2.2)

$$\Delta_s G^\circ = -RT \ln [L]_s \quad \text{eq.2.2}$$

The more negative the value obtained for $\Delta_s G^\circ$, the greater the solubility is. When investigating the solubility in a number of different solvents the required standard Gibbs energy of transfer $\Delta_t G^\circ$ from one solvent s_1 to another s_2 can be calculated from the following process:



Hence,

$$\Delta_t G^\circ = -RT \ln K_t = \Delta_s G^\circ (s_2) - \Delta_s G^\circ (s_1) \quad \text{eq.2.4}$$

In this equation K_t denotes the thermodynamic transfer constant, R is the gas constant ($8.314 \text{ J K}^{-1} \text{ mol}^{-1}$) and T is the absolute temperature in Kelvin. In doing so the contribution of the crystal lattice energy is eliminated. Therefore, it is possible to assess the difference in the solvation of the pharmaceutical in the two solvents. The pharmaceuticals were first tested in different solvents to investigate if these undergo solvation. Solvation experiments were carried out by exposing separately

pre-weighed crucibles containing the pharmaceutical to a saturated environment of different solvents in desiccators for several days. The crucibles were then weighed to check the uptake of solvent by the solid. From solubility data, $\Delta_s G^\circ$ were calculated for the samples when the compound was not altered by solvation¹⁹⁵⁻¹⁹⁷. The solvents investigated for the possibility to obtain solubility data were water, methanol, ethanol, acetonitrile, dichloromethane, chloroform, 1-octanol, dimethylsulphoxide and N, N-dimethylformamide.

The analytical technique used to determine the concentration of the drug in the saturated solution was UV spectrophotometry

2.3.2 Calibration curve for the analysis of pharmaceuticals

Stock solutions were made by dissolving a known amount of each pharmaceutical in the appropriate solvent, different volumes were taken and diluted in volumetric flasks (10 ml). Samples were measured using spectrophotometric measurements in the ultraviolet region. Calibration curves were obtained when absorbances, A , were plotted against molar concentration (mol dm^{-3}). The linear relationship (higher R values) obtained were used to determine the unknown concentration of the pharmaceutical in the saturated solution¹⁹⁸

2.3.3 Solubility of selected pharmaceuticals

Saturated solutions of targeted pharmaceutical (sodium diclofenac, aspirin, and clofibrac acid) in different solvents were mixed for one minute on a whirlimixer, sealed and left to equilibrate overnight in a water bath at 298.15 K. The solutions were filtered through a 0.22 Millipore and a known volume of each solution (2 ml) was transferred to an UV cell and diluted volumetrically with the respective solvent to obtain absorbance values in the linear range of the calibration curve for each system. All the experimental results are an average of at least three independent measurements. From the absorbance values, the concentration of the drug in the saturated solution was obtained by the use of the Beer's-Lambert law^{198,199}.

2.4 Determination of partition coefficients of selected drugs in the water-1-octanol solvent system

The partition coefficient (K_p) is calculated from the ratio of concentration of a solute in two partially or completely immiscible phases at equilibrium. This parameter is essential in many applications such as distribution of drugs between two immiscible layers and it is used to know the distribution of

chemicals in the environment. Usually one of the solvents is water, the other is a non-aqueous solvent such as 1-octanol. The partition coefficient K_p can be expressed by the following equation (eq.2.5)

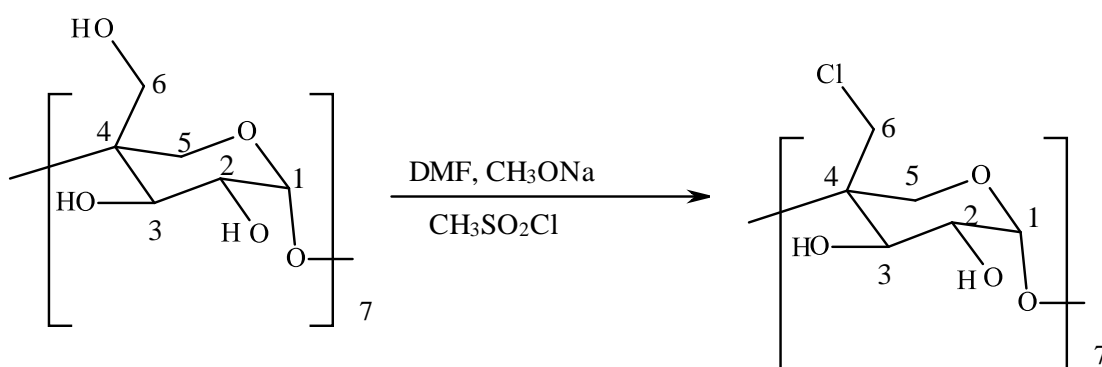
$$K_p = \frac{[D]_{org}}{[D]_{aq}} \quad \text{eq.2.5}$$

In this equation $[D]_{org}$ and $[D]_{aq}$ represents the molar concentration of the drug in the organic and aqueous phase respectively. For the determination of K_p , both solvents were mutually saturated with each other to avoid volume changes when mixed. The pharmaceuticals were dissolved in 1-octanol saturated with water. Equal volumes of solvents were mixed and left to equilibrate overnight at 298 K. The two phases were separated and the concentration of the drug in the aqueous phase was determined by UV/Vis spectrophotometry²⁰⁰.

2.5 Synthesis of the receptors

2.5.1 Synthesis and characterization of heptakis-(6-chloro-6-deoxy)- β -cyclodextrin(CIBCD)²⁰¹

The procedure used to synthesise heptakis-(6-chloro-6-deoxy)- β -cyclodextrin is shown in Scheme 2.1



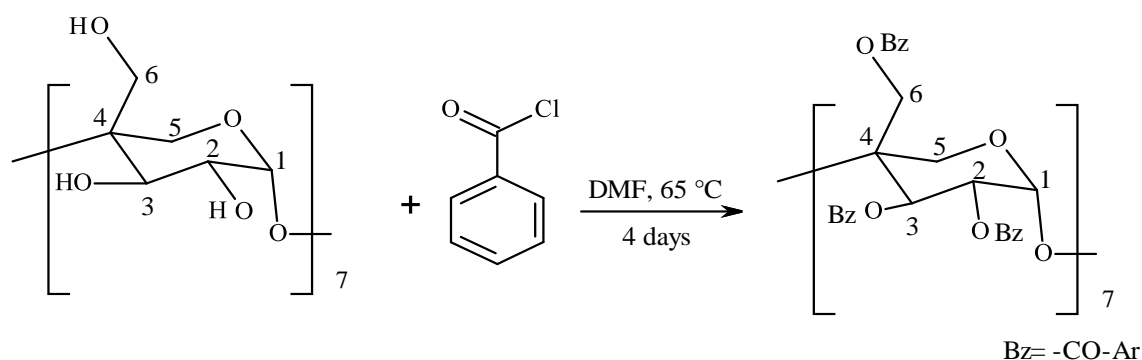
Scheme 2.1 Synthesis of heptakis-(6-chloro-6-deoxy)- β -cyclodextrin

In a three-necked round bottomed flask containing a solution of β -cyclodextrin (10.04 g, 8.81 mmol) in DMF, methanesulfonyl chloride (24.8 g, 230 mmol) was added and stirred at 65 °C for 4 days. The solvent was evaporated using a rotary evaporator. The residue was dissolved in methanol and

neutralized with sodium methoxide (3 M). The product was precipitated in ice water, the white solid obtained was filtered out and washed with cold methanol and dried under vacuum at 55 °C. ^1H NMR (500 MHz, d_6 -DMSO), δ in ppm, 5.96 (d, 1 H, 2-OH), 5.82 (s, 1 H, 3-OH), 4.94 (d, 1 H, 1-H), 4.13 – 3.89 (m, 2 H, 5-H, 3-H), 3.84 – 3.75 (m, 2 H, 4-H, 2-H), 3.61 (t, 1 H, 6a-H), 3.35 (s, 2 H, 6b-H), ^{13}C NMR (DMSO- d_6), δ in ppm, 102.04 (1-C), 83.57 (4-C), 72.43 (3-C), 71.96 (2-C), 71.17 (5-C), 44.95 (6-C). Appendix (Figs. 1-B & 2-B)

2.5.2 Synthesis of heptakis-(2, 3 , 6-tri-o-benzoyl)- β -cyclodextrin (BzBCD)²⁰¹

The compound was synthesised according to Scheme 2.2



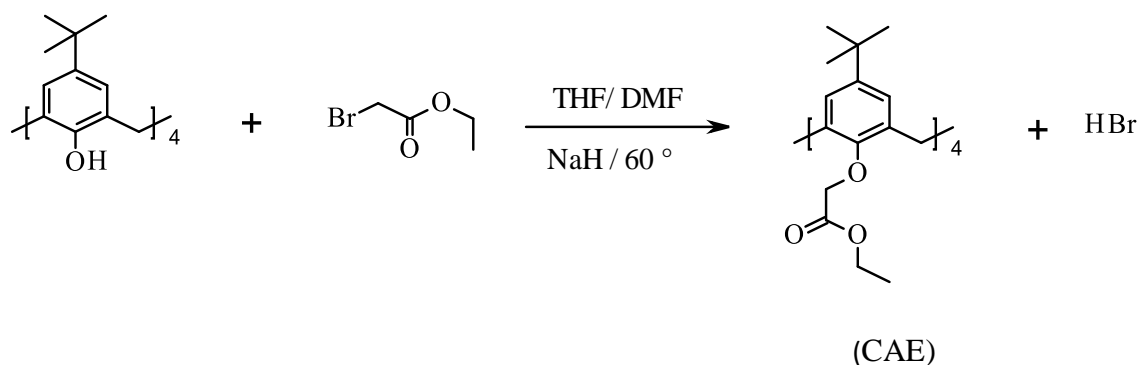
Scheme 2.2 Synthesis of heptakis-(2, 3 , 6-tri-o-benzoyl)- β -cyclodextrin

The synthesis of the perbenzoylated cyclodextrin was accomplished as described by Guillo *et al* ¹⁹⁸ . To a solution of β -cyclodextrin (5 g, 4.4 mmol) dissolved in DMF , benzoyl chloride (3.2 g, 0.45 mmol) was added and stirred at 65 °C for 4 days. The solvent was evaporated using a rotary evaporator, the residue was dissolved in methanol and neutralized with sodium methoxide (3 M) .The product was precipitated from ice water , filtered out and washed with methanol . The product was vacuum-dried at 55 °C and was obtained as a white solid. ^1H NMR (d_6 -DMSO), δ in ppm, 4.42 (H₄, 7 H), 4.9 (H₅ and H₆, 14 H), 5.13 (H₂, 7 H), 5.56 (H₆, 7 H), 5.75 (H₁, 7 H), 5.85 (H₃, 7 H), (Appendix, Fig. 3-B) Elemental analysis was carried out at the University of Surrey, calculated %, C; 67.5, H; 4.79, N; 0.0. Found %, C; 67.68, H; 4.53, N; 0.0.

2.5.3 Synthesis of 5, 11, 17, 27- *tert*-butyl-25, 26, 27, 28-(oxy-ethylethanoate) calix[4]arene (CAE)²⁰²

A new modified procedure has been carried out in the Thermochemistry Laboratory to synthesise the

compound according to the following Scheme



Scheme 2.3 Synthesis of 5, 11, 17, 27-*tert*-butyl-25, 26, 27, 28-(ethylacetoxyl) calix[4]arene (CAE)

In a 500 ml three-neck round bottom flask and under a nitrogen gas atmosphere, *p*-*tert*-butyl-calix[4]arene (5 g, 7.72 mmol) was dissolved in a mixture of freshly distilled THF and dry DMF (60:40, v/v), then sodium hydride (0.36 g, 0.016 mmol) was added carefully to the reaction mixture and stirred for 30 minutes. This was followed by the dropwise addition of ethyl bromoacetate (5.14 g, 3.78 mmol) to the reaction solution. The mixture was heated in an oil bath at 60 °C and followed by thin layer chromatography using a mixture of DCM: MeOH (7: 3 v/v) as the developing solvent mixture. After completion, the reaction was stopped and cooled down to room temperature, the resultant solution was filtered and the solvent evaporated using a rotary evaporator. A brown viscous product was obtained, dissolved in 100 ml dichloromethane and transferred to a separation funnel, washed with distilled water and then with brine. The organic layer was separated and dried over anhydrous magnesium sulphate, the mixture was filtered and the solvent evaporated under reduced pressure. A viscous colourless liquid was obtained. The crude product was dissolved in methanol and sonicated to break the oil. A white powder was obtained and filtered. Further purification was carried out by dissolving the product using a MeOH: DCM (15: 1) mixture which was refrigerated. Large needle-like crystals were obtained. Yield 5.5 g, 71.6 %, ¹H NMR (500 MHz in CDCl₃), δ in ppm, 6.77 (s, 8 H, Ar-H), 4.85 (d, 4 H, C-H_{axial}), 4.8 (s, 8 H, O-CH₂-CO), 4.2 (q, 8 H, O-CH₂CH₃), 3.19 (d, 4 H, C-H_{equatorial}), 1.28 (t, 12 H, CH₃), 1.05 (s, 36 H, CH₃), (Fig. 4-B- Appendix)

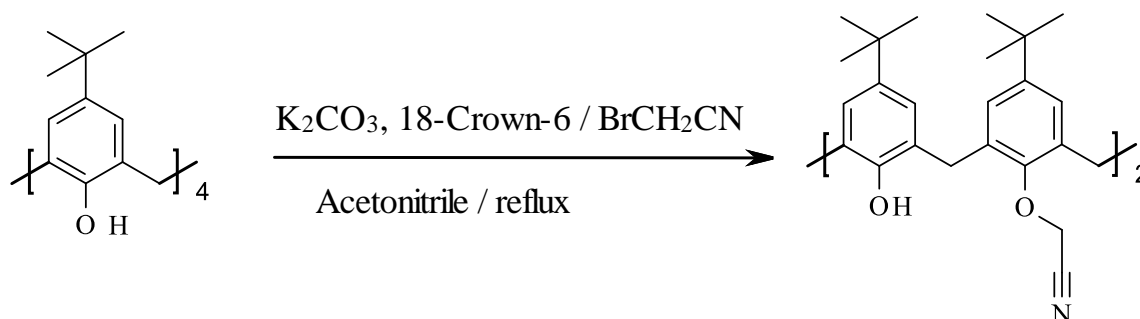
¹³C NMR (500 MHz in CDCl₃), δ in ppm, 14.22, 31.6, 33.38, 60.30, 71.34, 125.35, 133.46, 145.15, 152.59, 170.54

Microanalysis (C₆₀H₈₀O₁₂, M. Wt, 993.27) was carried out at the University of Surrey calculated % ; C; 72.58, H; 8.06, N 0.0. Found %: C, 72.35, H; 8.12, N; 0.0

Melting point: 155 °C, TGA and DSC analysis were carried out at the University of Surrey

2.5.4 Synthesis of 5, 11, 17, 23- tetra-*tert*-butyl, 25, 27-bis (2-cyanomethoxy)-26, 28-dihydroxycalix[4]arene (CA-(CN)₂)^{203,204}

The compound was synthesised according to the following Scheme

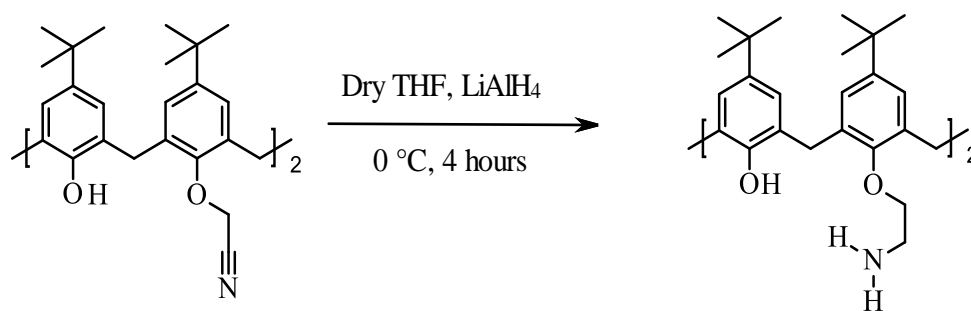


Scheme 2.4 Synthesis of 5, 11, 17, 23-tetra- *tert* -butyl, 25, 27 bis [2-cyanomethox] methoxy, 26, 28 -dihydroxycalix[4]arene

In a three-neck round bottom flask (500 ml) containing a magnetic stirrer at room temperature under a nitrogen gas atmosphere, *p-tert*-butyl calix[4]arene (10.293 g, 15.862 mmol), 18-crown-6 (1.004 g, 3.799 mmol) and potassium carbonate (18.087 g, 130.87 mmol) was dissolved in dry acetonitrile (200 ml). Bromoacetonitrile (7.394 g, 61.643 mmol) dissolved in acetonitrile (20 ml) was added dropwise. The reaction mixture was heated in an oil bath at 75 °C and refluxed for 24 hours under vigorous stirring. The reaction was monitored by thin layer chromatography using a mixture of hexane: ethyl acetate (8: 2) as the developing solvent. After 24 hours, the reaction mixture was allowed to cool to room temperature. The solvent was evaporated by a rotary evaporator and a yellow solid was obtained. The solid was dissolved in DCM, filtered gravitationally and the solvent was removed under reduced pressure, methanol was added to the resulting oil which was sonicated to break the oil. Afterwards the solid was filtered and washed with cold methanol. The solid was left in a vacuum drier at 90 °C. The product obtained in 70% yield was characterised by ¹H NMR spectroscopy. ¹H NMR (500 MHz, in CDCl₃), δ in ppm, 7.11 (s, Ar-H, 4 H), 6.72 (s, Ar-H, 4 H), 5.540 (s, OH, 2 H), 4.80 (s, O-CH₂, 4 H), 4.19 (d, CH_{axial}, 4 H), 3.42 (d, CH_{equatorial}, 4 H) 1.34 (s, CH₃, 18 H), 0.87 (s, CH₃, 18 H). (Fig.5-Appendix)

2.5.5 Synthesis of 5, 11, 17, 23-tetra-*p-tert*-butyl, 25, 27-bis[aminoethoxy], 26, 28-dihydroxycalix[4]arene [CA-(NH₂)₂]²⁰⁵

The compound was synthesised according to the following Scheme

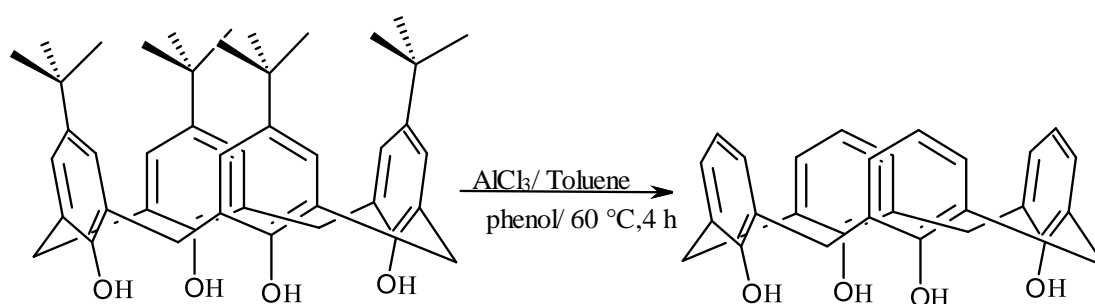


Scheme 2.5 Synthesis of 5, 11, 17, 23-tetra-*tert*-butyl, 25, 27-bis [aminoethoxy]-26, 28 dihydroxycalix[4]arene.

A solution of CACN (9 g, 21.45 mmol) was dissolved in dry THF (100 ml) and stirred in an ice bath until the temperature reached 0 °C, LiAlH₄ (1.896 g, 49.95 mmol) was dissolved in freshly dried THF, then added dropwise to the reaction mixture with continuous stirring for four hours and the temperature was kept at 0 °C. After completion, the reaction was monitored using TLC and hexane and ethyl acetate (8: 2, v/v) as the developing solvent. An aqueous solution of sodium hydroxide (10 ml, 20 %) was added, followed by distilled water (10 ml). A white precipitate was obtained. The undesired white precipitate was filtered gravitationally and the solvent was evaporated by using a rotary evaporator to obtain a white solid which was dried in a vacuum drier at 90 °C. The product obtained in 60 % yield was characterised by ¹H NMR spectroscopy, (500 MHz, in CDCl₃), δ in ppm, 7.03 (s, Ar-H, 4 H), 6.96 (s, Ar-H, 4 H), 5.2 (s, OH, 2 H), 4.34 (d, Ar-CH_{axial}-Ar, 4 H), 4.06 (t, OCH₂CH₂N, 4 H), 3.37 (d, Ar-CH_{equatorial}-Ar, 4 H), 3.3 (t, -O-CH₂-CH₂-N, 4 H), 1.2 (s, CH₃, 18 H), 1.09 (s, CH₃, 18 H). Fig. 6 Appendix -B

2.5.6 Synthesis of 25, 26, 27, 28-tetrahydroxycalix[4]arene²⁰⁶

The synthesis was carried out according to Scheme 2.6

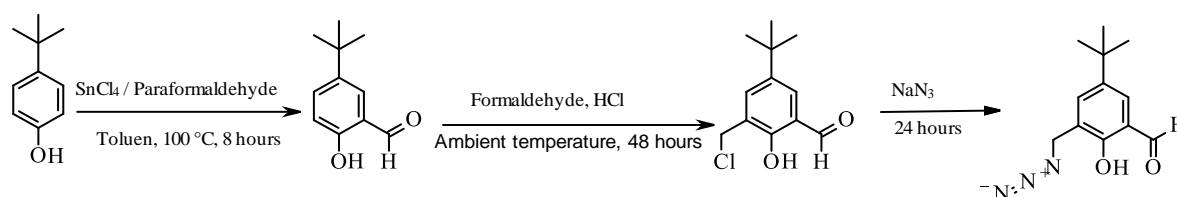


Scheme 2.6 Synthesis 25, 26, 27, 28-tetrahydroxycalix[4]arene

In a three-neck round bottom flask, a mixture of 4-*tert*-butylcalix[4]arene (5.13 g, 7.7 mmol) and phenol (4.35 g, 46.2 mmol) were dissolved in dry toluene (100 ml), stirred for 30 minutes at room temperature under a nitrogen gas atmosphere. Aluminium chloride (6.09 g) was added and the reaction mixture was stirred at 60° C for 6 h. The reaction was monitored by TLC using a hexane: ethyl acetate (8: 2) mixture as the developing solvent mixture. After completion of the reaction the mixture was cooled to room temperature, hydrochloric acid (100 ml, 0.2 M) was added dropwise and stirred for 30 minutes until the white precipitate disappeared. The reaction mixture was then transferred to a separating funnel. The upper organic layer was collected and the solvent was rotary evaporated. Then methanol (50 ml) was added to the concentrated mixture to obtain a white precipitate which was then recrystallized from methanol and dried over a vacuum oven. (3.02 g, 90 %). The compound was characterised by ¹H NMR spectroscopy in CDCl₃, δ in ppm, 10.18 (s, OH, 4 H), 7.05 (d, Ar-H, 8 H), 6.7 (t, Ar-H, 4 H), 4.25 (d, CH_{axial}, 4 H), 3.46 (d, CH_{equatorial}, 4 H) (Fig. 7 Appendix B)

2.5.7 Synthesis and characterization of 5-*tert*-butyl-3-azidomethyl-2-hydroxybenzaldehyde (AzAr)

The preparation of this receptor was carried out in three steps according to the following Scheme



Scheme 2.7 Synthesis and characterization of 5-*tert*-butyl-3-azidomethyl-2-hydroxybenzaldehyde

2.5.8 Synthesis and Characterization of 5-*tert*-butyl-2-hydroxybenzaldehyde²⁰⁷

The SnCl₄ (1.07 g, 4.1 mmol) was added to a magnetically stirred solution containing *p*-*tert*-butylphenol (6.01 g, 40 mmol) in dry toluene. Tri-*n*-butylamine was added dropwise to the reaction mixture with continuous stirring for 20 minutes. To the reaction mixture, paraformaldehyde (2.43g, 81 mmol) was added and the mixture was refluxed for 8 hours. After cooling the reaction mixture to room temperature, the solution was transferred into a separating funnel and then extracted with

diethyl ether (2×50 ml). The combined organic layer was washed with saturated brine and then dried over anhydrous sodium sulphate. The product formed was purified by a silica gel column chromatography using a hexane: chloroform (1: 1) mixture as eluent. Yield (4.5 g, 63 %), a yellow liquid was obtained upon evaporation of the solvents, ^1H NMR (500 MHz in CDCl_3), δ in ppm, 1.27 (s, 9 H), 6.76 (s, 1 H), 7.57 (d, 1 H), 7.50 (dd, 1 H), 9.89 (s, 1 H, aldehyde), 10.80 (s, 1 H, OH). Fig. 8-B Appendix

2.5.9 Synthesis and characterization of 5-*tert*-butyl-3-chloromethyl-2-hydroxybenzaldehyde²⁰⁸

A concentrated hydrochloric acid (12 M, 125 ml) was added to a mixture of 5-*tert*-butyl-2-hydroxybenzaldehyde (5.0 g, 28 mmol) and formaldehyde (25 ml, 35 %) in methanol and the solution was stirred for 2 days at room temperature. Water was added to the mixture, the product was extracted into dichloromethane (3×40 ml), and the organic layer was dried over anhydrous sodium sulphate. The dichloromethane was then evaporated under reduced pressure to afford the pure product as a yellow liquid. Yield (5.2 g, 82 %). ^1H NMR (500 MHz in CDCl_3), δ in ppm, 1.34 (s, 9 H), 4.70 (s, 2 H), 7.52 (d, 1 H), 7.67 (d, 2 H), 9.90 (s, 1 H), 11.28 (s, 1 H). Fig. 9B-Appendix

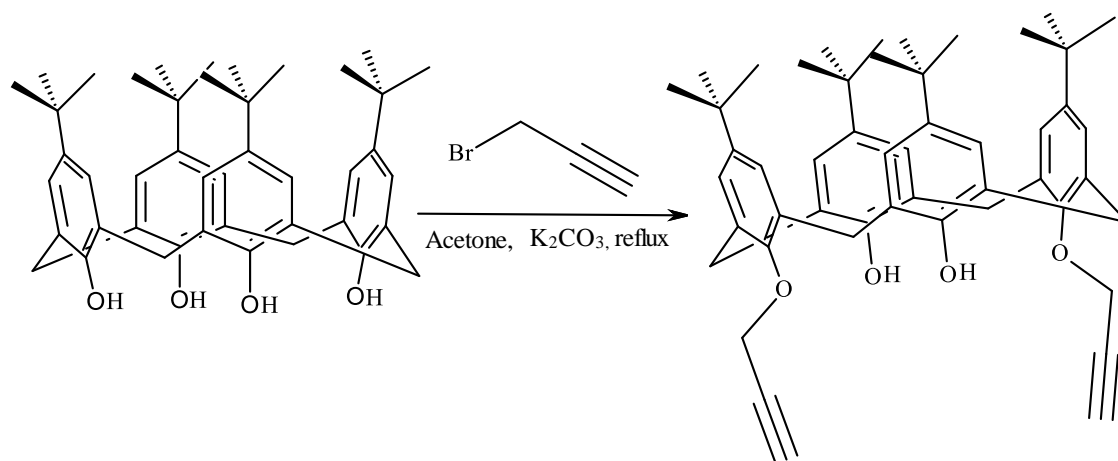
2.5.10 Synthesis of 5-*tert*-butyl-3-azidomethyl-2-hydroxybenzaldehyde²⁰⁸

The 5-*tert*-butyl-3-chloromethyl-2-hydroxybenzaldehyde (2.65 g, 11.89 mmol) was added to a solution of sodium azide (1.519 g, 23.37 mmol) in dimethylformamide (30 ml) under stirring for 12 hours. A mixture of water and ethyl acetate (100 ml, 50 %, v/ v) was added to the reaction mixture. The organic layer was separated and washed with water and brine. A yellow liquid was obtained upon evaporation of the organic solvent. Yield 89 %.

^1H NMR (500 MHz, CDCl_3), δ in ppm, 11.28 (broad s, 1 H), 9.9 (s, 1 H), 7.57 (dd, 1 H), 7.52 (s, 1 H), 4.45 (s, 2 H), 1.28 (s, 9 H). Fig. 10-B Appendix

2.5.11 Synthesis and characterization of 25, 27-dihydroxy-26-28-(dioxypargyl) *tert*-butylcalix[4]arene (ArCH)²⁰⁸

The synthesis of the compound was carried out according to the following Scheme



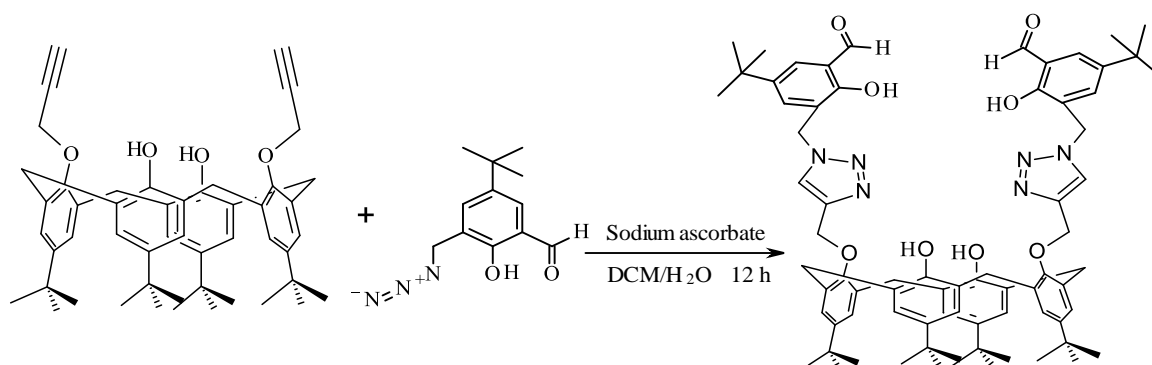
Scheme 2.8 Preparation of 25, 27-dihydroxy-26, 28-(dioxypargyl)-*tert*-butylcalix[4]arene

In a three-neck round bottom flask and under inert conditions, anhydrous potassium carbonate (5.1 g, 36.72 mmol) and *p-tert*-butylcalix[4]arene (10 g, 15.43 mmol) were dissolved in dry acetone (200 ml) and stirred at room temperature for 1 hour. A solution of propargyl bromide (6.49 g, 30.8 mmol) in acetone (50 ml) was added dropwise over a period of 30 minutes. The reaction mixture was refluxed for 24 hours and then cooled down to room temperature. The reaction mixture was filtered and then concentrated. Hydrochloric acid (100 ml, 2 M) was added and the product was extracted by dichloromethane (3 x 100 ml). The organic layer was separated, washed with water and then with brine, collected and dried over anhydrous sodium sulphate, filtered and the solvent evaporated by a rotary evaporator. The crude product was recrystallized from a dichloromethane: methanol (4: 1) mixture to afford a white solid (9.10 g, 82 % yield). ¹H NMR (500 MHz, in CDCl₃), δ in ppm, 7.07 (s, 4 H), 6.72 (s, 4 H), 6.46 (s, 2 H), 4.74 (d, 4 H), 4.73 (d, 4 H), 3.32 (d, 4 H), 2.54 (t, 2 H, alkyne), 1.30 (s, 18 H), 0.89 (s, 18 H). Fig. 11-B Appendix

Microanalysis was carried out at the University of Surrey, calculated %: C; 82.7, H; 8.27. Found %: C; 82.76, H; 8.36

2.5.12 Synthesis and characterization of 4-*tert*-butyl-azidocalix[4]arene²⁰⁸

The compound was synthesised according to the following Scheme



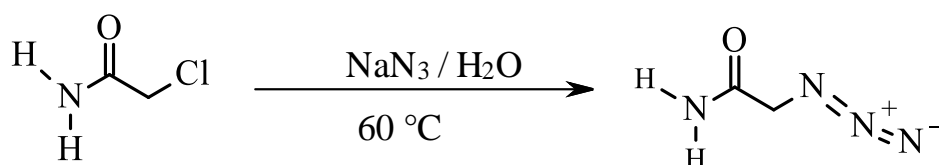
Scheme 2.9 Preparation of 4-*tert*-butyl-azidocalix[4]arene

Compound CAD (3.0 g, 4.14 mmol) was added to a solution of propargylated *p*-*tert*-butylcalix[4]arene (2.12 g, 9.53 mmol) in a mixture of dichloromethane and water (100 ml, 50: 50 v/v), then copper (II) sulphate pentahydrate, $\text{CuSO}_4 \cdot 5\text{H}_2\text{O}$ (0.124 g, 0.50 mmol) and sodium ascorbate (328.0 mg, 1.70 mmol) were added to the above reaction mixture and stirred for 12 hours at room temperature. After completion, the reaction mixture was transferred to a separation funnel and the organic layer was separated. The aqueous layer was extracted with dichloromethane (2×50 mL). The combined organic layer was washed with water and then with brine (2×100 mL) and dried over anhydrous sodium sulphate Na_2SO_4 , filtered and the solvent was evaporated by a rotary evaporator. The resulting product was purified by triturating with hexane and then the precipitate was filtered. Yield: 89.91%. ^1H NMR (CDCl_3 , 500 MHz), δ in ppm, 11.25 (s, 2 H), 9.83 (s, 2 H), 8.05 (s, 2 H), 7.63 (s, 2 H) 7.49 (d, 2 H), 7.21 (s, 2 H), 6.98 (s, 4 H), 6.73 (s, 4 H), 5.46 (s, 2 H), 5.2 (s, 2 H), 4.16 (d, 4 H), 3.16 (d, 4 H), 1.27 (s, 18 H), 1.26 (s, 18 H), 0.96 (s, 18 H). Fig. 12-B Appendix.

Microanalysis was carried out at the University of Surrey, calculated %: C; 74.6, H; 7.5, N; 7.05. Found %: C; 73.97, H; 7.84, N; 6.73

2.5.13 Preparation of 2-azidoacetamide²⁰⁹

The compound was prepared according to Scheme 2.10

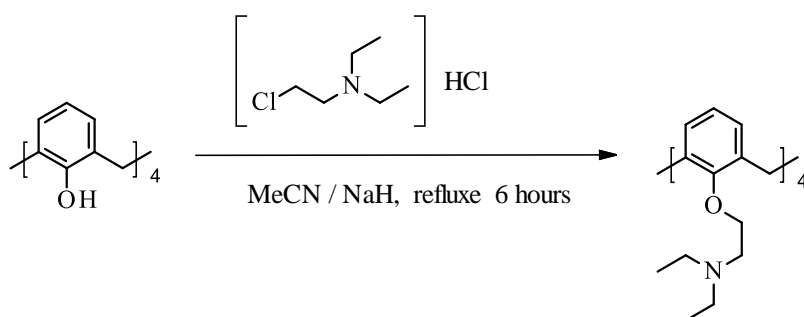


Scheme. 2.10 Preparation of 2-azidoacetamide.

In a three-neck round bottom flask, an aqueous solution of sodium azide (4 g, 61.5 mmol) was added slowly to 2-chloroacetamide (5 g, 126.5 mmol) in 100 ml of water. The reaction mixture was refluxed in an oil bath for 17 h at 60°C. The reaction mixture was allowed to cool. It was then concentrated and extracted by ethylacetate. The solvent was evaporated and the white solid product was recrystallized from diethyl ether to afford white crystals of 2-azidoacetamide. The yield was 87 %, mp: 57-58 °C, ¹H NMR (500 MHz, in CDCl₃), 3.9 (CH₂), 5.5-6.3 (d, NH₂). Fig. 13-B Appendix IR ν_{max} (cm⁻¹) 3371 and 3183 (N-H) Str., 2980-2910 (C-H) str., 2105 (N₃) str., 1622 and 1411 (C=O) str.

2.5.14 Synthesis of 25, 26, 27, 28-(diethylamino) ethoxycalix[4]arene CA-(NH₂)₄²¹⁰

The synthesis of 25, 26, 27, 28-(diethylamino)ethoxy calix[4]arene was carried out according to the following Scheme



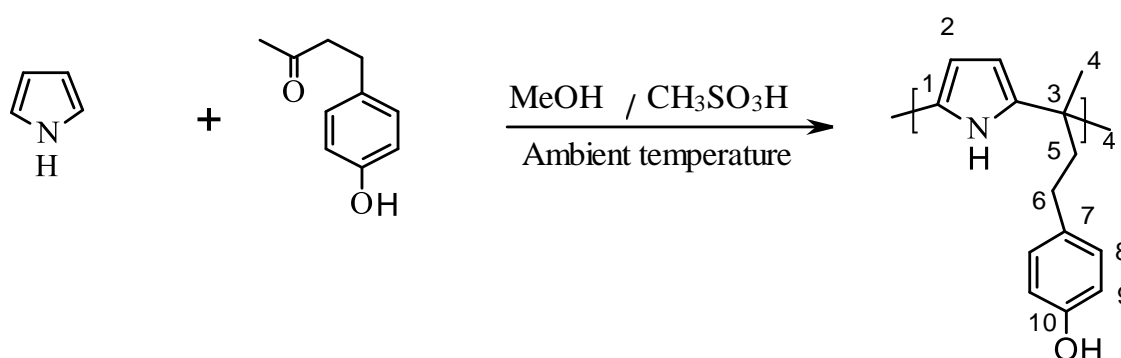
Scheme 2.11 Synthesis of 25, 26, 27, 28-(diethylamino)ethoxy calix[4]arene

A solution of 25, 26, 27, 28-tetrahydroxycalix[4]arene (2.52 g, 5.52 mmol) and sodium hydride (2.12 g, 88.36 mmol) was prepared in a THF: DMF (80: 20) solvent mixture (150 ml) under a nitrogen atmosphere. The mixture was stirred at 25 °C for 30 minutes. Then 2-diethylamino ethylchloride hydrochloride (6.09 g, 35.4 mmol) was added over a period of 30 minutes. The mixture was stirred for 6 hours at 80 °C. The progress of the reaction was monitored by TLC using a DCM: MeOH (9: 1) mixture. Following the completion of the reaction, the mixture was allowed to cool down to room temperature and the solvent was evaporated in a rotary evaporator. The resulting crude mixture was extracted into DCM (100 ml) and washed with water (100 ml). The organic phase was separated and dried over magnesium sulphate and then filtrated. The filtrate was evaporated by a rotary evaporator to a brown solid residue. The solid product was sonicated and then was recrystallised from methanol. White crystals were obtained (1.01 g, 40 % yield).

^1H NMR (500 MHz in CDCl_3), δ in ppm, 6.5 (m, Ar-H, 12 H), 4.4 (d, 4 H_{axial} , Ar- CH_2 -Ar, 4 H), 4.0 (t, 8 H, Ar-O- $\text{CH}_2\text{CH}_2\text{N}$, 8 H), 3.1 (d, Ar- CH_2 -Ar, 4 $\text{H}_{\text{equatorial}}$), 2.9 (t, CH_2 -N (CH_2CH_3)₂, 8 H), 2.5 (q, N- CH_2CH_3 , 8 H), 1.04 (t, N-(CH_2CH_3)₂, 24 H). Fig. 14-B Appendix

2.5.15 Synthesis of *meso*-tetramethyl-tetrakis-(4-hydroxyphenyl ethyl) calix[4]pyrrole (TTHCP)

This novel compound was synthesised at the Thermochemistry Laboratory by applying the modified procedure by Danil de Namor and co-workers³² to the procedure reported earlier²¹¹ according to Scheme 2.12



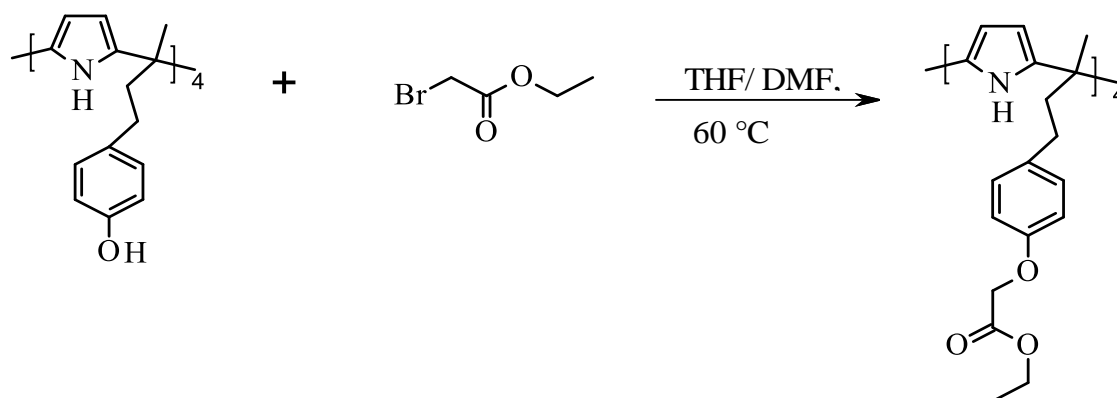
Scheme 2.12 Synthesis of *meso*-tetramethyl-tetrakis-(4-hydroxyphenylethyl)calix[4]pyrrole

In a three-neck round bottom flask (500 ml) containing a magnetic stirrer at ambient temperature, 4-[4-hydroxyphenyl]-2-butanone (12.24 g, 74.52 mmol), was dissolved in methanol (100 ml). Methanesulfonic acid (1 ml) was added to the solution and stirred for 30 minutes. Pyrrole (5 g, 74.53 mmol) was added dropwise to the reaction solution and the reaction was left overnight. The mixture was poured into a beaker containing distilled water (200 ml) and a brown solid precipitated. The compound was filtered, dried by air then collected and dissolved in diethyl ether. Then it was filtrated to remove the black tar from the solid. The solvent was evaporated using a rotary evaporator and the solid obtained was recrystallized from acetic acid and left to cool. Further purification by using acetone-acetonitrile mixture was applied to get a pure white powder which was dried in a vaccum. ^1H NMR (500 MHz, in d_6 -DMSO), δ in ppm, 9.32 (s, NH, 4 H), 9.08 (s, OH, 4 H), 6.83 (d, Ar -H, 8 H), 6.56 (d, Ar-H, 8 H), 5.78 (d, β -H pyrrole ring, 8 H), 2.25 (t, C_{meso} - CH_2 - CH_2 -Ar, 8 H), 2.05 (t, C_{meso} - CH_2 - CH_2 -Ar, 8 H), 1.56 (s, 12 H, CH_3). Fig. 15-B Appendix

^{13}C NMR (500 MHz, in $\text{d}_6\text{-DMSO}$), δ in ppm, 155.7 (C_{10}), 137.8 (C_9), 132.9 (C_8), 129.4 (C_7), 115.5 (C_1), 103.39 (C_2), 44.03 (C_6), 39.8 (C_5), 30.5 (C_4), 25.41 (C_3). Fig. 16 B Appendix

2.5.16 Synthesis of *meso*-tetramethyl-tetrakis-(4-ethylacetatophenoxyethyl) calix[4]pyrrole (TTECP)²⁰²

This super extended compound was synthesised for the first time in the Thermochemistry Laboratory by applying a new modified procedure according to Scheme 2.13



Scheme 2.13 Synthesis of *meso*-tetramethyl-tetrakis-(4-ethylacetato-oxyphenylethyl) calix[4]pyrrole

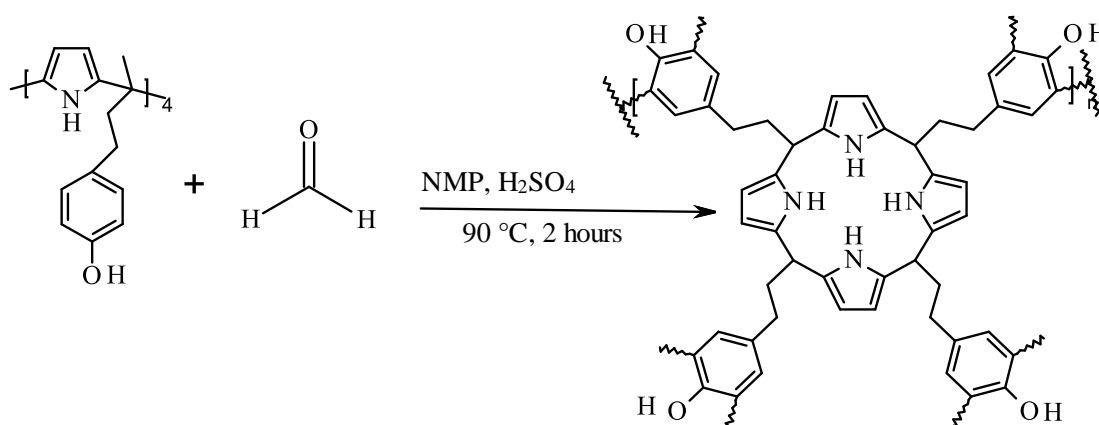
In a three-neck round bottom flask (250 ml) containing a magnetic stirrer at ambient temperature and under a N_2 atmosphere, *meso*-tetramethyl-tetrakis-(4-hydroxyphenylethyl)calix[4]pyrrole (2 g, 1.67 mmol), was dissolved and stirred in a mixture of freshly distilled THF and dry DMF (THF: DMF 60: 40, v/ v). Then sodium hydride (0.056 g, 2.24 mmol), was added carefully followed by dropwise addition of ethylbromo acetate (0.28 g, 1.67 mmol). The reaction mixture was heated in an oil bath at 60 °C under vigorous stirring. The reaction was monitored by thin layer chromatography using a DCM: MeOH (9: 1) mixture as the developing solvent. After the reaction was completed, the mixture was allowed to cool down to ambient temperature. The solvent was evaporated by a rotary evaporator and a colourless viscous liquid product was obtained, dissolved and extracted by DCM. It was then washed with distilled water and then with brine. The organic layer was collected and dried over anhydrous magnesium sulphate, filtered and the solvent evaporated using a rotary evaporator. A white powder was obtained, collected and recrystallised from methanol. The white powder obtained was filtered and dried, ^1H NMR (500 MHz, in CDCl_3), δ in ppm, 7.03 (s, NH, 4 H), 6.91 (d, Ar- H_{meta} , 8 H), 6.69 (d, Ar- H_{ortho} , 8 H), 5.95 (d, C-H, 8 H pyrrole rings), 4.54 (s, O- CH_2 -CO, 8 H), 4.25 (q, O-

$\text{CH}_2\text{-CH}_3$, 8 H), 2.30 (t, $C_{\text{meso}}\text{-CH}_2\text{-CH}_2\text{-Ar}$, 8 H), 2.10 (t, $C_{\text{meso}}\text{-CH}_2$, 8 H), 1.53 (s, CH_3 , 12 H) 1.28 (t, CH_3). Fig. 17 B Appendix

Elemental analysis was carried out at the University of Surrey. Calculated %; C; 72.7, H; 7.07, N; 4.68. Found % C; 72.19, H; 7.02, N; 3.95

2.5.17 Polymerisation of *meso*-tetramethyl-tetrakis-(4-hydroxyphenyl ethyl) calix[4]pyrrole (CPPOL)²¹²

The polymerisation reaction was carried out according to Scheme 2.14



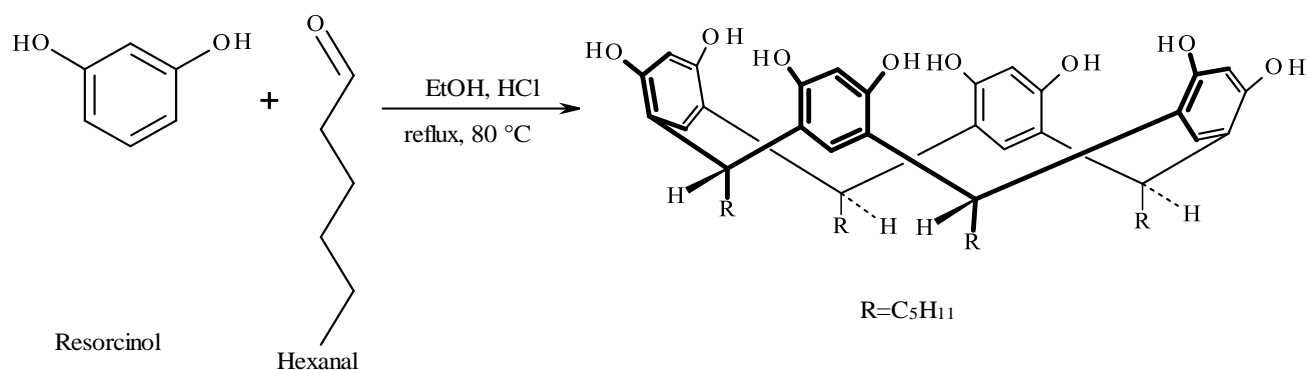
Scheme 2.14 Synthesis of calix[4]pyrrole oligomer

In a three-neck round bottom flask (250 ml), the calix[4]pyrrole derivative (2 g, 1.73 mmol) was dissolved in N-methyl pyrrolidone (25 ml), then sulphuric acid (2 ml) was added to the mechanically stirred solution, followed by the addition of formaldehyde (10 ml, 37 %) with vigorous stirring and heating to 90 °C. After 2 h, the solution became viscous and then it was converted into a dark brown solid which was washed with water then with ethanol. The solid product was collected and dried. Microanalysis was carried out at University of Surrey, found %: C; 67.35, H; 5.88, N; 5.72

FTIR, ν (cm^{-1}), 3335 (N-H), 3280-3192 (O-H), 3008 (C-H) str. Also, TGA, SEM, XRD and XPS have been also carried out at the University of Surrey.

2.5.18 Synthesis of 2, 8, 14, 20-tetrapentyl-1-resorc[4]arene (4, 6, 10, 12, 16, 18, 22-octahydroxy, 2, 8, 14, 20-tetrapentylresorc[4]arene^{213,214}(RC6)

The synthesis of the compound was carried out according to the Scheme 2.15

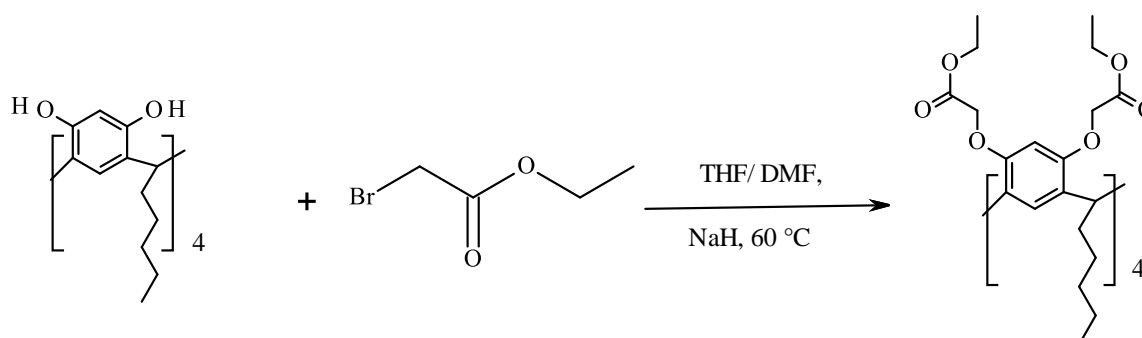


Scheme 2.15 Synthesis of C-pentyl-resorcin[4]arene

In a three-neck round bottom flask fitted to a reflux condenser, a solution of resorcinol (11 g, 99.8 mmol) in ethanol (100 ml), was stirred and cooled to 0 °C in an ice bath, hydrochloric acid (12 M, 2 ml) was added to the stirring solution which was followed by the careful addition of hexanal (12.1 ml, 99.9 mmol) maintaining the temperature at 0 °C. The reaction vessel was then removed from the ice bath under continuous stirring (one hour) and transferred to an oil bath heated to 80 °C for 16 hours. The reaction mixture was removed, allowed to cool down to ambient temperature and then refrigerated. The product was filtered and washed by an ice cold mixture of ethanol and water (1:1, v/v) to yield a yellow orange solid which was dried in *vacuo* at 80 °C. ¹H NMR (500 MHz, in CD₃CN), δ in ppm, 7.59 (s, Ar-OH, 4 H), 7.27 (s, Ar-H, 4 H), 6.21 (Ar-H, 8 H), 4.16 (t, CH_{bridge}, 4 H), 2.26-2.22 (m, CHCH₂CH₂, 8 H), 1.34-1.22 (m, CH₂CH₂CH₂, 24 H), 0.890 (t, CH₃, 12 H). Fig. 18-B Appendix

2.5.19 Synthesis of 4, 6, 10, 12, 16, 18, 22, 24-octa-oxy-ethylacetato-2, 8, 14, 20-tetrapentylresorcin[4]arene RC6-Es

The synthesis of the compound was carried out according to the Scheme 2.16



Scheme 2.16 Synthesis of C-pentylresorcin[4]arene ester

In a 500 ml three-neck round bottom flask and under a nitrogen gas atmosphere, C-pentylresorcin[4]arene (5 g, 6.5 mmol) was dissolved in a mixture of freshly distilled THF and dry DMF (60: 40, v/ v), then sodium hydride (0.16 g, 6.6 mmol) was added carefully to the reaction mixture and stirred for 30 minutes. This was followed by the dropwise addition of ethyl bromoacetate (1.09 g, 6.5 mmol) to the reaction solution. The mixture was heated in an oil bath at 60 °C. The reaction was followed by TLC using a DCM: MeOH (7: 3) mixture as the developing solvent system. After completion, the reaction was stopped and cooled down to ambient temperature. The resulting solution was filtered and the solvent evaporated using a rotary evaporator. A brown viscous product was obtained, dissolved in 100 ml dichloromethane and transferred to a separation funnel. Then it was washed with distilled water and brine, the organic layer was separated and dried over anhydrous magnesium sulphate. The mixture was filtered and the solvent was evaporated under reduced pressure. A viscous colourless liquid was obtained. The crude product was dissolved in methanol and sonicated to break the oil. Light yellow crystals were obtained, filtered, collected and then dried. Yield 3 g, 60 %, ¹H NMR (500 MHz, in CDCl₃), δ in ppm, 6.64 (s, Ar-H, 4 H), 6.23 (s, Ar-H, 4 H), 4.61 (t, C-H_{bridge}, 4 H), 4.3 (s (O-CH₂CO, 8 H), 1.86 (8 H, q (CHCH₂CH₂), 1.6-1.3 (m, CHCH₂CH₂CH₂CH₃, 24 H), 0.87 (s, CH₃, 12 H). Fig. 19 B Appendix

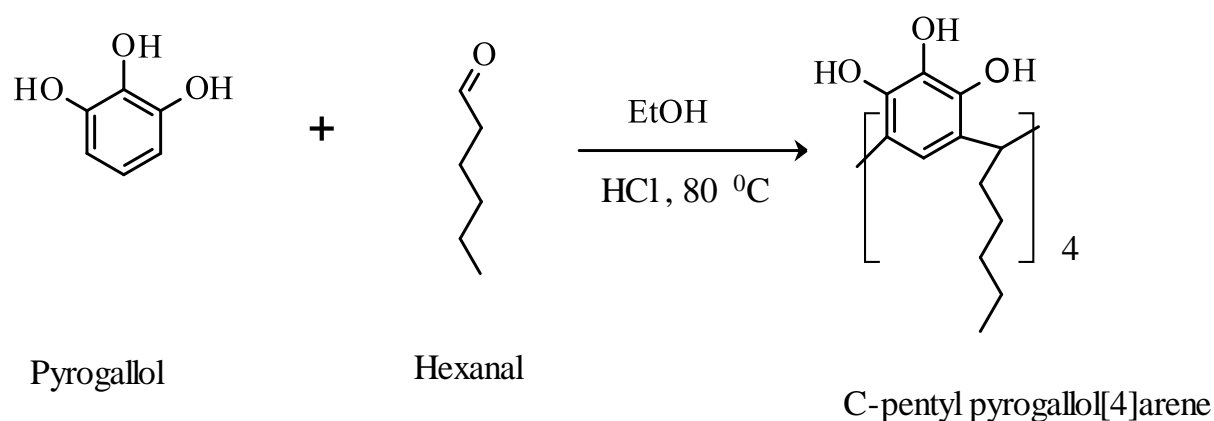
¹³C NMR (500 MHz, CDCl₃, δ in ppm), 14.14 (CH₃), 22.66 (CH₂), 27.67 (CH₂), 32.09 (CH₂), 34.47 (CH₂), 35.79 (CH₃), 51.92 (C_{bridge}), 60.97 (CO-OCH₂CH₃), 66.8 (OCH₂CO), 100.17 (Ph-C), 117.88, 128.54 (Ph-CH), 126.55 (Ph-CH), 154.9 (C-OH), 170.14 (C=O)

C₈₀H₁₁₂O₂₄

Microanalysis was carried out at the University of Surrey. Calculated %: C; 65.9, H; 7.69, N; 0.0
Found %: C; 64.12, H; 7.34, N; 0.0

2.5.20 Synthesis of 2, 8, 14, 20-tetradecyl-5, 11, 17, 23-tetrahydroxyresorc[4]arene (4, 5, 6, 10, 11, 12, 16, 17, 18, 22, 23, 24-dodecahydroxy-2, 8, 14, 20-tetrapentylresorcin[4]arene²¹⁵ (PG6)

The compound was synthesised following the same procedure used by Gerkensmeier and co-workers²¹⁵ according to the following Scheme



Scheme 2.17 Synthesis of C-pentylpyrogallol[4]arene

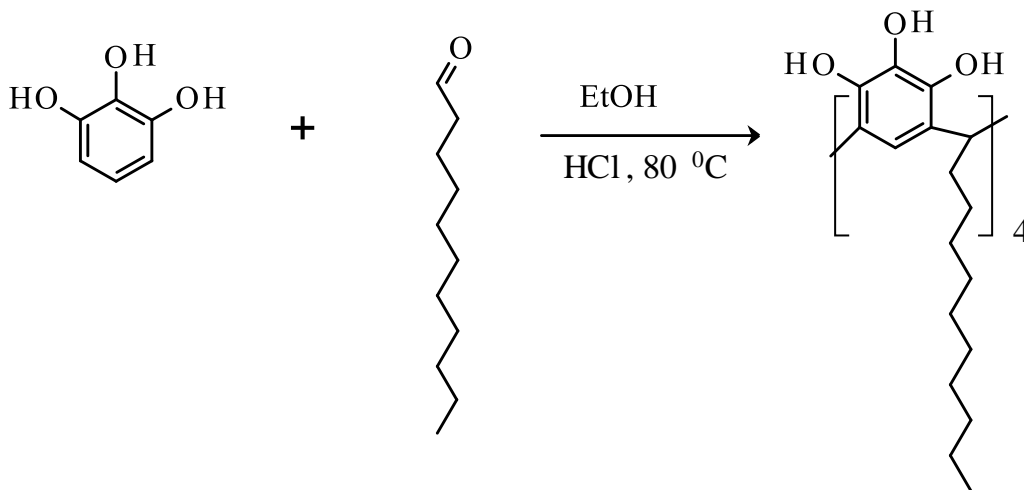
A pre-dried three-neck round bottom flask (500 ml) containing a magnetic stirrer and fitted to a condenser and dropping funnel was placed in an ice bath under an inert atmosphere. Pyrogallol (7.84 g, 62.2 mmol), was dissolved in ethanol (100 ml). Hydrochloric acid (12 M, 2 ml) solution in ethanol (20 ml) was added dropwise to the stirring solution maintaining the temperature at 0 °C. This was followed by the dropwise addition of hexanal (9.6 ml, 62.2 mmol) mixed with ethanol (25 ml). The reaction mixture was removed from the ice bath and heated in an oil bath at 80 °C under vigorous stirring for 16 hours. After the reaction was completed, the mixture was allowed to cool to ambient temperature. The mixture was poured into ice-water to obtain light purple solid which was filtered and washed by ice cold ethanol. The purple solid collected and dried *en vacuuum* at 80 °C. Pure white compound was obtained.

^1H NMR (500 MHz, in CDCl_3), δ in ppm, 8.77 (s, Ar-OH_{meta}, 4 H), 7.46 (s, Ar-OH_{para}, 4 H), 6.88 (s, Ar-OH_{meta}, 4 H), 6.84 (s, Ar-H, 4 H), 4.38 (t, CH_{bridge}, 4 H), 2.25-2.18 (m, CH-CH₂-CH₂, 8 H), 1.42-1.34 (m, CH₂-CH₂-CH₂-CH₂-CH₃, 24 H), 0.9 (t, CH₃, 12 H), Fig. 20-B Appendix

^{13}C NMR (500 MHz, in CDCl_3), δ in ppm, 138.49 (ArC-OH_{meta}, 4 C), 137.34 (ArC-OH_{meta}, 4 C), 131.37 (ArC-OH_{para}, 4 C), 125.39 (ArC_{ortho}, 4 C), 124.07 (ArC_{ortho}, 4 C), 113.76 (ArC, 4 C), 34.1 (CH, 4 C), 33.17 (CH-CH₂-CH₂, 4 C), 31.96 (CH-CH₂-CH₂, 4 C), 29.96 (CH-CH₂-CH₂, 4 C), 27.988 (CH₂-CH₂-CH₃, 4 C), 22.72 (CH₂-CH₂-CH₃, 4 C), 14.11 (CH₃, 4 C)

2.5.21 Synthesis of 2, 8, 14, 20-tetradecyl-5, 11, 17, 23-tetrahydroxyresorc[4]arene²¹⁵ [C-decylpyrogallol[4]arene] (PG11)

The synthesis of the compound was carried out following same procedure used in the synthesis of C-pentylpyrogallol[4]arene (Scheme 2.18)



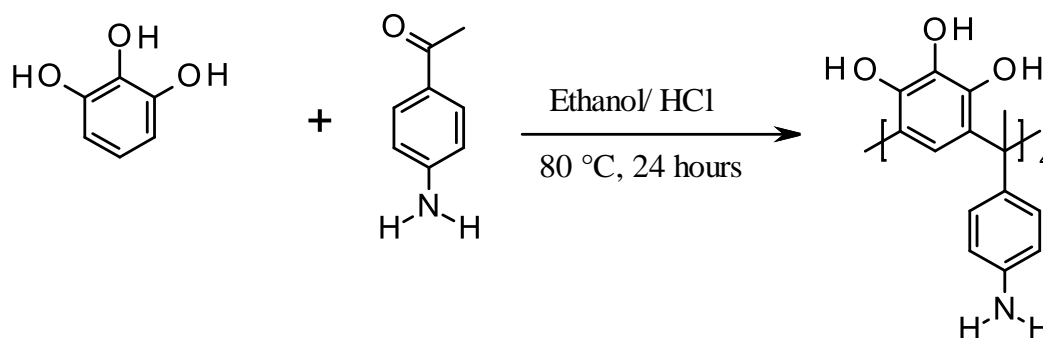
Scheme 2.18 Synthesis of C-decylpyrogallol[4]arene PG11

A pre-dried three-neck round bottom flask (500 ml) containing a magnetic stirrer and fitted to a reflux condenser was placed in an ice bath under an inert atmosphere. Pyrogallol (5 g, 39.9 mmol), was dissolved in ethanol (75 ml), and a hydrochloric acid (12 M, 2 ml) solution in ethanol (25 ml) was added dropwise to the stirring solution maintaining the temperature at 0 °C. This was followed by the dropwise addition of a solution of undecanal (6.75 g, 39.9 mmol) dissolved in ethanol (25 ml) to the reaction mixture. The reaction mixture was removed from the ice bath and heated in an oil bath at 80 °C under vigorous stirring for 16 hours. After the reaction was completed, the mixture was allowed to cool to room temperature, the mixture was poured into an ice-water to obtain a brown solid which was filtrated and washed with ice cold ethanol. The solid was collected and dried *en vacuo* at 80 °C.

¹H NMR (500 MHz, in CDCl₃), δ in ppm, 8.77 (s, Ar-OH_{meta}, 4 H), 7.46 (s, Ar-OH_{para}, 4 H), 6.87 (s, Ar-OH_{meta}, 4 H), 6.83 (s, Ar-H, 4 H), 4.38 (t, CH_{bridge}, 4 H), 2.23-2.17 (m, CH_{bridge}-CH₂-CH₂, 8 H), 1.54-1.2 (m, CH₂-CH₂-CH₂-CH₃, 24 H), 0.9 (t, CH₃, 12 H), Fig. 21-B Appendix

2.5.22 Synthesis of C-4-aminophenyl pyrogallol[4]arene

This compound was synthesised according to following scheme



Scheme 2.19 Synthesis of C-4-aminophenyl pyrogallol arene

In a 500 ml three neck round bottom flask containing a magnetic stirrer fitted with a reflux condenser, pyrogallol (4.66 g, 36.95 mmol) was dissolved in ethanol (50 ml), hydrochloric acid (2 ml, 12 M) mixed with ethanol (10 ml) were added dropwise under continuous stirring. Then *p*- aminoacetophenone (5 g, 36.99 mmol) was dissolved in ethanol (50 ml) and was added to the reaction mixture dropwise. Then the reaction mixture was heated in an oil bath at 60 °C. After 20 minutes the colour of the solution was changed to deep purple colour. The mixture was left overnight, then removed from the oil bath, cooled down to ambient temperature and then it was neutralised by an aqueous solution of sodium bicarbonate solution (10 %) and refrigerated, the obtained precipitate was collected by filtration and dried under vacuum. Microanalysis were carried out at the University of Surrey. Calculated %: C; 69.00, H; 5.30, N; 5.76. Found %: C; 68.35, H; 5.79, N; 6.97

2.6 Solubility measurements of receptors

Saturated solutions of each receptor were prepared in different solvents and kept in a water bath at 298.15 K for 24 hours to attain equilibrium between the solid and its saturated solution which were filtered by using Millipore filters 0.22 μm and a known volume of the solution was placed into a pre-weighed porcelain crucible, dried and the weight of the residual solid was gravimetrically determined. Solvation experiments were carried out by exposing separately pre-weighed crucibles containing the solid in a saturated environment of the appropriate solvent in a desiccator for several days. The crucibles were then weighed to check the uptake of solvent by the solid. From solubility data, $\Delta_s G^\circ$ were calculated for the samples that were not altered by solvation.

2.7 ^1H NMR measurements

^1H NMR measurements were carried out at 298 K using a Bruker AC-500 MHz. The investigations were carried out by dissolving each compound (30 mg) in the appropriate deuterated solvents (0.5

ml) in 5 mm NMR tubes using TMS as the internal reference. ^1H NMR titrations were carried out to determine the complexation between the receptor and the targeted guest by adding increasing amounts of known concentrations of guest solutions to the NMR tube containing a known concentration of the receptor. Chemical shift changes of the receptor after each addition were recorded. Subtracting the chemical shift for the free receptor δ_r from the chemical shifts of the complex, δ_c , the chemical shift changes, $\Delta\delta$, was calculated from the following equation (eq.2.6)

$$\Delta\delta = \delta_c - \delta_r \quad \text{eq. 2.6}$$

2.8 Conductometric measurements

Conductance measurements are very supportive tool to monitor the complexation process between the receptor and the targeted species by testing the variation of the electrical behaviour of the guest solution in the conductivity cell caused by the gradual addition of the host solution and to identify the stoichiometry of the interaction at 298.15 K. A brief introduction on conductance measurements is given. Conductance measurements follows Ohm's law in which the current I (amperes) in a conductor is directly proportional to the applied electric force E (volts) and inversely proportional to the resistance R (ohm's) of the conductor (eq.2.7)²¹⁶

$$I = E / R \quad \text{eq.2.7}$$

The resistance of an homogenous sample material, l , and cross sectional area, A , is given by eq.2.8

$$R = \rho l / A \quad \text{eq.2.8}$$

In this equation, ρ ; is a characteristic property of the material and is known as resistivity and it is measured in Ω cm.

$$\rho = R A / l \quad \text{eq.2.9}$$

The reciprocal of the resistivity is the conductivity, κ , is given as S.cm^{-1} where S is the notation used for the reciprocal of the resistivity ρ (Seimens or Ω^{-1}). Therefore eq.2.9 can be written in terms of κ

$$\kappa = I l / R A \quad \text{eq.2.10}$$

The conductivity of the solution under study was obtained by using the pre-determined value of the cell constant ($\theta = l / A$) and the measured value of the resistance R of the same sample as shown in eq.2.11

$$\kappa = I \theta / R \quad \text{eq.2.11}$$

In this equation, the cell constant units are cm^{-1} . The molar conductance, Λ_m , of an electrolyte is given by eq.2.12

$$\Lambda_m = 1000 \kappa / c \quad \text{eq.2.12}$$

In eq.2.12 c , is the concentration of the solution in mol dm^{-3} and the units of Λ_m are given in $\text{S.cm}^2 \text{mol}^{-1}$.

2.8.1 Determination of the conductivity cell constant

The conductivity cell constant, θ , was determined according to the method described by Jones and Bradshaw²¹⁷ by adding stepwise additions of a solution of potassium chloride in deionised water (0.1 mol dm^{-3}) to the conductivity cell containing deionised water (25 ml) at 298.15 K. Conductivity values were recorded after each addition. The molar conductance, $\Lambda_m (\text{S cm}^2 \text{mol}^{-1})$ was calculated from the equation derived by Lind, Zwolenik and Fuoss²¹⁸

$$\Lambda_m = 149.93 - 96.65 c^{1/2} + 58.74 c \log c + 198.4 c \quad \text{eq.2.13}$$

In eq.2.13, c , denotes to molar concentration (mol dm^{-3}) of potassium chloride solution. The cell constant, $\theta (\text{cm}^{-1})$ was calculated from the following equation

$$\theta = \Lambda_m c / \kappa \times 1000 \quad \text{eq.2.14}$$

2.8.2 Conductometric titrations at 298.15 K

Conductometric titrations involved the gradual addition of the receptor solution in acetonitrile to the conductivity cell containing the targeted guest in the same solvent at 298.15K. To achieve these measurements, the conductometric cell connected to a thermostated water bath was loaded with the guest solution in the appropriate solvent (25 ml). Then the electrodes were immersed into the solution cell under continuous stirring during the course of the titration. Accurate aliquots of the receptor were gradually added to the guest solution in the same solvent, the resistance was recorded after each addition once equilibrium was attained. Molar conductance Λ_m ($\text{S cm}^2 \text{ mol}^{-1}$) were plotted against the [receptor/ guest] concentration ratio. The stoichiometry of the complexation was identified by the graphical tangent method (intercept between the two lines prior and after the end point of the reaction).

2.9 Nano Isothermal Titration Calorimeter Nano-ITC

Isothermal titration calorimetry is a highly sensitive technique designed to determine rapidly and accurately the thermodynamic parameters associated with the complexation process between the host and the guest in solution (stability constant and enthalpy of a reaction). From these parameters, the Gibbs energy and the entropy of complexation can be calculated by applying the following equations

$$\Delta_c G^\circ = -RT \ln K_s \quad 2.15$$

$$\Delta_c G^\circ = \Delta_c H^\circ - T\Delta_c S^\circ \quad 2.16$$

In eqs. 2.15 and 2.16, $\Delta_c G^\circ$, R , T , K_s , $\Delta_c H^\circ$ and $\Delta_c S^\circ$ denote the standard Gibbs energy, the gas constant, the temperature (Kelvin), the stability constant, the standard enthalpy and entropy of complexation respectively

The Nano Isothermal Titration Calorimeter consists of the main features:

1. A burette stirring system.
2. A syringe (100 μl)
3. A reference cell (1 cm^3 each)
4. Thermoelectric devices.

The Nano ITC is connected to a personal computer that included the software delivered from the manufacturer with the information needed for the operation of the instrument and to analyse the data obtained to display the thermodynamic parameters for every single reaction taking place^{219, 220}.

2.9.1 Calorimetric measurements

The Nano- ITC measurements were carried out in degassed acetonitrile at 298.15 K. The host solution ($1 \times 10^{-3} \text{ mol dm}^{-3}$) was used in a 950 μl cell volume. Solutions of each guest ($2 \times 10^{-2} \text{ mol dm}^{-3}$) were added by an injection syringe programmed to inject 5 or 10 μl successively into the host solution in the same solvent with a 3 to 5 minutes' interval between each injection. The instrument was delivered with a program from the manufacturer to control the operation. The heat of dilution was determined from the titration curve after the receptor concentration was totally consumed. The obtained values were modelled using an independent nonlinear regression analysis. The fitting was done using a software

2.9.2 Calibration of the Nanocalorimeter

Calibration experiments were carried out to check the accuracy of the ITC. The complexation reaction between barium chloride with 18-crown-6 in aqueous medium at 298.15 K suggested by Briggner and Wadsö^{221,222} as a standard reaction was performed to calibrate the calorimeter. The calibration experiment was carried out by setting the instrument to inject automatically 5 μl from the injection syringe containing the aqueous solution of barium chloride ($1.5 \times 10^{-2} \text{ mol dm}^{-3}$) every five minutes to the reference cell which was loaded with 18-crown-6 solution ($1 \times 10^{-3} \text{ mol dm}^{-3}$) in deionised water. After completion of the reaction, the data were analysed by the software delivered with the instrument from the Manufacturer. From the titration information, the stability constant K_s and the enthalpy change ΔH were obtained. From these parameters, the Gibbs energy and entropy were calculated by applying equations 2.15 and 2.16 respectively

2.10 Determination of the stability constant and the composition of host-guest complexes by UV-Vis, ¹H NMR and calorimetric titrations

UV-Vis, ^1H NMR and calorimetry are the most commonly used analytical techniques for the determination of the stoichiometry and the stability constant of the host-guest complex for complexes of moderate or low stability. Titration measurements are performed by the addition of increasing concentration of one of the component (host or guest) to a fixed concentration of the other⁶⁷. The reversible complexation process between the host and the guest in a solvent (s) is described according to the following equation (eq.2.17)



Where H, G and $H.G$, are the notations used to indicate the host, the guest and the complex respectively. Therefore, the stability constant, K_s , can be expressed as follows

$$K_s = \frac{a_{H.G}}{a_H a_G} \quad \text{eq. 2.18}$$

In eq.2.18, $a_{H.G}, a_H$ and a_G denote the activity of the complex, host and guest respectively. On the assumption that the activity coefficients of reactants and product are equal to 1 (at low concentrations), the stability constant can be expressed by eq.2.19 in terms of molar concentrations,

$$K_s = \frac{[H.G]}{[H][G]} \quad \text{eq. 2.19}$$

The concentration of the host and the guest at equilibrium can be calculated from eq.2.20 and eq.2.21

$$[H] = [H]^\circ - [H.G] \quad \text{eq. 2.20}$$

$$[G] = [G]^\circ - [H.G] \quad \text{eq. 2.21}$$

In eqs.2.20 and 2.21, $[H]^\circ, [H], [G], [G]^\circ, [H.G]^\circ$, are the initial and final molar concentration of the host, the guest and the complex respectively. By replacing eqs. 2.20 and 2.21 in eq.2.19, it follows that

$$K_s = \frac{[H.G]}{[H]^\circ[G]^\circ - [H.G][G]^\circ - [H.G][H]^\circ + [H.G]^2} \quad \text{eq. 2.22}$$

Rearrangement of eq.2.22 leads to eq.2.23

$$K_s([H]^\circ[G]^\circ - [H.G][G]^\circ - [H.G][H]^\circ + [H.G]^2) = [H.G] \quad \text{eq. 2.23}$$

$$K_s[H.G]^2 - (K_s[G]^\circ - K_s[H]^\circ + 1)[H.G] + K_s[H]^\circ[G]^\circ = 0 \quad \text{eq. 2.24}$$

Eq.2.24 can be solved as follows

$$[H.G] = \frac{1}{2} \left([G]^\circ + [H]^\circ + \frac{1}{K_s} \right) - \sqrt{\left([G]^\circ + [H]^\circ + \frac{1}{K_s} \right)^2 + 4[H]^\circ[G]^\circ} \quad \text{eq. 2.25}$$

Or

$$[H.G] = \frac{[H]^\circ K_s [G]}{1 + K_s [G]} \quad \text{eq. 2.26}$$

In eq.2.26, the concentration of the complex $[H.G]$ is expressed as a function of K_s , which is the only unknown and can be determined by UV-Vis, ^1H NMR and calorimetric titrations.

In the UV-Vis spectrum, the complex has a particular absorption band,

$$A = \varepsilon_{H.G} [H.G] \quad \text{eq. 2.27}$$

Taking into account eq.2.25, it follows that

$$A = f(\varepsilon_{H.G}, K_s) \quad \text{eq. 2.28}$$

In the UV-Vis the change in the absorption band, ΔA_{obs} , during the titration is given by

$$\Delta A_{obs} = \varepsilon_{\Delta[H.G]} ([H.G]) \quad \text{eq. 2.29}$$

In ^1H NMR, the chemical shift changes, $\Delta\delta$, during the titration is

$$\Delta\delta = \delta_{\Delta HG} \frac{[H.G]}{[H]^\circ} \quad \text{eq. 2.30}$$

In the calorimetric titration, the change in the heat of complexation, Q , is given by eq.2.31

$$Q = \Delta H_{H.G} V ([H.G]) \quad \text{eq. 2.31}$$

In eq. 2.31, $\Delta H_{H.G}$, is the change in enthalpy of the reaction and V , is the volume of the guest added after each addition to the cell containing the host

Determination of stability constant based on absorbance, A

$$A = A_{H.G} + A_H + A_G \quad \text{eq. 2.32}$$

Assuming $[G]^\circ \gg [H]^\circ$, thus, $A^G > A^H$, it follows that

$$A = A_{HG} + A_G \quad \text{eq. 2.33}$$

$$\Delta A = A - A_0 \quad \text{eq. 2.34}$$

$$\Delta A = \varepsilon^{H.G}[H.G]b + \varepsilon^G[G]b + \varepsilon^{G_0}[G]_0b \quad \text{eq. 2.35}$$

$$\Delta A = \Delta\varepsilon[H.G]b \quad \text{with} \quad \Delta\varepsilon = \varepsilon^{H.G} - \varepsilon^G \quad \text{eq. 2.36}$$

$$\Delta A = b\Delta\varepsilon \frac{[H]_0 K_s [G]_0}{1 + K_s [G]_0} \quad \text{eq. 2.37}$$

And finally

$$\frac{1}{\Delta A} = \frac{1}{b\Delta\varepsilon[G]_0[H]_0 K_s} + \frac{1}{b\Delta\varepsilon[H]_0} \quad \text{eq. 2.38}$$

2.11 General procedure for the determination of optimum amount of the receptor for the uptake of targeted guest from aqueous solution at 298.15 K

Extraction experiments were carried out in an attempt to assess the efficiency of calix[4]arene derivatives and 3-aminopropyl functionalised silica (Sil-NH₂) to remove pharmaceuticals from water. The optimal conditions were determined by taking into account the effect of the amount of receptor and the pH of the solutions, The capacity of the receptor (or silica) defined as the maximum amount of the drug (mmol) per gram of material was determined

2.11.1 Effect of the amount of material on the extraction of pharmaceuticals

In order to calculate the optimal amount of the receptor to be used in the extraction experiment,

different amounts of the receptor (0.01, 0.02, ...,0.1 g) were added to a fixed concentration of the targeted guest in water, the mixtures were mixed well by whirlimixer and left overnight in a water bath at 298 K. Each solution was filtered and analysed by UV-Vis measurements. The percentage of extraction was calculated according to eq.2.39

$$\% E = \frac{C_i - C_e}{C_i} \times 100 \quad \text{eq.2.39}$$

In this equation, % E , is the extraction percentage of the targeted guest, c_i and c_e is the initial and final concentration of the guest (pollutants) before and after extraction respectively in mol dm^{-3} .

The capacity q of SiI-NH_2 was calculated from the eq.2.40

$$q = \frac{(c_i - c_e)V}{m} \quad \text{eq.2.40}$$

where c_i and c_e are the initial and final concentration of aspirin before and after extraction respectively in mol dm^{-3} , m is the mass of the material used for the removal of the pollutants, V is the volume of the solution in dm^3 and q is the capacity of the material used to remove the pollutants.

2.11.2 Effect of pH on the extraction

The effect of pH values on extraction of aspirin by 3-aminopropyl functionalised silica was tested by the addition of 0.08 g of SiI-NH_2 in the aspirin solutions (10 ml) containing $5.59 \times 10^{-3} \text{ mol dm}^{-3}$ of aspirin with different pH values. The mixtures were mixed on whirlimixer and left for six hours in a water bath at 298 K. The mixtures then filtered and analysed by UV-Vis spectroscopy. The percentage of extraction, % E , and the capacity, q , were calculated using eq.2.39 and 2.40

2.11.3 Kinetics of removal of pharmaceuticals by macrocycles and Si-NH₂

In order to assess the effect of the time required on the removal processes, a series of solutions with the same concentration prepared, fixed mass of receptor were added, mixed and filtrated after different contact times from 10 minutes to 18 h at 298 K by filter (Millipore 0.22), the UV-Vis measurements were used to determine the final concentration for each solution

2.12 Thermal Properties measurements TGA, DSC

These measurements include the thermogravimetric analysis, TGA and the Differential Scanning Calorimetry DSC. TGA and DSC are powerful and accurate thermoanalytical techniques used successfully in the investigation of the host-guest complexes by following the variation in the physicochemical properties of the materials in the solid state as a result of fixed rate increase of heating and cooling under an inert or potent atmosphere at constant pressure. The investigation of the complexation process can be determined by the comparison of the TGA and DSC thermograms for the host, guest and the complex. Getting different TGA thermograms indicating that the complexation of the host with guest has significant effect on their thermal stabilities while the obtaining of different thermodynamic parameters from the DSC thermograms such as shifting the value of melting enthalpies of the complex compared with its components to another temperature or vanishing during

the temperature scale of the sample cracking indicate that the complexation process was achieved successfully which means that the complexation process has led to an effect on their physicochemical properties²²³⁻²²⁵. TGA measurements were carried out to obtain information required in the next DSC measurements. In the TGA measurements, the solid sample was weighed accurately then placed in a platinum pan, the pan was inserted into the furnace, and the furnace was sealed. The sample was then heated from ambient temperature to a maximum temperature of 600 or 800 °C processed to 20 °C/min temperature rise. Between each analyses, the furnace was cooled by nitrogen gas to make sure that the instrument had reached ambient temperature. The sample mass was taken by using a microbalance. The onset temperature of weight loss and first derivative plot were obtained through the TA Universal Analysis, a software program delivered by the manufacturer of the instrument. Differential Scanning Calorimetric DSC technique is a thermal analysis used to study the change in the physical properties of the materials as a result of an increase or decrease of temperature at a constant rate with time in a fixed pressure. In the DSC runs, the solid sample was weighed, placed into an aluminium pan and an empty pan was used as a reference. To start the measurements, the instrument was cooled to – 25 °C using liquid nitrogen and then the empty reference pan was heated electrically at a rate of 10 °C/min and the heat transferred to the sample pan was recorded. The conditions used for these measurements are shown in Table 2.2. Melting points were calculated.

Table 2.1 Different conditions used during TGA analysis.

Sample name	Weight used mg	Temperature range	Ramped Temperature	N ₂ Gas flow
Sodium diclofenac NaDF	2.397	RT-800 °C	20 °C/min	60 cm ³ /min
Carbamazepine CBZ	4.314	RT-600 °C	20 °C/min	60 cm ³ /min
CAE	2.832	RT-800 °C	20 °C/min	60 cm ³ /min

C ₁₀ -pyrogallol[4] arene PG11	2.352	RT-800 °C	20 °C/ min	60 cm ³ / min
PG11+ CBZ	2.878	RT-600 °C	20 °C/ min	60 cm ³ / min
PG11+ aspirin	2.592	RT-600 °C	20 °C/ min	60 cm ³ / min
PG 11+ Diclofenac	3.909	RT-600 °C	20 °C/ min	60 cm ³ / min
PG11+ clofibric acid	3.157	RT-800 °C	20 °C/ min	60 cm ³ / min
Calixamine	2.704	RT-800 °C	20 °C/ min	60 cm ³ / min
Calixamin+aspirin	4.446	RT-800 °C	20 °C/ min	60 cm ³ / min
Calix-(NH ₂) ₂ +diclofenac	3.7910	RT-800 °C	20 °C/ min	60 cm ³ / min
Aspirin	5.802	RT-800 °C	20 °C/ min	60 cm ³ / min
Diclofenac	2.337	RT-800 °C	20 °C/ min	60 cm ³ / min
Clofibric acid	4.525	RT-800 °C	20 °C/ min	60 cm ³ / min

Table 2.2 The conditions applied for DSC analysis

Sample name	Weight used mg	Temperature range °C	Ramped Temperature	N ₂ Gas flow
Sodium diclofenac	3.7	- 25-250 °C	10 °C/ min	50 cm ³ / min
Carbamazepine CBZ	4.7	- 25-200 °C	10 °C/ min	50 cm ³ / min

Calix[4]arene tetraester CAE	3.8	- 25-260 °C	10 °C/ min	50 cm ³ / min
C ₁₀ -pyrogallol[4] arene PG11	2.8	- 25-250 °C	10 °C/ min	50 cm ³ / min
PG11+CBZ	3.5	- 25-190 °C	10 °C/ min	50 cm ³ / min
PG11+ aspirin	3.6	- 25-120 °C	10 °C/ min	50 cm ³ / min
PG 11+ Diclofenac	3.1	- 25-160 °C	10 °C/ min	50 cm ³ / min
PG11+clofibric acid	4.2	- 25-120 °C	10 °C/ min	50 cm ³ / min
Calixamine	2.2	- 25-220 °C	10 °C/ min	50 cm ³ / min
Calixamin+aspirin	3.9	- 25-100 °C	10 °C/ min	50 cm ³ / min
Calix-(NH ₂) ₂ +diclofenac	5.1	- 25-120 °C	10 °C/ min	50 cm ³ / min
Aspirin	5.6	- 25-120 °C	10 °C/ min	50 cm ³ / min
Diclofenac	2.2	- 25-150 °C	10 °C/ min	50 cm ³ / min
Clofibric acid	4.7	- 25-120 °C	10 °C/ min	50 cm ³ / min

Chapter III

Results &

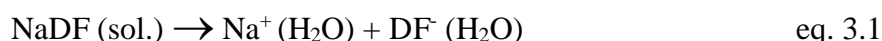
Discussion

3.1 Solubility of drugs in different solvents

Under the IUPAC-NIST Solubility Data Series, Acree²²⁶ proceeded with a critical evaluation on the solubility of non-steroidal anti-inflammatory drugs in pure organic solvents as well as in organic solvent mixtures. Drugs included within the context of this work were diclofenac, ibuprofen, sodium diclofenac and salicylic acid. In order to familiarise with the experimental work related to solubility measurements of drugs in different solvents, two drugs were selected, sodium diclofenac and carbamazepine and the results are now discussed

3.1.1 Solubility of sodium diclofenac in different solvents

Solvation and solubility measurements were carried out as described in Section 2.1 and results in water, methanol (MeOH), ethanol (EtOH), acetonitrile (MeCN), tetrahydrofuran (THF), 1-octanol (1-Oct), dimethyl sulfoxide (DMSO), N, N-dimethylformamide (DMF), ethyl acetate (EtAc), 1-butanol (BuOH) and hexane (Hex) are displayed in Table 3.1. For comparison purposes also included are the literature recommended values reported by Acree²²⁶. The derivation of standard solution Gibbs energy, ΔG_s° requires that the composition of the solid in equilibrium with the saturated solution should be the same. Therefore, solvation was tested in the various solvents. Sodium diclofenac NaDF, is expected to be fully dissociated in water as shown in eq.3.1



Therefore, the thermodynamic solubility product, K_{sp} can be represented as shown in eq. 3.2

$$K_{sp} = [\text{Na}^+] [\text{DF}^-] \gamma_{\pm}^2 \quad \text{eq. 3.2}$$

In eq.3.2 values between brackets denote molar concentrations and γ_{\pm} is the mean molar activity coefficient which can be calculated according to the limited Debye-Hückel equation (eq.3.3)

$$\log \gamma_{\pm} = -0.509 z_+ z_- \sqrt{I} \quad \text{eq.3.3}$$

In equation 3.3, z_+ , z_- , are the net charge for the cationic and anionic moieties respectively and I is the ionic strength which is defined in eq.3.4

$$I = \frac{1}{2} \sum cz^2 \quad \text{eq. 3.4}$$

In eq.3.4, c, is the concentration of the solution in mol dm⁻³ units

The calculated ionic strength for sodium diclofenac solution in distilled water in this work is

$$I = 0.069 \text{ mol dm}^{-3}$$

This value is not in agreement with the value reported earlier²²⁷ ($I = 0.16 \text{ mol dm}^{-3}$) Therefore, the mean molar activity

$$\gamma_{\pm} = 0.735 \quad \Rightarrow \quad K_{sp} = 2.57 \times 10^{-3}$$

The data are referred to the standard state (1 mol dm^{-3}) for ions and therefore the units are cancelled

Thus the ΔG_s° is given by eq.3.5

$$\Delta G_s^\circ = -RT \ln K_{sp} \quad \text{eq. 3.5}$$

In eq. 3.5, R is the gas constant and T is the absolute temperature in Kelvin. The data are referred to the standard state of 1 mol dm^{-3} for the solid and for the saturated solution.

In solvents of moderate dielectric constant such as MeOH, EtOH, BuOH, MeCN ions and ion-pairs will be present in the saturated solution. In order to calculate the ΔG_s° for the dissociated salt it is necessary to have knowledge of the ion-pair association constant, K_s . These values are not available in the literature for this particular drug. Therefore, the ΔG_s° is not reported in Table 3.1. In solvents of low dielectric constant such as 1-Oct, THF and Hex, ion pairs will be predominantly in the saturated solution. Therefore, the ΔG_s° is referred to the process in eq.3.6



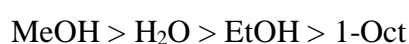
In this case, the ΔG_s° can be obtained directly from eq.2.2. Therefore, the Gibbs energies of transfer, $\Delta_t G^\circ$ from water to low permittivity solvents reported in Table 3.1 are referred to the following process



Table 3.1 Solubility and standard Gibbs energies of solution of sodium diclofenac in different solvents at 298.15 K.

Solvent	K_{sp}	$\Delta G_s^\circ / \text{kJ mol}^{-1}$	$\Delta G_t^\circ (\text{H}_2\text{O} \rightarrow \text{S}_2) \text{ kJ mol}^{-1}$
H ₂ O	$(6.69 \pm 0.04) \times 10^{-2}$	14.78 ± 0.2	0.00
MeOH	$(5 \pm 0.01) \times 10^{-1}$	-----	-----
EtOH	$(3 \pm 0.02) \times 10^{-2}$	-----	-----
MeCN	$(1.52 \pm 0.01) \times 10^{-3}$	-----	-----
THF	$(7.53 \pm 0.01) \times 10^{-3}$	20.56 ± 0.1	5.78
DMF	$(2.25 \pm 0.01) \times 10^{-2}$	9.41 ± 0.1	-5.37
DMSO	$(2.91 \pm 0.05) \times 10^{-2}$	8.76 ± 0.3	-6.02
EtAc	$(5.1 \pm 0.03) \times 10^{-3}$	8.14 ± 0.2	-6.64
1-BuOH	$(4.3 \pm 0.04) \times 10^{-4}$	-----	-----

It is clear from Table 3.1 that in protic solvents (able to enter hydrogen bond formation) the solubility of NaDF follows the sequence



For other solvents, the following pattern was found



Water will be used as the main solvent for sodium diclofenac as it is the primary focus of this study to remove this pharmaceutical from water. Unlike sodium diclofenac, carbamazepine CBZ is a non-electrolyte and therefore the standard solution Gibbs energy can be directly calculated from the solubility of the drug in the appropriate solvent provided the solvation phenomenon is not observed when the solid is exposed to a saturated atmosphere of the solvent. The results obtained are now presented and discussed

3.1.2 Solubility of carbamazepine (CBZ) in different solvents

Solubility data for the CBZ drug in different solvents at 298.15 K are shown in Table 3.2. From the solubility value, both the Gibbs energy of solution and then the transfer Gibbs energy $\Delta_t G^\circ$ of the drug from one solvent to another using water as reference solvent were calculated

Table 3.2 Solubility of carbamazepine CBZ in different solvents at 298.15 K and derived standard Gibbs energies of solution and transfer from water

Solvent	Solubility/ mol dm ⁻³	$\Delta_s G^\circ$ / kJ mol ⁻¹	$\Delta_t G^\circ$ (kJ mol ⁻¹) H ₂ O→s ₂ (H ₂ O)
Water	$(7.66 \pm 0.04) \times 10^{-4}$	17.78 ± 0.2	0.00
MeCN	$(4.25 \pm 0.04) \times 10^{-3}$	13.39 ± 0.2	- 4.48
DCM	$(1.8 \pm 0.03) \times 10^{-2}$	9.96 ± 0.2	- 3.37
DMSO	$(1.66 \pm 0.03) \times 10^{-2}$	10.13 ± 0.2	- 7.65
Hex	$(5.0 \pm 0.06) \times 10^{-1}$	1.71 ± 0.3	- 15.96
MeOH	$(4.4 \pm 0.04) \times 10^{-1}$	2.03 ± 0.2	- 15.64
EtOH	$(1.6 \pm 0.05) \times 10^{-1}$	4.54 ± 0.3	- 13.13
DMF	$(3.7 \pm 0.02) \times 10^{-2}$	8.17 ± 0.1	- 9.61

From the above data it can be seen that CBZ is least soluble in water and is most soluble in hexane than in any other solvent. The structure of CBZ itself has a hydrophobic region due to the aromatic groups but the amide moiety confers to it a certain degree of hydrophilic character and therefore even though its hydrophobic presence seems to be reflected in the low solubility observed in water and the highest solubility found in hexane. It seems that protophilic dipolar aprotic solvents such as DMF and DMSO containing basic oxygen atoms are able to interact through hydrogen bond formation with

the amide functional groups of the drug given that the solubility of the drug in these solvents is higher than that in water.

Again the carbonyl oxygen of the amide functional group in CBZ can interact with the alcohols through hydrogen bond formation. It is important to emphasise that water is the most strongly 'structured' solvent (tri-dimensional nature of molecules associated) while this is not the case for protic solvents such as the alcohols (chains). Therefore, the latter are more likely to interact with the drug than water and the results shown in Table 3.2 corroborate this statement. As a result of the low solubility of CBZ in water, this drug is more favourably transferred to non-aqueous media as reflected in the negative transfer Gibbs energies. In an attempt to obtain experience on the determination of partition coefficients of drugs and its relationship with solubility as described below, four drugs were selected and these are diclofenac, clofibric acid carbamazepine, aspirin and sodium diclofenac²²⁸⁻²³¹.

3.2 Determination of partition coefficients for diclofenac, clofibric acid, carbamazepine, aspirin and NaDF in the water-1-octanol solvent system

The relationship between solubility of a drug and its partition coefficient, K_p , is described as follows; the solubility of a non-electrolyte, D , as described by eq.3.8 is an equilibrium between the solid and its saturated solution in a given solvent, s_1



The equilibrium constant, $K (s_1) = [D] (s_1)$ given that the activity of the solid is by convention =1 For solvent s_2 , the process is described as follows,



Therefore, $K (s_2) = [D] (s_2)$. The ratio between these equilibrium constants is the transfer equilibrium constant, K_t as defined by eq.3.9

$$K_t = K(s_2) / K(s_1) \quad \text{eq.3.11}$$

K_t differs from the partition coefficient, K_p (eq.3.12) in that in the former, pure solvents are involved while in the latter, the mutually saturated (satd) solvents are involved.

$$K_p = [D] (\text{satd } s_2) / [D] (\text{satd } s_1) \quad \text{eq.3.12}$$

In solvents of low mutual solubility, K_t is approximately equal to K_p but differs considerably for solvents for which their mutual solubility is high. This issue has been addressed by Danil de Namor and co-workers²³².

High values of partition coefficients are important and imply that the drug is able to penetrate through the biological cell membrane which is a low permittivity medium to target the receptor site, this means these drugs have low solubility in water and when excreted as a metabolite or as a parent compound to the environment it will take long time to decompose and will be distributed through a wide range of aquatic area. The determination of the partition for these pharmaceuticals have been reported by many researchers¹⁹⁹ but the values obtained are not in accord with each other and this may be due to different factors such as the conditions applied or companies using different procedures to synthesise the chemicals and therefore different crystal structures are obtained. These differences in the crystal structure can have an effect on the solubility and as a result different values are obtained for the parameters related to the solubility. Usually 1-octanol and chloroform are used as solvents representative of the biological membrane due to their low permittivity (dielectric constant)

Values obtained in this work for the partition coefficients of these drugs in the water-1-octanol solvent system obtained (expressed as $\log K_p$) are considered acceptable when compared with the values reported in the literature shown Table 3.3. The dissociation constants of the drugs expressed as pK_a values at 298 K are also included in this Table

Table 3.3 Partition coefficients of drugs in the water-1-octanol solvent system at 298.15.K

Pharmaceutical	$\log K_p$	pK_a
Diclofenac	2.2 ^a , 1.9 ^b , 4.51 ^b	4.16 ^b
Clofibric acid	3.3 ^a , 2.88 ^b	3.2 ^b
Carbamazepine	2.32 ^a , 1.5 ^b , 2.25 ^b	14 ^b
Aspirin	2.02 ^a	3.49

^a This work, ^b ref. 199

It can be seen that within the experimental error not much differences are found in the partition of these drugs from water saturated with 1-octanol to 1-octanol saturated with water.

Having gained experience on solubility measurements and derived thermodynamic parameters as well in the determination of partition coefficients, among all the macrocycles synthesised and characterised, only few were selected for complexation with drugs. These are the functionalised cyclodextrin, Bz- β -CD and the calix[4]arene ester, CAE for sodium diclofenac. For drugs containing carboxylic acids in their structures, such as clofibrac acid, diclofenac, aspirin and ibuprofene, the calix[4]arene amine derivative CA-(NH₂)₂ was the receptor selected for further studies. Preliminary studies in the solid state were carried out with a pyrogallol derivative, PG11 and carbamazepine. The reason for this selection of receptors is explained through the text

3.3 Complex formation of sodium diclofenac NaDF with the per-benzoylated- β -cyclodextrin receptor (BzBCD)

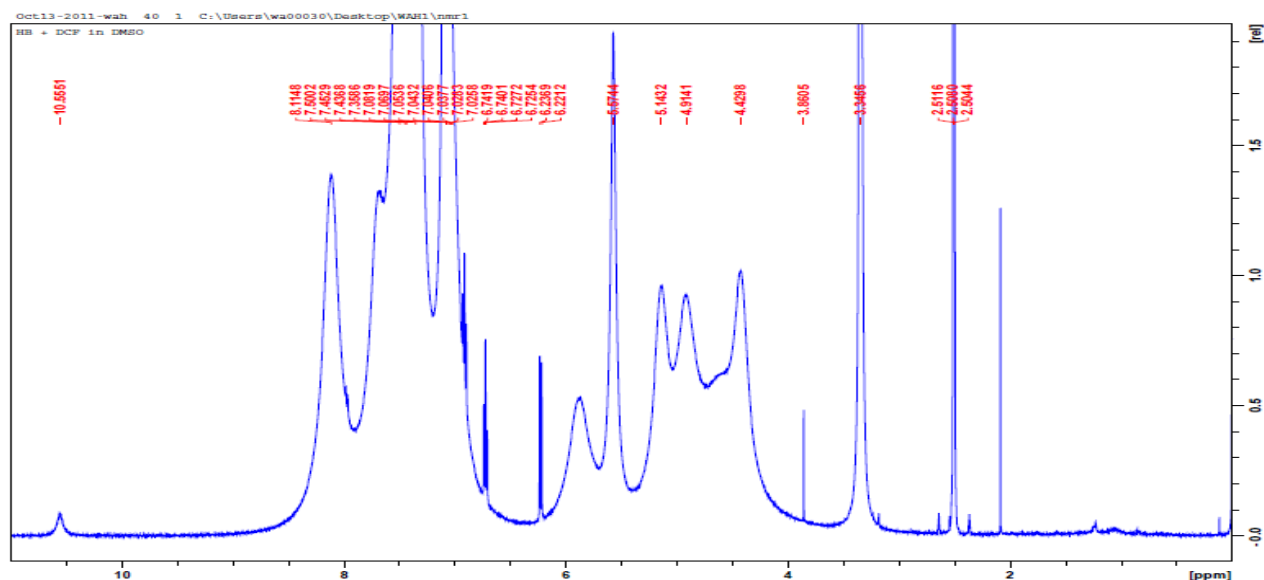
There are a number of possible interactions between NaDF and the functionalised cyclodextrin. It is clear from the chemical structure of the perbenzoylated- β -cyclodextrin. The later contains ester groups which are known to interact with the sodium cation through ion-dipole interactions^{113,114}. On the other hand, the NH functionality of the drug can interact with the oxygen atom of the receptor *via* hydrogen bond formation. Another possibility is that the hydrophobic region of the receptor can interact with the hydrophobic region of the drug. Different techniques were used to investigate whether or not sodium diclofenac interacts with the per-benzoylatec- β -cyclodextrin and if so, to identify possible sites of interaction.

3.3.1 ¹H NMR complexation studies

The ¹H NMR spectrum of the sodium diclofenac with the perbenzoylated cyclodextrin in DMSO-d₆ at 298 K (Fig. 3.1) shows significant changes in the chemical shifts for the sodium diclofenac protons especially for the N-H proton and a downfield shift ($\Delta\delta = 0.5$ ppm) was observed (Table 3.4) which may indicate that there is interaction between this proton and the oxygen atom of the receptor. In addition to strong π - π interaction between the aromatic systems of the sodium diclofenac and the benzoyl groups of the receptor which could be attributed to the formation of host-guest complex through the inclusion of the sodium diclofenac in the receptor cavity^{233,234}

Table 3.4 Chemical shift changes for the NH proton of sodium diclofenac resulting from complexation with per-benzoylated- β -cyclodextrine in DMSO-d₆ at 298 K

Compound	Related proton	chemical shift δ / ppm	δ / ppm	$\Delta \delta$ / ppm
Sodium diclofenac	N-H	10.06	10.56	0.5

**Fig. 3.1** ¹H NMR spectrum for the complex resulted from the complexation of sodium diclofenac and per-benzoylated- β - cyclodextrin in DMSO-d₆ at 298 K

3.3.2 Photophysical properties of the host-guest complex

UV-Vis spectroscopy was also used to investigate the complexation process. The study of the complexation of per-benzoylated β -cyclodextrin and sodium diclofenac were carried out in 1-octanol at 298 K. The selection of 1-octanol was based on the fact that this non-aqueous solvent is representative of the cell membrane due to its low permeability. The titration experiment was carried out by the addition of increasing concentrations of the receptor in 1-octanol to the UV cell containing the solution of sodium diclofenac (5.029×10^{-5} M) in same solvent. The increase of the concentration of the receptor in the cell solution containing sodium diclofenac caused an increase of the absorption band intensity and changed the shape of the absorption band (Fig. 3.2). It can be seen from the plot of absorbance against the wavelength λ (nm) that the absorption band ($n \rightarrow \pi^*$) of the carbonyl group at λ_{\max} 292 nm was shifted to a shorter wavelength due to the solvent-drug interaction through the formation of hydrogen bonding between n electrons and the solvent which can lead to decrease the

energy of the n state without any effect on π orbitals. This means that the energy required for the transition increased and the wavelength will moved shorter while the intensity of the peaks increased (hyperchromic effect) in spite of the decrease in the absorbance of the pharmaceutical which may attributed to the effect of the receptor to lowering the aggregation and promote the dissociation of NaDF to form the complex with the receptor²³⁵⁻²³⁷. The red shifting of $\pi \rightarrow \pi^*$ transition is attributed to the conjugation process for π systems of the aromatic rings. These are indications that there is possible interaction between the receptor and sodium diclofenac. Given that glucose is one of the components of the β -cyclodextrin derivative, this compound was added to the drug solution. The intensity of the peaks was not affected by this addition.

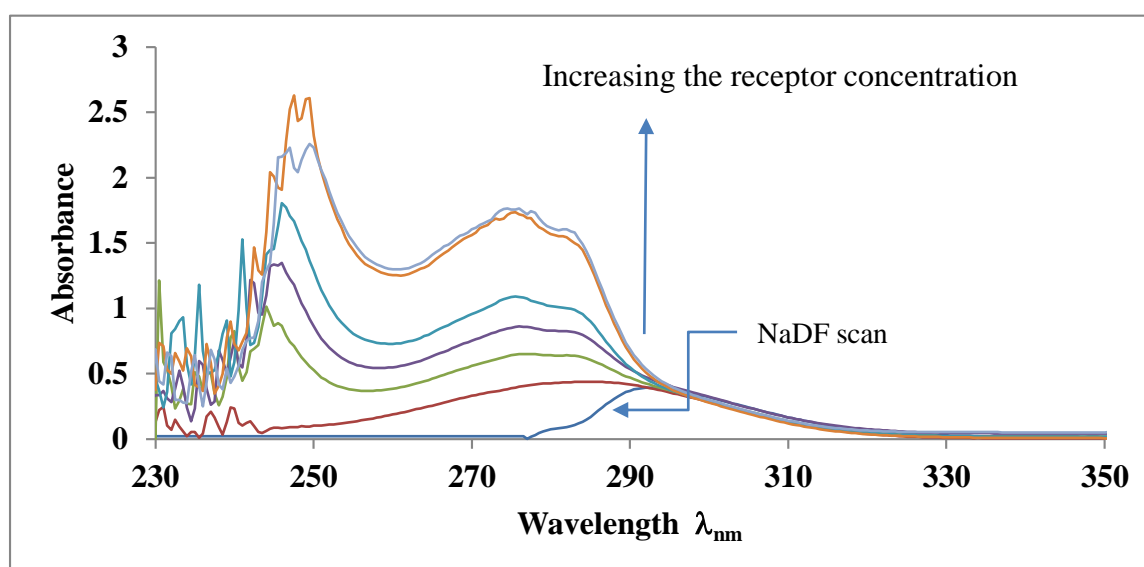


Fig. 3.2 UV-Vis spectrum for the titration of sodium diclofenac solution in 1-octanol (bottom scan, $5.029 \times 10^{-5} \text{ mol dm}^{-3}$) as a result from the addition of different concentrations (3.08×10^{-5} , 4.6×10^{-5} , 6.17×10^{-5} , 7.7×10^{-5} , 9.2×10^{-5} and $1.08 \times 10^{-4} \text{ mol dm}^{-3}$) of perbenzoylated β -cyclodextrin receptor,

Assuming that the complexation reaction between sodium diclofenac NaDF and the receptor L occurred in 1: 1 stoichiometric ratio, thus the complexation can be expressed by equation eq.3.13



In equation 3.13 [NaDF], [BzBCD] and [NaDFBzBCD] denote the molar concentration of sodium diclofenac, the per-benzoylated- β - cyclodextrin receptor and the complex respectively. Therefore,

the stability constant, K_s (expressed in terms of concentrations) for the complexation process is defined in eq.3.14 on the assumption that one molecule of the receptor takes up one unit of the drug

$$K_s = \frac{[NaDFBzBCD]}{[NaDF][BzBCD]} \quad \text{eq. 3.14}$$

The difference between the solutions having the maximum absorbance in the presence of the receptor, A , and its absence, A° is denoted as ΔA_{max} . The change in absorbance with the concentration of the receptor can be represented in eq.3.15

$$A = A^\circ + \frac{\Delta A_{max} K_s [BzBCD]}{1 + K_s [BzBCD]} \quad \text{eq. 3.15}$$

In eq. 3.15, A , A° are the measured absorbance at a given wavelength for the drug solution with and without receptor and ΔA_{max} , represents the change in the absorbance between the complex and the free drug. The stability constant, K_s of the reaction can be calculated from equation 3.16. Plotting $[BzBCD] [NaDF] / [A - A^\circ]$ against the concentration of the receptor (Fig. 3.3) the stability constant was calculated from the slope (slope = $1/K_s$, $\log K_s = 4.01$)²³⁸. It is clear from Fig. 3.3 that the linearity of the equation deviates at the highest concentration of the receptor, which means that as the concentration of the receptor increases the receptor may undergo aggregation instead of complexation with sodium diclofenac.

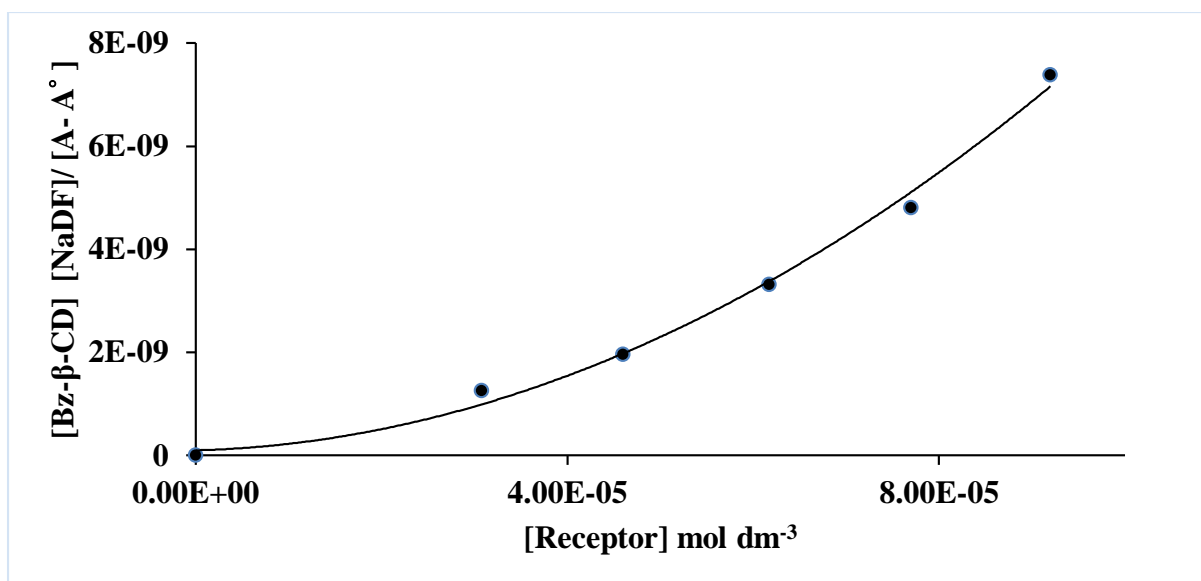


Fig. 3.3 Plot of $[BzBCD] [NaDF] / [A - A^\circ]$ against the concentration of the receptor in mol dm⁻³

In an attempt to corroborate the data obtained by UV-Vis spectrophotometry and to verify the composition of the complex, conductmetric measurements are now discussed. However due to the

difficulties encountered in the use of 1-octanol in the conductometry cell, 1-butanol was the solvent used for conductometric measurements

3.4 Conductometric measurements

3.4.1 Determination of the conductivity cell constant

The cell constant was determined using the method described in the Experimental Section. The numerical values of molar conductance and the cell constant of an aqueous solution of KCl (0.1 mol dm⁻³) at 298.15 K are shown in Table 3.5

Table 3.5 Molar conductance of an aqueous solution of KCl at 298.15 K for the calculation of the cell constant, (θ)

Λ_m (S.cm ² .mol ⁻¹)	θ (cm ⁻¹)
147.07	1.03
146.12	1.08
145.42	1.09
144.84	1.07
144.34	1.09
143.91	1.07
143.15	1.07
142.82	1.07
142.52	1.07

The average value for the cell constant obtained at 298.15 K, θ (cm⁻¹) was 1.07 ± 0.01 cm⁻¹

3.4.2 Conductometric measurements of sodium diclofenac with heptakis-(2, 3 , 6-tri-o-benzoyl)- β -cyclodextrin in 1-butanol at 298.15 K

The solution of the non-steroidal inflammatory sodium diclofenac in 1-butanol has low conductivity due to the association (ion-pair formation) of this salt in butanol as a result from the low dielectric constant of the solvent. Addition of the receptor solution into the sodium diclofenac solution led to an increase of the conductivity values as shown in Fig. 3.4. The conductivity increase is due to the fact that more ions are present in solution. Indeed, the complex consists of a cation larger than the free sodium cation. As a result, the new salt NaBzBCDDF is expected to be more dissociated than

NaDF. After the ligand/ drug concentration ratio reaches a value of 0.5, an excess of the receptor shifts the equilibrium to the right leading to a further increase in conductance. In conclusion, a 2: 1 complex is the most probably formed between NaDF and heptakis-(2, 3 , 6-tri-o-benzoyl)- β -cyclodextrin in this solvent.

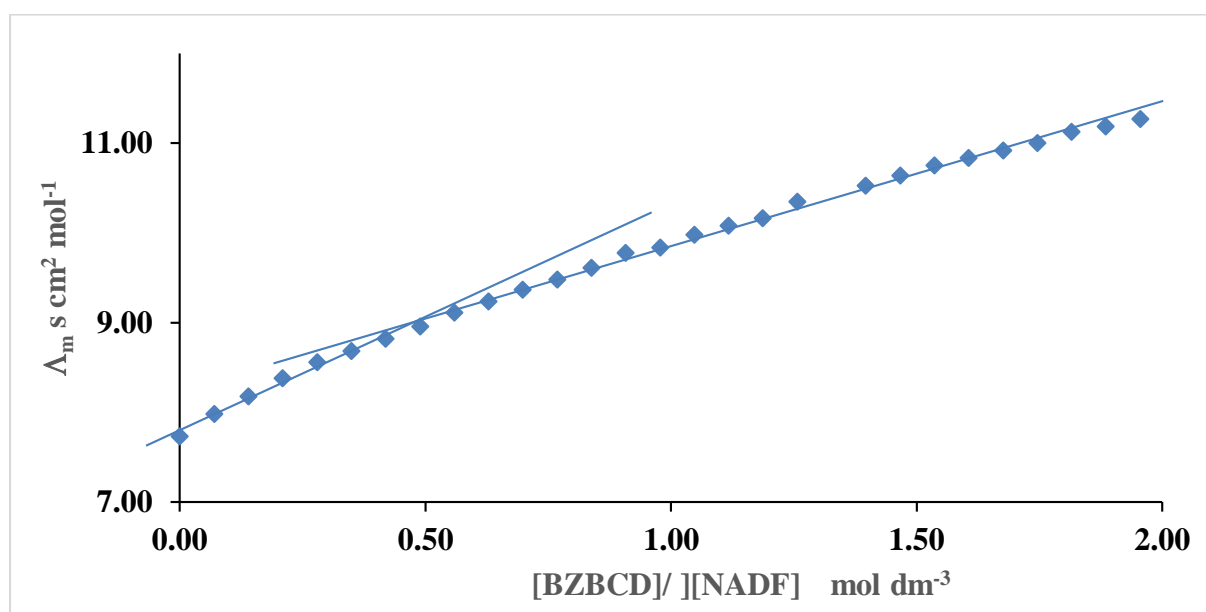


Fig. 3.4 A plot of molar conductance of sodium diclofenac in 1-butanol against the [ligand]/ [drug] concentration at 298.15 K, $[\text{NaDF}] = 1.25 \times 10^{-4} \text{ mol dm}^{-3}$ (the experiment was carried out once).

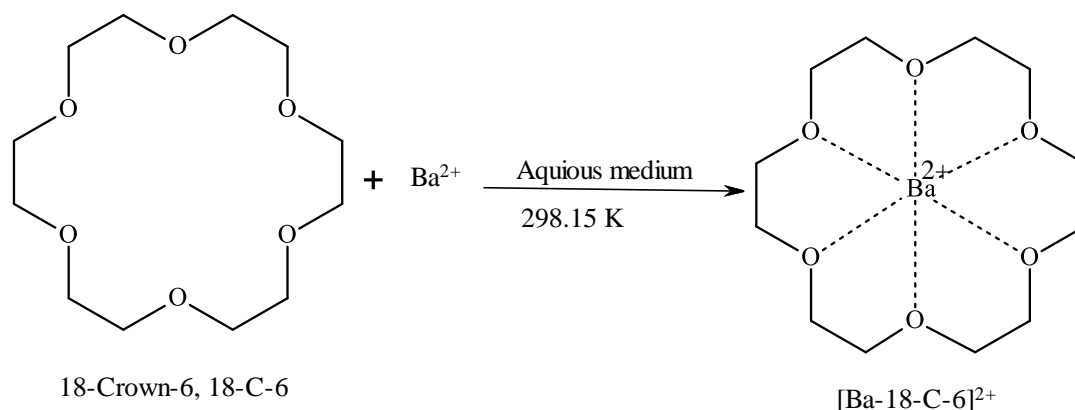
3.5 Complexation studies of sodium diclofenac with heptakis-(2, 3 , 6-tri-O-benzoyl)- β -cyclodextrin in 1-octanol using Nano-Isothermal titration calorimetry (Nano-ITC)

Before proceeding with the determination of thermodynamic data of complexation, the ITC calorimeter was calibrated and therefore in the following section, the calibration of the instrument is discussed

3.5.1 Calibration of the Nano-Isothermal Titration calorimetry (Nano-ITC)

A standard titration experiment between 18-Crown-6 and barium chloride in de-ionised water at 298.15 K was carried out to determine the reliability of the instrument. An aqueous solution of 18-crown-6 ether ($1 \times 10^{-3} \text{ mol dm}^{-3}$) was loaded in the reference cell and a solution of barium chloride in de-ionised water ($1.5 \times 10^{-2} \text{ mol dm}^{-3}$) injected automatically to the sample cell. A typical baseline

and fitting curve were obtained (Fig.3.5) indicating that the experiment was carried out carefully and the instrument was highly accurate



Scheme 3.1 The standard reaction between barium chloride and 18-crown-6 ether in aqueous medium at 298.15 K

From the data obtained from this titration, thermodynamic parameters for the complexation process such as stability constant ($\log K_s$) and the change in enthalpy, $\Delta_c H$ were calculated from the software provided with the instrument. The standard Gibbs energy, $\Delta_c G^\circ$ and entropy $\Delta_c S^\circ$, were calculated according to the following equations

$$\Delta_c G^\circ = -RT \ln K_s \quad \text{eq.3.16}$$

In eq.3.16 K_s represents the stability constant, $\Delta_c G^\circ$ is the standard Gibbs energy change of complexation, R is the gas constant ($8.314 \text{ J mol}^{-1} \text{ K}^{-1}$) and T is the temperature in Kelvin. The standard entropy change, $\Delta_c S^\circ$ for the complexation was calculated according to the following equation

$$\Delta_c G^\circ = \Delta_c H^\circ - T\Delta_c S^\circ \quad \text{eq.3.17}$$

A typical calibration curve was obtained (Fig. 3.5) indicating that the stoichiometry of the reaction is 1: 1 $[\text{18-Crown-6}]/[\text{Ba}]^{2+}$ and the thermodynamic parameters obtained for the complexation of 18-crown-6 with BaCl_2 in water at 298.15 K are shown in Table 3.6. It was found that the obtained values were in good agreement with the values reported earlier in the literature.

Table 3.6 Thermodynamic parameters of complexation of barium with 18-crown-6 measured by ITC in aqueous medium at 298.15 K.

Log K_s	$\Delta_c G^\circ / \text{kJ mol}^{-1}$	$\Delta_c H^\circ / \text{kJ mol}^{-1}$	$\Delta_c S^\circ / \text{J K mol}^{-1}$	Reference
3.60 ± 0.06	$- 20.8 \pm 0.3$	$- 29 \pm 2$	$- 27$	This work
$\approx 3.45 - 3.87$	$\approx - 21.9$	$- 29 - 33$	$- 33$	Ref. 219

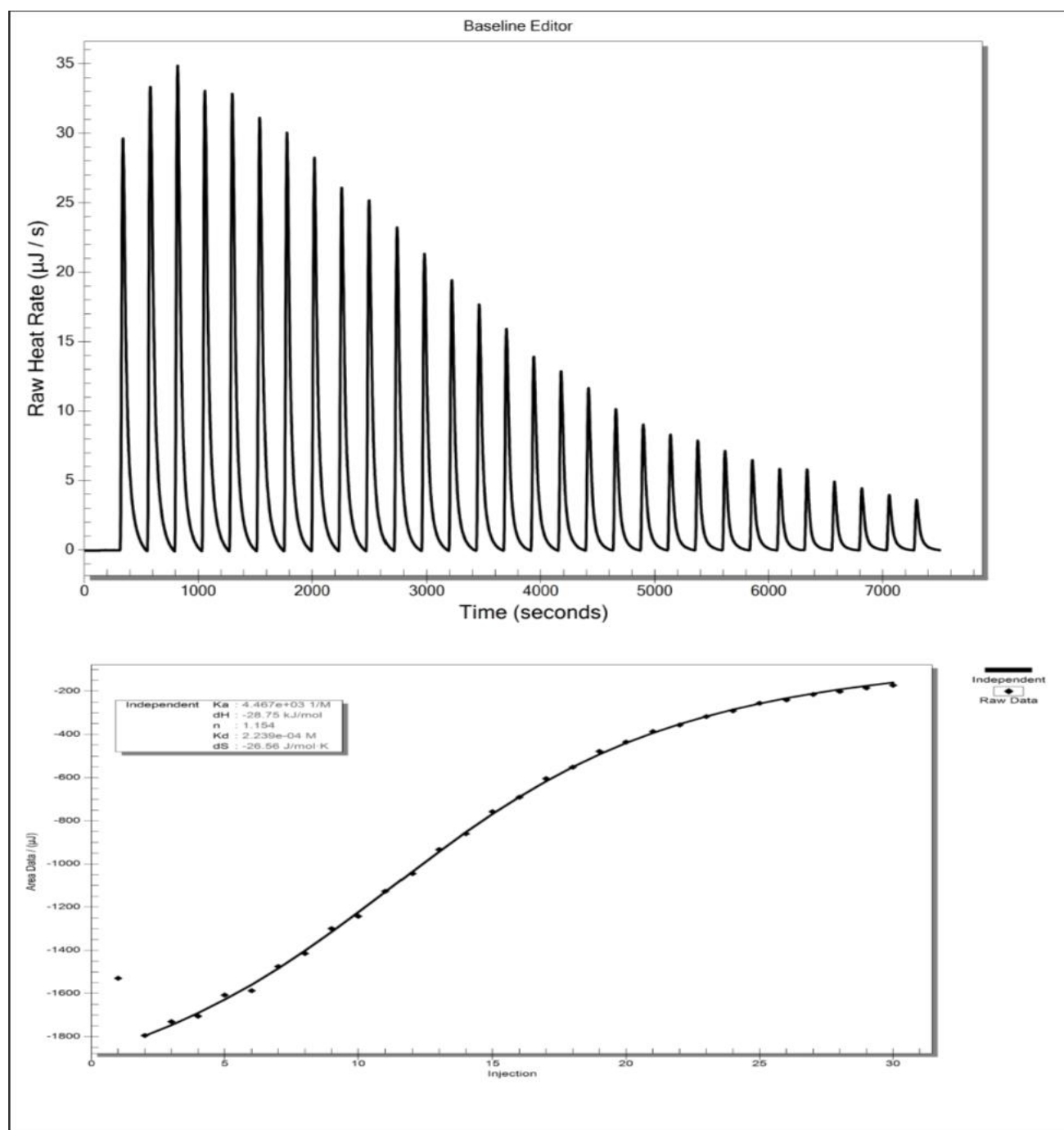


Fig. 3.5 Isothermal titration calorimetry for the complexation of 18-crown-6 ($1 \times 10^{-3} \text{ mol dm}^{-3}$) with BaCl_2 ($1.5 \times 10^{-2} \text{ mol dm}^{-3}$). The curve shows the change in enthalpy after each injection as a result of complexation.

3.6 Determination of the thermodynamic parameters of complexation of sodium diclofenac with heptakis-(2, 3 , 6-tri-o-benzoyl)- β -cyclodextrin in 1-octanol at 298.15 K

The experimental work to determine the complexation of BzBCD and NaDF in 1-octanol by titration calorimetry at 298.15 K was carried out by the addition of NaDF in 1-Oct into the ITC cell loaded with the receptor solution in the same solvent. The baseline of the titration curve shown in Fig.3.6 indicated that the complexation process was achieved successfully. The heat evolved is very small implying that the process was driven by weak forces and therefore the stability of the complex is entropy controlled as shown in Table 3.7. The data fits into a 1: 1 (drug: receptor) stoichiometric ratio as found by UV-Vis spectroscopy. Good agreement is found between the two sets of data. The advantage of nanocalometry relative to UV-Vis spectrophotometry is that the former gives the contribution of enthalpy to the stability of the complex and by the use of eq. 3.17 the entropy could be calculated

Table 3.7 Thermodynamic parameters of complexation of the cyclodextrin derivative with sodium diclofenac at 298.15 K.15 in 1-octanol

Titration type	$\log K_s$	$\Delta_c G^\circ / \text{kJ mol}^{-1}$	$\Delta_c H^\circ / \text{kJ mol}^{-1}$	$\Delta_c S^\circ / \text{J K}^{-1} \text{mol}^{-1}$
By ITC measurements	4.04 ± 0.01	-23.07 ± 0.06	-0.45 ± 0.02	79
UV/ Vis measurements	4.01 ± 0.001	-22.90 ± 0.01		

Unfortunately, the use of the per-benzoylated as a solid phase to remove sodium diclofenac from water could not be investigated due to the aggregation of the receptor in the aqueous medium To overcome this limitation, a calix[4] arene ester derivative, CAE was explored as discussed below

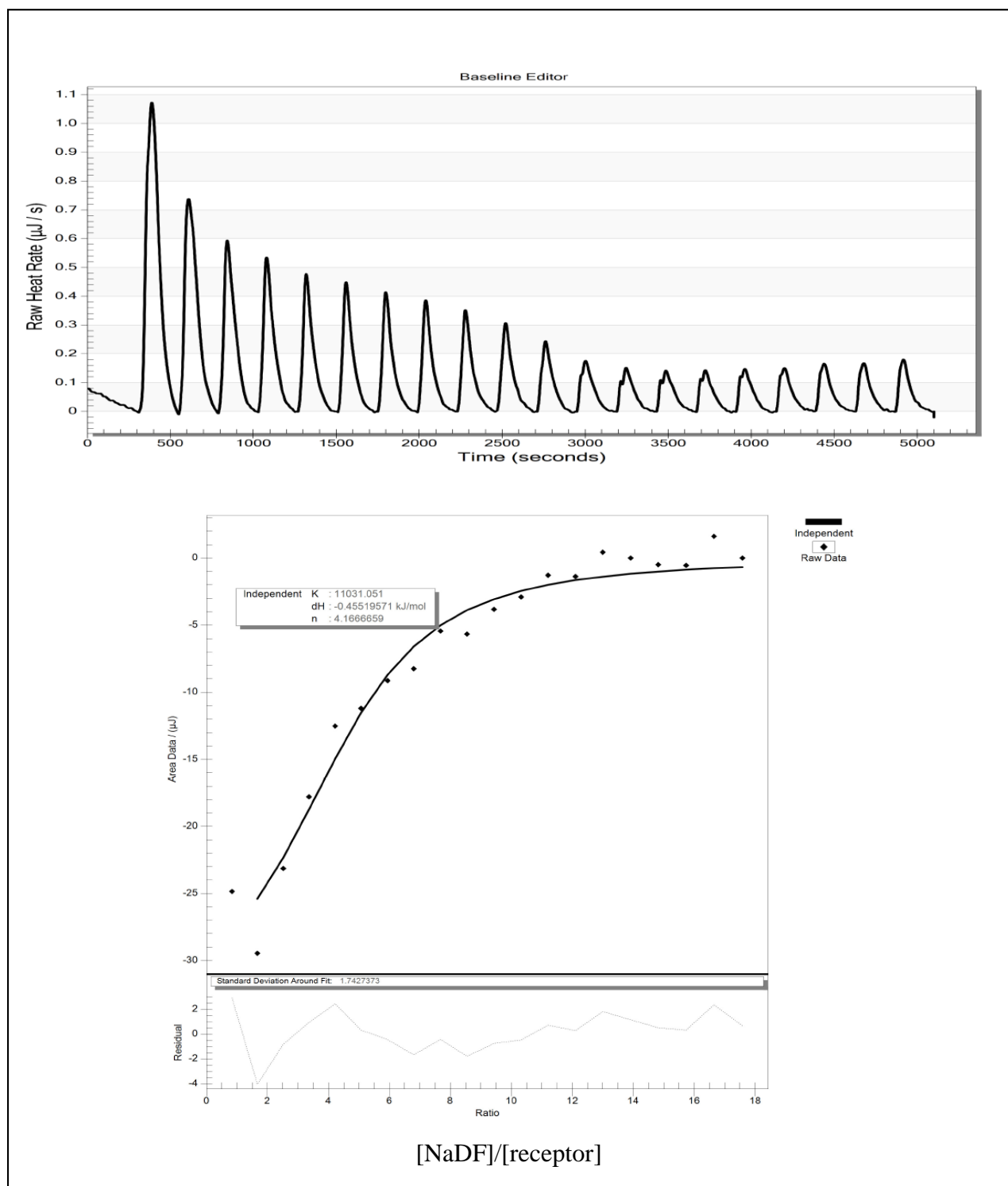


Fig. 3.6 Isothermal titration calorimetry for the complexation of sodium diclofenac [Guest] and perbenzoylated- β - cyclodextrin in 1-octanol at 298.15 K. Top: the heat evolved after each addition of sodium diclofenac to the receptor sloution and bottom plotted against the molar ratio. $[\text{NaDF}] = 1 \times 10^{-3} \text{ mol dm}^{-3}$

3.7 Complexation studies of sodium diclofenac and 5, 11, 17, 27- *tert*-butyl-25, 26, 27, 28-(oxy-ethylethanoate)calix[4]arene (CAE)

3.7.1 ¹H NMR complexation studies

The esterification of *p-tert*-butyl calix[4]arene has been carried out in one step and the compound was obtained in a high degree of purity which is very important for complexation studies. The modified procedure used here differs from those previously reported. In the procedures used earlier the authors²³⁹ introduced ethyl bromoacetate in several portions in order to give time for the activation of the phenolic hydroxyl group. Other workers did not give a detailed account of the procedure¹¹⁴ and used a base like sodium bicarbonate which appears to be time consuming (5 days)²¹². It was concluded in the literature that there is a probability that the ester group could be reduced to alcohol in the presence of a base, but the anhydrous solvent used prevents the reduction to alcohol which means that the use of the hydrated solvent can facilitate the reduction to alcohol due to the protonation of the carbonyl groups which can deviate the reaction towards the alcohol product. Also controlling the pH of the reaction (pH = 7) was a suitable way to direct the reaction to produce the targeted receptor. The ¹H NMR spectrum confirmed the structure of the compound in addition to the microanalysis (see Experimental Part). The obtained receptor adopts a distorted *cone* conformation as it is clear from the difference in the chemical shift value $\Delta\delta = 1.47$ ppm between the axial and equatorial protons¹¹⁷. Initially, the complexation studies were carried out using ¹H NMR studies in deuterated acetonitrile. The spectrum for the complex (Fig.3.7) showed that the receptor complexed with the drug and significant changes in the chemical shift for the axial and equatorial protons of the methylene bridge protons of the receptor were observed (Table 3.8). The low solubility of the sodium diclofenac in acetonitrile retarded the progress with the titration experiment as to determine the thermodynamic parameters associated with this process by isothermal titration calorimetry. Another complexation study has been carried out to investigate the complexation process using DMSO-d₆ as a dipolar aprotic solvent but the spectrum obtained shows that the receptor interacted strongly with this solvent and this interaction prevent the ¹H NMR titration experiment. However, the binding affinity of the receptor to complex with the sodium cation (picrate or perchlorate counter ion) have been reported with details by McKerverey *et al*¹¹³ and Danil de Namor *et al*²⁴⁰ and have demonstrated that the cation was nested perfectly in the lower rim polar semi-cavity with the cooperation of the acetonitrile solvent occupying the hydrophobic cavity of the receptor. Here the affinity of the solid receptor to complex with the sodium cation was exploited for the removal of the sodium diclofenac

from water after proceeding with the fundamental studies to determine the composition of the complex. In doing so conductance measurements were carried out prior to these measurements.

Table 3.8 Chemical shift changes for the receptor protons as a result from the addition of sodium diclofenac in CD₃CN at 298 K

Proton	Ar-H	C-H _{Axial}	OCH ₂ CO	O-CH ₂ CH ₃	H _{Equatorial}	O-CH ₂ -CH ₃	C-CH ₃
δ	6.77	4.85	4.8	4.2	3.38	3.28	1.05
Δδ	0.0	Vanished	-0.05	0.1	0.04	0	0

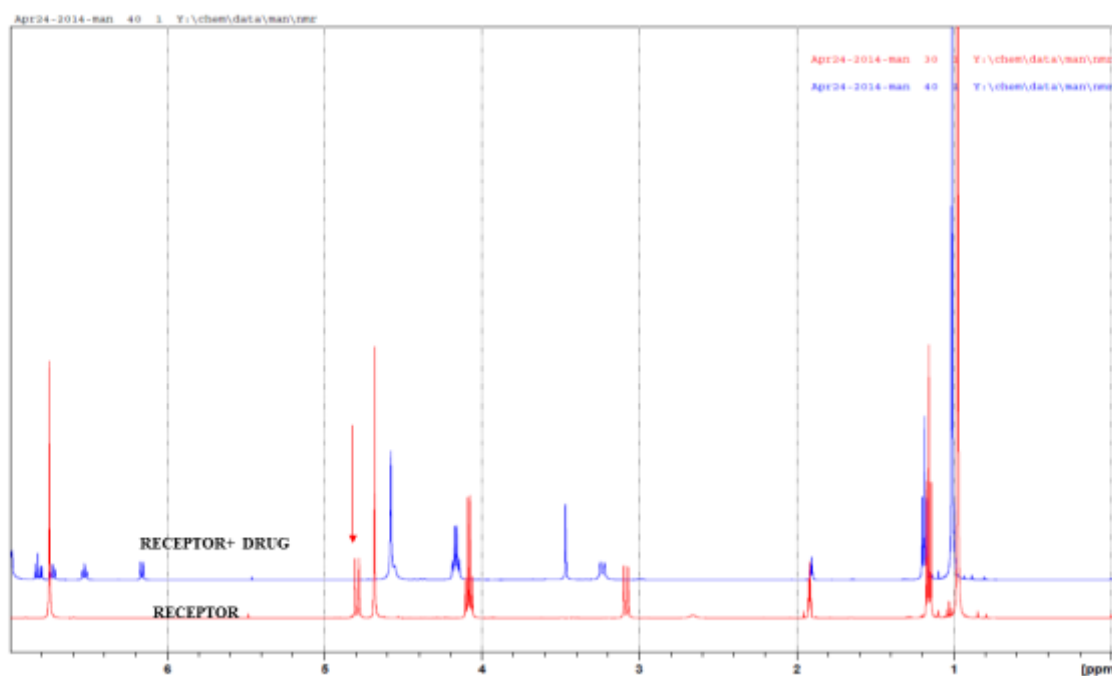


Fig. 3.7 ¹H NMR spectra for the complexation of *p-tert*-butylcalix[4]arene tetraeseter (3×10^{-2} mol dm⁻³) with sodium diclofenac in CD₃CN at 298 K. The lower spectrum for the free receptor and the upper for the complex with sodium diclofenac (1×10^{-3} mol dm⁻³)

3.7.2 Conductometric measurements of sodium diclofenac with 5, 11, 17, 27- *tert*-butyl-25, 26, 27, 28-(oxy-ethylacetate)calix[4]arene (CAE) in acetonitrile at 298.15 K

The solution of sodium diclofenac in acetonitrile has low conductivity due to the association (ion-pair formation) of this salt in acetonitrile. Addition of the calix[4]arene tetraester solution into the sodium diclofenac solution ($4.8 \times 10^{-4} \text{ mol dm}^{-3}$) led to an increase in the conductivity values as shown in Fig. 3.8 The conductivity increase is due to the fact that more ions are present in solution. Indeed, the complex consists of a cation larger than the free sodium cation. As a result, the new salt [NaCAE]DF is expected to be more dissociated than NaDF. After the ligand/ drug concentration ratio reaches a value of 1, an excess of the receptor shifts the equilibrium to the right leading to a further increase in conductance. In conclusion a 1: 1 complex is formed between NaDF and the calix[4]arene ester in acetonitrile

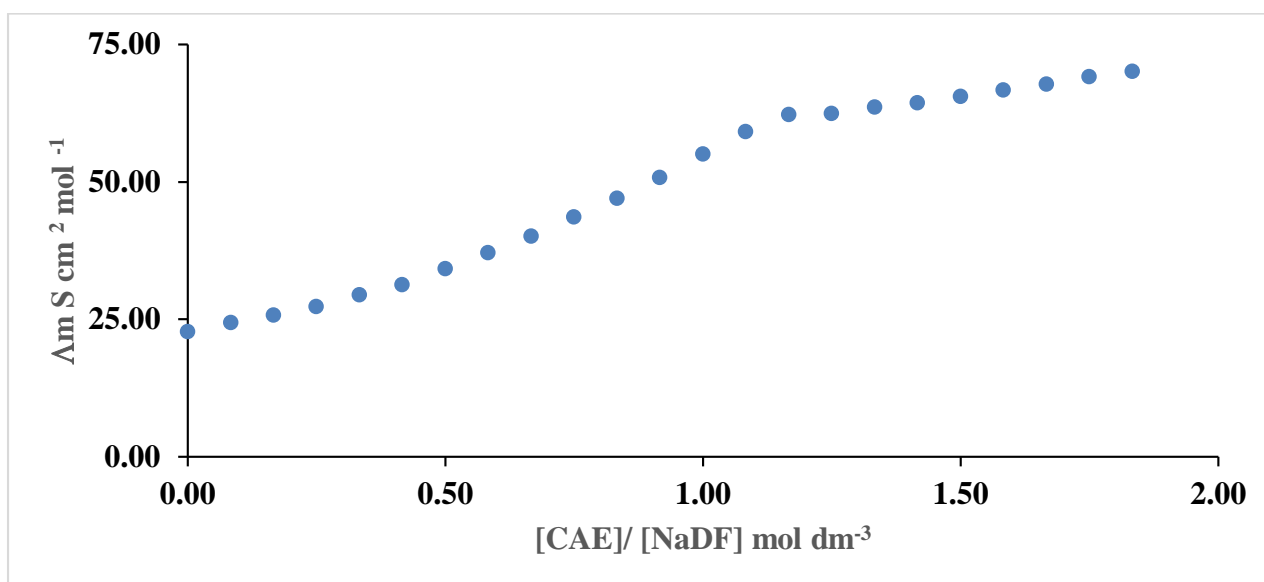
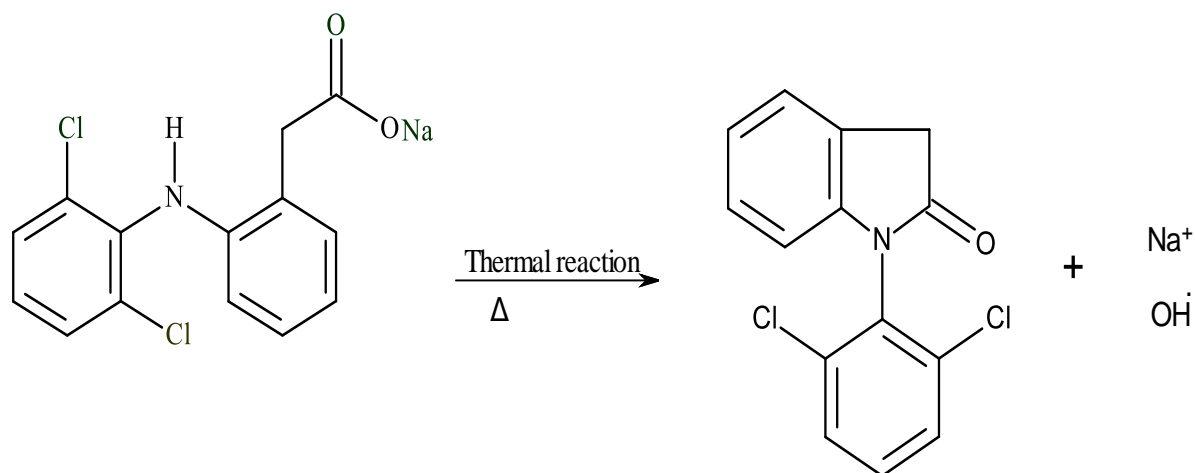


Fig. 3.8 A plot of molar conductance against the receptor/ drug concentration ratio for the system involving *p-tert*-butylcalix[4]aren tetraester and sodium diclofenac NaDF in acetonitrile ($4.8 \times 10^{-4} \text{ mol dm}^{-3}$) at 298.15 K.

To investigate further the complexation of NaDF with the calix[4]arene ester, thermogravimetric analysis were carried out.

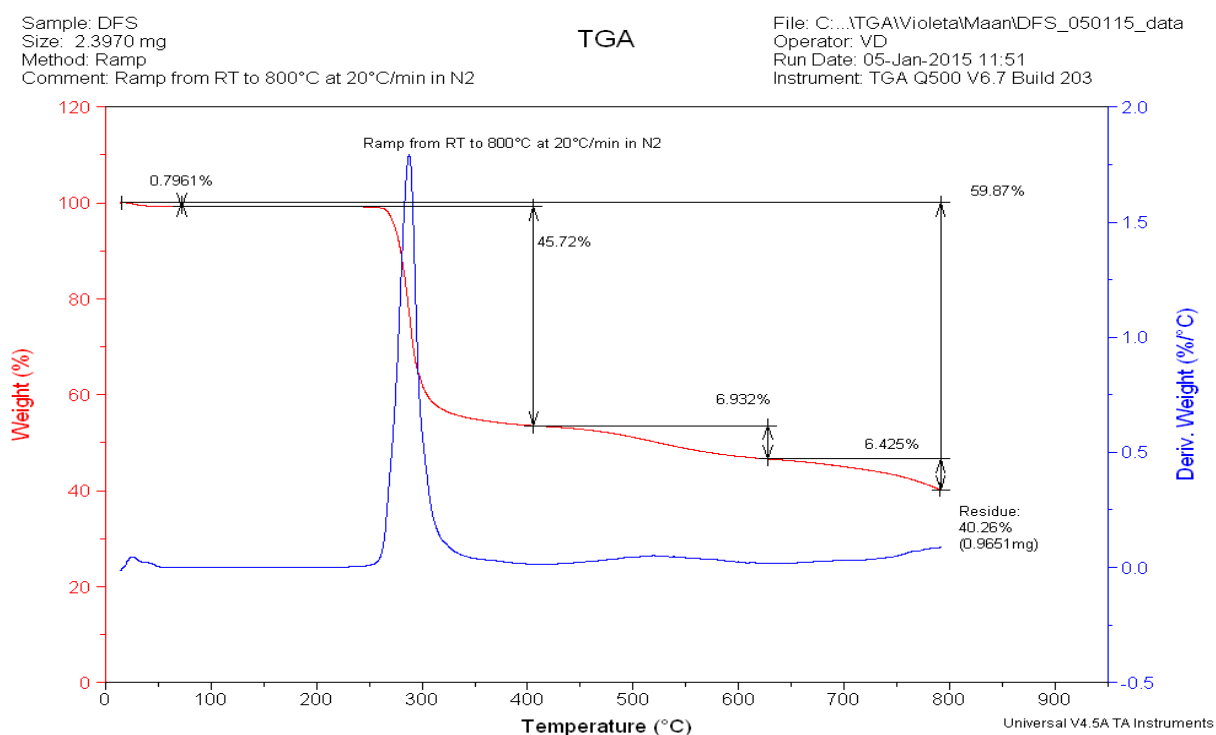
3.7.3 Investigation of the complexation between sodium diclofenac and 5, 11, 17, 27- *tert*-butyl-25, 26, 27, 28-(oxy-ethylacetato)calix[4]arene by thermogravimetric analysis TGA and DSC

The thermogravimetric analysis was carried out as described in the Experimental Part. The TGA thermograms for sodium diclofenac, the receptor (CAE) and the complex are shown in Figs 3.9-3.12. The TG analysis was carried out under a nitrogen gas atmosphere in the rate flow of 50 cm³/min and the temperature was raised from 0 °C to 800 °C. The complexation process between the calix[4]arene tetraester receptor with sodium diclofenac was confirmed by comparing the thermogravimetric behaviour of the pure compounds with that of the complex formed. TGA thermograms for calix[4]arene tetraester CAE, NaDF and the complex formed (Fig. 3.9) provided significant evidence that the complexation process between CAE and NaDF was implemented successfully. It is known that there is a direct correlation between the rigidity of a solid and its thermal stability. Comparison between these thermograms indicated that the thermal stability of the complex is lower than the thermal stability of the free receptor as a result of the increasing flexibility of the complex to achieve the conformational changes required for complex formation. The required reorganization processes to achieve the complexation process obliged the receptor to be sufficiently flexible to compensate the energy losses during the conformational changes and to stabilise the complex formed²⁴¹. This means that the rigidity decreases and, as a consequence, reduction of the thermal stability occurred. In addition to the results obtained from TG analysis, the DSC thermograms for the pure compounds and the complex indicated that the complexation between the NaDF and the receptor is achieved. The DSC curve for sodium diclofenac is not in accord with the DSC thermogram reported earlier in the literature and this may be due to the oxidation of the pharmaceutical (Scheme 3.1)²⁴². This can be attributed to the quantity of nitrogen gas delivered to the sample which was not enough to prevent the oxidation reaction or to the increase in the heat rate to 20 °C/min which may have accelerated the oxidation reaction. Therefore, the curve reported in the literature is considered to give the interpretation related to the DSC curve of sodium diclofenac. The DSC thermogram reported in the literature²⁴¹ indicated that the melting point of sodium diclofenac is 280 °C. The DSC thermogram of the free receptor (Fig. 3.14) have shown a sharp endothermic peak at 155.04 °C with a heat of fusion; $\Delta H = +14.878 \text{ kJ mol}^{-1}$ representing the melting point of the pure receptor. The results obtained clearly have indicated that the melting point of the complex shifted to a lower temperature than that for the free receptor as a result of the complexation process (Fig. 3.15). It should be emphasised that this is the first DSC analysis reported in the literature for the calix[4]arene tetraester and its complexation involving any pharmaceutical.



Sodium diclofenac

1-(2, 6-dichlorophenyl) indolin-2-one

Scheme 3.2 The cyclisation of the sodium diclofenac due to thermal reaction²⁴²**Fig. 3.9** TGA Thermogram for pure sodium diclofenac

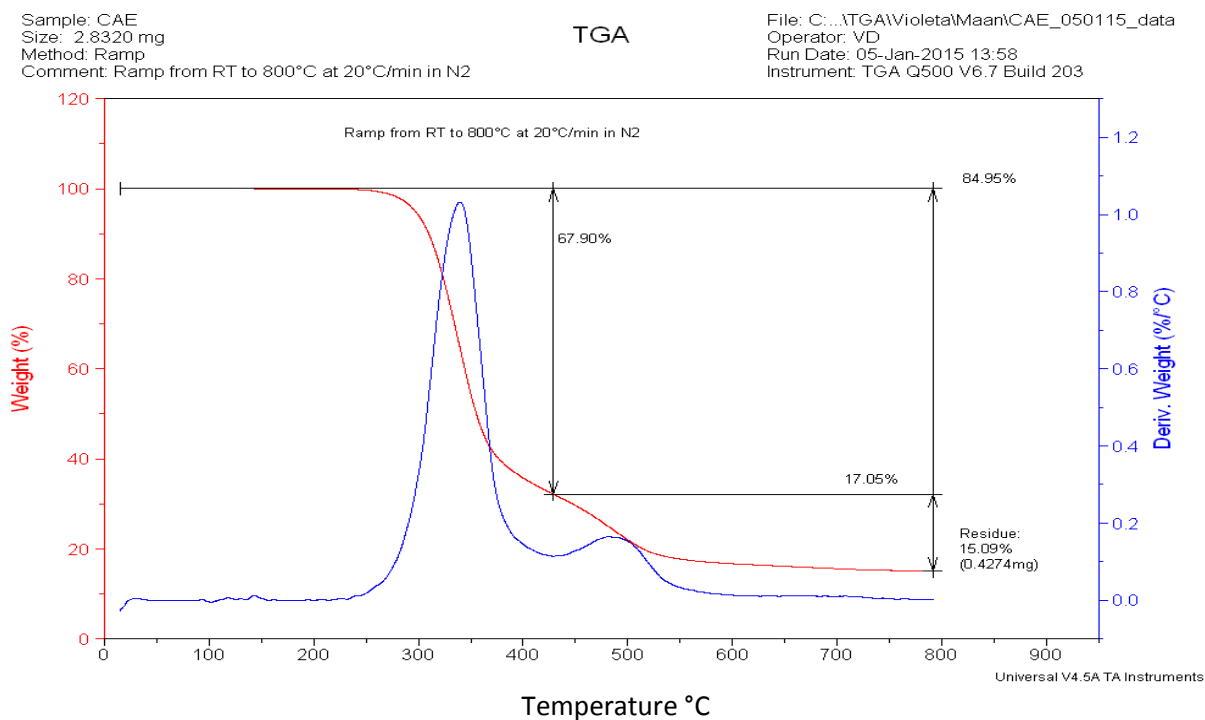


Fig. 3.10 TGA thermogram analysis curve as it was obtained for *p*-*tert*-butylcalix[4]arene tetraester

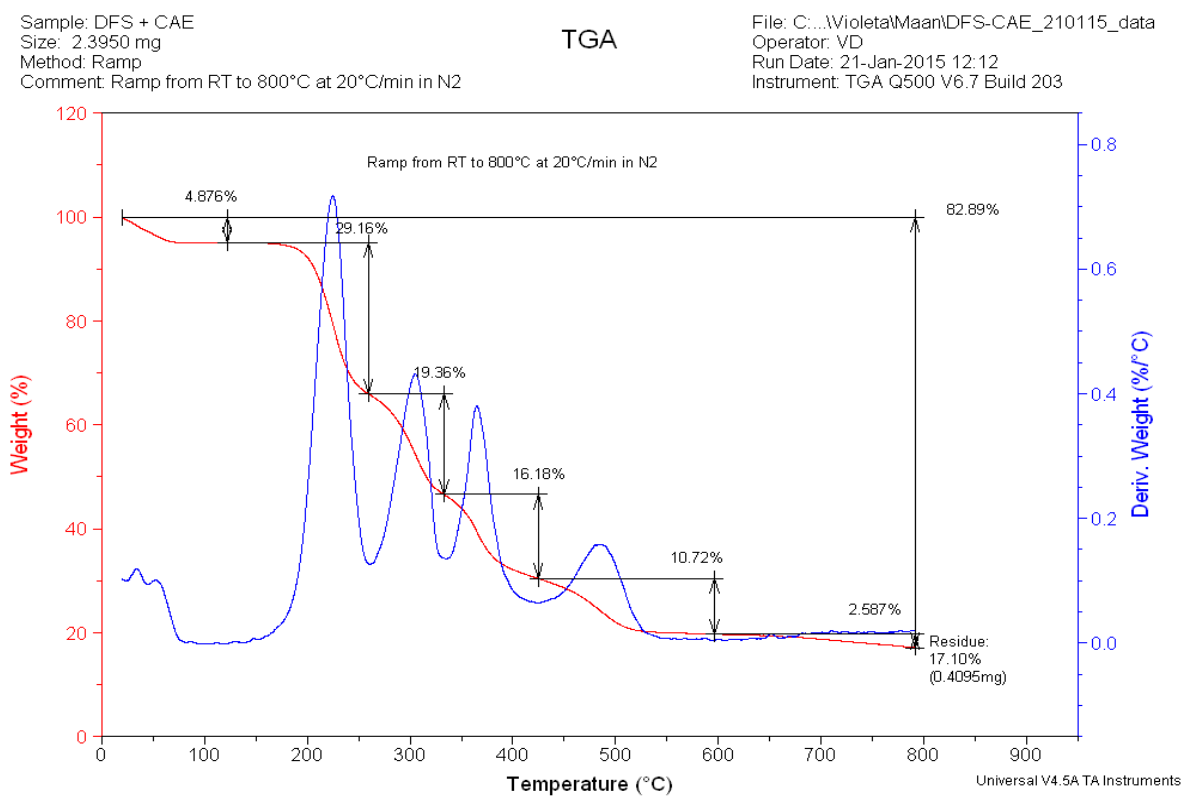


Fig. 3.11 TGA thermogram for the complex formed between sodium diclofenac NaDF and the CAE receptor

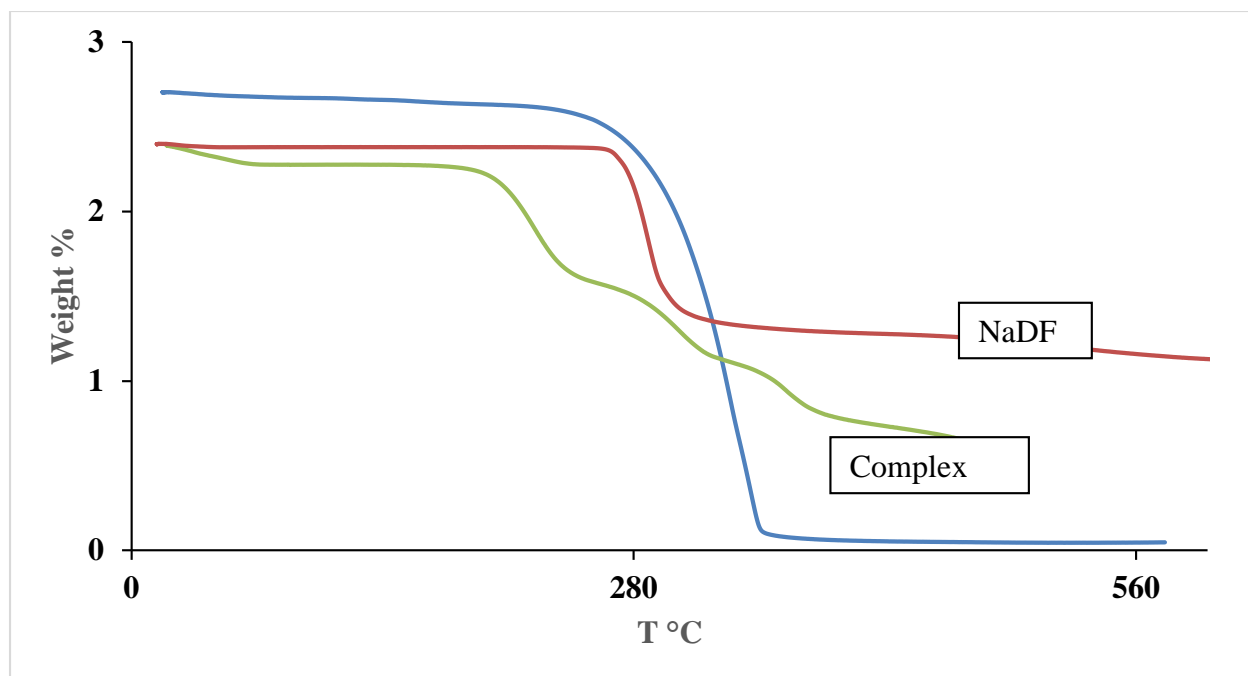


Fig. 3.12 TGA curves for the sodium diclofenac NaDF, calix[4]arene tetraester (CAE) and the complex formed.

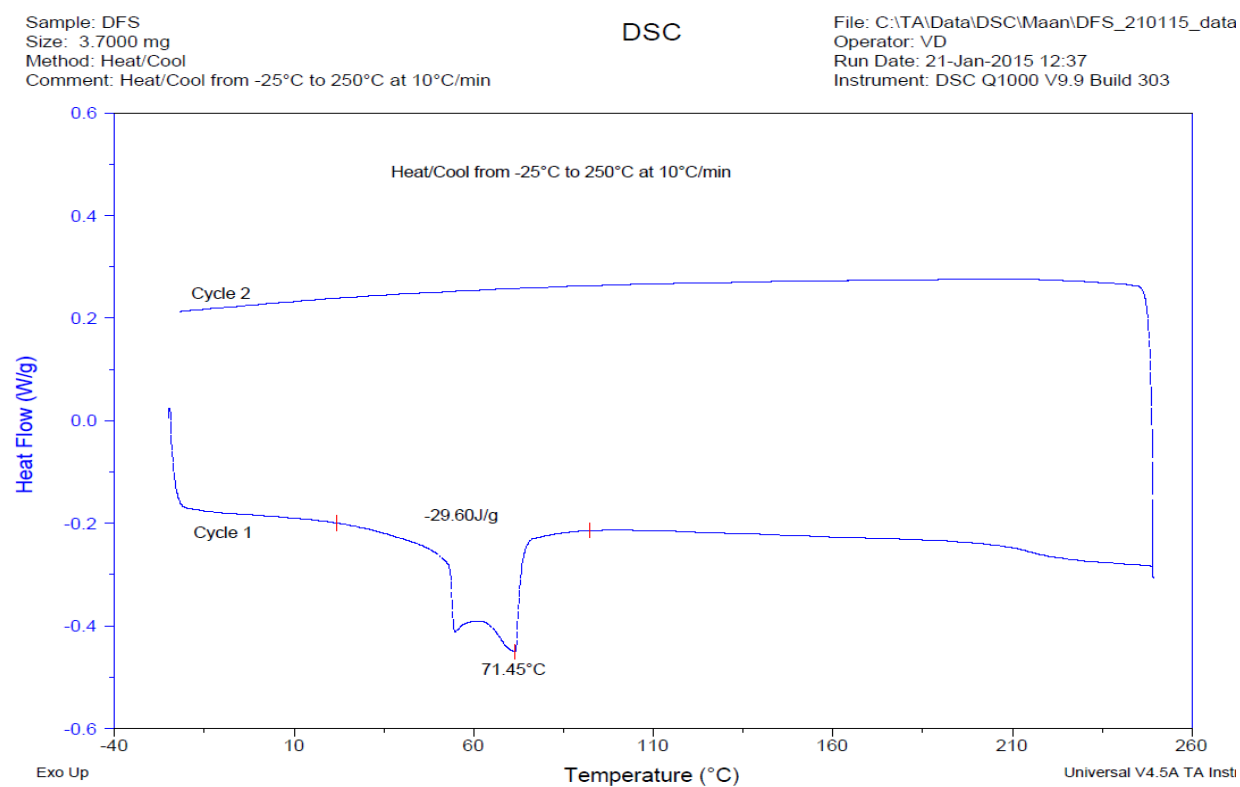


Fig. 3.13 DSC thermogram of the sodium diclofenac

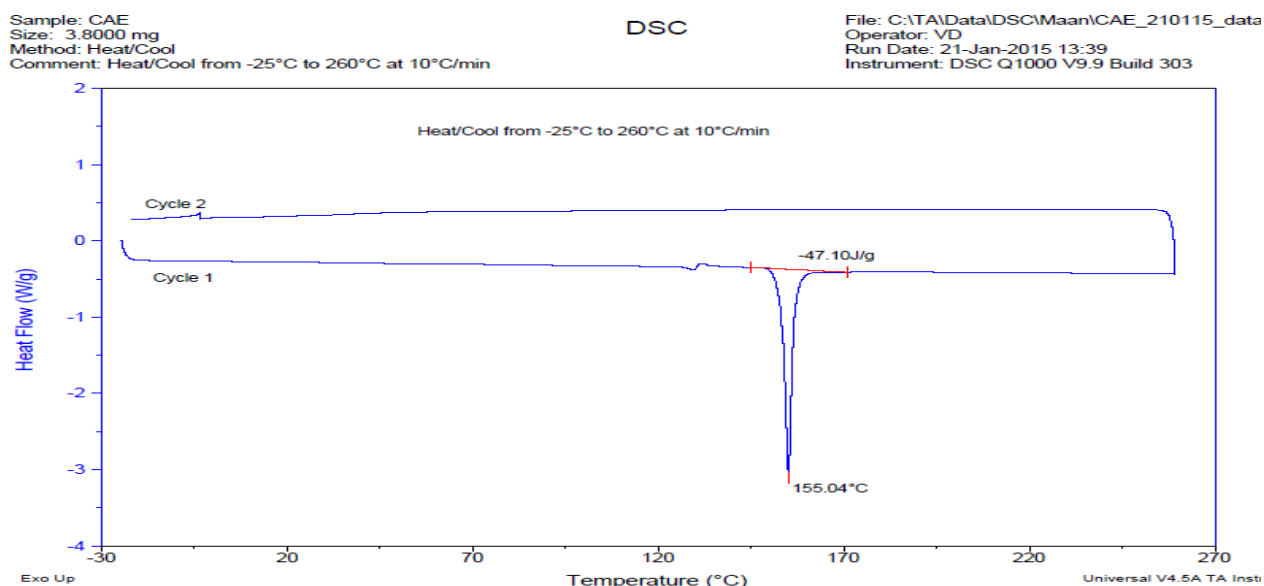


Fig. 3.14 DSC thermogram for the CAE receptor

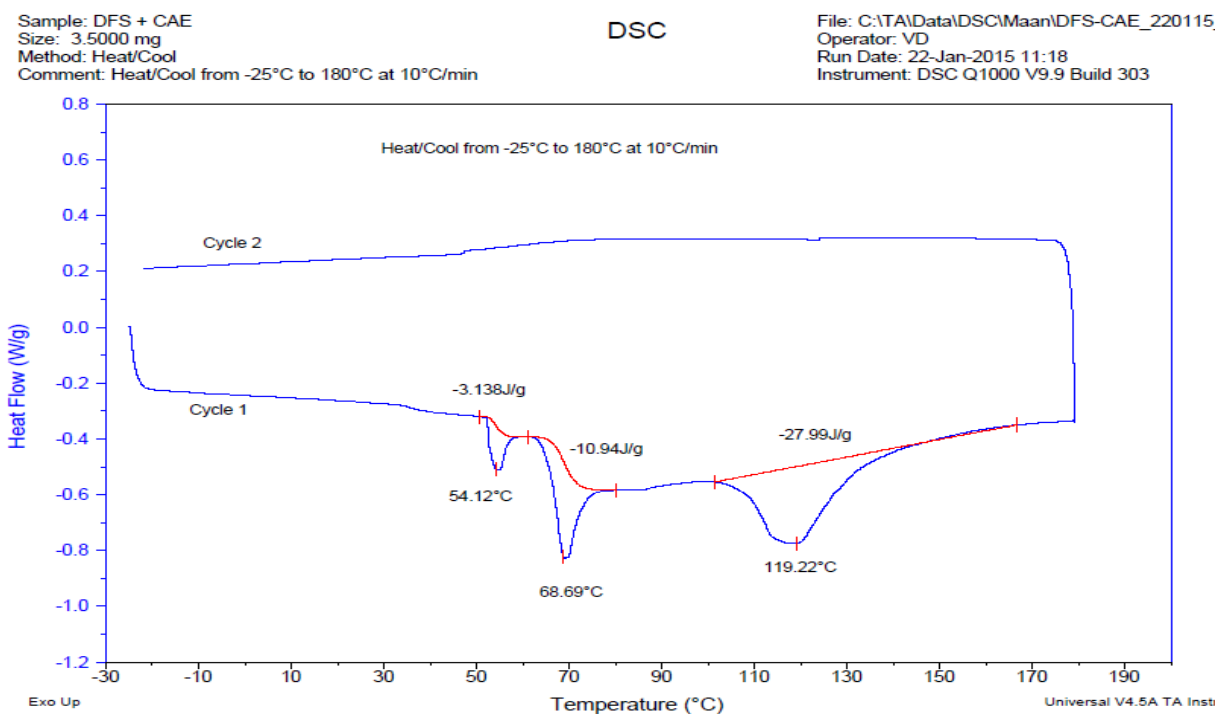


Fig. 3.15 DSC analysis for the complex formed between sodium diclofenac and calix[4]arene tetraester.

Having obtained some information regarding the complexation process in solution (conductance measurements) and in the solid state (thermal analysis) the ability of calix[4]arene tetraester to remove the drug from water was investigated.

3.8 Removal of sodium diclofenac from water by using calix[4]arene tetraester from water.

Extraction experiments were carried out under several experimental conditions as shown below

3.8.1 Determination of the optimum amount of calix[4]arene tetraester for the uptake of sodium diclofenac from aqueous solution at 298 K

In order to determine the optimum mass of the calix[4]arene tetraester for the removal of sodium diclofenac from water, batch experiments were carried out. Different weights of the calix[4]arene tetraester was added to a fixed concentration of aqueous solution of sodium diclofenac (2×10^{-4} mol dm^{-3} , 10 ml). The mixtures were mixed for 10 minutes on a whirlimixer, sealed and left in a water bath at 298 K. The mixtures were filtered and the concentration of the drug at equilibrium was determined using a UV-Vis spectrophotometer at $\lambda_{\text{max}} = 272$ nm. Table 3.9 indicates that the percentage of NaDF removed from aqueous solution by the receptor increases with increasing the mass of the material, and then the material reaches saturation as shown in Fig. 3.16.

This is expected as the weight of the receptor increases, the amount of sites available for interaction with the sodium cation increases

Table 3.9 Effect of the amount of calix[4]arene tetraester on the extraction of sodium diclofenac from aqueous solution (10 ml) at 298 K

[conc.] _{initial} mol dm^{-3} (10 ml)	Receptor added (solid in mole)	[Conc.] _{equilibrium} mol dm^{-3}	[Conc.] _{removed} mol dm^{-3}	% E
2×10^{-4}	1.01×10^{-5}	7.93×10^{-5}	1.21×10^{-4}	60.35
2×10^{-4}	2.01×10^{-5}	7.63×10^{-5}	1.24×10^{-4}	61.85
2×10^{-4}	3.02×10^{-5}	7.03×10^{-5}	1.30×10^{-4}	64.85
2×10^{-4}	4.03×10^{-5}	7.03×10^{-5}	1.30×10^{-4}	64.85
2×10^{-4}	5.03×10^{-5}	7.1×10^{-5}	1.29×10^{-4}	64.50
2×10^{-4}	6.04×10^{-5}	7.1×10^{-5}	1.29×10^{-4}	64.50

The % E was calculated using the eq.2.39 and the concentration of the NaDF at equilibrium was calculated using UV-vis measurements (see Fig. 1-A Appendix)

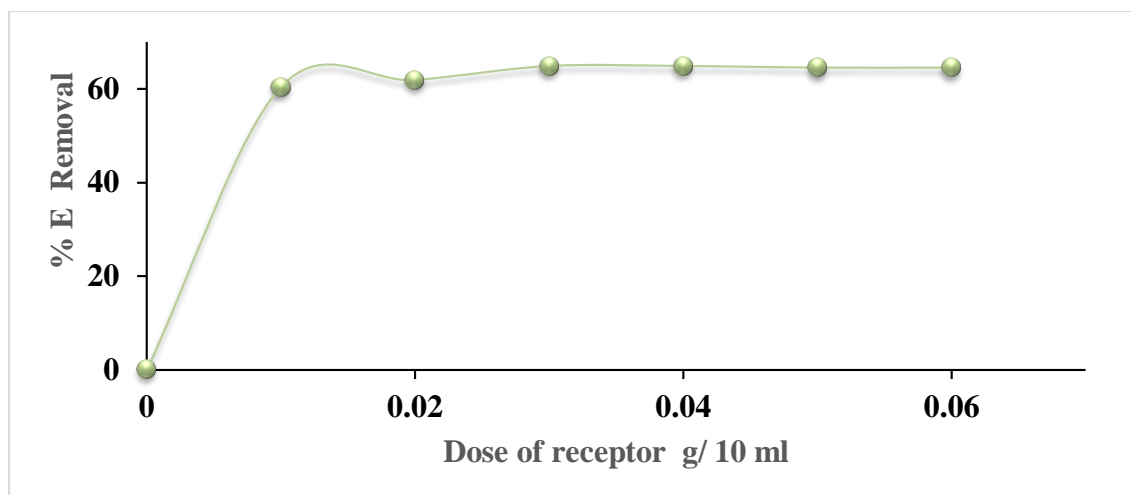


Fig. 3.16 The effect of mass on the uptake of NaDF from aqueous solution by calix[4]arene tetraester at 298.15 K

The data obtained shows that the optimum mass of the material to remove NaDF from aqueous solution was found to be 0.03 g for a volume of aqueous solution of 10 ml.

3.8.2 Determination of the capacity of calix[4]arene tetraester to uptake NaDF from aqueous solution at 298.15 K

The capacity (quantity of NaDF extracted from the solution per unit quantity of material) was determined by equilibrating a fixed mass of calix[4]amine tetraester (0.03 g) with a volume of 10 ml of the aqueous solution containing different concentrations of NaDF (Table 3.10). Thus Fig. 3.17 shows the amount of NaDF (mmol) extracted per gram of dry calix[4]arene tetraester. It is observed that the degree of extraction of calix[4]arene tetraester is dependent on the concentration of the NaDF present but the percentage of extraction is not attained when the concentration of the drug is about $8.9 \times 10^{-5} \text{ mol dm}^{-3}$ decreased when the concentration is about $1.03 \times 10^{-4} \text{ mol dm}^{-3}$ and this may refer to the increasing of the interferences at high concentrations .

Table 3. 10 Illustrate the initial equilibrium and removed concentration of NaDF by calix[4]tetraester.

$[\text{NaDF}]_{\text{initial}}$	$[\text{NaDF}]_{\text{equilibrium}}$	$[\text{NaDF}]_{\text{removed}}$	Capacity (mmol g^{-1})	% E
3.45×10^{-5}	1.70×10^{-5}	1.75×10^{-5}	0.005	50.70
4.60×10^{-5}	1.90×10^{-5}	2.70×10^{-5}	0.009	58.60
5.75×10^{-5}	2.30×10^{-5}	3.45×10^{-5}	0.011	60.00
6.90×10^{-5}	2.50×10^{-5}	4.40×10^{-5}	0.014	63.70
8.05×10^{-5}	2.80×10^{-5}	5.25×10^{-5}	0.017	65.20
9.20×10^{-5}	3.10×10^{-5}	6.10×10^{-5}	0.020	66.30
1.03×10^{-4}	4.00×10^{-5}	6.30×10^{-5}	0.021	61.16

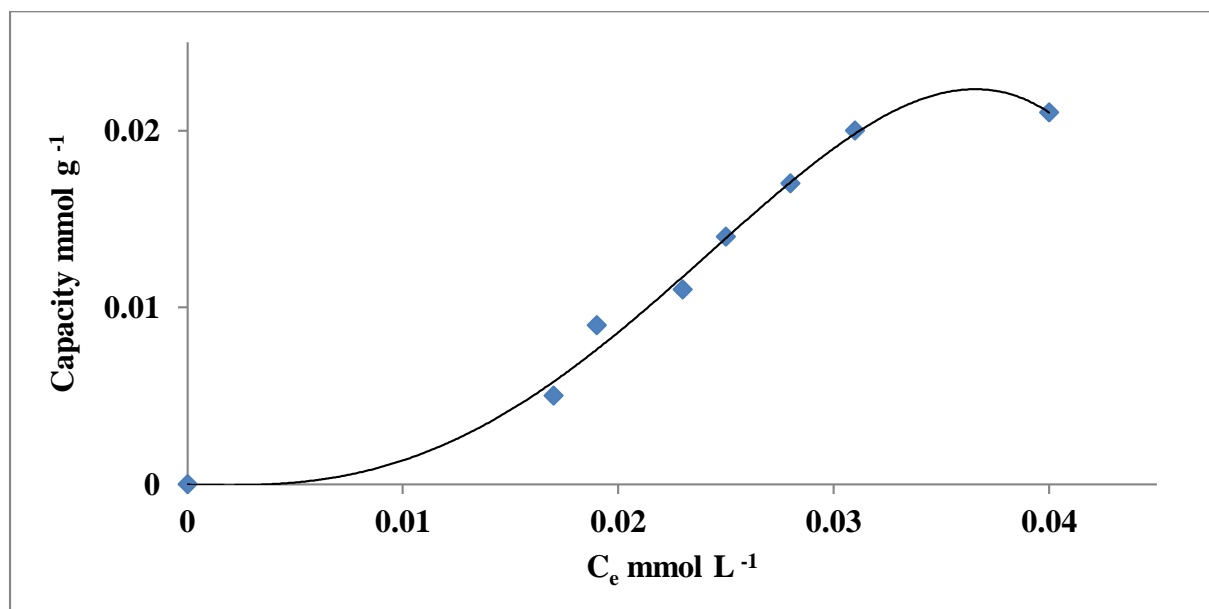


Fig. 3.17 Uptake isotherm for sodium diclofenac from aqueous solution by CAE at 298.15 K.

3.8.3 Determination of the pH effect on the uptake of NaDF from aqueous solution by the calix[4]arene tetraester CAE at 298 K

The influence of pH value on the removal of sodium diclofenac by CAE was assessed in order to achieve the best removal condition, the assesment process was tested by the addition of solid receptor CAE (0.03 g) to a fixed concentration of aqueous solution of NaDF ($6.9 \times 10^{-5} \text{ mol dm}^{-3}$, 10 ml) at different pH at 298 K. The mixtures were mixed for 10 minutes on a whirlimixer, sealed and left in a water bath at 298. The mixtures were filtered and the concentration of the drug at equilibrium determined using a UV-Vis spectrophotometer at 272 nm. The obtained results are displayed in Table 3.11 and plotted. Fig. 3.18 shows that the efficiency of the receptor to uptake NaDF from water in low and high level of pH is dramatically decreased which means that the extraction percentage of NaDF moved down due to the sensitivity of ester group to acids and bases.

Table 3.11 Effect of pH on the extraction of sodium diclofenac by CAE receptor (3.02×10^{-5} mole) at 298 K

pH solution	[NaDF] _{initial} mol dm ⁻³	[NaDF] _{eq} mol dm ⁻³	E %
1	6.9×10^{-5}	6.72×10^{-5}	2.61
3	6.9×10^{-5}	3.73×10^{-5}	46.0
4	6.9×10^{-5}	2.49×10^{-5}	63.8
5	6.9×10^{-5}	2.84×10^{-5}	58.9
6	6.9×10^{-5}	3.52×10^{-5}	49.0
7	6.9×10^{-5}	3.82×10^{-5}	44.6
8	6.9×10^{-5}	4.89×10^{-5}	29.0

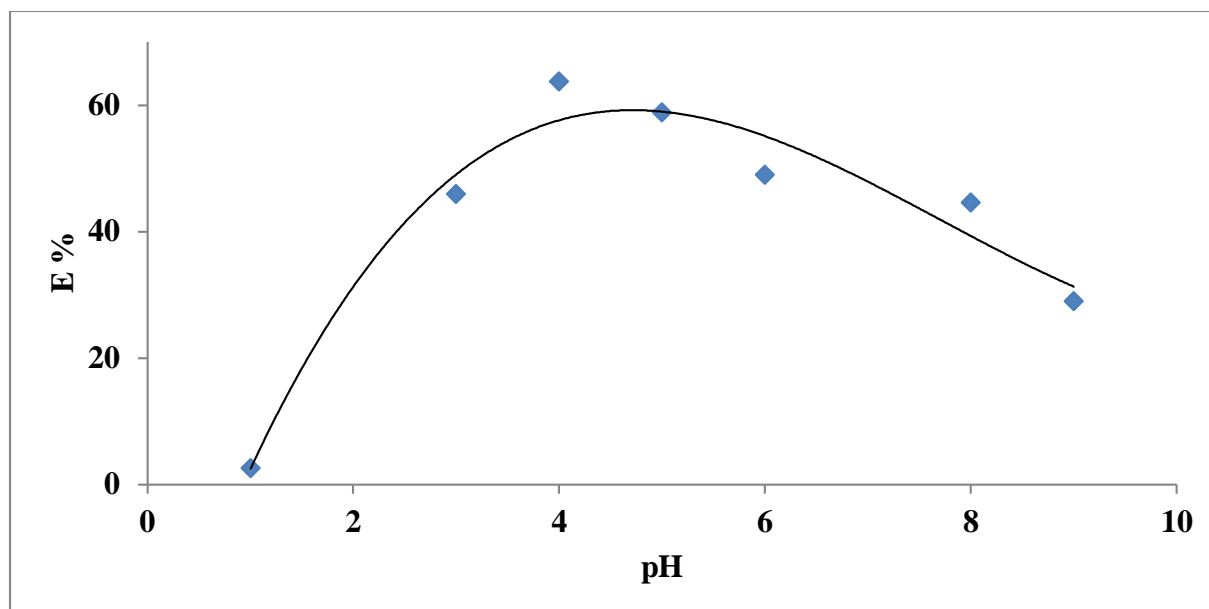


Fig. 3.18 The effect of pH on the on the sodium diclofenac uptake (6.9×10^{-5} mol dm⁻³, 10 ml) by 5, 11, 17, 27- *tert*-butyl-25, 26, 27, 28-(oxy-ethylacetato)calix[4]arene (CAE, 3.02×10^{-5} mole)

The results obtained for the removal of NaDF from water by the calix[4]aren ester were encouraging. It was thought that it was of interest to explore the complexing ability of a calix[4]arene amine based receptor containing amino functional groups for currently used

3.9 Complexation studies of CA-(NH₂)₂ and pharmaceuticals

3.9.1 ¹H NMR complexation studies of diclofenac, clofibric acid, aspirin and ibuprofen with the 5, 11, 17, 23-tetra-*tert*-butyl, 25, 27-bis[aminoethoxy]26, 28 - dihydroxycalix[4]arene [(CA(NH₂)₂] receptor in CD₃CN at 298 K

The chemical structure for the receptor and the pharmaceuticals are shown in the Fig.3.19

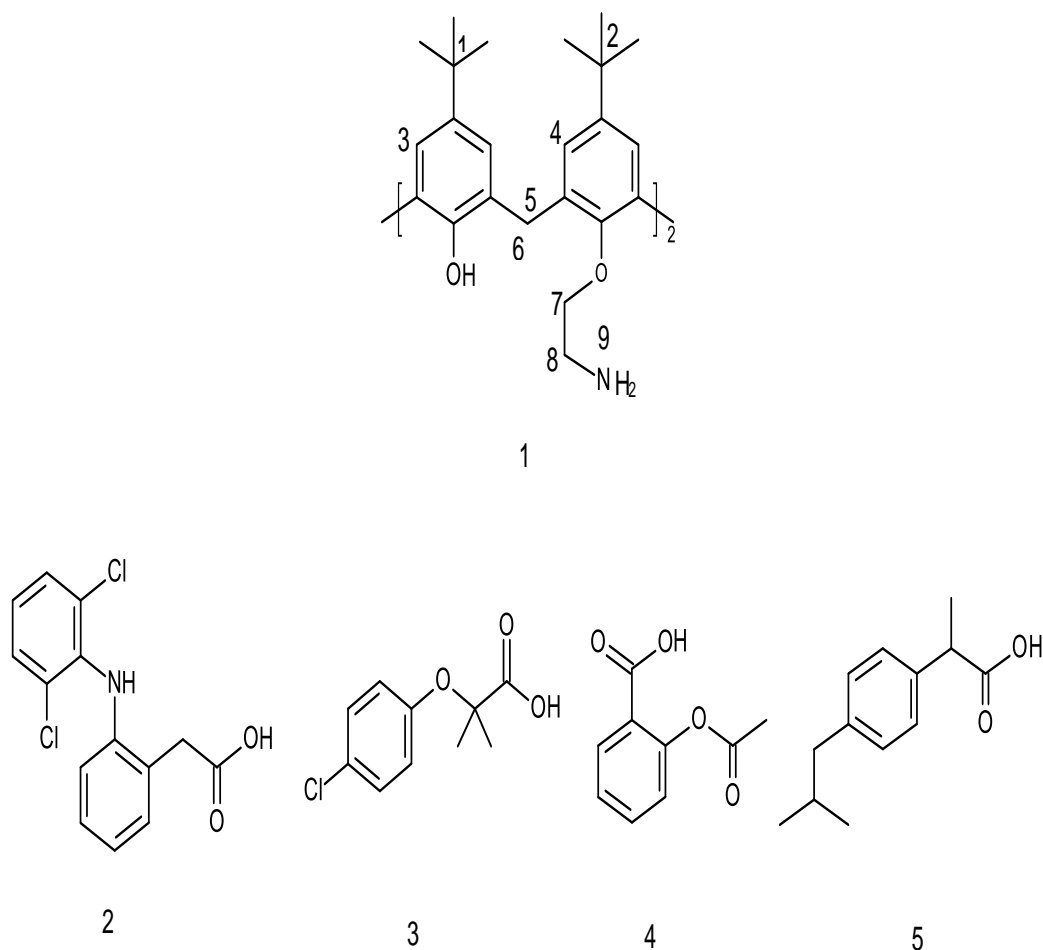


Fig. 3.19 Chemical structures of (1) receptor (CA-(NH₂)₂), (2) diclofenac, (3) clofibric acid (4) aspirin and (5) ibuprofen

As described in the Experimental Section, ¹H NMR titration experiments were carried out to investigate the active sites of complexation of the receptor with the pharmaceuticals and to obtain information regarding the stoichiometry of the complexation. As far as the ¹H NMR measurements are concerned, the results in CD₃CN at 298 K are listed in Table 3.12 which shows the chemical shifts of the free receptor, δ , and the chemical shift changes, $\Delta\delta$, for the receptor upon the addition of the pharmaceutical. These were calculated from eq.3.17

$$\Delta\delta(\text{ppm}) = \delta(\text{complex}) - \delta(\text{free}) \quad \text{eq.3.17}$$

In eq.3.17, $\Delta\delta$ is the chemical shift observed, δ (complex) is the chemical shift for the complex resulting from the addition of the targeted drug, δ (free) is the chemical shift for the free receptor. As far as the free receptor is concerned quite clearly the calix[4]arene amino derivative adopts a *quasi* perfect 'cone' conformation in solution as reflected in the difference observed in the chemical shifts of the axial and equatorial protons ($\Delta\delta_{\text{ax-eq}} = 1.03$ ppm)^{110,117}. This conformation is due to the presence of hydrogen bond formation between the phenolic hydrogens and the ethereal oxygens of the pendant arms of the receptor. This was previously demonstrated by Danil de Namor and co-workers¹⁸⁵ for an homologous receptor, namely 5,11,17,23-*tetrakis*-[(diethylamine)ethoxy]calix[4]arene [CA(Et₂)₂] in the solid state (X-ray diffraction studies) and in solution. In fact the $\Delta\delta_{\text{ax-eq}} = 1.02$ ppm in CD₃CN for this homologous receptor is practically the same as that for CA(NH₂)₂. Furthermore acetonitrile was found in the hydrophobic cavity of the receptor. Also the X-ray structure of 5,11,17,23-*tetrakis*-[(diethylamine)ethoxy]calix[4]arene showed acetonitrile in the hydrophobic cavity of the receptor. Previous studies by Danil de Namor^{185,240} in this solvent demonstrated that this process is also observed in solution. In fact this is also the case for the receptor involved in this work as assessed from the chemical shift changes observed for the aromatic protons of this receptor in moving from CDCl₃ to CD₃CN where downfield chemical shifts of 0.21 and 0.19 ppm are observed. Further conformational changes are also observed in the bridging methylene protons during the complexation or protonation process. The equatorial protons become less shielded relative to the free receptor particularly for clofibric acid and diclofenac (-0.21 ppm) while for aspirin this effect is less pronounced (-0.11 ppm) while the equatorial protons are slightly deshielded relative to the uncomplexed receptor. Hardly any changes for the equatorial and axial protons are found for ibuprofen and this may be attributed to the presence of the isobutyl group in the chemical structure of this drug which may reduce the possibility of ibuprofen to interact with the receptor in addition to the ion-pair formation for the drug in acetonitrile. A direct consequence of that, is a decrease in the shift difference between each pair of doublets of the ArCH₂Ar system, from the free to the complex ligands (from 1.03 to 0.76 ppm for aspirin and to 0.66 ppm for clofibric acid and diclofenac), Significant downfield chemical shift changes are observed for H-7, H-8 and the NH proton as a result of an interaction between the amino group of the receptor and the proton of the carboxylic functional group of the drug. The most significant chemical shift changes are found for the NH proton. In an attempt to explain the differences observed in the $\Delta\delta$ values for the NH proton for these pharmaceuticals (Table 3.13-Appendix) the pK_a values in water are considered¹⁹⁹ (pK_a values are 3.0, 3.5, 4.16, 4.38 for clofibric acid, aspirin, diclofenac and ibuprofen respectively) due to the unavailability of these data in acetonitrile. Although the absolute pK_a values of these in the latter solvent are expected to differ significantly from those in water due to the medium effect,

the sequence would be the same. It is therefore concluded that the downfield shift of the NH proton of CA-(NH₂)₂ is strongly dependent of the degree of dissociation of the acid. This is further corroborated by ¹H NMR titrations carried out in CD₃CN. Representative examples for the titration of the receptor with diclofenac (Table 3.1-Appendix, Fig. 3.20) and clofibric acid (Table 3.2-Appendix, Fig. 3.21) in acetonitrile at 298 K are given where Δδ values obtained by the addition of these drugs to CA-(NH₂)₂ are plotted against the drug/receptor molar ratio where the most pronounced chemical shift changes are observed for the NH protons and to a lesser extent for H-7 and H-8. Regarding aspirin, overlapping between the spectra of receptor and aspirin prevent the calculation of the chemical shift changes after each addition of this drug.

From Figs. 3.20 and 3.21 it is found from the chemical shift changes of the NH proton that at [Drug]/[receptor]= 0.5 there is a break which indicates that the stoichiometry of complexation between calix[4]arene amine with diclofenac and clofibric acid appears to be 2: 1 [Drug]/ [receptor]. To corroborate it further and to determine the composition of the receptor: drug complex conductance measurements were carried out.

Table 3.12 ¹H NMR complexation study to check the affinity of the receptor to complex with the pharmaceuticals in CD₃CN at 298 K.

[Drug] / [receptor]	H1	H2	H3	H4	H5	H6 _{ax}	H7	H8	N-H
δ _{ppm} Free receptor	1.20	1.16	7.24	7.17	3.39	4.32	4.01	3.22	2.17
Δδ (Diclofenac/ L)	-----	0.01	0.01	-----	-----	-0.21	0.14	0.17	0.21
Δδ (Clofibric/L)	-----	-----	-----	-----	0.06	-0.21	-0.09	0.15	0.32
Δδ (Ibuprofen+L)	-----	-----	-----	-----	0.01	0.05	0.02	0.03	0.05
Δδ (Aspirin+L)	-----	-----	-----	-----	0.08	-0.11	0.25	0.24	0.29

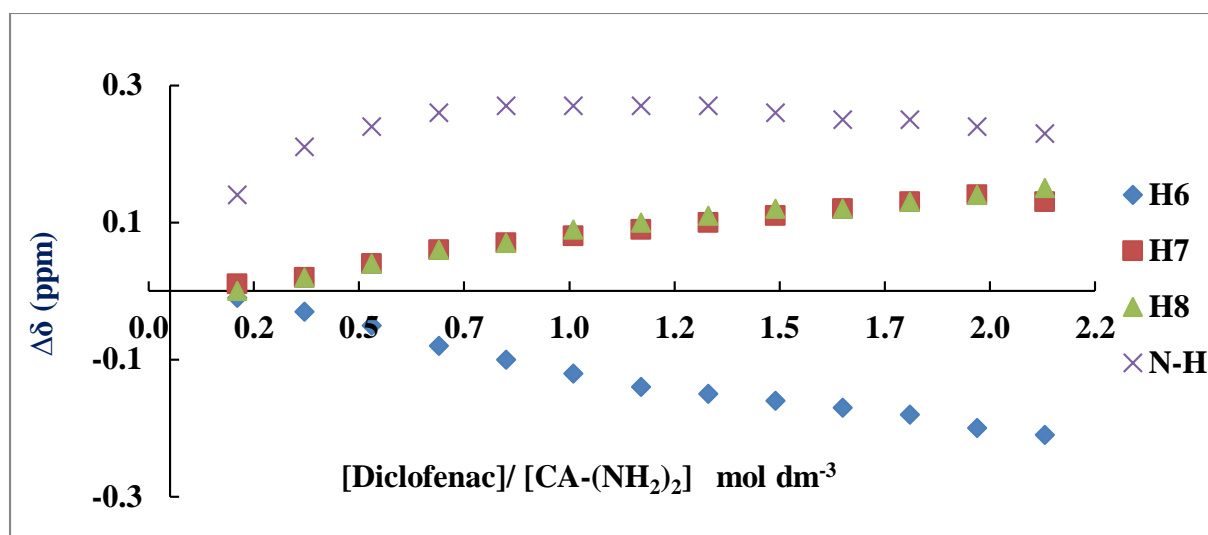


Fig. 3.20 The chemical shift changes for the 5,11,17,23 tetra-*tert*-butyl, 25, 27-bis[aminoethoxy], 26, 28 dihydroxycalix[4]arene upon addition of diclofenac against the [Drug]/ [receptor] ratios in CD₃CN at 298 K. [CA-(NH₂)₂] = 2 × 10⁻³ mol dm⁻³, [DCF] = 4 × 10⁻³ mol dm⁻³ (see Table 3.1-Appendix)

The chemical shift changes for the CA-(NH₂)₂ protons as a result from the addition of increasing concentration from clofibric acid are presented in Table 3.2-Appendix. As shown in Fig. 3.21 that the addition of clofibric acid to the receptor solution led to significant changes in chemical shift changes

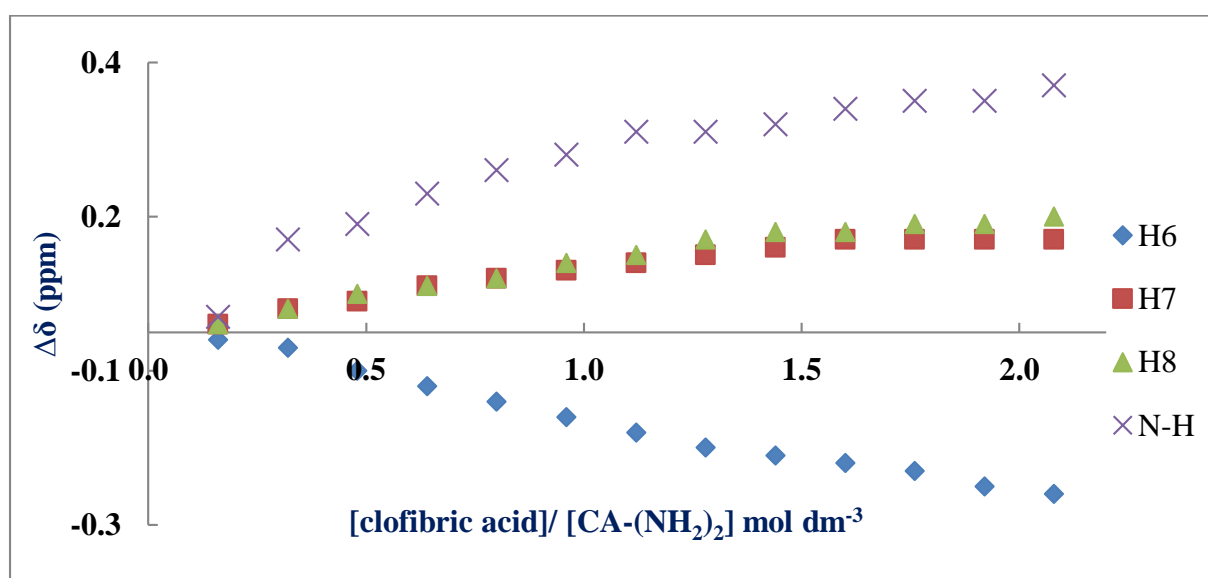


Fig. 3. 21 Chemical shift changes for the 5,11,17,23 tetra-*tert*-butyl, 25, 27-bis[aminoethoxy], 26, 28 dihydroxycalix[4]arene upon addition of clofibric acid against the [drug]/ [receptor] ratios at 298 K. [CA-(NH₂)₂] = 2 × 10⁻³ mol dm⁻³, [CLF] = 4 × 10⁻³ mol dm⁻³, 0.04 ml for each addition

Conductometric measurements were carried out with the aim of assessing the stoichiometry of the drug-receptor interaction

3.9.2 Investigation of the complexation of the pharmaceuticals with CA-(NH₂) in acetonitrile by conductance measurements

3.9.2.1 Conductometric measurements for the pure receptor CA-(NH₂)₂ in acetonitrile at 298.15 K

Following the calibration of the instrument to establish the cell constant ($\theta \approx 1.07 \text{ cm}^{-1}$, Table 3.4) the conductance of calix[4]arene amine was established in dry acetonitrile at 298.15K. (Fig. 3.22) shows the conductometric titration plot of the molar conductance Λ_m versus the increasing analyte concentration for calix[4]arene amine. Conductivity values obtained revealed that no significant change is caused by the addition of the receptor solution to the conductivity cell containing freshly dried acetonitrile. This indicates that the receptor does not undergo ionization or protonation process by acetonitrile as the solvent. It should be noted that although in the plot appears that Λ_m increases, the values are extremely low

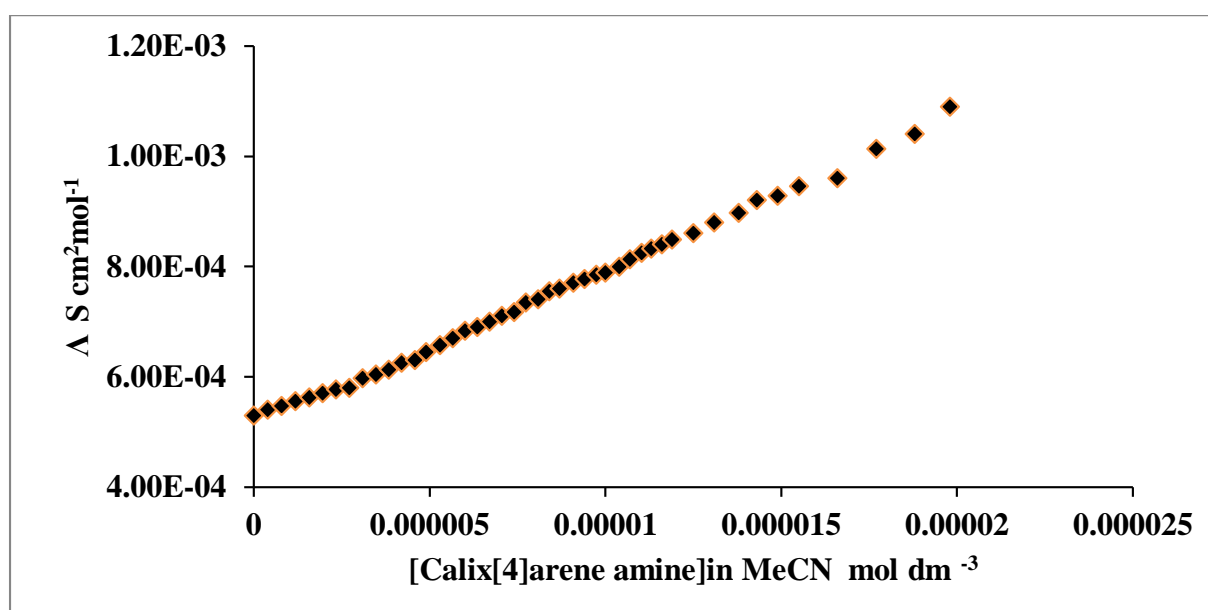
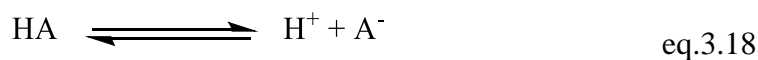


Fig. 3.22 Conductivity curve of the free receptor in acetonitrile ($5.29 \times 10^{-4} \text{ mol dm}^{-3}$) titrated into the cell containing 25 ml of pure acetonitrile at 298.15 K

Investigation of drug-receptor interactions by conductometric studies will be in the next section

The selected drugs in this study are weak acids which are able to dissociate in solution according to eq.3.18

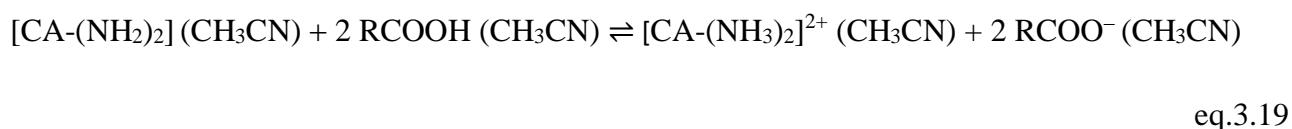


Therefore, monitoring the binding of drugs with the receptor by testing the variation of the electrical conductivity of their solution is a suitable strategy to follow the achievement of complexation. Conductometric titrations of diclofenac, clofibric acid and aspirin with calix[4]arene amine were carried out in acetonitrile as described previously in the Experimental Part at 298.15 K.

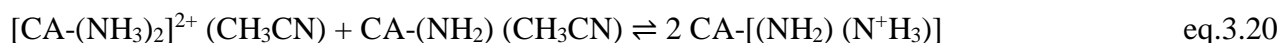
3.9.2.2 Conductometric titration studies of diclofenac DF and CA(NH₂)₂ in acetonitrile at 298.15 K

The conductivity values of the titration experiments are listed in Tables 3.3-Appendix. It can be observed from a plot of molar conductance, Λ_m (S.cm².mol⁻¹) versus [receptor]/ [Drug] concentration ratio (Fig. 3.23) that upon the addition of increasing concentrations of the receptor solution to diclofenac, the molar conductance increases and this indicates that the interaction process occurred through a proton transfer reaction to form host-guest complex salts and the stoichiometric ratio for the interaction is 1: 2 [receptor]/[diclofenac] .

Fig. 3.23 shows that the molar conductance, Λ_m , before the addition of the CA-(NH₂)₂ receptor is very low. This is an indication that the diclofenac is fully associated (ion pair formation) in acetonitrile. However, upon the addition of the receptor an increase in molar conductance is observed from A to B due to the transfer of two protons from the drug to the two amino functional groups of the receptor. The reaction is represented as follows



Further addition of the receptor leads to the formation of two units of [CA-(NH₂) (NH₃)]⁺. As the concentration of the receptor increases (B to C), a proton from the double protonated calix[4]arene amine derivative appears to be transferred to the free receptor resulting in the formation of two monoprotonated receptors as shown in the following equation



From C to D the increase in conductance occurs due to the excess of receptor which displaces the equilibrium to the right

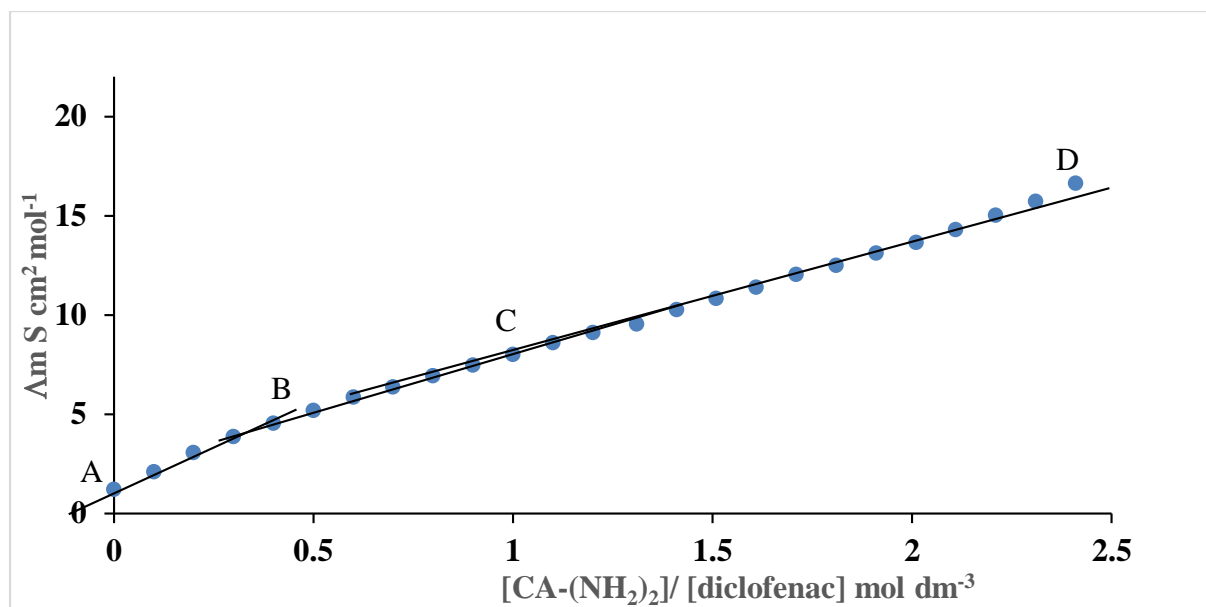


Fig. 3.23 Change in molar conductance resulting from the addition of receptor against the [receptor]/[drug] concentration ratio in acetonitrile at 298.15 K, [Diclofenac] = 1.6×10^{-3} mol dm⁻³, see Table 3.3-Appendix

3.9.2.3 Conductometric titration studies of clofibric acid with CA-(NH₂)₂ in acetonitrile at 298.15 K

Conductance values for clofibric acid with CA-(NH₂)₂ in acetonitrile at 298.15 K are listed in Table 3.4-Appendix. It can be observed from the plot of molar conductance, Λ_m (S.cm².mol⁻¹) versus [receptor]/[clofibric acid] concentration ratio (Fig. 3.24) that upon the addition of increasing concentrations of the receptor solution to the clofibric acid solution, the conductance values increase (A to B) indicating the transfer of two protons from the drug to the receptor given that the [receptor]/[clofibric acid] ratio is 0.5, therefore the composition of the adduct formed is 1: 2. The pattern followed from B to C and from C to D is similar to that observed for diclofenac and this receptor in this solvent

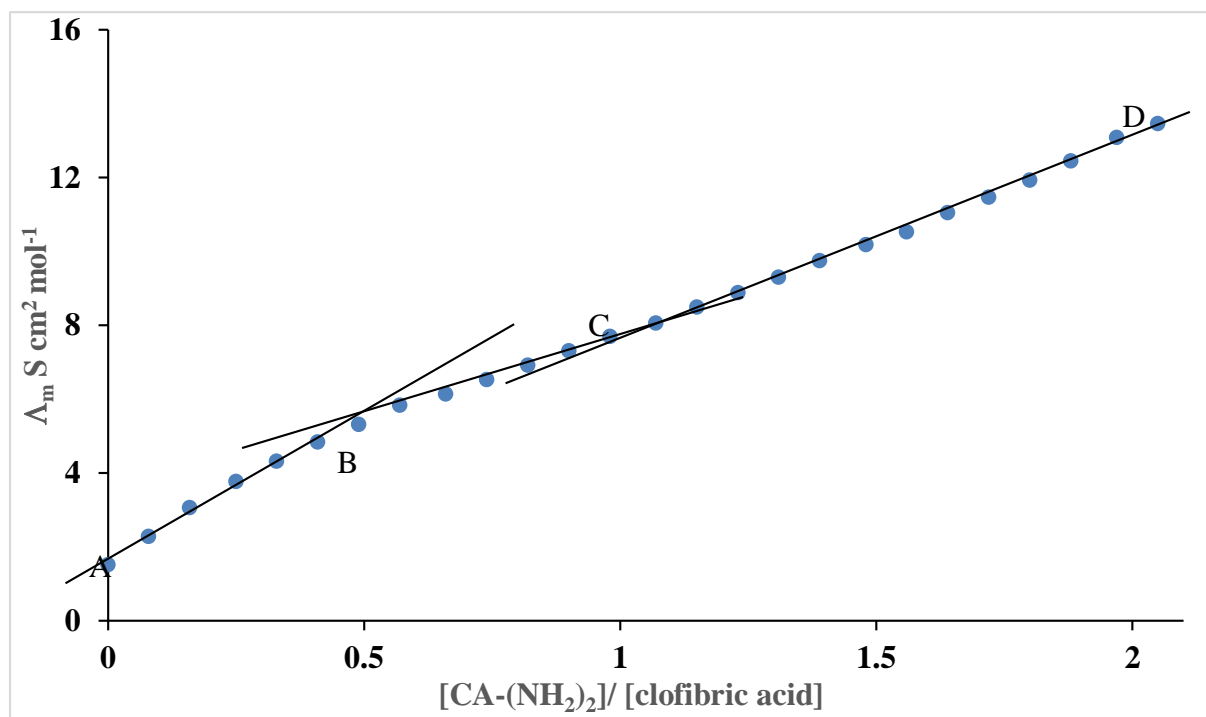


Fig. 3.24 Change in molar conductance resulting from addition of the receptor against the [receptor]/ [clofibric acid] concentration ratio in acetonitrile at 298.15 K. The concentration of clofibric acid solution in MeCN is $1.96 \times 10^{-3} \text{ mol dm}^{-3}$, see Table 3.4-Appendix

3.9.2.4 Conductometric titration of aspirin with CA-(NH₂)₂ in acetonitrile at 298.15 K

The conductance values of the titration experiments are listed in Table 3.5-Appendix. It can be observed from plots of molar conductance, Λ_m ($\text{S} \cdot \text{cm}^2 \cdot \text{mol}^{-1}$) versus [receptor]/ [aspirin] concentration ratio (Fig. 3.25) that upon the addition of increasing concentrations of the receptor solution to the aspirin solution the conductance increases (A to B) and this indicates that the interaction process occurred through the transfer of one proton from the drug to the receptor to form host-guest complex salts of general formula $(\text{CA-NH}_2\text{-N}^+\text{H}_3) \cdot (\text{R-CO}_2^-)$ and the stoichiometric ratio for the interaction is found to be 1: 1 [receptor]/ [aspirine]

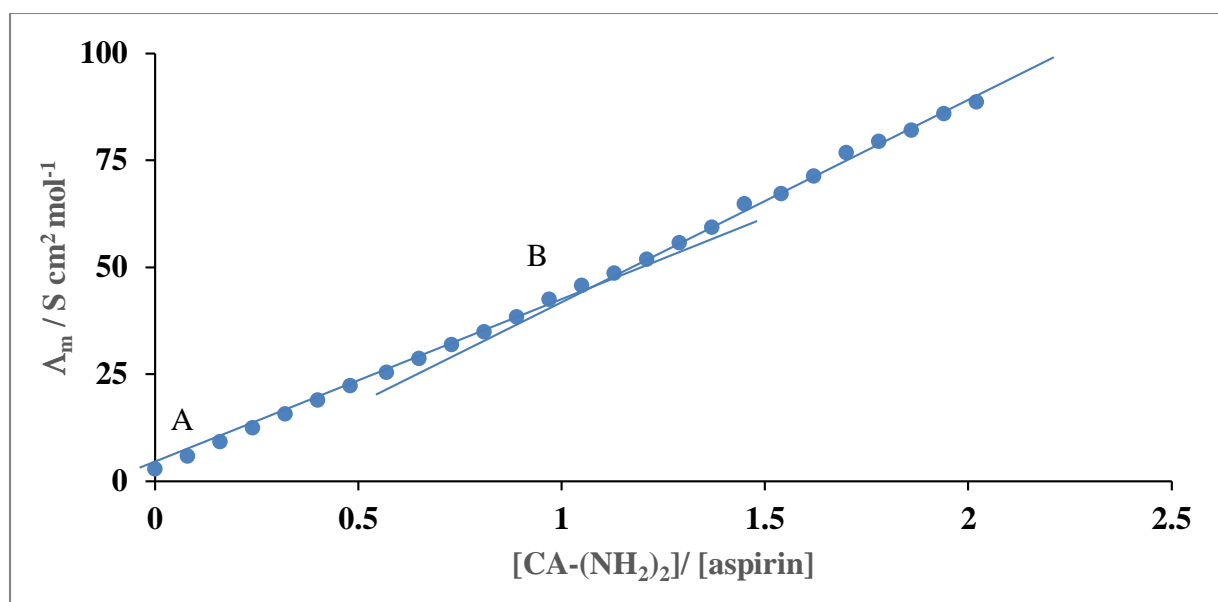


Fig. 3.25 Conductance changes of aspirin solution in dry acetonitrile resulting from the gradual addition of calix[4]arene amine against the [receptor]/ [drug] concentration ratio at 298.15 K. The concentration of aspirin is 1.79×10^{-4} mol dm⁻³, see Table 3.5-Appendix

In order to get further information regarding the complexation of CA-(NH₂)₂ with the drugs, UV titrations were carried out

3.10 Photophysical properties of the drug bindings

3.10.1 UV titration of diclofenac with calix[4]arene amine in acetonitrile at 298.15 K

The titrations were carried out in same manner with those above discussed in conductance measurements. The receptor solution in dry acetonitrile was added to the UV cell containing the diclofenac in the same solvent. The absorption spectrum obtained from a plot of absorbances against the wavelengths is shown in Fig. 3.26. The rapid change in the spectrum observed after each addition of the receptor solution to the drug solutions indicates that an interaction occurs between the receptor and the drug. Also, the absorption bands of the complexed diclofenac are red shifted as compared with the absorbances of the free drug ($n \rightarrow \pi^*$ at $\lambda_{\max} = 277$ nm) which confirms the formation of the complex. The red shifting of the $n \rightarrow \pi^*$ transitions are attributed to the polarity of acetonitrile which has the ability to stabilise the excited state through the reduction the energy of the π^* orbitals which means that the total energy of the $n \rightarrow \pi^*$ transition required are reduced and this make the wavelength longer^{236,237}. By plotting absorbances values against the [receptor]/ [Drug] concentration ratios (Table 3.6-Appendix) the stoichiometry of the complexation can be identified (Fig. 3.27) The stoichiometric

ratio obtained is not in accord with the stoichiometry obtained from the conductance measurements and this may be attributed to the presence of N-H group in the chemical structure of diclofenac and can act as a proton donor–acceptor at the same time and can compete with the acidic proton to interact with the receptor and therefore the spectrum is disturbed. Therefore, ITC measurements were carried out to confirm the stoichiometry of the reaction which was obtained by ^1H NMR. From titration experiments we can conclude the red shift for the maximum absorbance band occurred because of the polarity of the solvent which can stabilise the transition state of the complex.

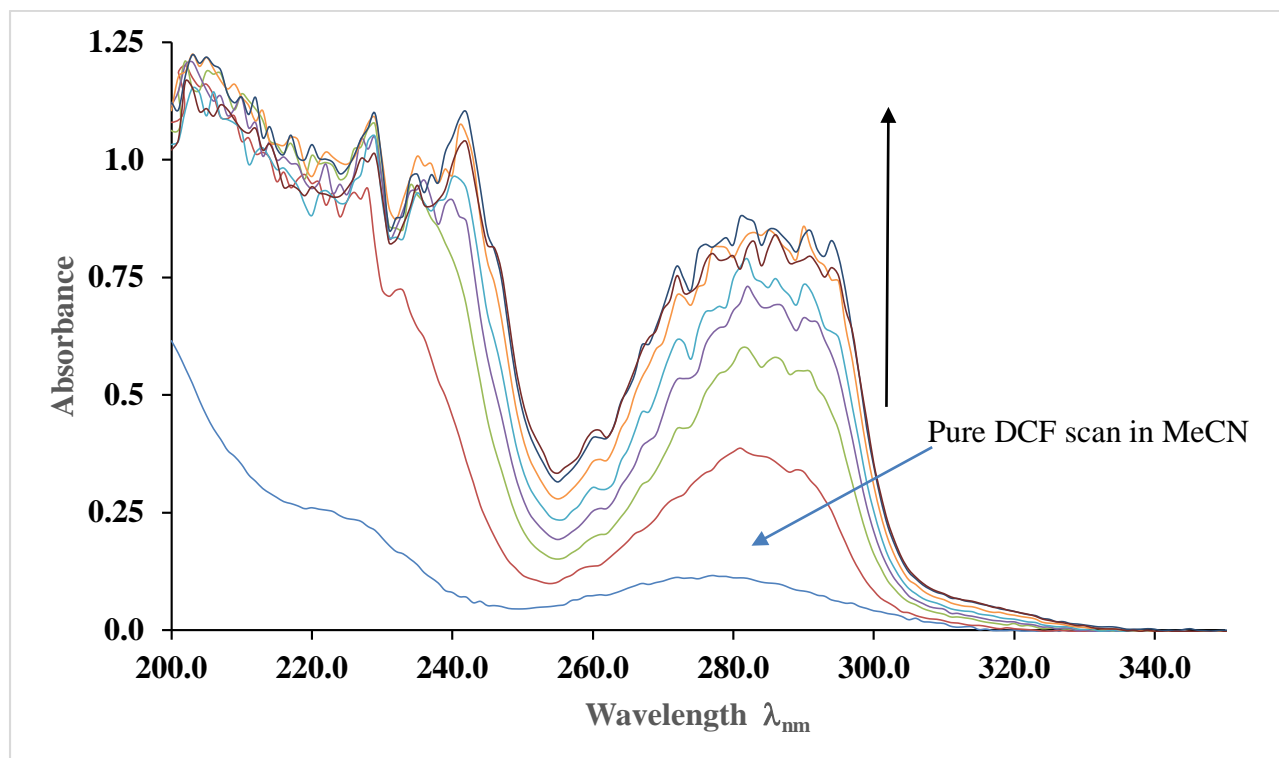


Fig. 3.26 UV-Vis titration spectrum of diclofenac in acetonitrile ($1.12 \times 10^{-4} \text{ mol dm}^{-3}$, bottom scan) showing the increase in the absorbance bands intensity resulting from the addition of *p-tert*-butyl calix[4]arene amine [CA-(NH₂)₂], see Table 3.6-Appendix

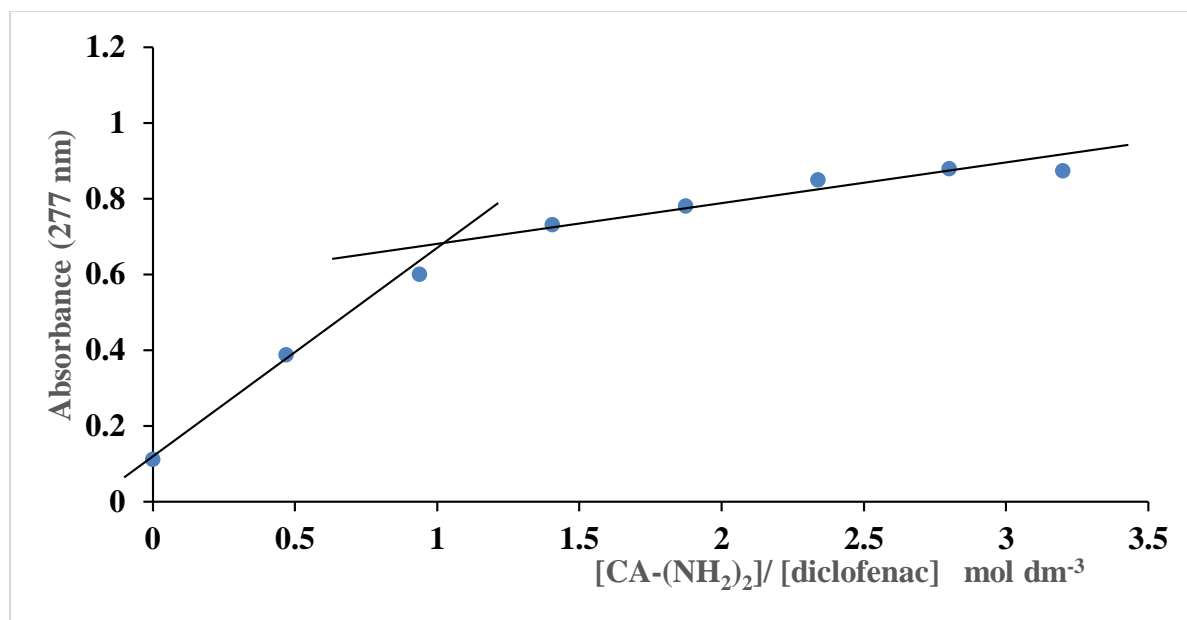


Fig. 3.27 Plot of the absorbance of the diclofenac against the [receptor]/ [diclofenac] concentration ratio in acetonitrile at 298.15 K, see Table 3.6-Appendix

3.10.2 UV titration of clofibric acid with calix[4]arene amine in acetonitrile

UV-Vis spectra were recorded on the range 200-400 nm using 1 cm quartz cell. Successive additions of the receptor solution in dry acetonitrile were added to the UV cell containing the clofibric acid in the same solvent. The absorption spectrum obtained from the plot of the absorbances against the wavelength is shown in Fig. 3.28. It is observed that the receptor exhibits high affinity to bind with the clofibric acid as reflected in the rapid change observed after each addition of the receptor solution to the drug solution. The absorption bands of the complexed clofibric acid red shifted relative to those for the free drug ($n \rightarrow \pi^*$ at $\lambda_{\max} = 280$ nm) which confirms the formation of the complex. As concluded above the shifting of the $n \rightarrow \pi^*$ transition attributed to the lowering of the energy for π^* orbitals resulting from the using of polar solvent. The energy of π^* orbitals are reduced which means that the total energy required for the $n \rightarrow \pi^*$ transitions are reduced and this made the wavelength longer^{236,237}. A plot of the absorbance values against the [receptor]/ [drug] concentration ratios (Table 3.6-Appendix), Fig. 3.29 gives the stoichiometry of the complexation. It's clear that in the case of clofibric acid, two protons are taking up per unit of receptor in agreement with the results obtained from conductance measurements.

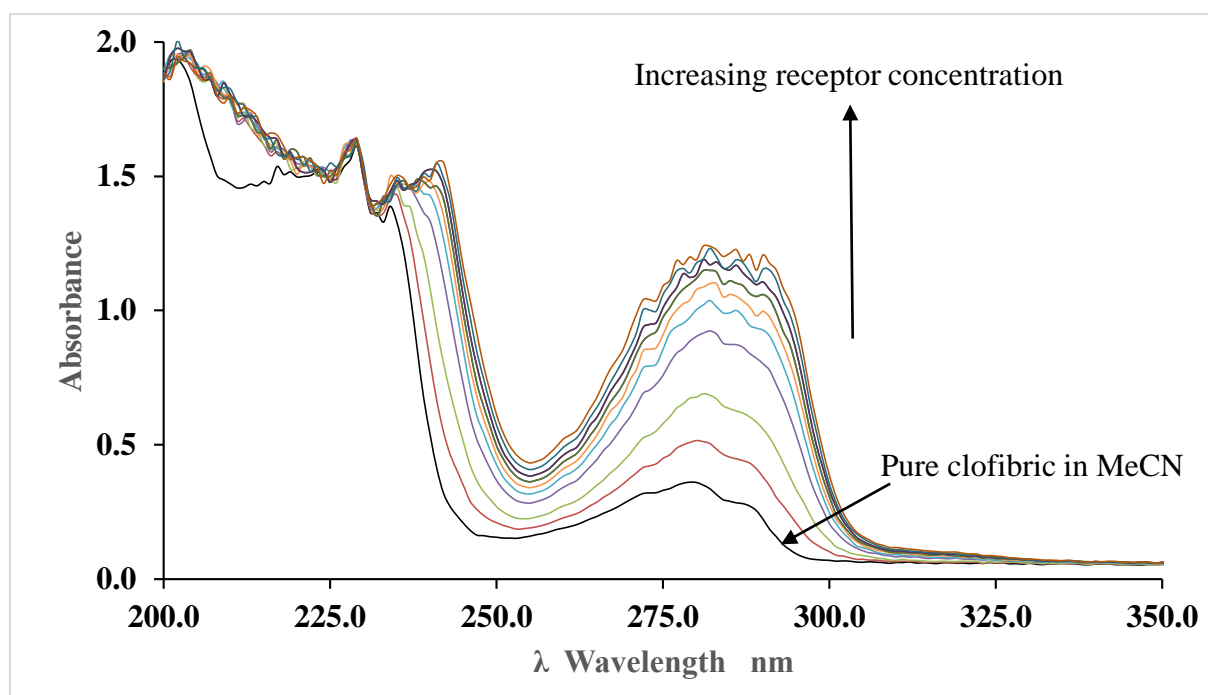


Fig. 3.28 UV-Vis titration spectrum of clofibric acid in acetonitrile ($3.35 \times 10^{-4} \text{ mol dm}^{-3}$) showing the increase in the absorbance bands resulting from the gradual addition of increasing concentration of CA-(NH₂)₂ solution in acetonitrile at 298 K, see Table 3.7-Appendix

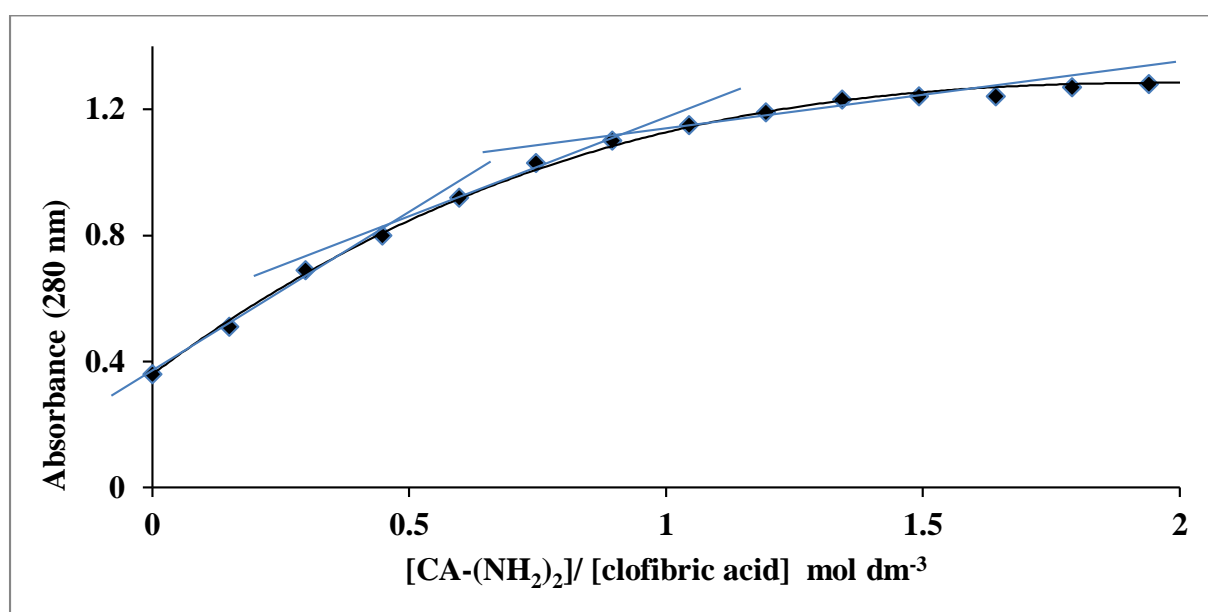


Fig. 3.29 Plot of the absorbance of clofibric acid in acetonitrile against [receptor]/ [drug] concentration ratio

3.10.3 UV-Vis titration of aspirin with CA-(NH₂)₂ receptor at 298 K

The UV-Vis spectrum was recorded on the 200-400 nm range using a 1 cm quartz cell. The titrations were carried out to make sure that the complexation process is achieved. Addition of CA-(NH₂)₂ solution in acetonitrile to the aspirin solution has led to considerable changes in the spectral picture of aspirine (Fig. 3.30). It can be concluded from the absorption spectrum obtained from the plot of the absorbances against wavelength (Fig. 3.30) that the receptor exhibits high affinity to bind with the aspirin and a rapid change in the spectrum is observed after each addition of the receptor solution to the drug. The absorption bands of the complex formed red shifted relative to the absorbance of the free drug ($n \rightarrow \pi^*$ at $\lambda_{\max} = 276$ nm) caused by the using of polar aprotic solvent. The polarity of the solvent can lower the energy of the π^* orbitals which can reduce the total energy required for the $n \rightarrow \pi^*$ transitions with longer wavelength which confirms the formation of the complex. From Fig.3.31 and Table 3.8-Appendix, the stoichiometry of complexation can be identified. It is clear that a 1: 1 [aspirin]/ [receptor] complexes is obtained^{236,237}

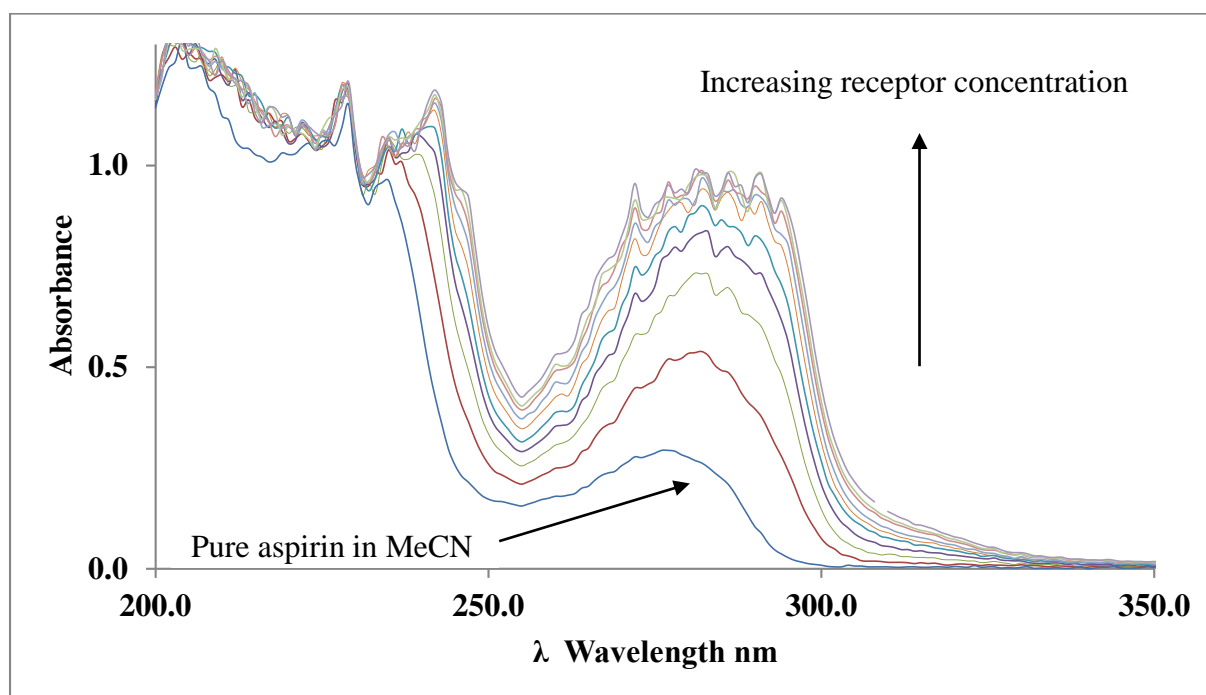


Fig. 3.30 UV-Vis spectrum of aspirin solution in acetonitrile resulting from gradual addition of CA-(NH₂)₂ solution in acetonitrile at 298 K. The concentration of the diclofenac is 2.99×10^{-4} , see Table 3.8-Appendix

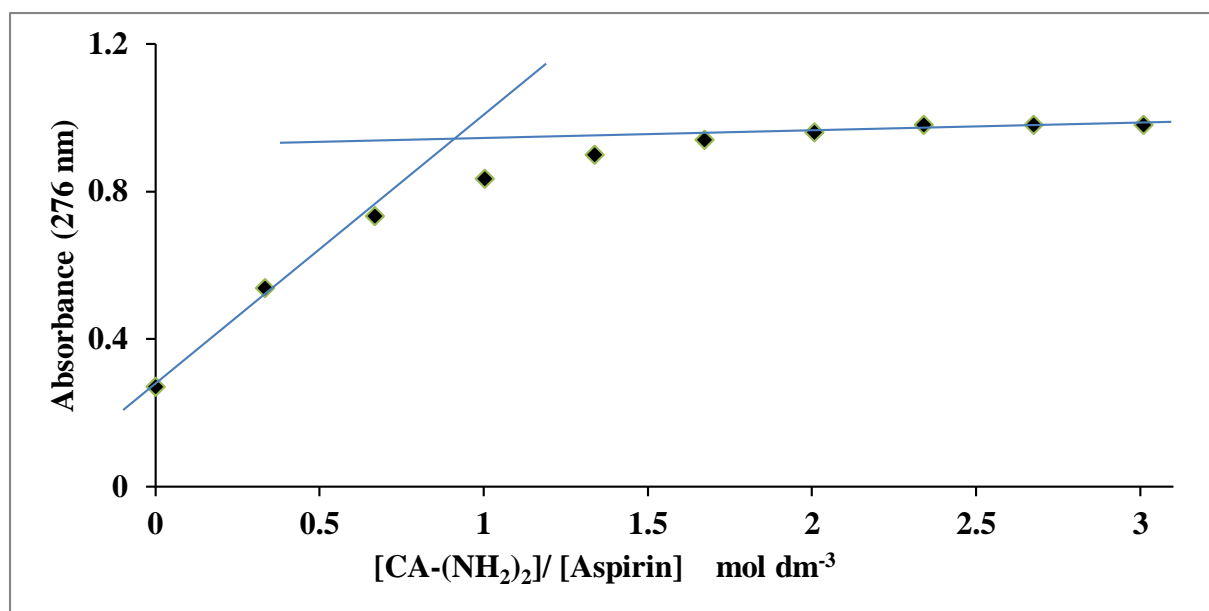


Fig. 3.31 Variation in absorbance values of aspirin resulting from addition of increasing concentrations of the receptor at 298 K, see Table 3.8-Appendix

3.11 Thermodynamic parameters of complexation of pharmaceuticals with CA-(NH₂)₂ in acetonitrile at 298.15 K

The Nano isothermal titration calorimeter (ITC) was used to investigate the thermodynamic parameters for the interaction of *p-tert*-butyl calix[4]arene amine with aspirin, clofibric acid, diclofenac and ibuprofen. It is a powerful and highly accurate tool for evaluating the thermodynamic parameters associated to the complexation process which can give quantitative information about the degree of the interaction between the receptor and the targeted drugs.

The thermograms obtained are shown in Figs. 3.32, 3.33, and 3.34. The stability constants (expressed as $\log K_s$), the standard enthalpy, $\Delta_c H^\circ$ and entropy, $\Delta_c S^\circ$ for the interaction of aspirin, clofibric acid and diclofenac with the calix[4]arene amine derivative in acetonitrile at 298.15 K are listed in Table 3.13. The standard deviations of the data are also included. The data for aspirin fits into a 1: 1 (host: guest) complex while those for clofibric acid and diclofenac into 1: 2 complexes as shown previously from conductance data. As previously stated thermodynamics does not provide structural information. However, it is indisputable that any model proposed must fit the experimental data. Therefore, the thermodynamic data are referred to the following processes,

For 1:1 complexes of aspirin, clofibric acid and diclofenac, eq.3.21 is representative of the process taking place in solution, in doing so the results obtained from conductance data that these pharmaceuticals are predominantly as ion pairs in acetonitrile



For 1: 2 complexes of clofibric acid and diclofenac,



For aspirin the process is enthalpy controlled. The same applies for the 1: 1 complexes of clofibric acid and diclofenac. However, the formation of 2: 1 complexes is enthalpically unfavoured and entropically controlled. These results are striking and suggest that a great disorder in the structure of the receptor occurs to allow the entrance of the second proton. X-ray crystallographic studies of an analogous receptor CA-[N(Et₂)₂], with perchloric acid has shown the double protonation of the receptor as well as the loss of the solvent upon protonation while the hydrogen bond between the ethereal oxygen and the phenolic oxygen still remains. The conformational change that CA-(NH₂)₂ undergoes in moving from the free to the protonated ligand as shown by ¹H NMR studies in CD₃ CN indicates a flattened ‘cone’ conformation for the latter relative to the *quasi* ‘cone’ conformation of the former and as a result the hydrophobic cavity is able to lose the solvent. This process will lead to an increase in entropy. Given that energy would be required to remove the solvent from the cavity, the process would be enthalpically unfavoured. This interpretation is corroborated by the data reported in Table 3.13. Comparison of the protonation constants of CA-(NH₂)₂ with clofibric acid and diclofenac in acetonitrile at 298.15 K relative to those for CA-[N(C₂H₅)₂] and HClO₄ in the same solvent and temperature (log K_{s1} = 15.68, log K_{s2} = 14.36) demonstrates the effect of the strength of the acid on the protonation process as well as the basic nature of the amine moieties in the pendant arms given that the basicity of the tertiary amine in CA-[N(Et₂)₂] is higher than that of CA-(NH₂)₂ (primary amine). The thermodynamic data reveal that CA-(NH₂)₂ is selective for these drugs in the following sequence

Clofibric acid > diclofenac > aspirin in acetonitrile

In order to get further insight regarding the different hosting capacity of CA-(NH₂)₂ for aspirin relative to clofibric acid and diclofenac, molecular simulation calculations were carried out. The outcome is shown in Figs. 3.35-3.37 where the presence of a carbonyl oxygen in *ortho* position with respect to the carboxylic group in aspirin leads to two contact points involving the amine functionalities in each of the pendant arms of the receptor. Thus a proton transfer reaction occurs where one of the amino functionality is protonated (as shown from conductance measurements) while the remaining one enters hydrogen bond formation with the carbonyl oxygen of the ester group of aspirin. It seems that the presence of acetonitrile in the hydrophobic cavity of the ligand pre-organise the receptor to interact with the drug. The molecular modelling shows the interaction of two units of drug per unit of receptor in the case of diclofenac and clofibric acid (Figs. 3.35-3.37).

In the following section thermal analysis for the receptor, drug and complex in the solid state are discussed.

Table 3.13 Thermodynamic parameters of the binding between the drugs and calix[4]arene amine receptor in acetonitrile at 298.15 K

Drug interaction [L]/[D]	log K _s	Δ _c G° / kJ mol ⁻¹	Δ _c H° / kJ mol ⁻¹	Δ _c S° J mol ⁻¹ K ⁻¹
Aspirin 1:1	log K _s = 3.92 ± 0.1	Δ _c G° = - 22.4 ± 0.6	Δ _c H ₁ ° = - 23.0 ± 0.3	Δ _c S° = - 2
Clofibric acid 1:2	log K _{s1} = 7.3 ± 0.05	Δ _c G° ₁ = - 41.4 ± 0.3	Δ _c H° ₁ = - 48.1 ± 0.7	Δ _c S° ₁ = - 23
	log K _{s2} = 6.14 ± 0.12	Δ _c G° ₂ = - 35.7 ± 0.7	Δ _c H° ₂ = + 14 ± 3	Δ _c S° ₂ = 1.68 × 10 ²
Diclofenac 1:2	log K _{s1} = 5.83 ± 0.7	Δ _c G° ₁ = - 33 ± 4	Δ _c H° ₁ = -34.5 ± 0.12	Δ _c S° ₁ = - 4
	log K _{s2} = 5.1 ± 0.6	Δ _c G° ₂ = - 29 ± 3	Δ _c H° ₂ = + 17 ± 3	Δ _c S° ₂ = 1.5 × 10 ²

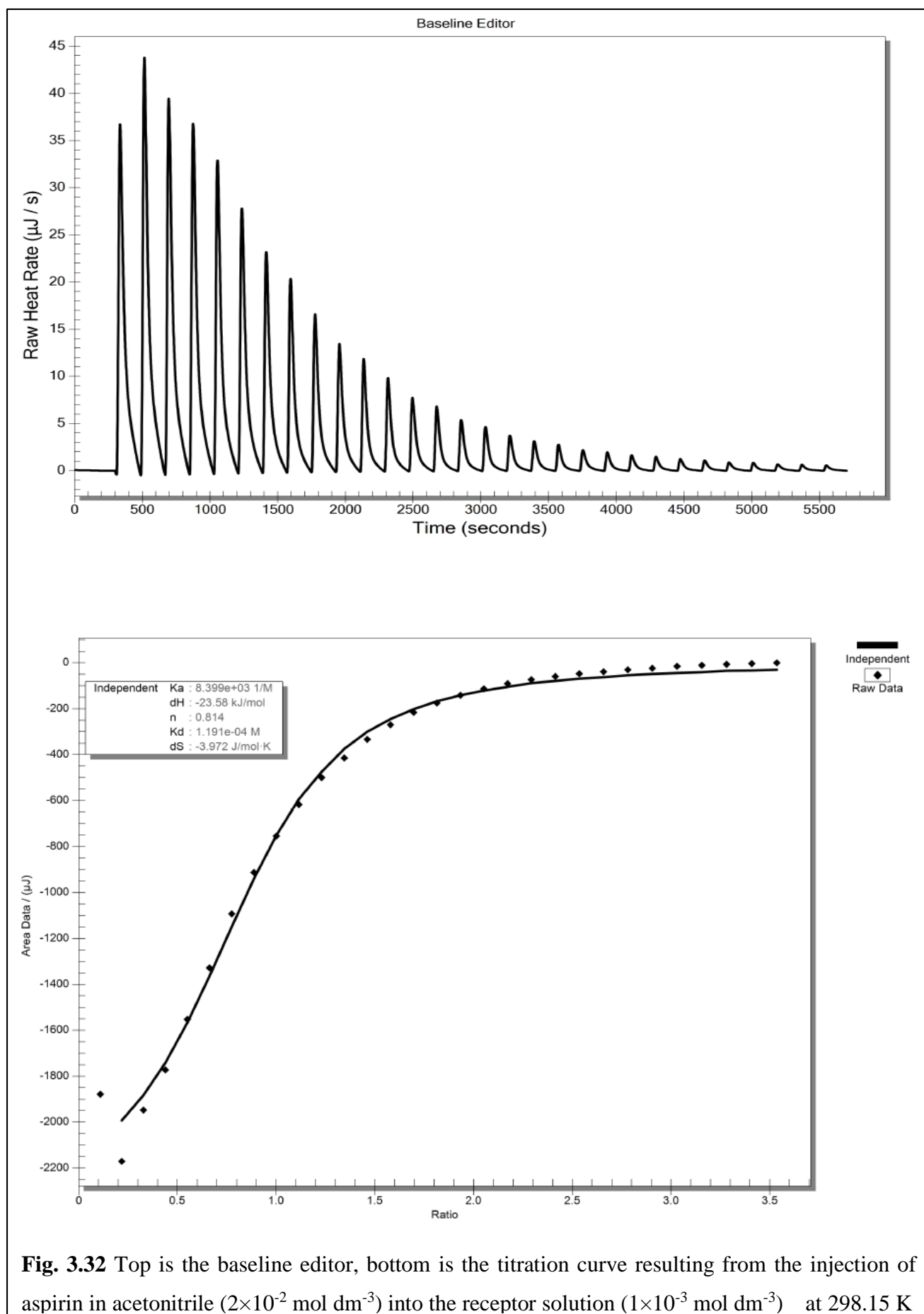


Fig. 3.32 Top is the baseline editor, bottom is the titration curve resulting from the injection of aspirin in acetonitrile ($2 \times 10^{-2} \text{ mol dm}^{-3}$) into the receptor solution ($1 \times 10^{-3} \text{ mol dm}^{-3}$) at 298.15 K

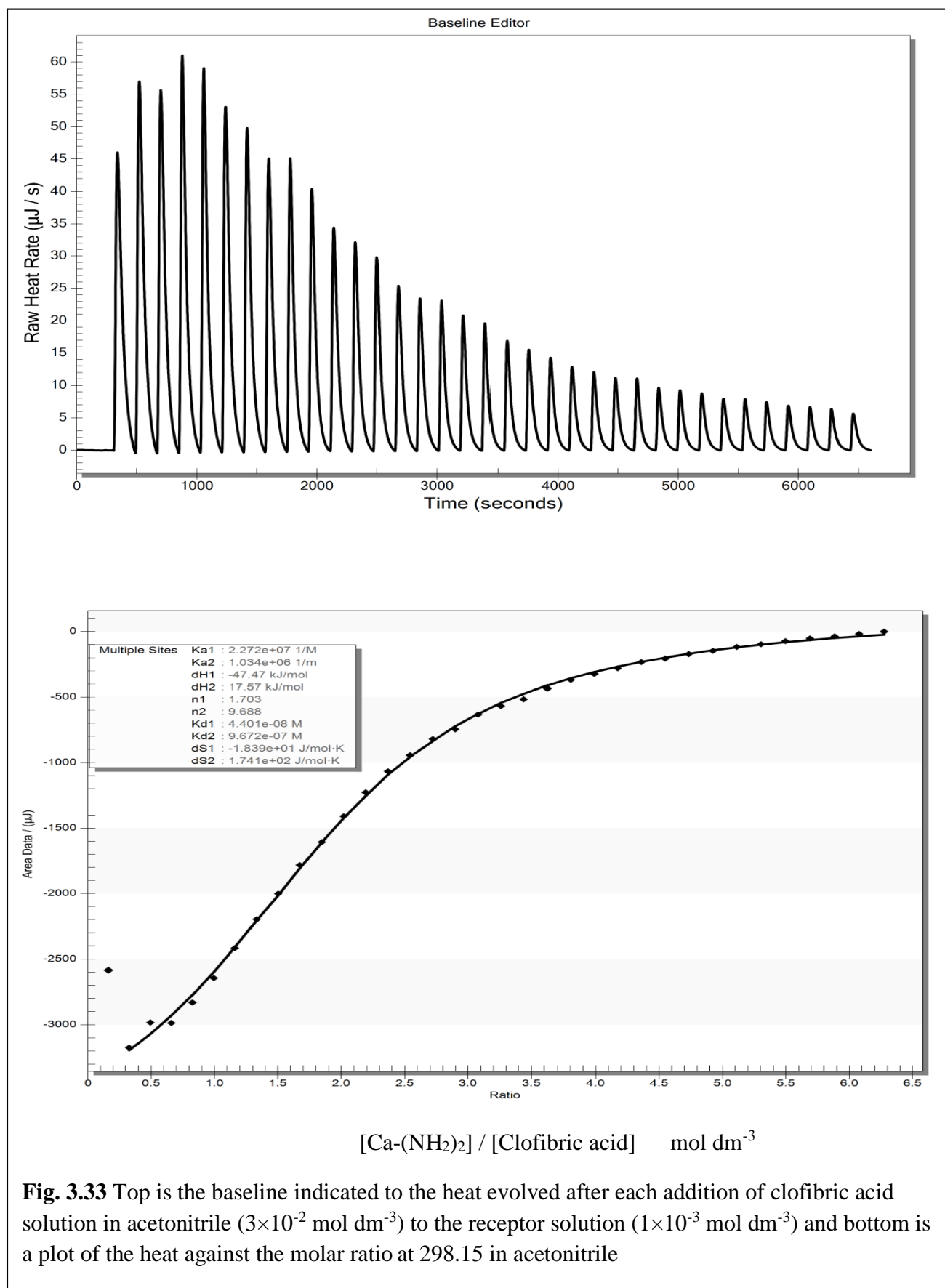


Fig. 3.33 Top is the baseline indicated to the heat evolved after each addition of clofibric acid solution in acetonitrile ($3 \times 10^{-2} \text{ mol dm}^{-3}$) to the receptor solution ($1 \times 10^{-3} \text{ mol dm}^{-3}$) and bottom is a plot of the heat against the molar ratio at 298.15 in acetonitrile

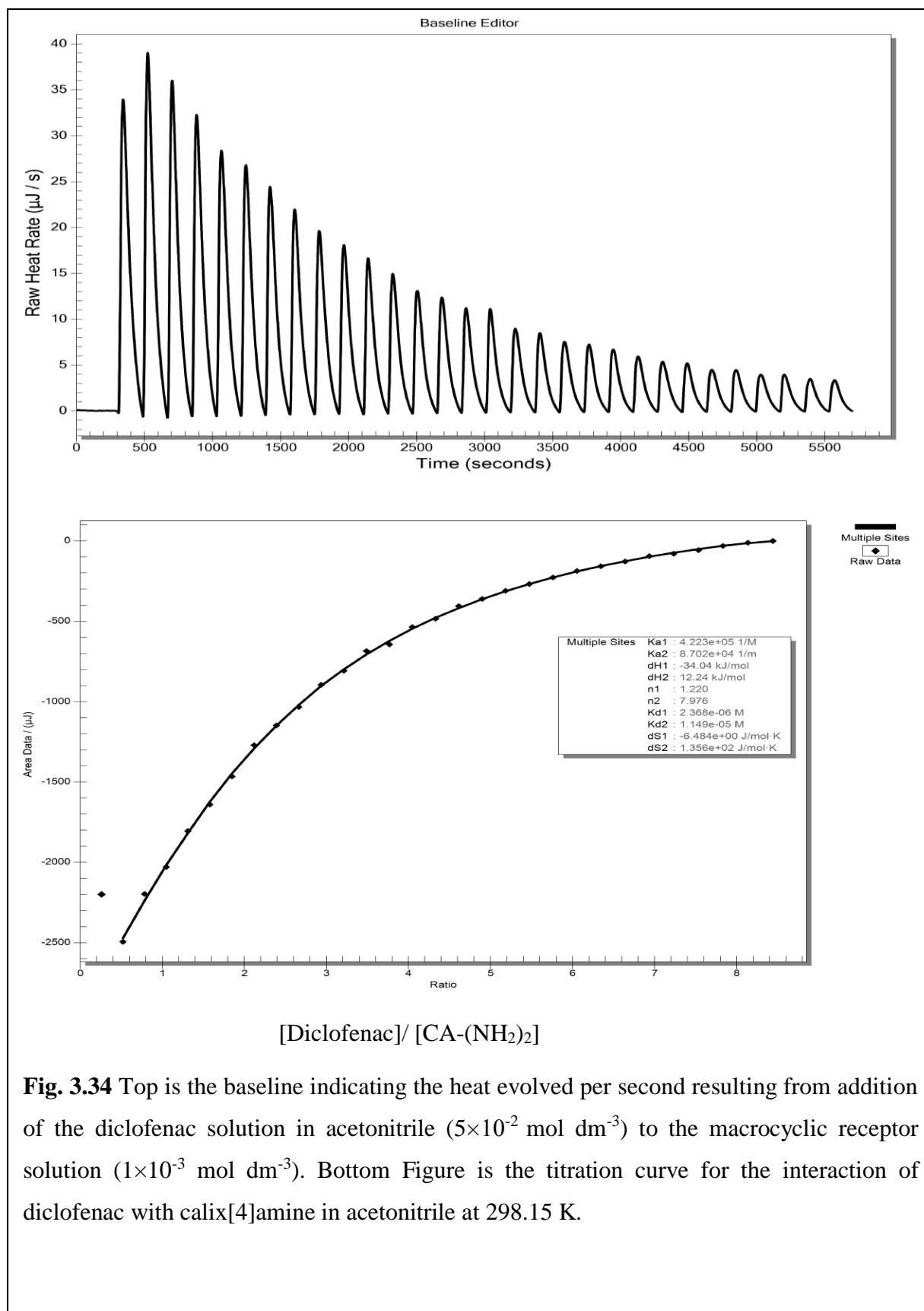


Fig. 3.34 Top is the baseline indicating the heat evolved per second resulting from addition of the diclofenac solution in acetonitrile ($5 \times 10^{-2} \text{ mol dm}^{-3}$) to the macrocyclic receptor solution ($1 \times 10^{-3} \text{ mol dm}^{-3}$). Bottom Figure is the titration curve for the interaction of diclofenac with calix[4]amine in acetonitrile at 298.15 K.

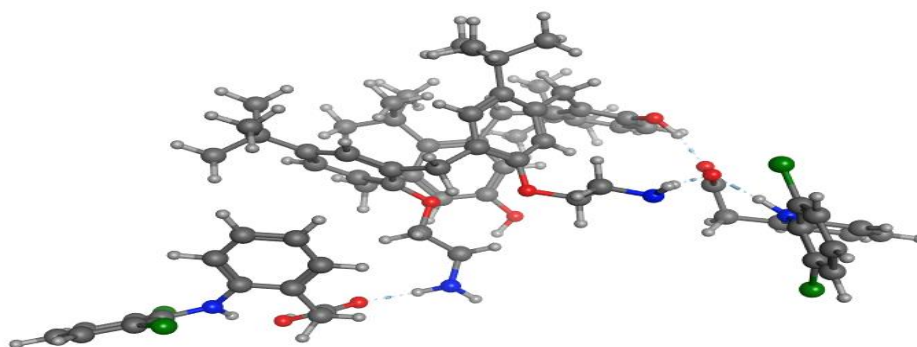


Fig. 3.35 Molecular modelling of the interaction of diclofenac with calix[4]arene amine

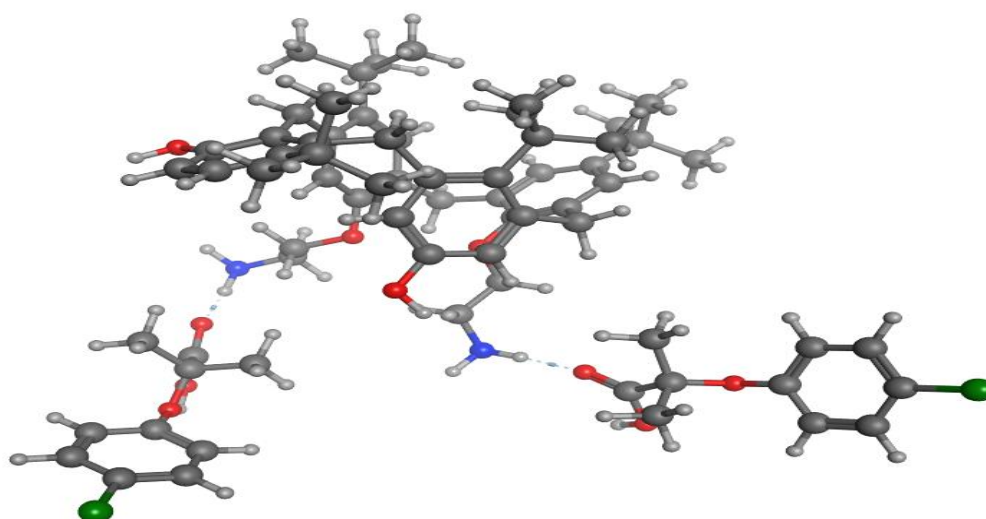


Fig. 3.36 Molecular modelling of the interaction of clofibric acid and calix[4]arene amine

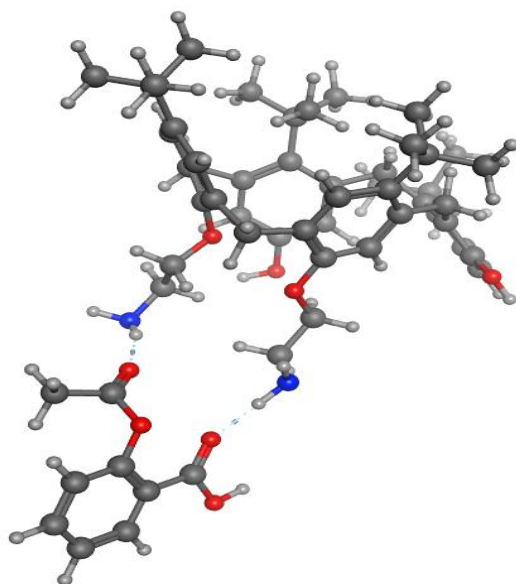


Fig. 3.37 Molecular modelling of the interaction of aspirin and calix[4]arene (CA-NH₂)₂

3.12 Investigation of the interaction between diclofenac, clofibric acid and aspirin with CA-(NH₂)₂ by using thermogravimetric analysis TGA and differential scanning calorimetry DSC

Further investigations on the interaction process between CA-(NH₂)₂ and the pharmaceuticals have been carried out by following the changes in the thermal behaviour of the free drugs, the receptor and the complexes. The TG thermograms obtained for diclofenac, receptor and the complex formed (Fig. 3.38) have displayed that the TG thermogram for the complex differs from those for the pure compounds which means that the thermal properties of the complex shifted to a lower temperature as compared with that for the free receptor as a result from the complexation process indicating that the complexation process was achieved successfully. Similar results were obtained for the complexation of the receptor with clofibric acid (Fig. 3.39) and the complexation of the receptor with aspirin (Fig. 3.40) which means that the thermal properties of the the complex formed in both cases differ from the TG thermogram of the pure compounds. These results confirm that the pharmaceuticals and the receptor incorporated in the complexation led to differ in their chemical structures.

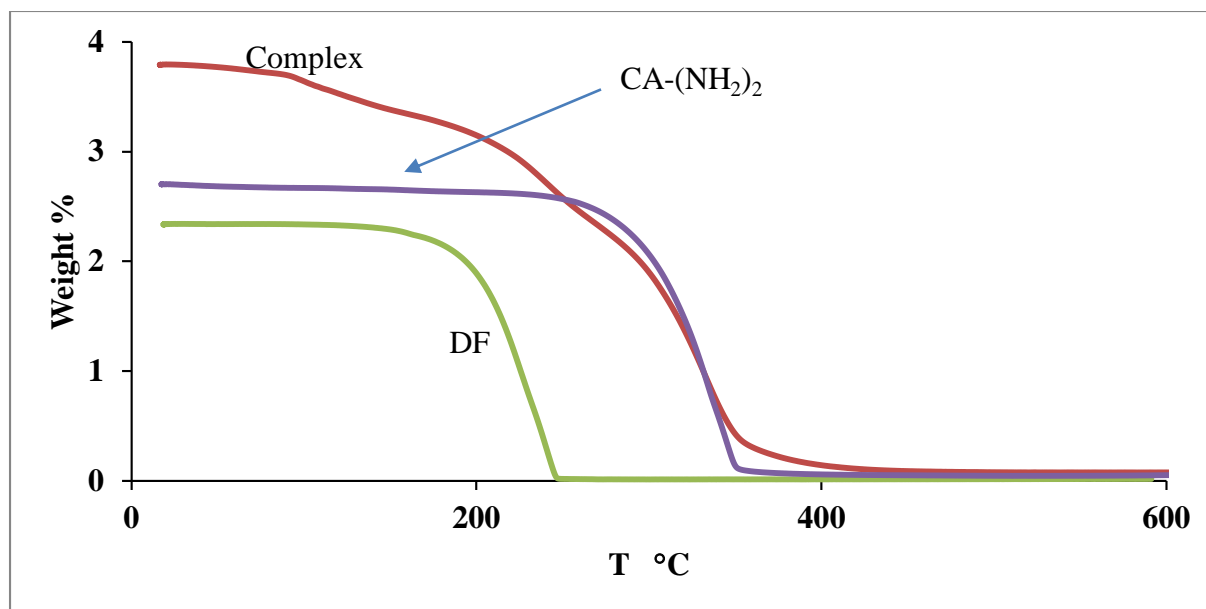


Fig. 3.38 TGA thermograms for diclofenac (DF), CA-(NH₂)₂ and the complex

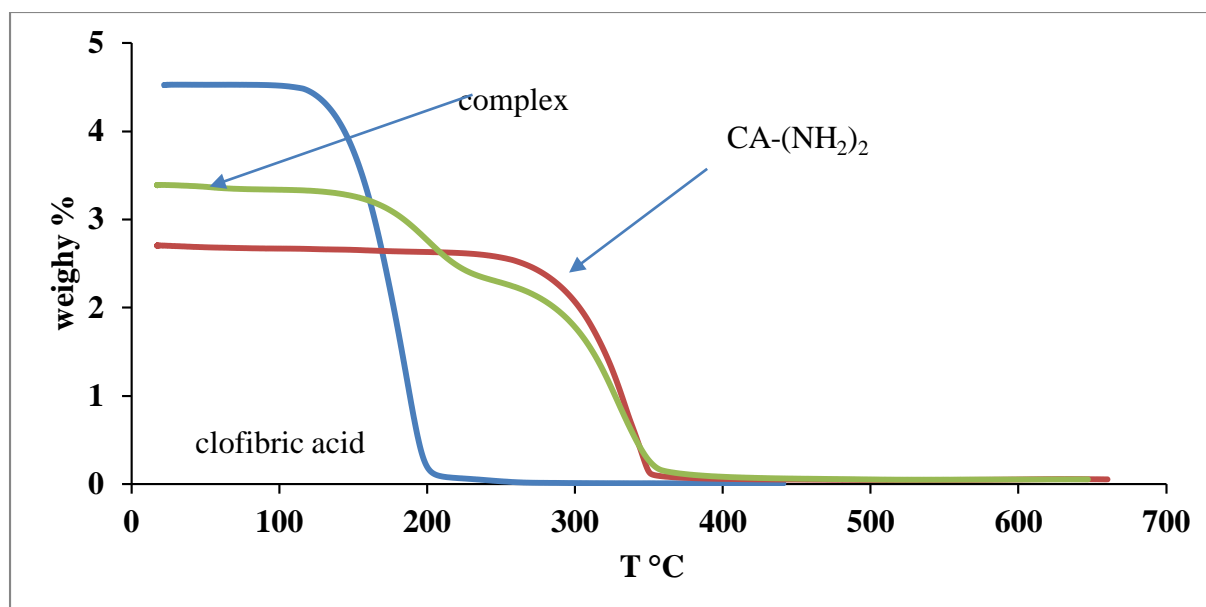


Fig. 3.39 TGA thermogram for the complexation process between CA-(NH₂)₂ and the receptor

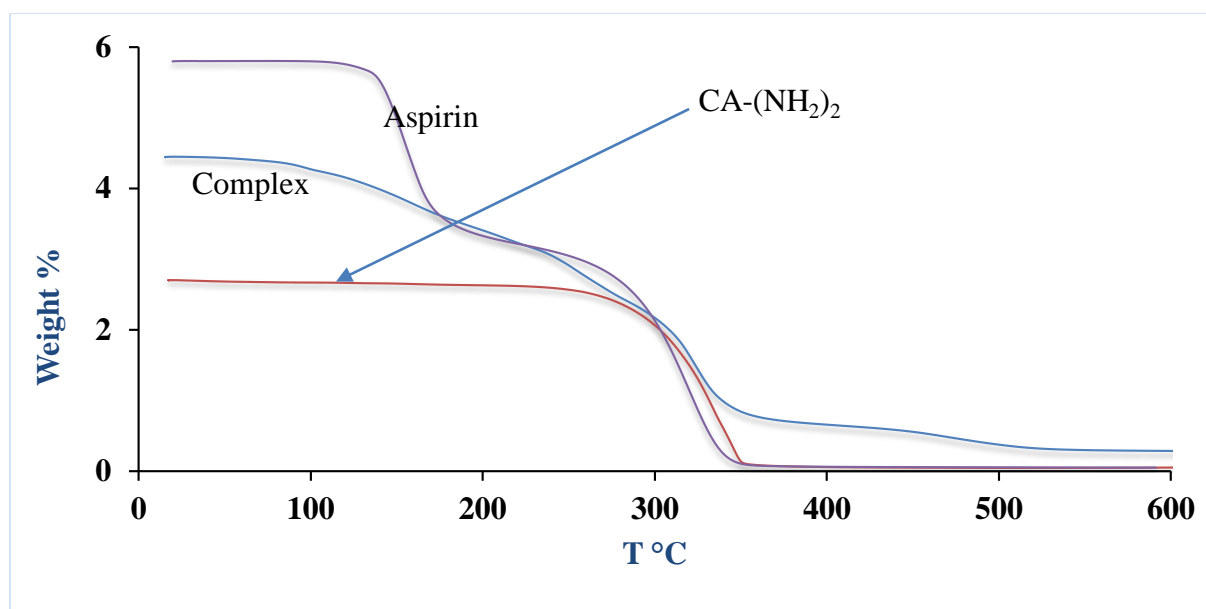


Fig. 3.40 TGA thermogram for the complexation of aspirin with CA-(NH₂)₂

Having carried out fundamental studies on interactions exploring CA-(NH₂)₂ and pharmaceuticals in the next section, the extracting properties of this calix[4]arene receptor for the removal of drugs from water are discussed

3. 13 Extraction of clofibric acid and diclofenac from water by CA-(NH₂)₂

The affinity of the CA-(NH₂)₂ receptor to remove clofibric acid and diclofenac from water was investigated as a representative example given that two units of the drug were taken up per unit of receptor. In doing so, a number of parameters were considered in order to find the optimal conditions for the removal process. Among them, the effect of the mass/ solution ratio, the pH of the aqueous solution. The removal capacity of the material for these drugs was also determined. These are now discussed.

3.13.1 The effect of mass on the extraction of clofibric acid from water.

The effect of the receptor dose on the extraction process was determined by the addition of different weights of the receptor to a fixed concentration of the drug solutions in water (4.09×10^{-4} mol dm⁻³, 10 ml). The mixtures were mixed for 10 minutes on a whirlimixer, sealed and left in a water bath at 298 K. The mixtures were filtered and the concentration of the drug at equilibrium was determined using a UV-Vis spectrophotometer at $\lambda_{\max} = 278.5$ nm. The percentage of extraction was calculated by using equation 2.39. Table 3.14 lists the initial concentration of the drug prior to the addition of the receptor, C_i , the equilibrium concentration, C_{eq} , both in the aqueous solution in the molar scale,

the mass of the receptor and the percentage of extraction, % E at 298 K. It can be seen from the table that when the mass of the receptor reaches 0.01 g, no further changes in the % E takes place (Fig. 3.41), given that no material is available for interaction

Table 3.14 The clofibrac acid concentration before and after the extraction, adsorbent used and extraction percentages (total volume of the drug solution is 10 ml)

$[C_i]$ mol dm ⁻³ 10 ml	$[C_{eq}]$ mol dm ⁻³	quantity of CA-(NH ₂) ₂ in mole (solid)	Mole ratio Solid L/ drug	% E
4.09×10^{-4}	8.63×10^{-5}	1.63×10^{-5}	3.98	78.90
4.09×10^{-4}	6.74×10^{-5}	2.72×10^{-5}	6.65	83.55
4.09×10^{-4}	6.95×10^{-5}	5.70×10^{-5}	13.93	83.10
4.09×10^{-4}	6.85×10^{-5}	6.94×10^{-5}	16.97	83.20
4.09×10^{-4}	6.50×10^{-5}	8.18×10^{-5}	20.00	84.10
4.09×10^{-4}	6.95×10^{-5}	1.02×10^{-4}	24.93	83.04
4.09×10^{-4}	8.42×10^{-5}	1.25×10^{-4}	30.56	79.40

In Table 3.22 $[C_i]$, $[C_{eq}]$ and % E denote initial, equilibrium concentration and percentage of extraction respectively

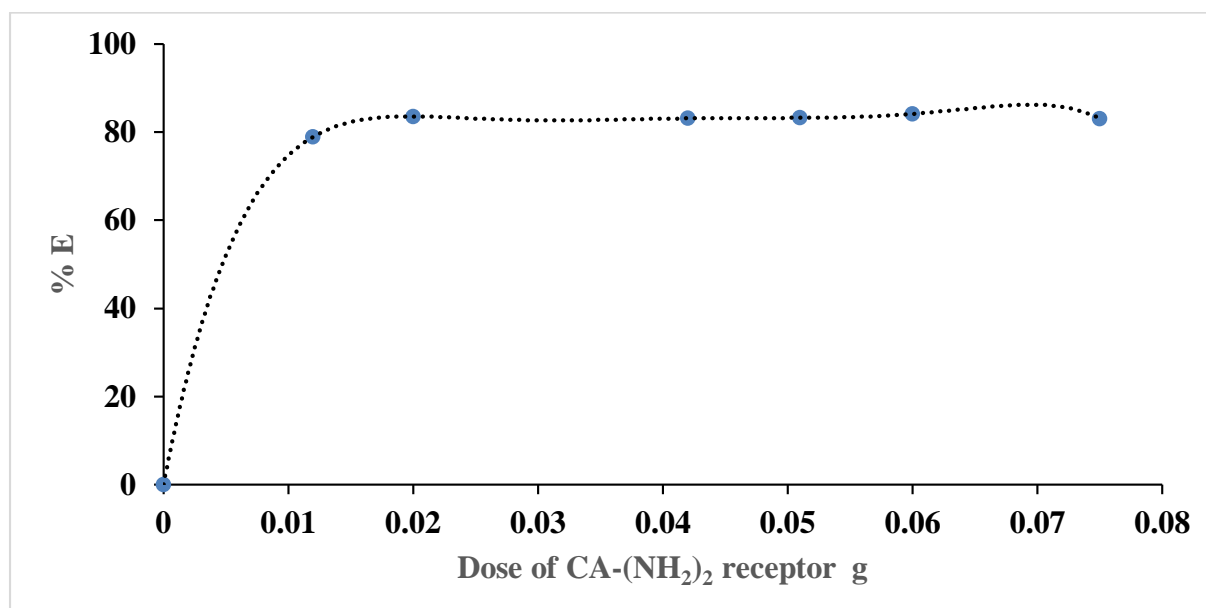


Fig. 3.41 The effect of receptor dose on the uptake of clofibrac acid from aqueous solution at

298.15 K.

3.13.2 The effect of pH of the aqueous solution on the extraction of clofibric acid from water by CA-(NH₂)₂ at 298 K

The controlling pH of solutions were carried by using buffer tablets from Fisher Scientific. The effect of pH on the extraction of clofibric acid from water by (CA-NH₂)₂ is shown in Fig. 3.42. The results show that at low pH, the % E of the drug by the receptor is very low due to the protonation of the receptor, as the pH increases the % E increases consistently once the amino functional group of the receptor is fully free to interact with the proton of the carboxylic group of the drug. Therefore the pH in the alkaline range will increase the activity of the lone pair of electrons on the nitrogen to interact with acidic proton of the pharmaceutical

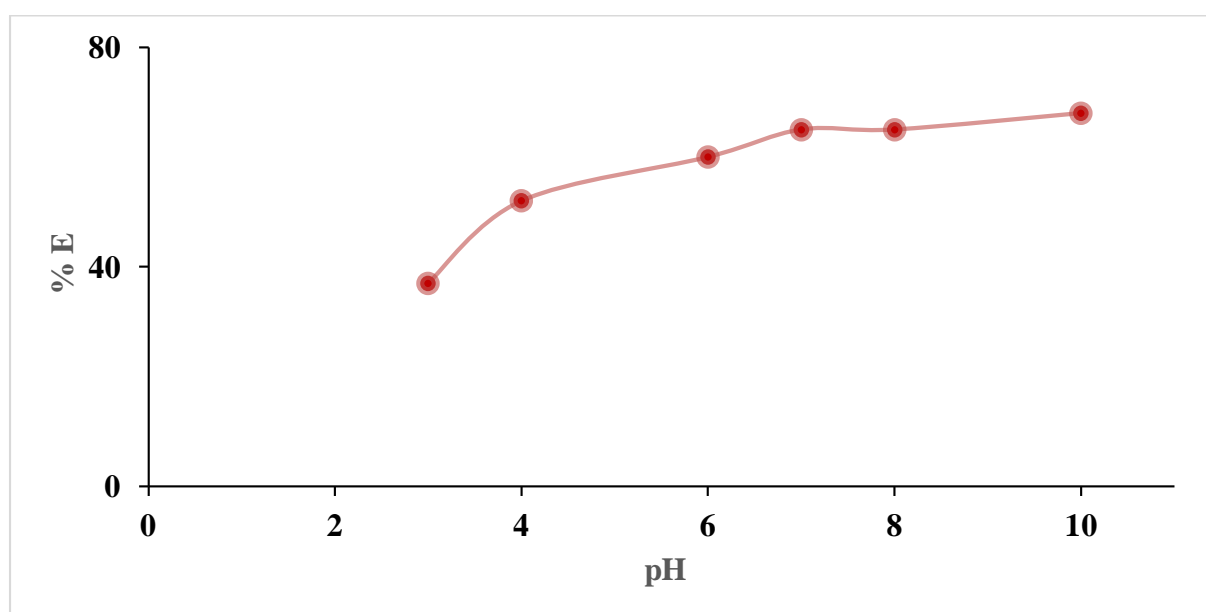


Fig. 3.42 The effect of pH on the extraction of clofibric acid (4.09×10^{-4} mol dm⁻³, 10 ml) by using CA-(NH₂)₂

3.13.3 Calculation of the capacity of the CA-(NH₂)₂ receptor to extract clofibric acid

The experiment was carried out by adding 0.01 g of the receptor to different concentrations (9×10^{-5} , 1.39×10^{-4} , 1.95×10^{-4} , 2.45×10^{-4} , 3.6×10^{-4} , 4.4×10^{-4} mol dm⁻³, 10 ml) of the clofibric acid in aqueous medium. The capacity of the receptor was calculated according to eq.2.40 and the obtained values were plotted against the concentration at equilibrium state (Fig. 3.43)

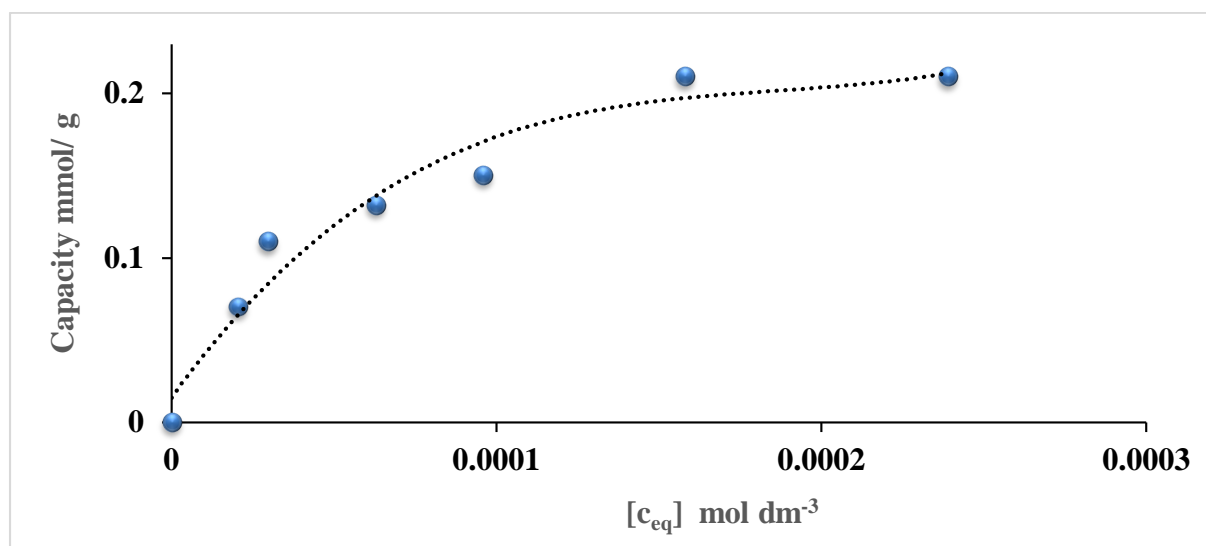


Fig. 3.43 The capacity of the calix[4]arene amine towards clofibric acid

3.14 Extraction of aspirin from water by CA-(NH₂)₂

The extraction of aspirin from water was carried in the same way as for clofibric acid. Table 3.15 and Fig. 3.44 shows that the receptor has low efficiency to remove aspirin from water (% E) and the increase of aspirin concentration in aqueous solution led to decrease the efficiency of the receptor to complex with aspirin which means that the water can compete with the receptor to form hydrogen bonding with aspirin molecules which leads to the formation of aspirin-aspirin homodimer through the protons of carboxylic groups and also intermolecular hydrogen bond between the acidic proton of carboxylic acid with the adjacent acetoxy group is expected to be formed²⁴⁴.

Table 3.15 Initial and equilibrium concentration of aspirin before and after the extraction and the percentages of extraction from water by CA-(NH₂)₂

C_i / mol dm ⁻³	C_{eq} / mol dm ⁻³	% E
1.96×10^{-4}	1.23×10^{-4}	37.2
3.93×10^{-4}	2.86×10^{-4}	27.2
5.90×10^{-4}	4.6×10^{-4}	22.0
7.80×10^{-4}	7.3×10^{-4}	6.90
9.80×10^{-4}	9.35×10^{-4}	4.50
1.18×10^{-3}	1.13×10^{-3}	4.23

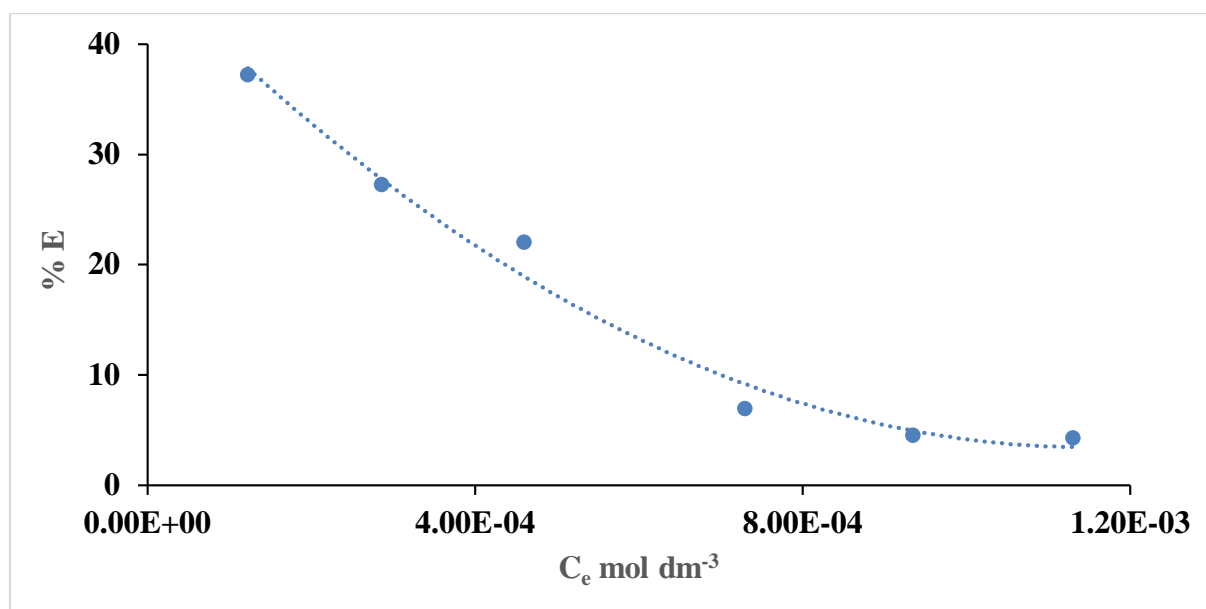


Fig. 3.44 Extraction of aspirin from water by CA-(NH₂)₂ at 298 K

From the above results it is concluded that CA-(NH₂)₂ is a suitable extracting agent for clofibric acid and diclofenac but the extraction ability of this receptor for aspirin was very poor. This is in accord with the results obtained from fundamental studies which demonstrated that CA-(NH₂)₂ is able to take two protons from the drug in the case of clofibric acid and diclofenac but only one from aspirin

Given the results obtained by calix[4]arene amine derivative in its interaction with pharmaceuticals in which it was demonstrated that the amine functionality is the active site of the interaction, experimental work was carried out to remove aspirin from water by 3-aminopropyl functionalised silica (Sil-NH₂). This drug was selected due to the low degree of extraction found with the calix[4]arene amine derivative

3.15 Aspirin removal by aminopropyl silica

The removal of aspirin from water by aminopropyl silica was investigated under different experimental conditions such as the effect of the amount of receptor and the pH of the aqueous solution on the extraction process. The capacity of aminopropyl silica to remove aspirin was also investigated.

3.15.1 Dose effect

In order to find the optimum amount of aminopropyl functionalised silica (Sil-NH₂), different amounts of this material were added to aqueous solutions containing a fix concentration of aspirin ($5.59 \times 10^{-3} \text{ mol dm}^{-3}$, 10 ml). The mixture was left to equilibrate in a water bath overnight at 298.15 K. Solutions were filtered and the pH meter (AB 15 pH meter Fisher Scientific) was standardised with buffer solutions (pH = 4 and 9.2) and the solution pH was measured. Blank experiments showed that no aspirin was extracted in the absence of silica. The percentage of aspirin extracted was calculated by eq. 2.39. The results are shown in Table 3.16 and graphically represented in Fig. 3.45

Table 3.16 Percentage of extraction of aspirin as a function of the dose of Sil-NH₂ at 298 K

$[C]_i \text{ mol dm}^{-3}$	$[C]_e \text{ mol dm}^{-3}$	Mass of Sil-NH ₂ g	% E
5.59×10^{-3}	2.59×10^{-3}	0.02	53.5
5.59×10^{-3}	1.83×10^{-3}	0.03	67.2
5.59×10^{-3}	1.31×10^{-3}	0.04	76.5
5.59×10^{-3}	1.31×10^{-4}	0.05	87.2
5.59×10^{-3}	7.10×10^{-4}	0.06	90.5
5.59×10^{-3}	5.29×10^{-4}	0.07	95.5
5.59×10^{-3}	2.30×10^{-4}	0.08	99.1
5.59×10^{-3}	5.20×10^{-4}	0.09	99.6
5.59×10^{-3}	3.24×10^{-5}	0.10	99.9

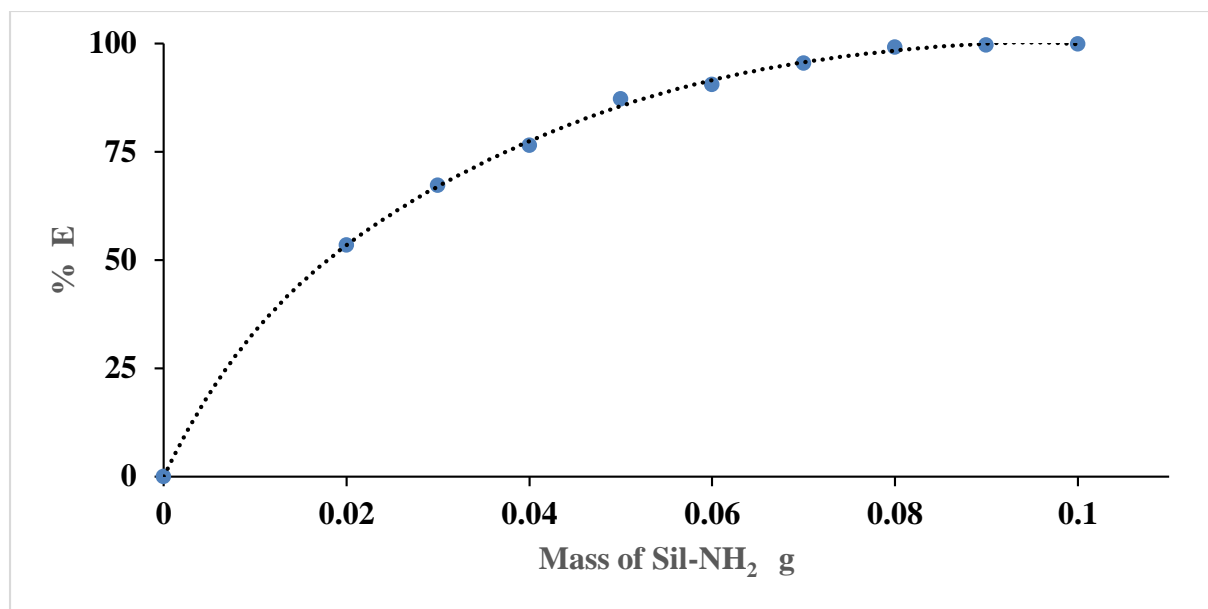


Fig. 3.45 The effect of the mass of Sil-NH₂ on the uptake of aspirin from aqueous solution ($5.59 \times 10^{-3} \text{ mol dm}^{-3}$, 10 ml) at 298 K.

The results show that as the amount of silica increases the % E extraction increases as the sites of interaction (amino active sites) in the material increase until saturation occurs. It is concluded that between 0.08 to 0.10 g are the optimum mass to be used for almost complete removal of aspirin from water

3.15.2 Effect of pH of the aqueous solution on the removal of aspirin by Sil-NH₂ at 298 K

Fig. 3.46 (plot of % E vs the pH of the aqueous solution of aspirin) shows that no extraction of aspirin occurs at low pH given that the amino group is protonated therefore unable to remove the drug from water. As the pH increases the % E increases substantially and at $\text{pH} \approx 4$ almost 100% of aspirin is removed from water due to the change of the acidic pharmaceutical to the ionic form which can be interacted with the amino group. In other words the acidic materials with low pK_a value will leads to rise the number of ions in solution and as a result the percentage of extraction will increased.

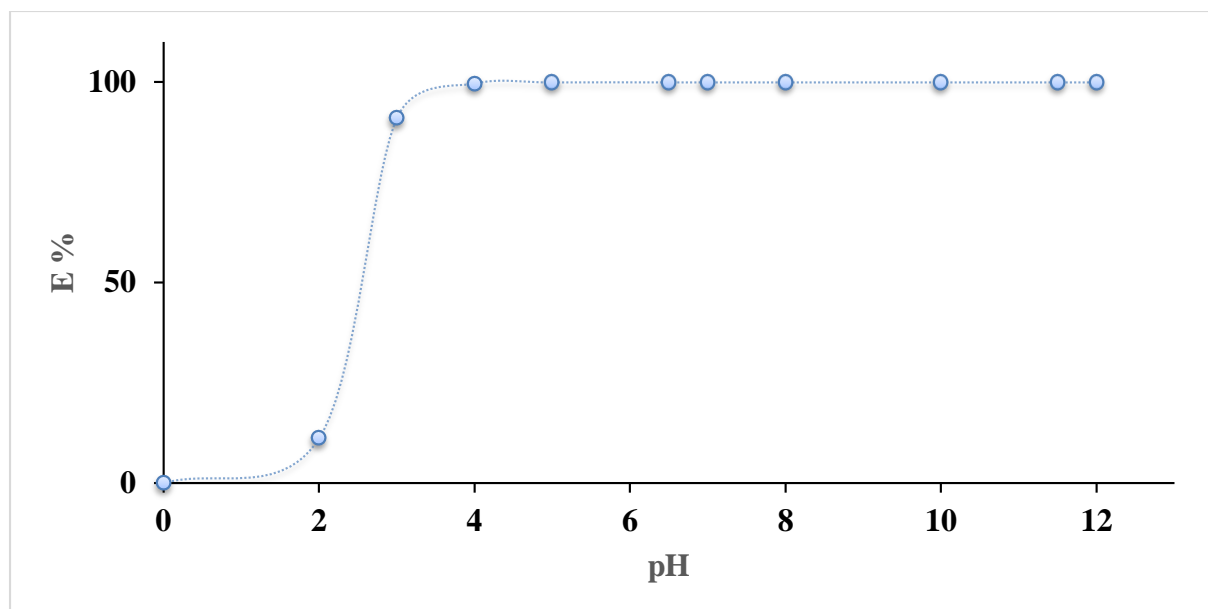


Fig. 3.46 Effect of pH of the aqueous solution on the extraction of aspirin from water (5.59×10^{-5} mol dm⁻³, 10 ml) by Sil-NH₂ at 298 K

3.15.3 Kinetics of removal

Using a solution of aspirin (5.59×10^{-3} mol dm⁻³) and 0.05 g of silica, it was found that after 5 minutes about 90 % of aspirin was removed, an indication the kinetics of the removal process is very fast

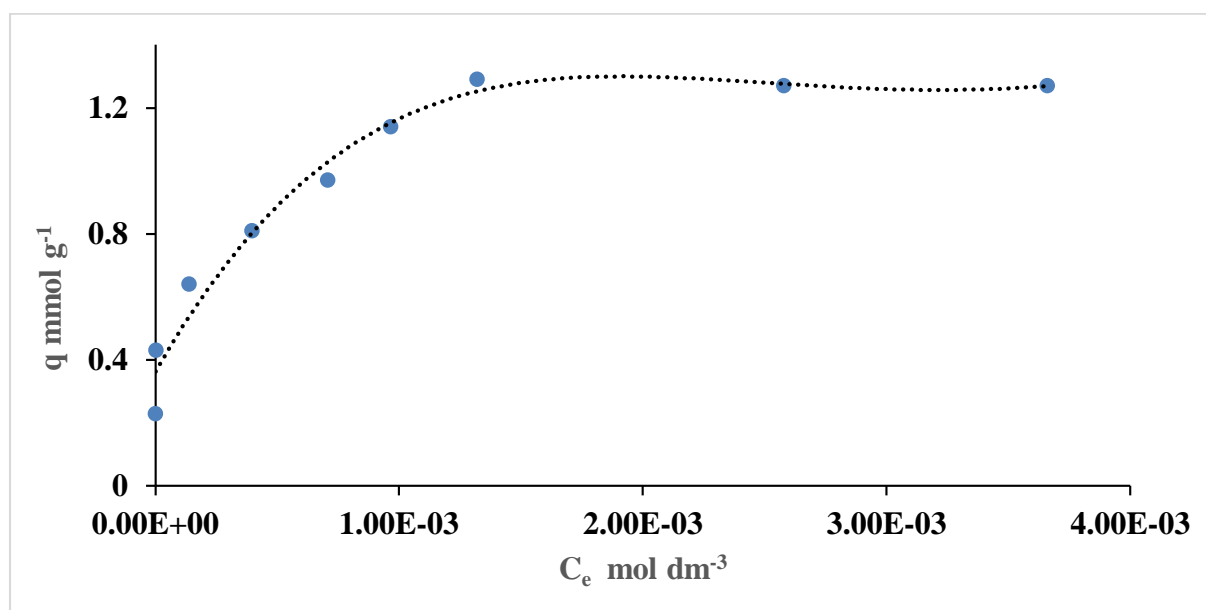
3.15.4 Determination of the capacity of Sil-NH₂ for the removal of aspirin from water at 298 K

The capacity of aminopropyl silica (maximum amount of aspirin per gram of silica) was determined by using a batch procedure. Eq. 2.40 was used to calculate the capacity, q , where c_i and c_e are the initial and equilibrium concentration of aspirin respectively in the molar scale, V the volume of solution (10 cm⁻³) and m denotes the mass of silica (0.05 g)

Details are given in Table 3.17 and shown graphically in Fig. 3.47

Table 3.17 Initial, equilibrium concentration and the capacity of silica to remove aspirin from water

$[C_i]$ mol dm ⁻³	$[C_{eq}]$ mol dm ⁻³	q / mmol g ⁻¹
1.12×10^{-3}	8.59×10^{-7}	0.23
2.24×10^{-3}	3.17×10^{-6}	0.43
3.36×10^{-3}	1.39×10^{-4}	0.64
4.48×10^{-3}	3.98×10^{-4}	0.81
5.59×10^{-3}	7.08×10^{-4}	0.97
6.70×10^{-3}	9.66×10^{-4}	1.14
7.80×10^{-3}	1.32×10^{-3}	1.29
8.95×10^{-3}	2.58×10^{-3}	1.27
1.00×10^{-2}	3.66×10^{-3}	1.27

**Fig. 3.47** Capacity of Sil-NH₂ to uptake aspirine from aqueous solution at 298 K

From Table 3.25, it can be concluded that the capacity, q , of 3-aminopropyl-functionalised silica gel to remove aspirin from aqueous solution is 1.27 mmol g⁻¹. The results are striking and indicate that the aminopropyl silica is an efficient material for the removal of aspirin from water to an extent that its capacity to remove this drug from water is much higher than the capacity of CA-(NH₂)₂ to remove clofibric acid from water. Experimental work on the use of aminopropyl silica to remove clofibric acid, diclofenac is now undergoing in the Thermochemistry Laboratory. Despite that the 3-aminopropyl functionalised silica is effective to remove aspirin and might be effective to remove some of acidic pharmaceuticals but the removal process is relying only on the acid-base reactions

which can make the removal process not efficient in real water samples due to the presence of many of acidic and basic pollutants. Also, most of the manufactured drugs are hydrophobic in order to interact with the cell membrane which can diminish the use of silica as receptor for these pollutants due to the hydrophilicity of silica. On the other side, the CA-(NH₂)₂ has its own special features such as the high hydrophobicity, can be modified, recycled easier than silica and also can be applied as drug carrier in drug delivery system due to the presence of amino group which is found in the structure of the amino acids which are the main component in living systems

Preliminary experiments were carried out to assess the interaction of C-decylpyrogallol[4]arene, PG11, and carbamazepine, CBZ, and this is discussed in the following section

3.16 Complexation of C-decylpyrogallol[4]arene with carbamazepine

The complexation process has been carried out by ¹H NMR in acetonitrile. It's found that the macrocyclic receptor has affinity to complex with the carbamazepine and therefore the effect of the complexation process on the thermal behaviour of the drug will be discussed

3.16.1 Investigation of the complexation of PG11 and CBZ by thermal analysis

Thermal studies TG, DTG and DSC analysis have been carried out to investigate whether or not PG11 interacts with CBZ and if so, to investigate the effect of complexation on the physico-chemical properties of the drug. The CBZ was heated from -25 to 200 °C at 10 K/ min to detect the melting process, followed by cooling down at the same temperature range, in order to observe the drug crystallization. TGA analysis for the complexation between CBZ and C-decylpyrogallol[4]arene confirmed that the complexation process was implemented successfully, the comparison between the TGA thermograms obtained for the pure compounds (Fig. 3.48-3.49) and the complex formed (Fig. 3. 50). Also, the DSC thermograms obtained for the pure compounds and the complex gives strong support that the complex is formed and this can be interpreted as follows, for the pure CBZ, the endothermic peak at 169.33 °C with the heat of 7.788 Jg⁻¹ reflects the amorphous character of the drug and also can give information about the effect of the temperature on the structure. Another peak existed at 192.38 °C with a heat of fusion 90.75 Jg⁻¹ which indicates the melting point of the drug. On cooling, an exothermic peak is observed at 170.42°C which indicates the conversion of the melted material to its solid state but the difference between these two peaks revealed that the phase transition from stable state to another occurred which means that the heat delivered to the drug induces phase transitions causing variations in the locations of the molecules to a new location in the molecular system. The thermogram of the free receptor heated from -25 °C to 250 °C to detect the melting point

of the receptor was followed by cooling at the same temperature in order to investigate the crystallisation. The thermogram shows a broad peak at 142.65 °C which indicates the melting point of the host with the heat of fusion -42.23 Jg^{-1} and the broadening may attribute to the residual of the solvent used in the crystallization due to the depth of the cavity formed. There is no phase transition between two phases resulted from the heat delivered to the sample because of the rigidity of the macrocyclic host resulting from the presence of four benzene rings and the hydrogen bonding between these rings that can prevent the rotation and traslocation to another state which means that the compound has ability to work as a molecular store²⁴¹. Completely different thermogram was obtained for the complex compared with the free host and guest as shown in Fig. 3. 36. The curve indicated that conformational changes in the receptor structure occurred which means that the complexation process led to defects in the molecular structure of the host and the guest and this is essential to promote the complexation process. This was reflected by the appearance of five signals in the DSC thermogram, and also the possibility of the macrocycle to be sufficiently flexible to achieve the complexation process which can lead to promote phase transition in the host structure. There are three endothermic peaks shifted from their free form. TG and DTG analysis of the pure compounds and the complex were carried out at the range of ambient temperature to 800 °C with a temperature increase rate 10°C/minute in a nitrogen gas atmosphere

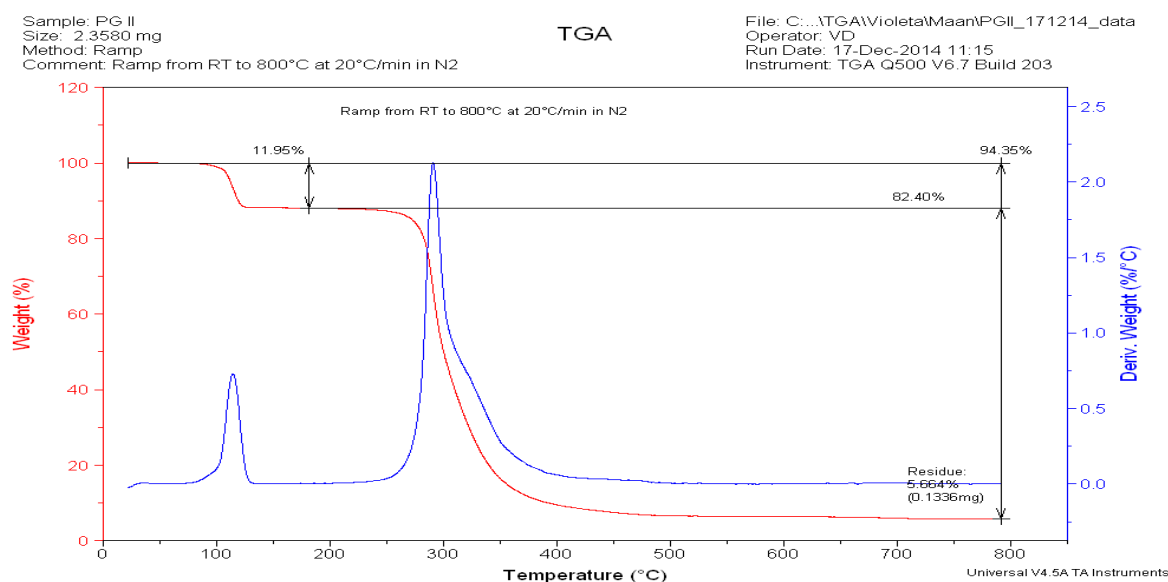


Fig. 3.48 TGA thermogram for the C-decylpyrogallol[4]arene receptor

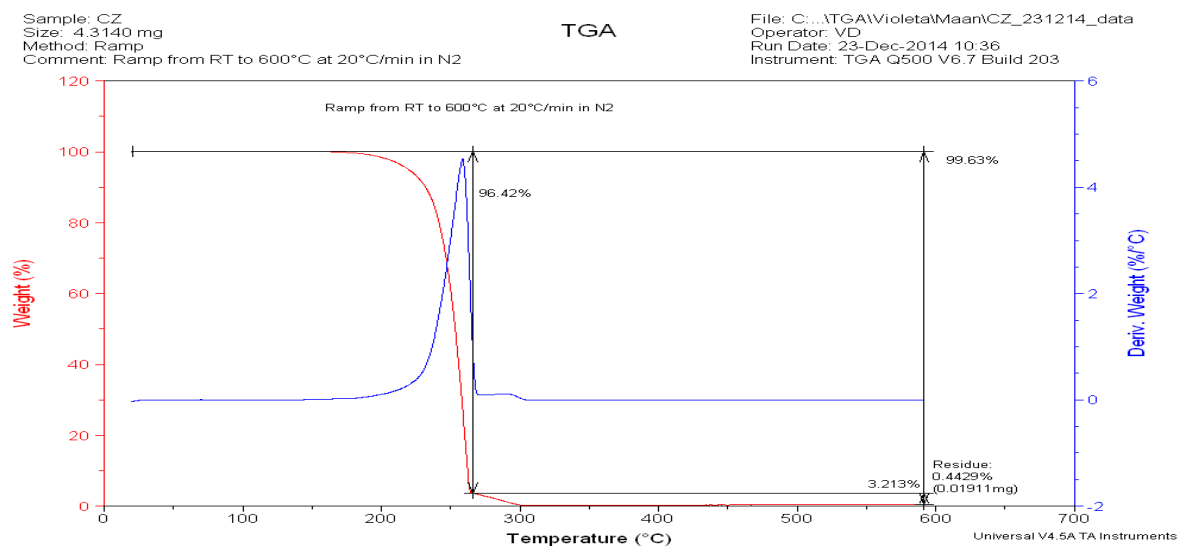


Fig. 3.49 TGA thermogram for the CBZ

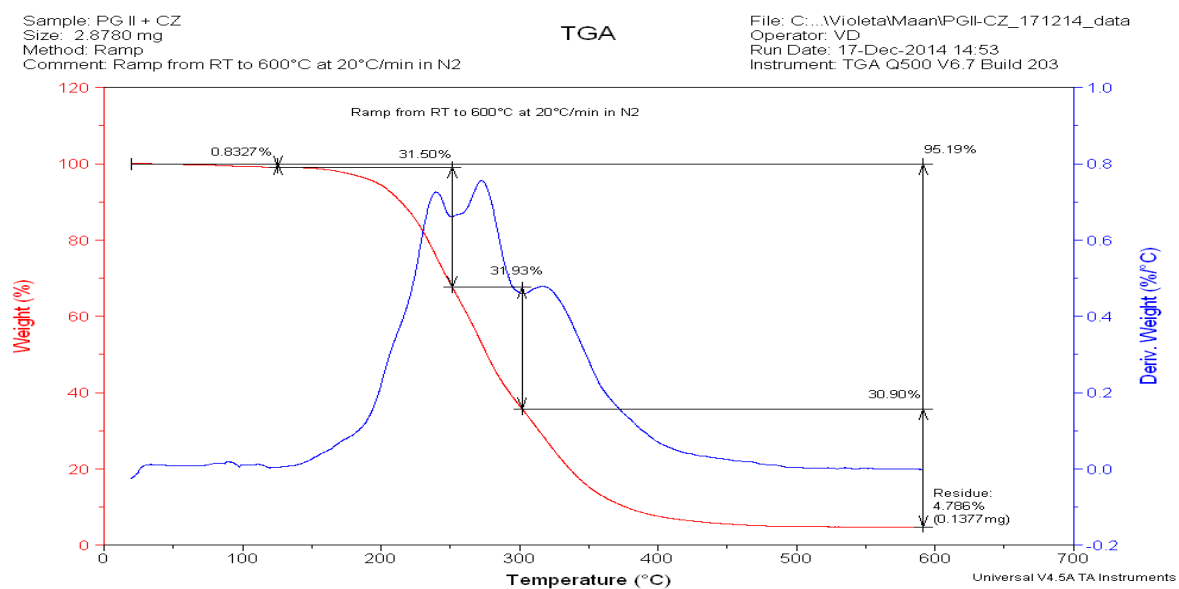


Fig. 3.50 TGA thermogram of the complex formed between CBZ and C-decylpyrogallol[4]arene

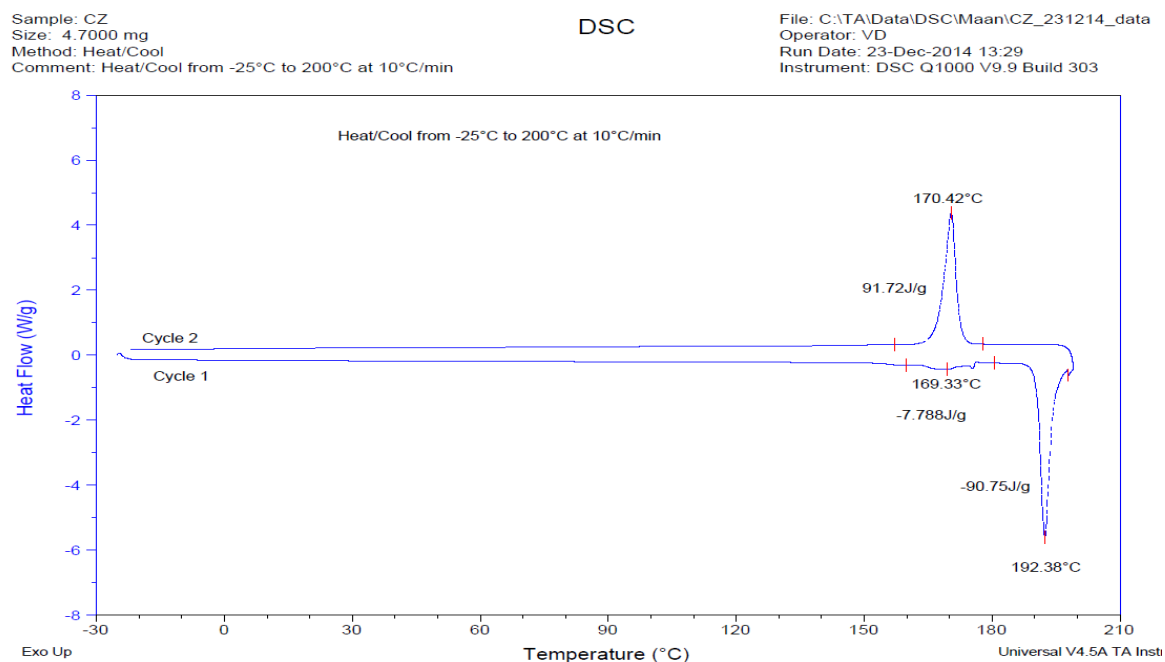


Fig. 3.51 DSC thermogram for the carbamazepine showing structural phase transition

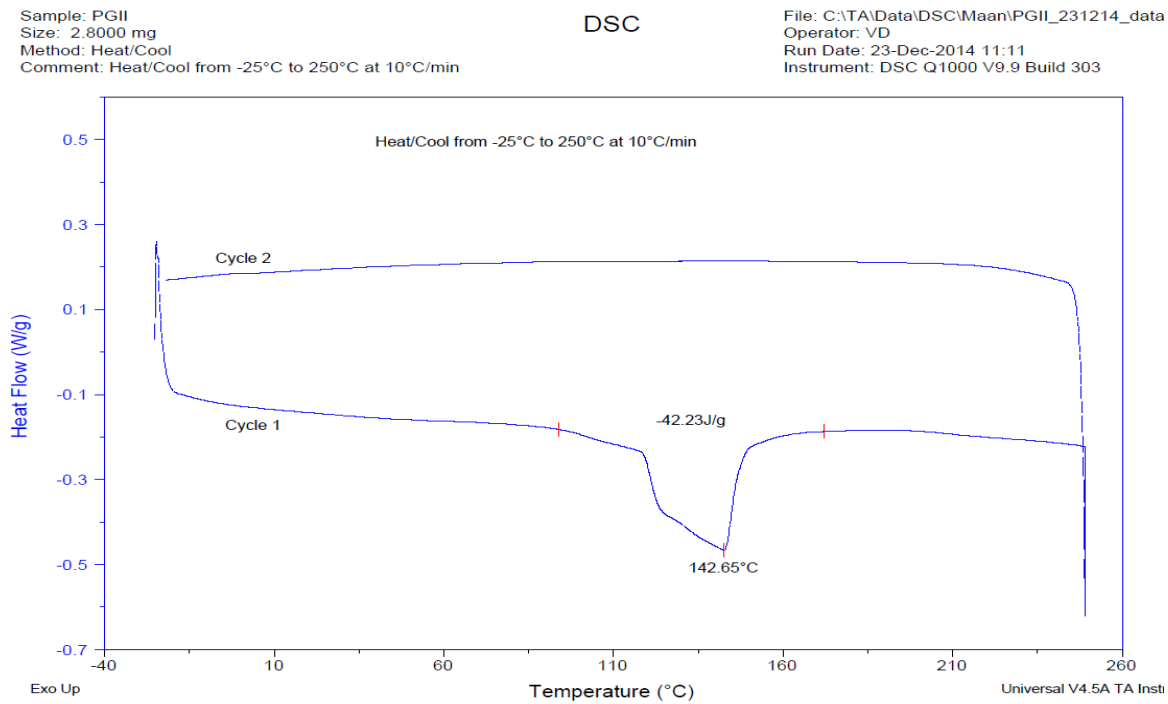


Fig. 3.52 DSC thermogram for C-decypyrogallol[4]arene

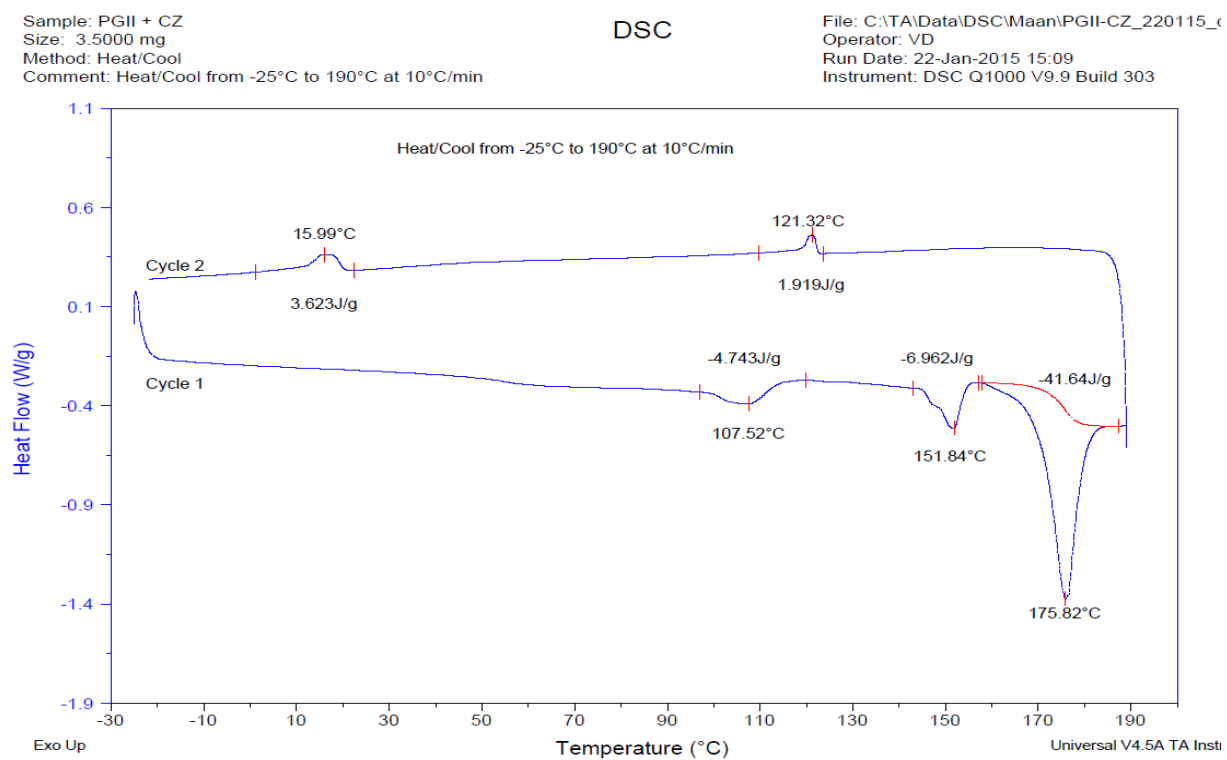


Fig. 3.53 DSC thermogram for the complex formed between C-decylpyrogallol[4]arene and CBZ

Chapter IV

Results &

Discussion

4.1 *Meso*-tetramethyl-tetrakis-(4-hydroxyphenyl ethyl)calix[4]pyrrole TTHCP and *meso*-tetramethyl-tetrakis-(4-ethylacetatophenoxyethyl) calix[4] pyrrole TTCP

Here we engineered, synthesised and characterised two novel derivatives based on calix[4]pyrrole. Both of them are characterised by a deep cavity with multiple functional groups and also multiple walls and these are first produced using a new procedure. The real progress achieved with this synthesis is that all of the calix[4]pyrrole derivatives synthesised earlier rely on the addition of phenol groups to the *meso* position without a pendant arm²¹¹ like these two novel receptors. The addition of ethylene groups in the pendant arms could have an effect on the flexibility of the receptors to drive the interaction with different guests which is essential to give freedom for the conformational changes required in the complexation process. Also the presence of phenol ring inspired the polymerisation.

In addition to these unique behaviour of the new receptors, the addition of ester groups is very important to increase the solubility of the receptor in different solvents. The receptor containing ester groups can act as a ditopic ion-pair receptor and may have an application as ion transporter through the cell membrane due to the low toxicity of calix[4]pyrrole. The chemical structures for these compounds are shown in Fig. 4.1

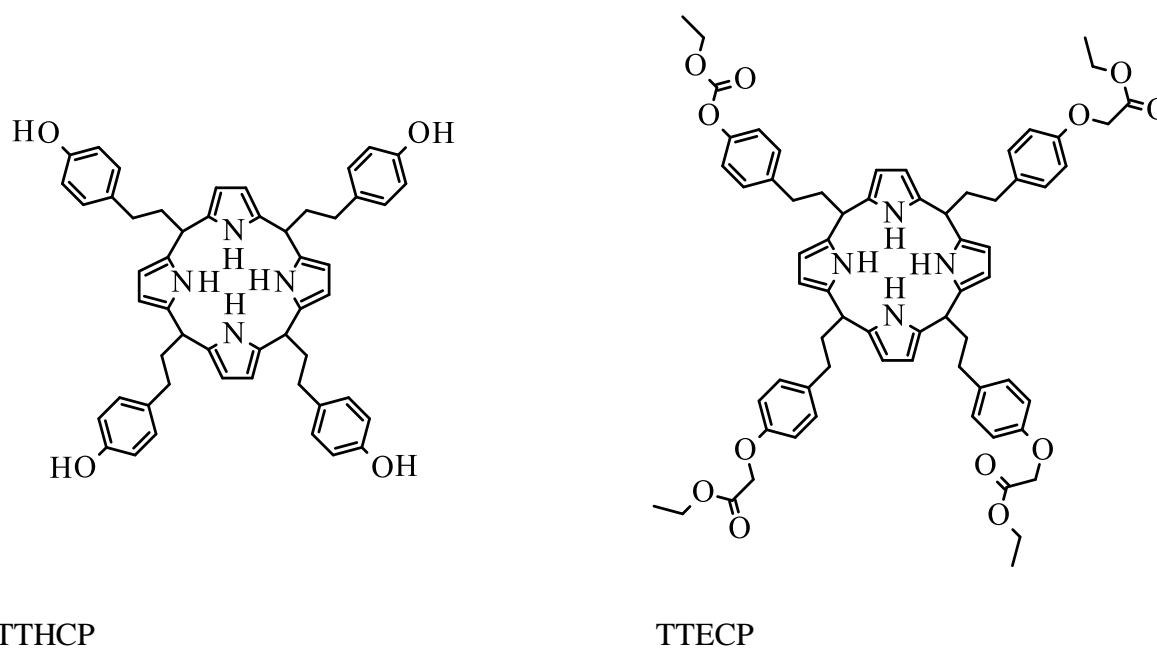


Fig. 4.1 Chemical structure of novel calix[4]pyrrole derivatives (a) *meso*-tetramethyl-tetrakis-[2-(4-hydroxyphenyl)ethyl]calix[4]pyrrole TTHCP and *meso*-tetramethyl-tetrakis-[2-(4-ethylacetatophenoxy)ethyl] calix[4]pyrrole TTECP

4.1.1 Characterisation of *meso*-tetramethyl-tetrakis-[2-(4-hydroxyphenyl)ethyl]calix[4]pyrrole TTHCP

^1H NMR data in $\text{d}_6\text{-DMSO}$ at 298 K (Fig. 4.2) confirmed that the calix[4]pyrrole derivative was obtained in high purity which is important for the next study. A set of peaks referring to different protons in different environments appear in the spectrum, the singlet peak at 9.32 ppm corresponds to the **NH** proton and that at 9.08 ppm refers to **OH**, the sets of doublets at 6.84 and 6.57 ppm are assigned to the phenyl protons. The resonance of protons of the pyrrolic ring appears as a doublet at 5.7 ppm, the singlet peak at 3.3 ppm is due to the presence of water in $\text{d}_6\text{-DMSO}$. The two sets of triplets at 2.27 and 2.06 ppm refer to the methylene protons while the singlet peak at 1.5 ppm corresponds to the methyl group at the *meso* position as shown in Fig. 4.1. Having characterised the receptor, solubility measurements in a variety of solvents at 298.15 were carried out.

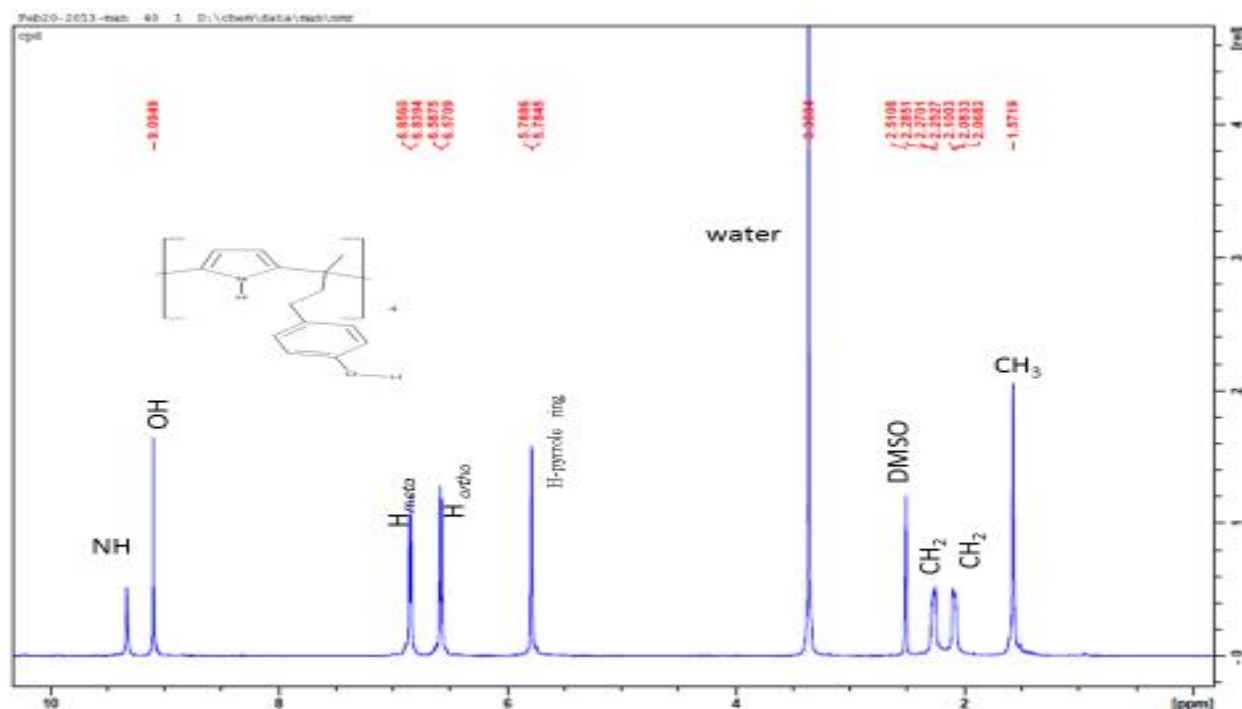


Fig. 4.2 ^1H NMR spectrum for *meso*-tetramethyl-tetrakis-(4-hydroxyphenyl ethyl) calix[4]pyrrole TTHCP in DMSO-d_6

4.1.2 Solubility of TTHCP in various solvents at 298.15 K

The solvation properties of TTHCP in various solvents can be assessed through the calculation of the transfer Gibbs energies from a reference solvent (acetonitrile) to other solvents. The solubility of the ligand in different organic solvents are reported in Table 4.1 at 298.15 K. Standard Gibbs energies of solution $\Delta_s G^\circ$ were calculated using the following equation

$$\Delta G^\circ = -RT \ln K_s \quad \text{eq.4.1}$$

$$\Delta_t G^\circ (\text{TTHCP}) (s_1 \rightarrow s_2) = \Delta_s G^\circ (\text{TTHCP}) (s_2) - \Delta_s G^\circ (\text{TTHCP}) (s_1) \quad \text{eq.4.2}$$

In equation 4.1, K is the equilibrium constant which is equal to the ligand concentration in the saturated solution on the assumption that the activity coefficient of a low concentration non-electrolyte in solution is equal to unity. It is not possible to calculate the Gibbs energy of solution if the ligand undergoes solvation as previously stated. The standard transfer Gibbs energy, $\Delta_t G^\circ$ was calculated using acetonitrile as reference solvent as shown in Table 4.1

Table 4.1 Solubility data and derived standard Gibbs energies of solution of TTHCP in different solvents at 298.15 K. Transfer Gibbs energies from acetonitrile to other solvents is ($\Delta_t G^\circ_{\text{MeCN} \rightarrow s_2}$) at 298.15 K

Solvent	Solubility mol dm ⁻³	$\Delta_s G^\circ / \text{kJ mol}^{-1}$	$\Delta_t G^\circ_{\text{MeCN} \rightarrow s_2} / \text{kJ mol}^{-1}$
H ₂ O	Not soluble	-----	-----
MeCN	$(1.3 \pm 0.1) \times 10^{-3}$	16.5 ± 0.6	0.00
MeOH	$(2.1 \pm 0.4) \times 10^{-4}$	21.0 ± 2	4.5
EtOH	$(1.8 \pm 0.3) \times 10^{-4}$	21.4 ± 1.7	4.5
DMSO	$(2.0 \pm 0.2) \times 10^{-2}$	10 ± 1	6.5
DMF	$(3.4 \pm 0.3) \times 10^{-2}$	8 ± 1.7	- 8.5
Hexane	Not soluble	-----	-----
Chloroform	Not soluble	-----	-----
CH ₂ Cl ₂	Not soluble	-----	-----
Acetone	$(14 \pm 0.1) \times 10^{-3}$	14.3 ± 0.6	- 2.2

From the standard transfer Gibbs energy of the receptor from acetonitrile (Table 4.1) it can be shown that among dipolar aprotic solvents, the receptor is better solvated in DMF, DMSO and acetone than acetonitrile. It was previously reported by Danil de Namor and Shehab that DMSO and DMF interact with the -NH- functionality of the pyrrole rings of the macrocycle through their basic oxygen atoms. As far as the alcohols are concerned, these are poor solvators of the ligand relative to acetonitrile as reflected in their transfer Gibbs energies (unfavourable)

4.1.3 Complexation of TTHCP with anions, ^1H NMR studies

^1H NMR experiments reveal that the receptor interacts significantly with the fluoride anion F^- (Fig. 4.3, Table 4.2) and the dihydrogen phosphate (Fig. 4.4, Table 4.2). In fact, the strong downfield shift change of the $-\text{NH}-$ proton with the fluoride anion is much greater than that for the phosphate anion in this solvent. The result obtained for the OH proton indicates that interaction may take place with this proton. It is also shown for the phosphate anion that some interaction with the phenyl proton occurs.

^1H NMR experiments have revealed that the receptor complexed significantly with the fluoride and H_2PO_4^- anions and there is significant contribution for the phenolic hydroxyl group and through the pyrrolic NH functional group with the complexation of these anions (Fig. 4.3).

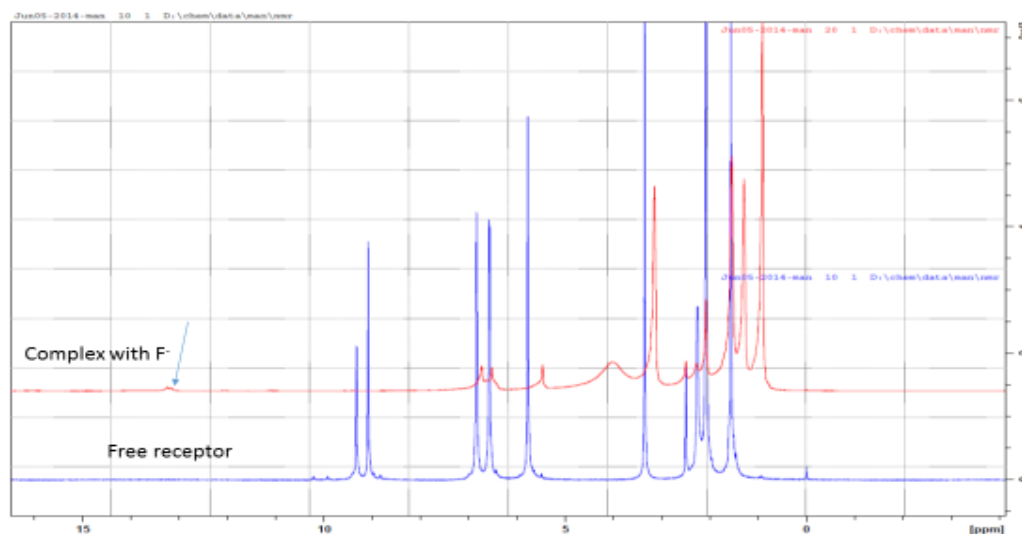


Fig. 4.3 ^1H NMR spectrum of TTHCP and its fluoride complex (Bu_4N^+ as counter ion) in DMSO-d_6 at 298 K.

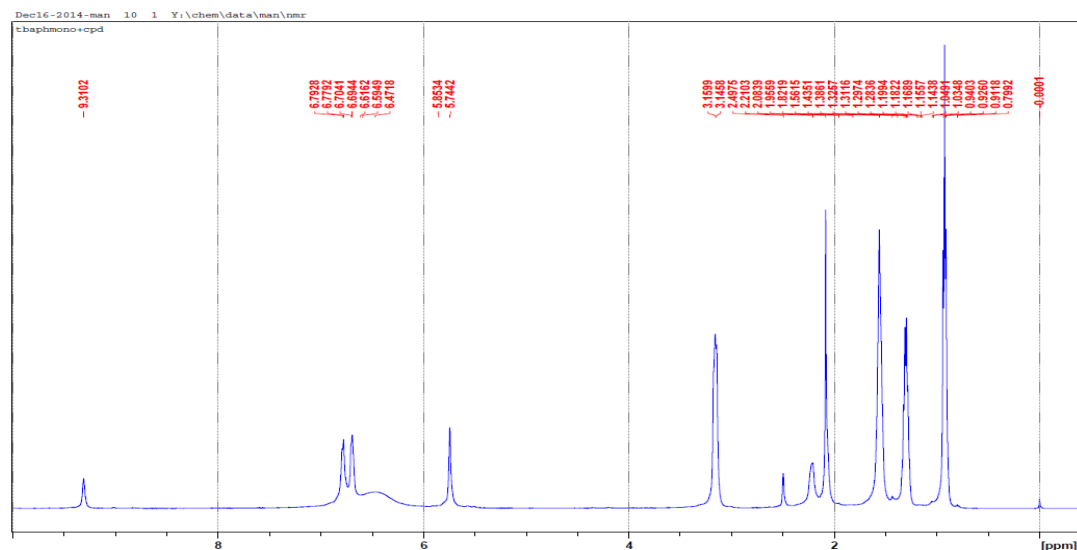


Fig. 4.4 ^1H NMR spectrum for the complex formed between *meso*-tetramethyl-tetrakis-(4-hydroxyphenyl ethyl)calix[4]pyrrole TTHCP and tetra-*n*-butylammonium phosphate ($\text{Bu}_4\text{NH}_2\text{PO}_4$) at 298 K in DMSO-d_6

Table 4.2 ^1H NMR chemical shifts (δ) and chemical shift changes ($\Delta\delta$) of CPD protons upon the addition of fluoride, phosphate, and bromide as tetra-*n*-butylammonium salts in DMSO-d_6 at 298 K

Proton	δ_{ppm} (N-H)	δ_{ppm} (O-H)	δ_{ppm} (Ar-H _{meta})	δ_{ppm} (Ar-H _{ortho})	δ_{ppm} (C-H-pyrrole)
CPD proton	9.42	9.08	6.84	6.56	5.76
CPD + TBAF	12.9	Vanished	6.98	6.62	5.62
$\Delta\delta$ ppm	3.48		0.14	0.06	- 0.14
CPD+TBAPh	9.31	Vanished	6.78	6.69	5.79
$\Delta\delta$ ppm	- 0.14	Vanished	- 0.06	0.13	0.03
CPD +TBABr	Overlapped	Overlapped	-----	-----	-----

Following ^1H NMR studies on the interaction of TTHCP and the anions in DMSO-d_6 , conductance measurements were carried out in order to identify the composition of the complex. For comparison purposes with other calix[4]arene receptors, acetonitrile was used as the solvent for conductance and thermodynamic studies

4.2 Conductometric titration of anion salts with TTHCP in MeCN at 298.15 K

Given that the ^1H NMR studies were confirmed the complexation between TTHCP and anions, further investigations were carried out by using conductometric measurements and it will be discussed next

4.2.1 Conductance measurements of *meso*-tetramethyl-tetrakis-(4-hydroxyphenyl ethyl)calix[4]pyrrole TTHCP with fluoride (tetra-n-butylammonium as counter ion) in acetonitrile at 298.15 K

The main goal of the conductance measurements is to corroborate further the interaction between the calix[4]pyrrole derivative and the fluoride anion and to identify the stoichiometry of the interaction. As shown in Fig. 4.5 (plot of the molar conductance Λ_m ($\text{S cm}^2 \text{mol}^{-1}$) against [receptor]/ [anion] concentration ratio (Table 4.3-Appendix), the molar conductance decreases significantly upon addition of the receptor (A to B) until the ratio reaches a value of 0.5, at this point all the fluoride anions in the solution were consumed indicating the formation of a 1 [receptor]: 2 $[\text{F}^-]$ complex $[\text{TTHCPF}_2]^{2-}$ (eq.4.3)



The decrease in conductance is attributed to the size of the complex relative to the free anion. Further addition of the receptor leads to a break in the conductance (B to C) at a [receptor]/ [anion] concentration ratio of unity which may attributed to the transfer of one fluoride anion to the free receptor as shown in the following equation



From C to D the molar conductance does not change significantly

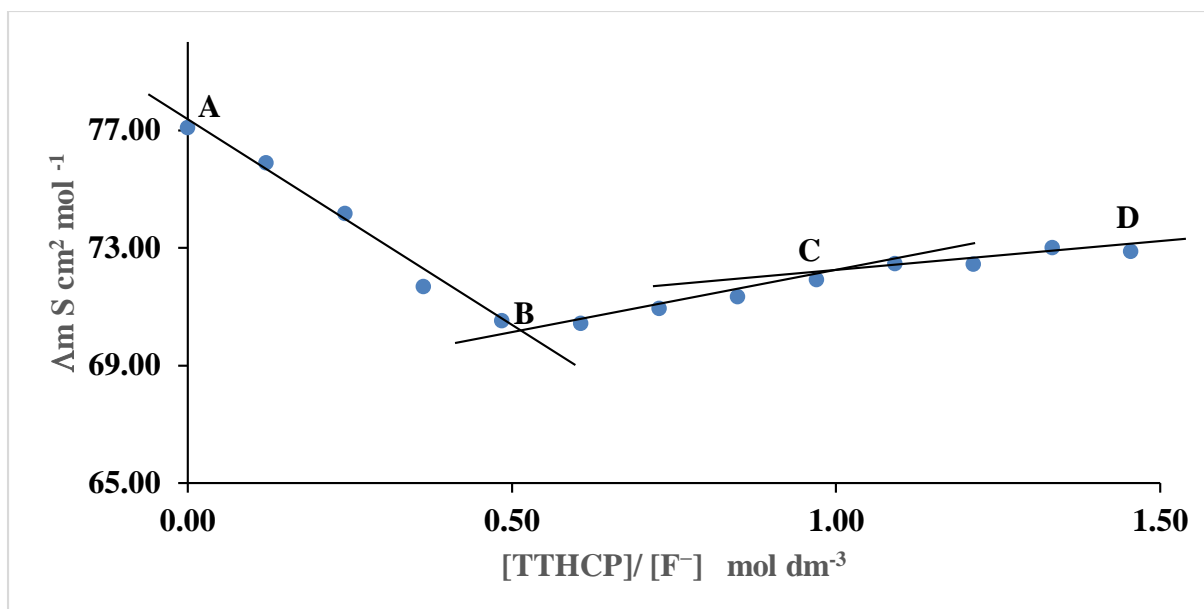


Fig. 4.5 Conductometric titration of TTHCP against $\text{Bu}_4\text{NH}_2\text{PO}_4$ in acetonitrile ($1 \times 10^{-4} \text{ mol dm}^{-3}$) at 298.15 K.

Conductometric measurements involving TTHCP and the dihydrogen phosphate anion in acetonitrile are now discussed

4.2.2 Conductance measurements for the complexation of dihydrogen phosphate $\text{Bu}_4\text{NH}_2\text{PO}_4$ with TTHCP in acetonitrile at 298.15 K

As shown in Fig. 4.6 the solution of tetra-*n*-butylammonium phosphate monobasic in acetonitrile is conductive. The addition of calix[4]pyrrole solution to the phosphate anion solution has led to a dramatic decrease in the molar conductance as a result of the hosting of the phosphate anion by the receptor (A to B). A plot the molar conductance Λ_m ($\text{S cm}^2 \text{ mol}^{-1}$) against [receptor] / [anion] concentration ratio (Table 4.4-Appendix), the stoichiometry of the reaction is found to be 2 $[\text{H}_2\text{PO}_4^-]$: 1 [TTHCP] which means that one molecule of the receptor hosted two phosphate anions to form $[\text{TTHCP}(\text{H}_2\text{PO}_4)_2]^{2-}$ as shown in eq.4.5



A comparison between these results and those previously reported by Danil de Namor and Shehab³² reveals that the parent calix[4]pyrrole interacts with only one unit of the anion. Therefore, the functionalization of the parent compound has increased the hosting ability of the receptor to uptake this anion. Further addition of the receptor to the phosphate solution does not lead to any significant change in the conductance

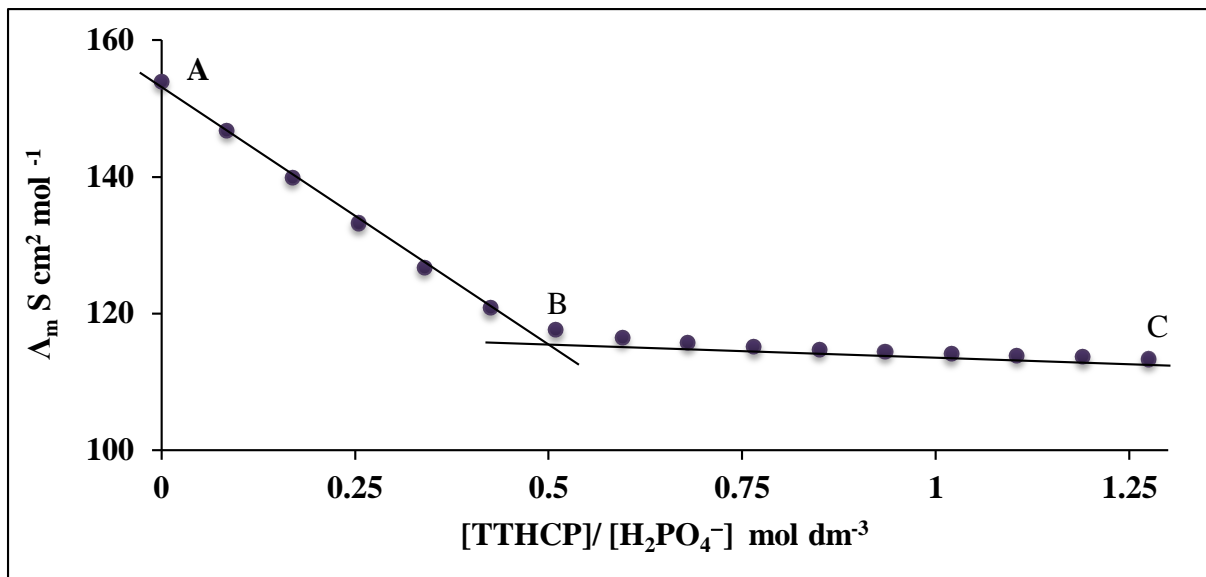


Fig. 4.6 Conductivity titration between TTHCP and tetrabutylammonium phosphate ($\text{Bu}_4\text{NH}_2\text{PO}_4$) in acetonitrile at 298.15 K, $[\text{Bu}_4\text{NH}_2\text{PO}_4] = 9.4 \times 10^{-5} \text{ mol dm}^{-3}$.

The following section reports the thermodynamic studies on the complexation of this receptor TTHCP with the halides and phosphate anions (as tetra-*n*-butyl ammonium counter ion) by the use of titration calorimetry

4.3 Thermodynamic parameters for the complexation of TTHCP with fluoride and phosphate anions (tetra-*n*-butylammonium counter ion) in acetonitrile at 298.15 K

The isothermal titration calorimetry was used to investigate the thermodynamic parameters of the complexation processes between the macrocyclic receptor with fluoride and phosphate anions (tetra-*n*-butylammonium counter ion) in acetonitrile. The Nano-ITC cell was loaded with the receptor solution in acetonitrile ($1 \times 10^{-3} \text{ mol dm}^{-3}$) and the injection syringe with the guest solution (fluoride or phosphate as tetra-*n*-butylammonium counter ion) in acetonitrile and the instrument was programmed to inject the guest solution (5.14 μl) every three minutes. It seems from the thermodynamic data in Fig. 4.7 for fluoride and Fig. 4.8 for H_2PO_4^- that the receptor has high affinity to interact with these anions (phosphate and fluoride) and stable complexes are formed with high stability constants as shown in Table 4.3 with stoichiometric ratios of 2: 1 guest: host. The high hosting ability of the receptor for these anions may be attributed to the flexibility of the receptor and the depth of the cavity.

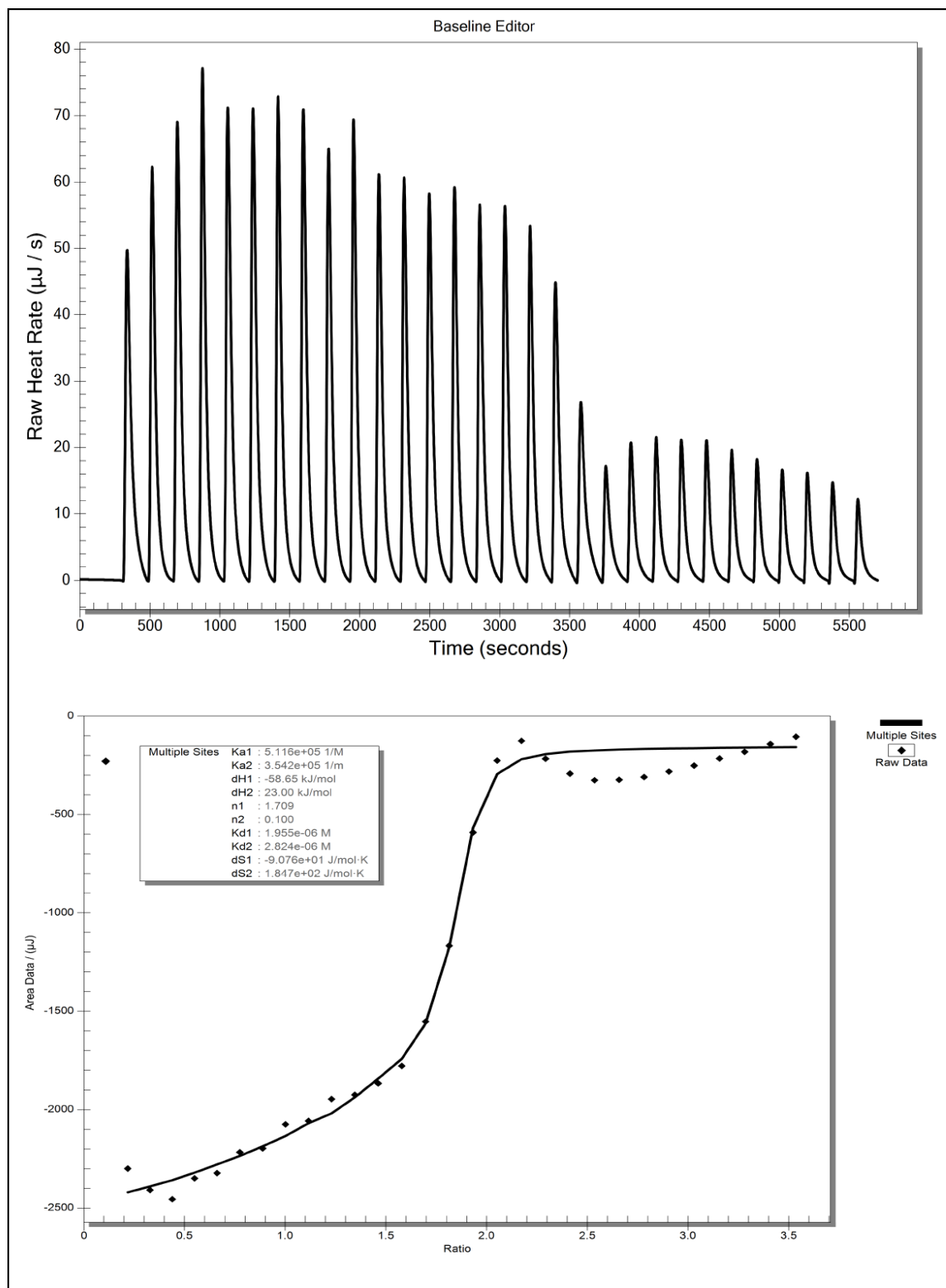


Fig. 4.7 Isothermal titration calorimetry for the complexation of TTHCP solution in acetonitrile ($1 \times 10^{-3} \text{ mol dm}^{-3}$) with fluoride (tetrabutylammonium counter ion) in acetonitrile ($2 \times 10^{-2} \text{ mol dm}^{-3}$) at 298.15 K

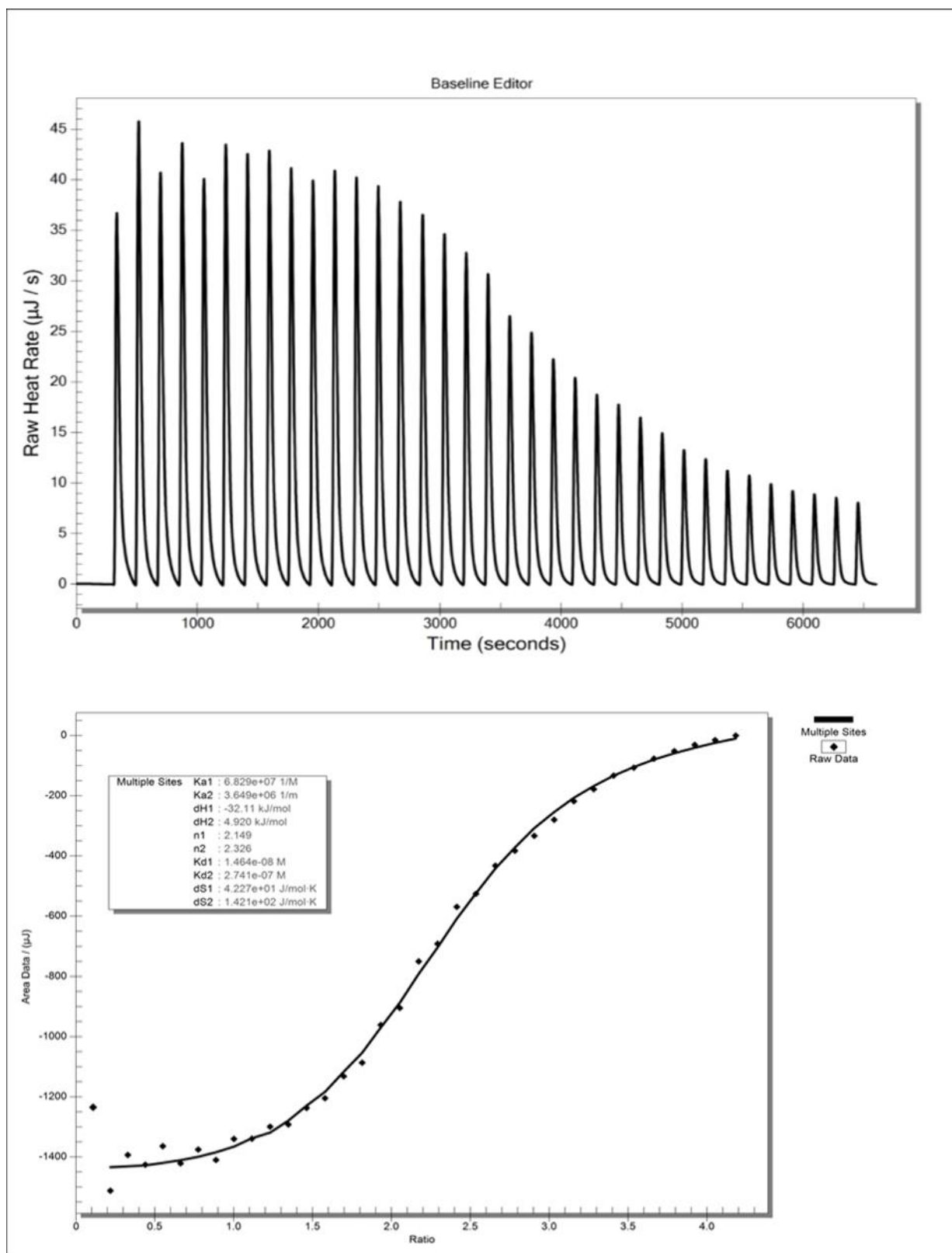


Fig. 4.8 Isothermal titration calorimetry for the complexation of TTHCP in MeCN ($1 \times 10^{-3} \text{ mol dm}^{-3}$) with phosphate (tetrabutylammonium counter ion) in acetonitrile ($2 \times 10^{-2} \text{ mol dm}^{-3}$) at 298.15 K.

Table 4.3 The thermodynamic parameters for the interaction of *meso*-tetramethyl-tetrakis-(4-hydroxyphenyl ethyl) calix[4]pyrrole TTHCP and phosphate, fluoride, chloride, as tetrabutylammonium counter ion in acetonitrile at 298.15 K

[Guest]/ [host]	log K	$\Delta H^\circ / \text{kJ mol}^{-1}$	$\Delta G^\circ / \text{kJ mol}^{-1}$	$\Delta S^\circ / \text{J mol}^{-1}\text{K}^{-1}$
[Fluoride]/ [CPD]	$K_1 = 5.71$	$\Delta H^\circ_1 = - 58.6$	$\Delta G^\circ_1 = - 32.59$	$\Delta S^\circ_1 = 46$
2: 1	$K_2 = 5.54$	$\Delta H^\circ_2 = 23$	$\Delta G_2 = - 31.62$	$\Delta S^\circ_2 = 38$
[Phosphate]/ [CPD]	$K_1 = 7.83 \pm 0.03$	$\Delta H_1 = - 32.11$	$\Delta G^\circ_1 = - 44.72$	$\Delta S^\circ_1 = 42$
2: 1	$K_2 = 6.55$	$\Delta H_2 = 4.9$	$\Delta G^\circ_2 = - 37.45$	$\Delta S^\circ_2 = 142$

The results in Table 4.3 shows that highly stable complex are formed in acetonitrile, as far as the fluoride is concerned, the formation of the 1: 1 (receptor: anion) complex is enthalpically controlled. The loss of entropy is due to the conversion of 2 units (anion and receptor) into one (the complex). However, the formation of the 1: 2 (receptor: anion) receptor is entropically controlled and enthalpy destabilised. This pattern is typical of processes in which desolvation occurs upon complexation. Desolvation requires energy to remove the solvent either from the host or from the guest and therefore the reaction is endothermic and entropically favourable. As for as the H_2PO_4^- and TTHCP is concerned, the 1: 1 process is favourable in enthalpic and entropic terms. As a result, a TTHCP has a higher affinity to complex with H_2PO_4^- in acetonitrile than for the fluoride anion. These results are relevant to Experimental Processes given that the waste processes of phosphoric acids produce untreated waste water containing large amounts fluoride leading to serious environmental problems therefore attempts to produce a material with selective properties may lead to a new approach for the separation of these two species. On this basis the possibility of using the phenol-formaldehyde reaction to synthesise a dimer or polymer was explored and the results are presented in the next Section

4.4 Polymerisation of *meso*-tetramethyl-tetrakis-(4-hydroxyphenyl ethyl) calix[4]pyrrole TTECP

The phenol-formaldehyde polymerisation is a well known reaction in Chemistry since over a century ago. Here the polymerisation of the calix[4]pyrrole derivative containing phenolic hydroxyl groups was polymerised in acidic media. FTIR and SEM (Fig. 4.9) analysis provide further addition to the experimental evidence like the change in color, solubility and the viscosity which confirmed the formation of the polymer. The polymer formed is not soluble in any organic solvent. It has a high porosity according to the SEM and the BET analysis. The difference between the FTIR spectra for the monomer and the polymer is a further evidence for the formation of the polymer, disappearance of the C-H stretching of the hydrogen neighbour to the hydroxyl of the phenolic ring is the remarkable difference between the two IR spectrums. As shown from XR-ray diffraction analysis (Fig. 4.10) results obtained also confirmed the porosity of the polymer. EDX and the microanalysis confirmed that the carbon C, hydrogen H and the nitrogen N, are the main elements in the polymer skeleton. It is found that the polymer formed contain sulphur Fig. 4.11 in addition to the main elements and this due to the use of sulphuric acid as a catalyst in the synthesis of the polymer and the presence of the catalyst as a pollutant with the polymer formed is considered an ordinary case due to the porosity of the polymer. The results obtained from BET analysis confirmed that the obtained polymer is porous with a surface area = $0.9 \pm 0.1 \text{ m}^2 \text{ gm}$ and the physico-chemical properties are shown in Table 4.4

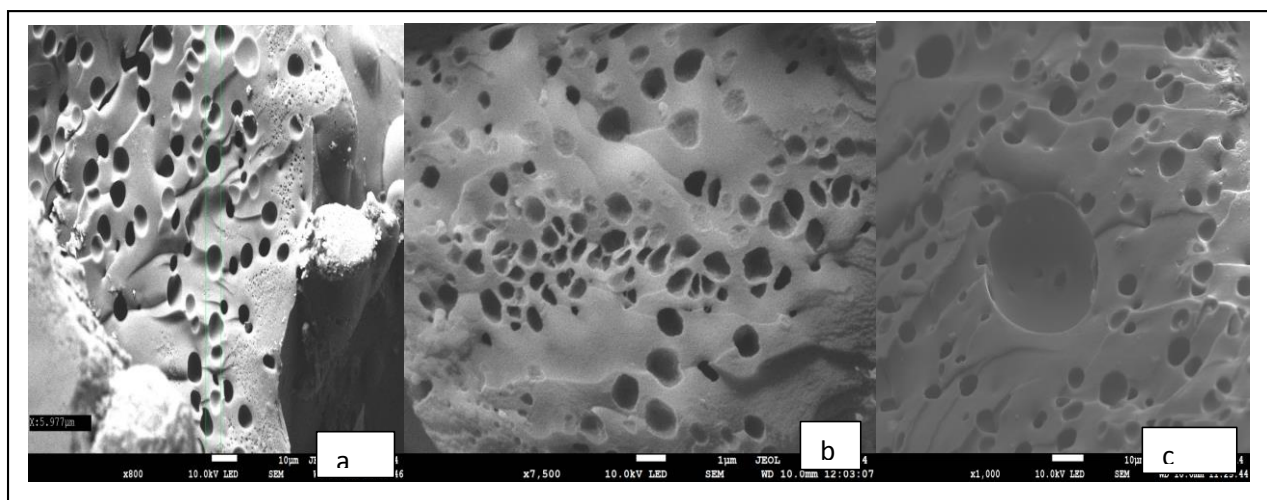


Fig. 4.9 SEM analysis for the polymer formed showing the porosity of the structure in different regions a, b and c.

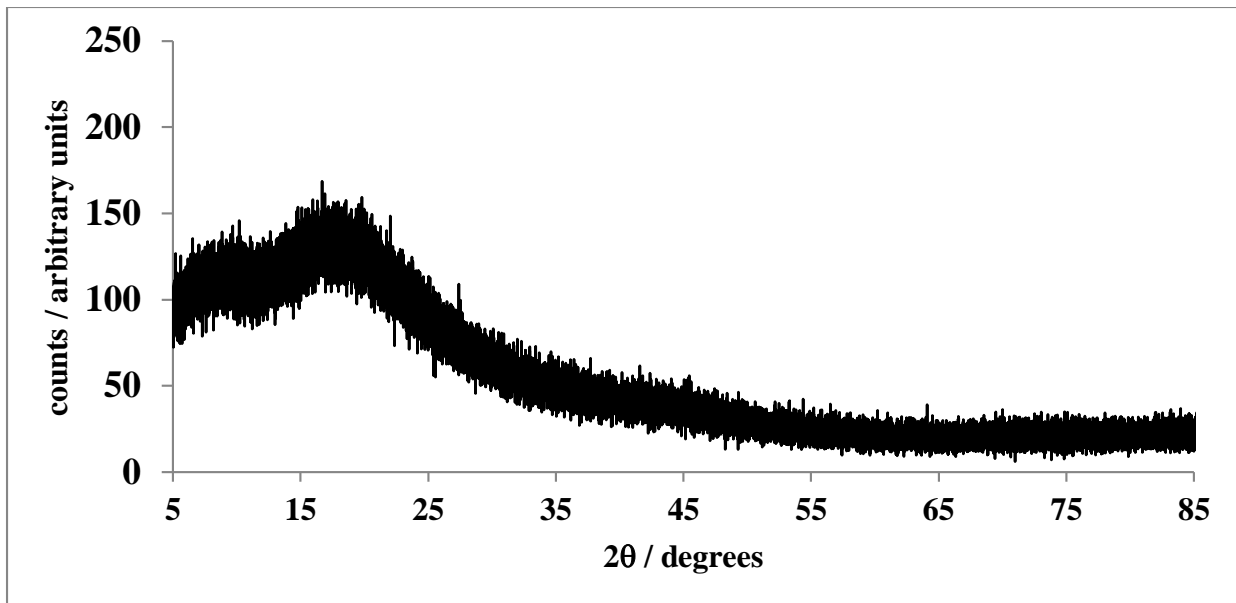


Fig. 4.10 Shows the X-Ray diffractogram of the sample. It is characteristic of an amorphous compound with little or no crystal structure

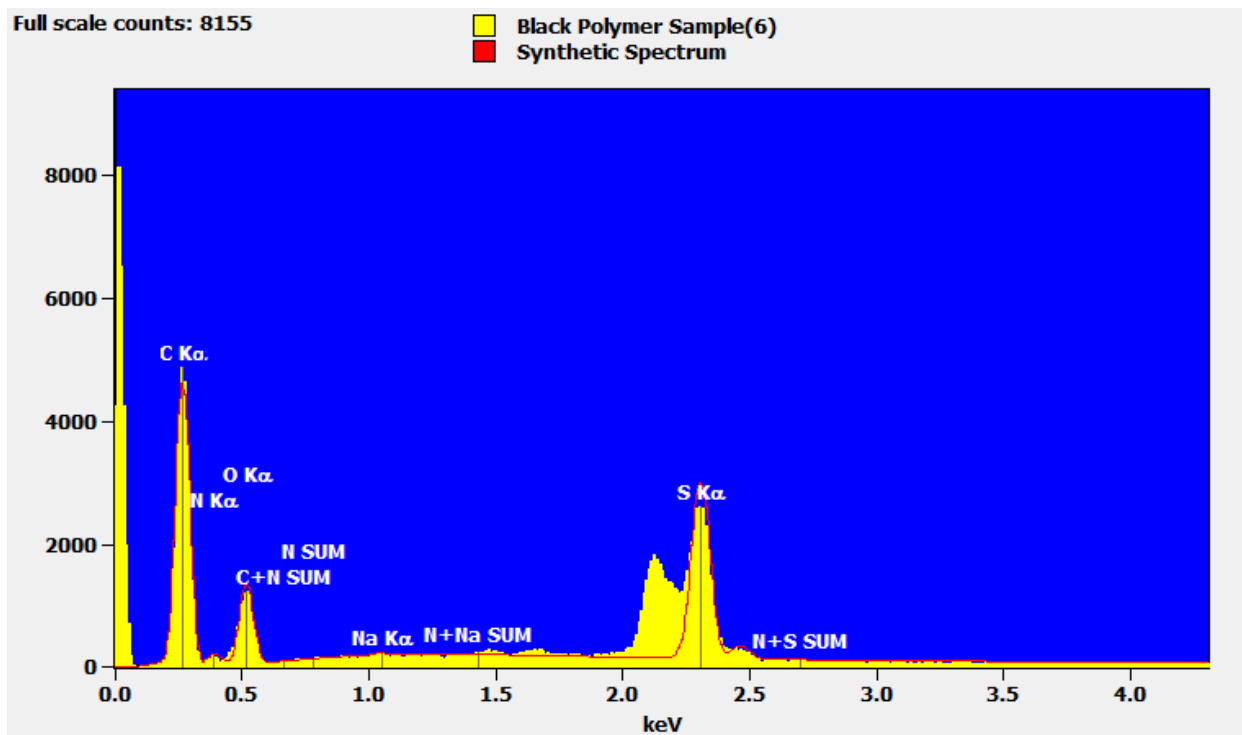


Fig. 4.11 EDS spectrum for the polymer formed

Table 4.4 Physical properties of the polymer obtained from BET analysis

Properties	Value
Sample density (g cm ⁻³)	1 g cm ⁻³
BET surface area (m ² g)	0.9016 ± 0.1036 m ² g
Molecular cross-sectional area/ nm ²	0.1620 nm ²

4.5 Characterisation of the novel *meso*-tetramethyl-tetrakis-[4-(oxyethylacetato)phenyl] ethyl calix[4]pyrrole TTECP

The addition of ester groups to the TTHCP is of interest due to their known affinity to complex with cations. It also makes the cavity of the functionalised calix[4]pyrrole deeper. The ¹H NMR spectrum of compound (Fig.4.12) indicated that the targeted compound in addition to ¹³C NMR, ¹³C DEPT and the microanalysis were obtained. It is clear from the spectrum that the compound differs from the TTHCP compound which is used in the synthesis of the TTECP. The single peak at 9.27 ppm refers to N-H protons, two peaks at 6.95 and 6.69 ppm correspond to the aromatic protons of the benzene rings, the two doublets at 5.7 and 5.68 ppm are assigned to the pyrrolic protons. A single peak at 4.7 ppm refers to the methylene next to the carbonyl group. A quartet peak at 4.14 ppm refers to the methylene protons and the triplet signal refers to the methyl protons (Table 4.5)

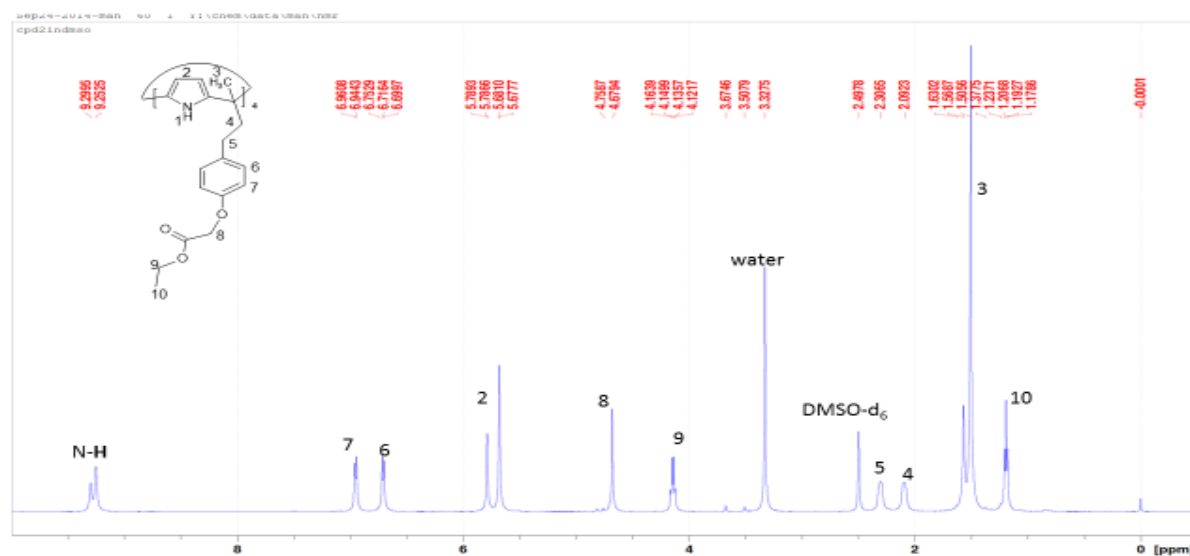


Fig. 4.12 ¹H NMR spectrum of *meso*-tetramethyl-tetrakis-[4-(oxy-ethylethanoato)-phenyl]ethyl calix[4]pyrrole TTHCP in DMSO-d₆ at 298 K

Table 4.5 Chemical shifts (δ_{ppm}) of different protons of the *meso*-tetramethyl-tetrakis-(4-ethylacetatophenoxyethyl) calix[4]pyrrole TTECP in DMSO- d_6 and CD $_3$ CN at 298 K

δ_{ppm} (DMSO- d_6)	Related proton	δ_{ppm} (CD $_3$ CN)	Related proton	$\Delta \delta$
1.19	Triplet (t, CH $_3$, 12 H)	1.28	(t, O-CH $_2$ -CH $_3$, 12 H)	0.09
1.58	Singlet (s, CH $_3$)	1.53	(t, CH $_3$, 12 H)	0.05
2.10	Triplet (t, C-CH $_2$)	2.1	(t, CH $_2$, 8 H)	0.00
2.30	Triplet (t, CH $_2$ -Ph)	2.3	(t, CH $_2$, 8 H)	0.00
4.14	Quartet (q, O-CH $_2$ -CH $_3$)	4.25	(q, O-CH $_2$, 8 H)	- 0.11
4.7	Singlet (s, O-CH $_2$ -CO)	4.54	(s, O-CH $_2$ -CO, 8 H)	0.16
5.68, 5.78	Doublet (dd, C-H) pyrrolic	5.95	(d, C-H) pyrrole ring	0.01
6.7	Doublet (H- <i>ortho</i> phenyl ring)	6.69	(d, H-Ortho, 8 H)	0.01
6.95	Doublet (H- phenyl ring)	6.91	(d, H- phenyl ring)	0.04
9.27	Doublet (N-H) pyrrole ring	7.03	(s, N-H) pyrrole ring	2.24

Before proceeding with the complexation with anions and the cations it's very important to study the solubility of the receptor in different organic solvents in order to select the appropriate medium for the complexation

4.5.1 Solubility measurements of *meso*-tetramethyl-tetrakis-(4-ethylacetatophenoxyethyl) calix[4]pyrrole (TTECP)

Solubility measurements were carried out to gain information about the solvation process and to select the appropriate solvent for next studies. From the solubility data obtained (Table 4.6) the standard solution Gibbs energy in the appropriate solvent was calculated. Using acetonitrile as a reference solvent to calculate the standard transfer Gibbs energy from acetonitrile to other solvents was calculated

Table 4.6 Solubility data for TTECP in different solvents at 298.15

Solvent	Solubility (mol dm ⁻³)	$\Delta_s G^\circ$ (kJ mol ⁻¹)	$\Delta_t G^\circ_{s_1 \rightarrow s_2}$ (kJ mol ⁻¹)
H ₂ O	Not soluble	-----	-----
MeCN	$(1.1 \pm 0.1) \times 10^{-2}$	11.1 ± 0.6	0.00
MeOH	$(4.5 \pm 0.4) \times 10^{-3}$	13 ± 2	1.90
EtOH	$(4 \pm 0.2) \times 10^{-3}$	14 ± 1	2.90
DMSO	solvation	-----	-----
DMF	solvation	-----	-----

The results show that TTECP is better solvated in acetonitrile than in alcohols

4.6 ¹H NMR complexation studies

Chemical shift of the TTECP receptor and chemical shift changes by the addition of anion salts (BU₄N as counter-ion) are shown in Table 4.7. The results shown in this Table reflect the significant chemical shift change observed by the addition of the fluoride salt to the receptor in a similar manner to that observed with the TTHCP receptor indicating that this anion interact with the –NH-protons of the pyrrole rings. This is again not the case for the H₂PO₄⁻ anion which seems to interact with the ester groups. A downfield shift is found in the aromatic protons.

Conductance measurements were carried out to identify the composition of the complex and these are now discussed

Table 4.7 Chemical shifts (δ_{ppm}) for the free calix[4]pyrrole tetraester receptor TTECP and its chemical shifts changes ($\Delta\delta_{\text{ppm}}$) as a result from complexation with the fluoride, phosphate, bromide (as tetra-n-butylammonium salts counter ion) anions in acetonitrile at 298 K

Related proton	δ_{ppm} (N-H)	δ_{ppm} (Ar-H _{meta})	δ_{ppm} (Ar-H _{ortho})	δ_{ppm} (C-H _{pyrrole})
Receptor proton	9.32	6.84	6.56	5.76
Rceptor + TBAF	13.2	6.7	6.52	5.46
$\Delta\delta$ ppm	3.78	-0.14	-0.04	-0.03
Receptor + TBAPh	9.31	6.78	6.69	5.79
$\Delta\delta$ ppm	0.01	-0.06	0.13	0.03
Recetor + TBABr	d (10.65)	7.4	6.74	5.67
$\Delta\delta$ ppm	1.33	0.56	0.18	-0.8

4.7 Conductance measurements for the complexation of *meso*-tetramethyl-tetrakis-[4-(oxy-ethylaethanoato) phenyl]ethylcalix[4]pyrrole (TTECP) with the halides and phosphate anions(tetra-*n*-butylammonium counter ion)

Given that in the ^1H NMR studies overlapping was found with the addition of chloride and bromide salts, chloride anion was tested by conductometry

4.7.1 Conductance measurements for the titration of TTECP with BU_4NF in acetonitrile at 298.15 K

Fig. 4.13 shows a plot of the molar conductance against the receptor: anion concentration ratio. A substantial decrease in conductance is observed from A to B as a result of complex formation. This is a size effect which decrease the mobility of the complex relative to the free anion. From B to C a slight increase in conductance is found due to a displacement of the equilibrium to the right in the presence of an excess of the receptor in this solvent.

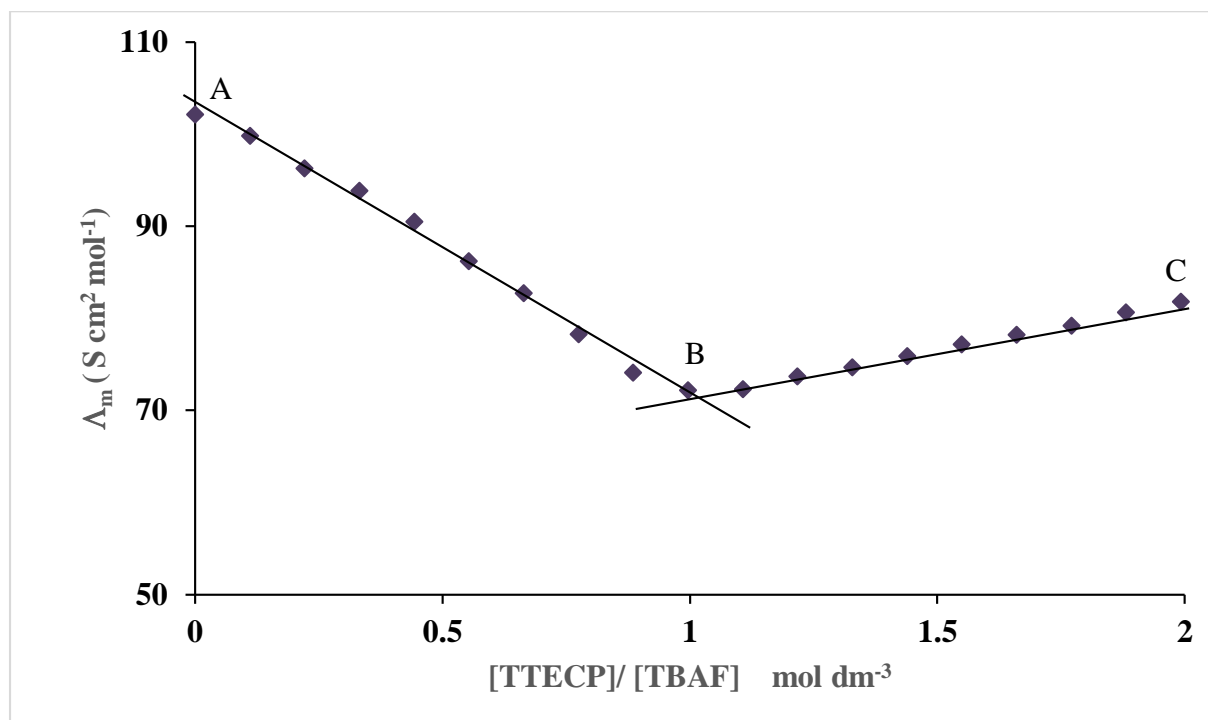


Fig. 4.13 Conductometric titrations of fluoride (BU_4N^+ as counter-ion) in acetonitrile with TTECP in acetonitrile at 298.15 K, $[\text{BU}_4\text{NF}]$ is $1 \times 10^{-4} \text{ mol dm}^{-3}$

4.7.2 Conductometric titrations of chloride (Bu_4N^+ as counter-ion) with TTECP in acetonitrile at 298.15 K

Fig. 4.14 shows a plot of the molar conductance against the receptor/ guest concentration ratios in acetonitrile. The pattern shown is typical of most systems involving macrocycles. The conductance decreases from A to B due to the lower mobility of the receptor-anion complex relative to the free chloride salt. The increase from B to C results from the addition of excess of TTECP which displaces the equilibrium to the right. The complex composition is 1: 1 (receptor: chloride). Therefore, the process taking place is represented by eq. 4.6

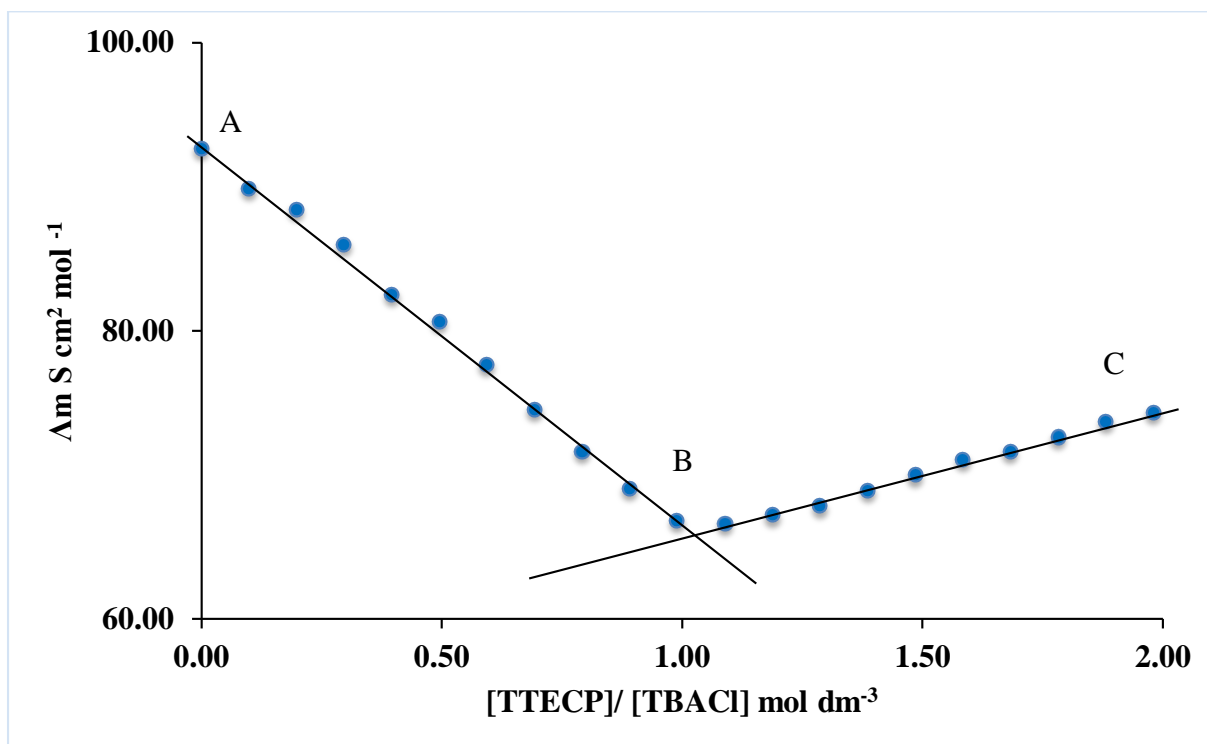


Fig. 4.14 Conductometric titration curve of TTECP against tetra-n-butylammonium chloride $\text{Bu}_4\text{NH}_2\text{Cl}$ solution ($1.09 \times 10^{-4} \text{ mol dm}^{-3}$) in acetonitrile at 298.15 K

4.7.3 Conductometric titration of tetra-n-butylammonium bromide (Bu_4NBr) with TTECP in acetonitrile at 298.15 K

It is clear from plot of changes in conductance values of Bu_4NBr as a result from the addition of the receptor solution TTECP in the same solvent (Fig. 4.15) that there is no significant change in conductivity values which mean that the free receptor is unable to capture the bromide anions which means that the coordination of bromide with Bu_4N^+ is more favourable than with the calix[4]pyrrole derivative

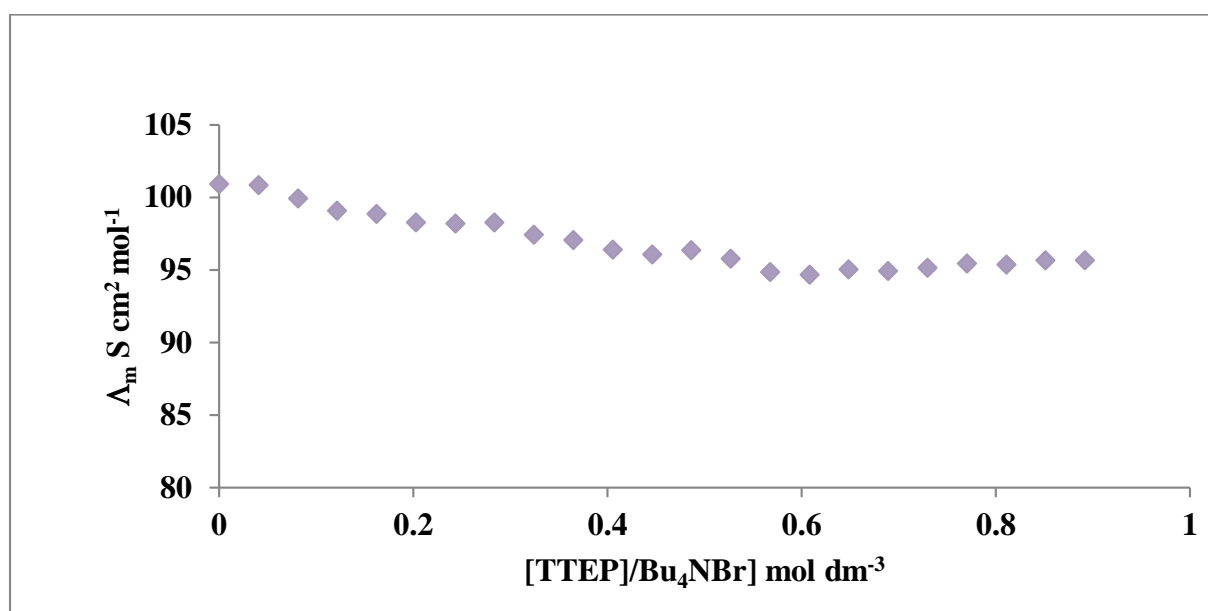
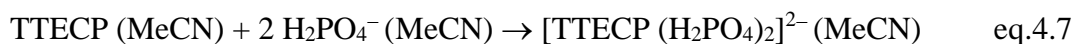


Fig. 4.15 Conductometric titration of tetra-n-butylammonium bromide ($1.48 \times 10^{-4} \text{ mol dm}^{-3}$) with TTECP in acetonitrile at 298.15 K.

4.7.4 Conductometric titration of tetra-n-butylammonium phosphate ($\text{Bu}_4\text{NH}_2\text{PO}_4$) with TTECP in acetonitrile at 298.15 K

As shown in Fig.4.16, the sharp break in conductance is found at the [receptor]/ $[\text{H}_2\text{PO}_4]^-$ concentration ratio of 0.5 which means that two anions are taking up per unit of receptor as shown in eq.4.7



On the basis of the conductometric studies, the hosting ability of TTECP is greater for H_2PO_4^- than for F^- and Cl^- anions

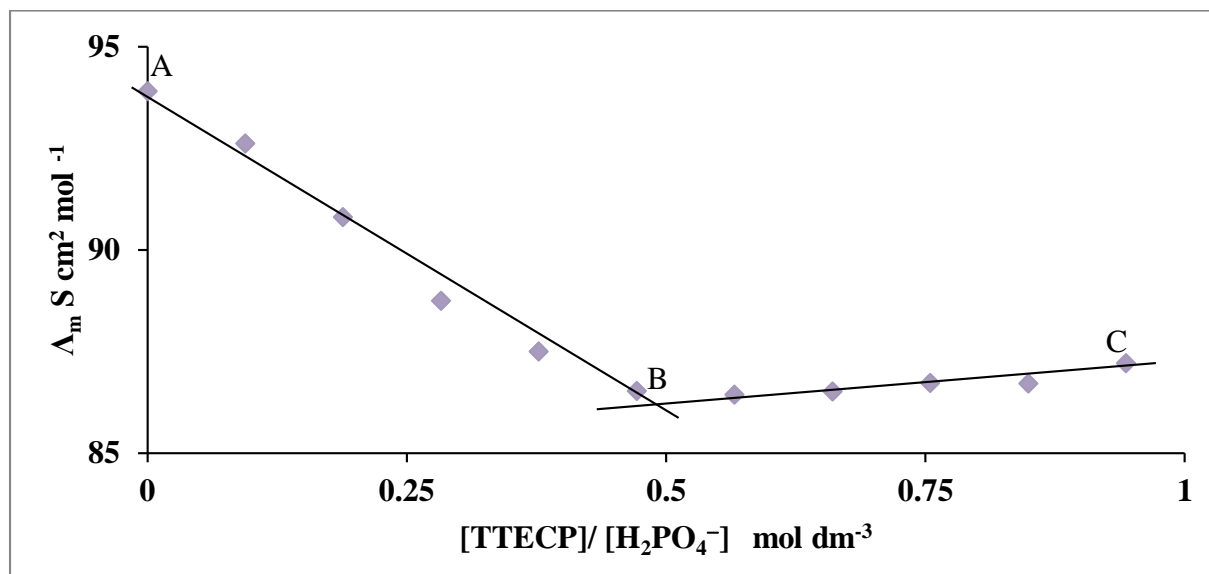


Fig. 4.16 Molar conductance of $\text{Bu}_4\text{NH}_2\text{PO}_4$ against the $[\text{TTECP}]/[\text{H}_2\text{PO}_4^-]$ in acetonitrile at 298.15 K, $[\text{Bu}_4\text{NH}_2\text{PO}_4]$ is $1 \times 10^{-4} \text{ mol dm}^{-3}$

4.7.5 Thermodynamic parameters of complexation of *meso*-tetramethyl-tetrakis-[4-(ethylacetatophenoxyethyl)calix[4]pyrrole TTECP with fluoride, bromide and anions (tetra-*n*-butylammonium as counter-ion) in acetonitrile at 298.15 K

Further investigations for the complexation of the TTECP with the halides and phosphate anions (tetra-*n*-butylammonium salts) were carried out by using isothermal titration calorimetry in acetonitrile at 298.15 K.

Titration calorimetry was the analytical method used to obtain the stability constant (expressed as $\log K_s$) and the enthalpy of complexation of TTECP and anions (F^- , Cl^- , Br^- and H_2PO_4^-) in acetonitrile at 298.15 K. For this receptor the isothermal titration calorimeter was used. Thermograms for F^- , Cl^- , Br^- and H_2PO_4^- and their interaction with TTECP are shown in Figs. 4.17- 4.20 respectively. Stability constants, standard Gibbs energies, enthalpies and entropies are listed in Table 4.8

As far as fluoride is concerned, the process is enthalpy and entropy favoured but enthalpy controlled. The strength of complexation of this receptor with chloride is approximately the same. The data suggest that TTECP is unable to recognise selectivity between these two anions. Again the process is enthalpy controlled. However, the stability of the bromide complex is lower. The enthalpy and entropy contribution are typical of most binding processes in that the loss of entropy results from the combination of two species (host and guest) to give one unit of the complex. The process is enthalpy controlled.

A different picture emerges with the complexation data involving the H_2PO_4^- anion. Thus the formation of the 1: 1 complex occurs with a gain in entropy, typical of processes in which strong desolvation, either of the host or the guest or both takes place. It seems that the entropic and enthalpic contribution to the stability of the complex is approximately the same. The entrance of a second anion to the receptor to form the 1: 2 (receptor: anion) causes conformational changes to keep the two anions as far apart as possible. This aspect and desolvation may be the roots of the high entropic contribution observed and the endothermic character of the reaction as observed from $\Delta_c H^\circ$ reported for this anion and this ligand in Table 4.8

In summary, TTECP has a high affinity for phosphate relative to the halides and shows high stability constant compared with most of calix[4]pyrrole derivatives prepared^{147,245}. In addition, the hosting ability of this receptor for the H_2PO_4^- is greater than that for the halides. It is therefore concluded that although this receptor is not able to distinguish between fluoride and chloride, in terms of the separation process between the former anion and phosphate, it seems to be more suitable than TTHCP due to the high affinity and high hosting capacity for the phosphate anion. Further experimental data in wastewater solutions containing both anions would be required to confirm the outcome of this thermodynamic study given that the kinetics of the process also play an important role in extraction process

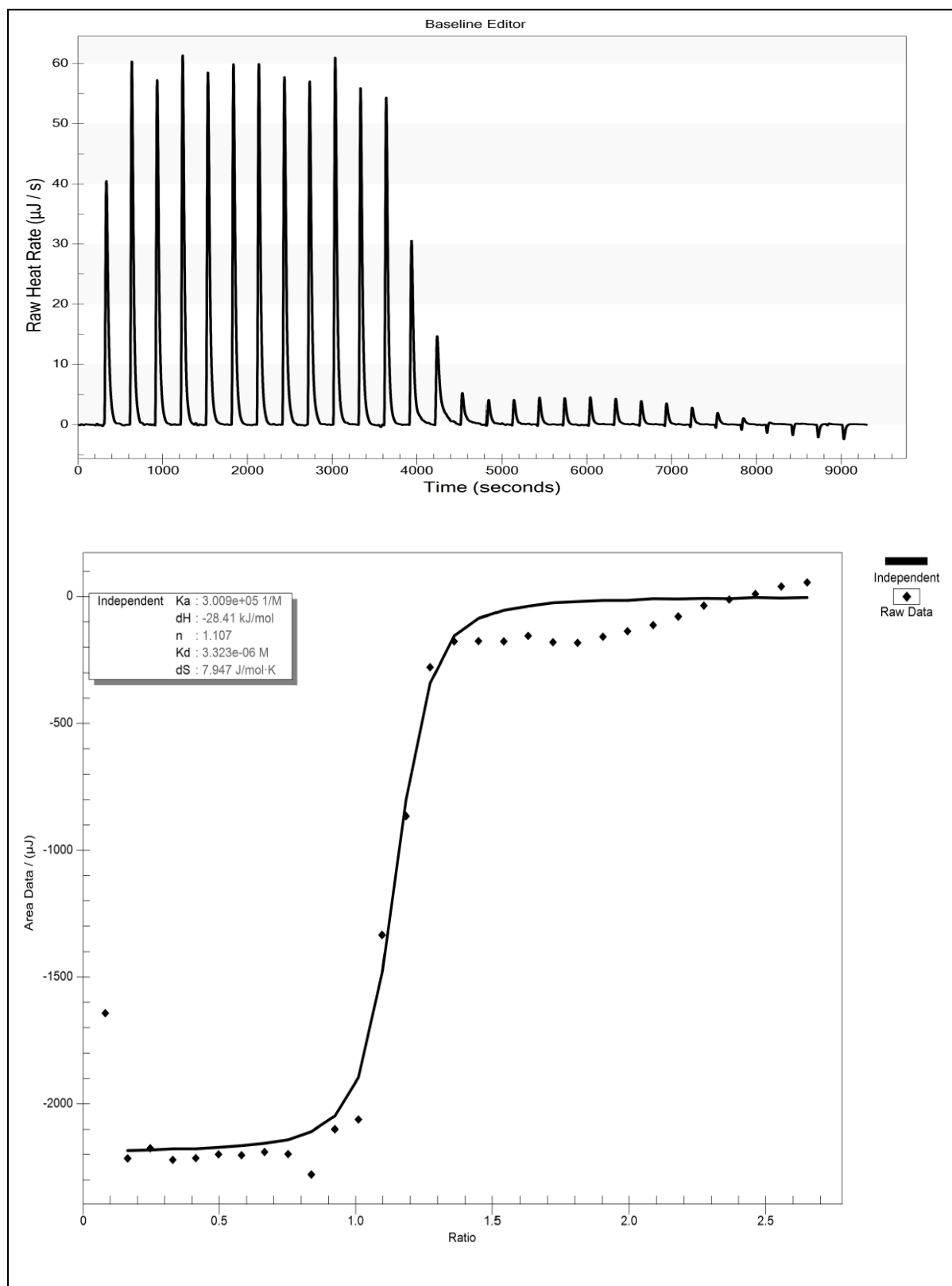


Fig. 4.17 Interaction of fluoride (tetrabutylammonium fluoride, Bu_4NF ($2 \times 10^{-2} \text{ mol dm}^{-3}$) as counter ion and CP-Tetraester in acetonitrile ($1 \times 10^{-3} \text{ mol dm}^{-3}$) at 298.15 K

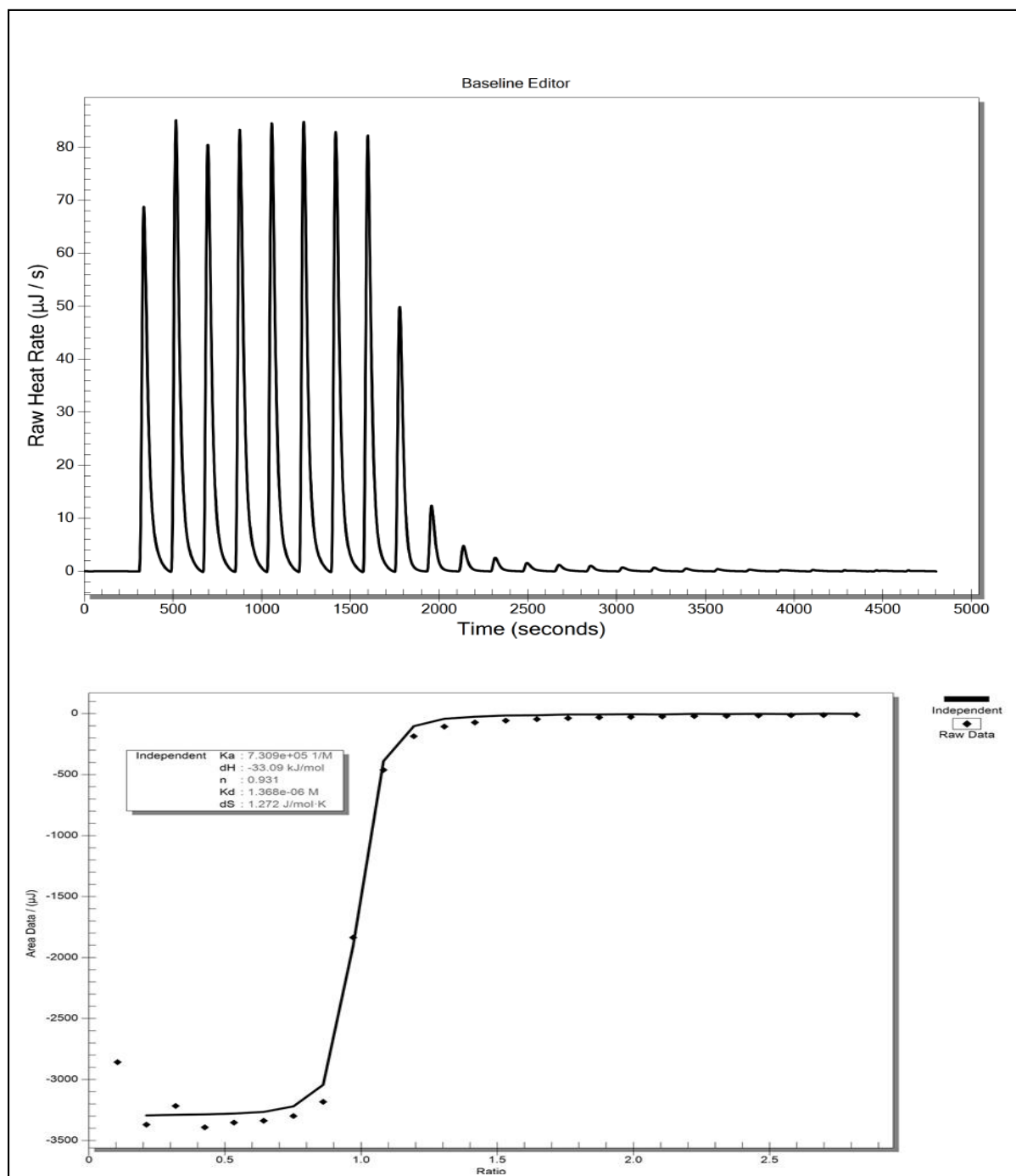


Fig. 4.18 Nano-isothermal titration calorimetry of the Interaction of CP-tetraester ($1 \times 10^{-3} \text{ mol dm}^{-3}$) with tetrabutylammonium chloride (Bu_4NCl) in acetonitrile ($2 \times 10^{-2} \text{ mol dm}^{-3}$) at 298.15

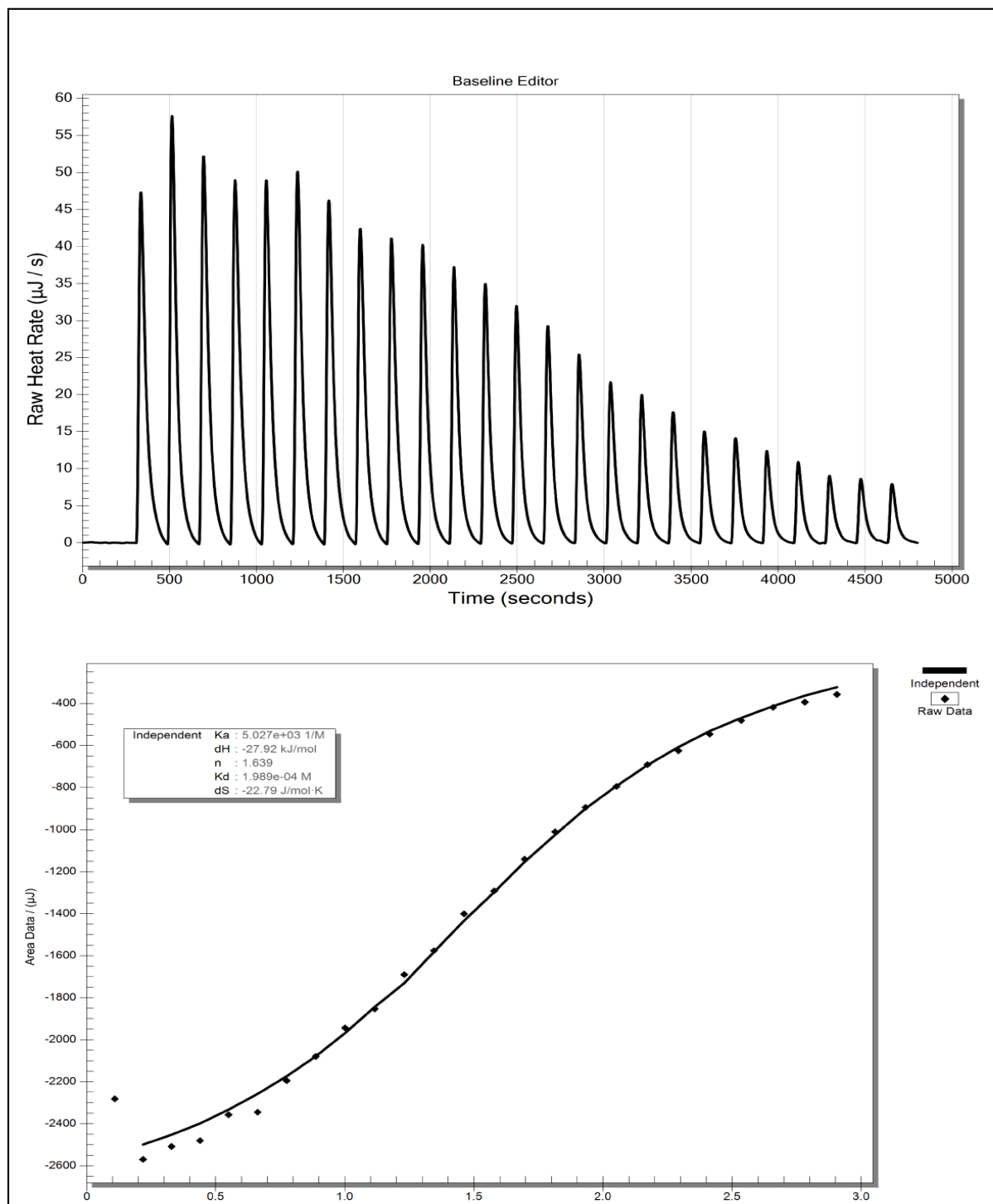


Fig. 4.19 Nano isothermal titration calorimetry for the interaction of the TTECP solution in acetonitrile ($1 \times 10^{-3} \text{ mol dm}^{-3}$) and tetra-*n*-butylammonium bromide (Bu_4NBr) in acetonitrile ($2 \times 10^{-2} \text{ mol dm}^{-3}$) at 298.15 K, top, is the baseline editor, and bottom is the titration curve.

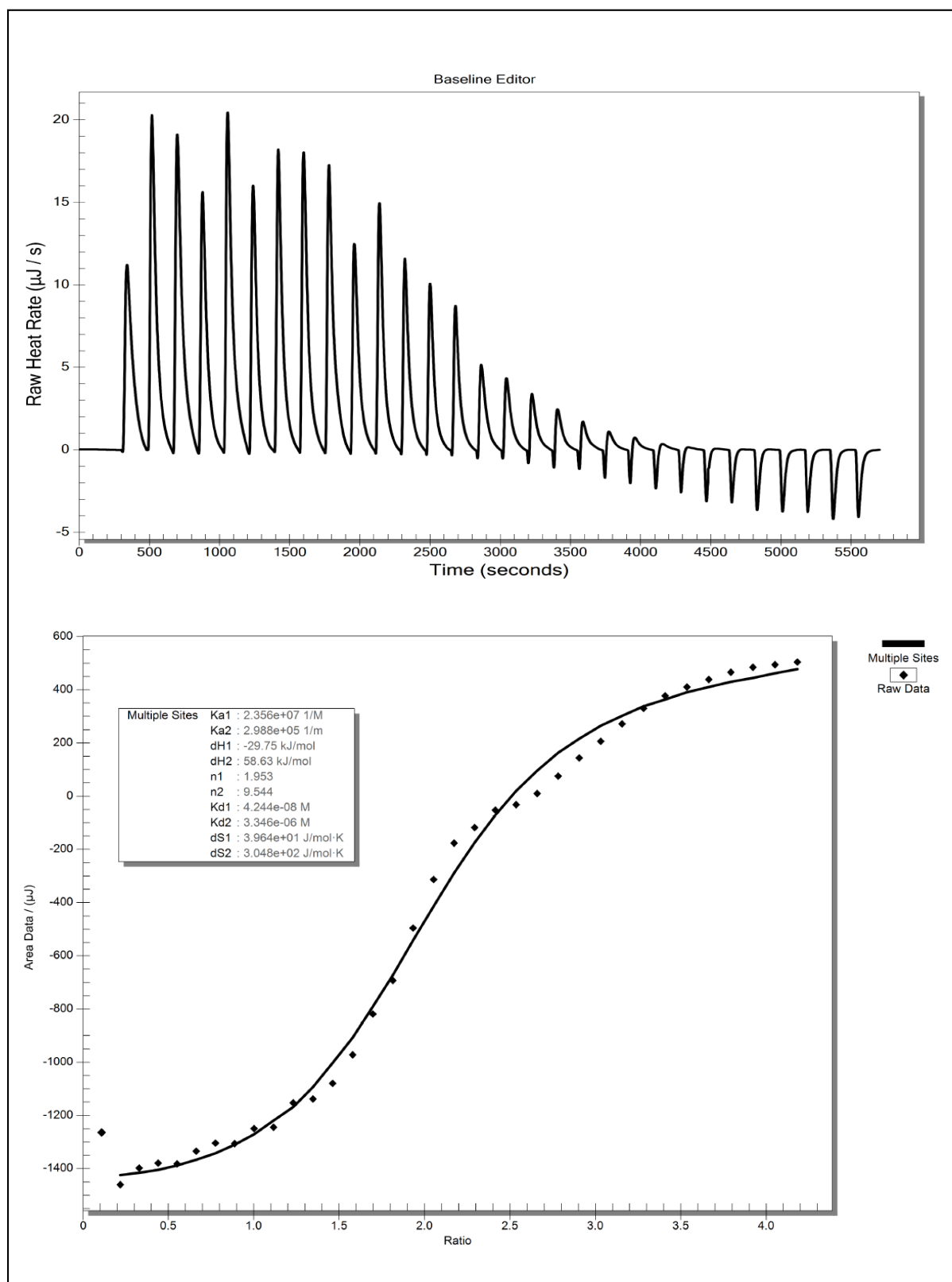


Fig.4.20 Nano ITC for the complexation of the Bu_4NPO_4 ($2 \times 10^{-2} \text{ mol dm}^{-3}$) and TTECP in acetonitrile ($1 \times 10^{-3} \text{ mol dm}^{-3}$) at 298.15 K

Table 4.8 The thermodynamic parameters for the interaction of calix[4]pyrrole ester [L] and phosphate, fluorid, chloride, as tetrabutylammonium counter ion in acetonitrile at 298.15 K

[Anion]/ [L]	log K_s	$\Delta_c H^\circ / \text{kJ. mol}^{-1}$	$\Delta_c G^\circ / \text{kJ mol}^{-1}$	$\Delta_c S^\circ / \text{J mol}^{-1}\text{K}^{-1}$
[H ₂ PO ₄] ⁻ / [L] 2: 1	log K_{s1} = 7.37 ± 0.03 log K_{s2} = 5.47 ± 0.02	$\Delta_c H^\circ_1 = -29.75 \pm 0.05$ $\Delta_c H^\circ_2 = 58.6 \pm 0.1$	$\Delta_c G^\circ_1 = -42.07 \pm 0.2$ $\Delta_c G^\circ_2 = -31.23 \pm 0.1$	$\Delta_c S^\circ_1 = 3.9 \times 10^1$ $\Delta_c S^\circ_2 = 3.1 \times 10^2$
[F] ⁻ / [L] 1: 1	log K_s = 5.48 ± 0.02	$\Delta_c H^\circ = -28.4 \pm 0.05$	$\Delta_c G^\circ = -31.26 \pm 0.1$	$\Delta_c S^\circ = 8$
[Cl] ⁻ / [L] 1: 1	log $K_s = 5.79 \pm 0.02$	$\Delta_c H^\circ = -33.8 \pm 0.06$	$\Delta_c G^\circ = -33.09 \pm 0.05$	$\Delta_c S^\circ = 1.99$
[Br] ⁻ / [L] 1: 1	log $K_s = 3.6 \pm 0.01$	$\Delta_c H^\circ = -27.9 \pm 0.05$	$\Delta_c G^\circ = -21.11 \pm 0.06$	$\Delta_c S^\circ = -23$

FINAL CONCLUSIONS

From the above discussion the following conclusions are drawn

A number of macrocycles have been synthesised and characterised by ^1H NMR and microanalysis. These are based on modified naturally occurring receptors such as cyclodextrins (heptakis-(6-chloro-6-deoxy)- β -cyclodextrin and heptakis-(2, 3, 6-tri-O-benzoyl)- β -cyclodextrin) and synthetic macrocycles such as calix[4]arenes (5, 11, 17, 23-*tert*-butyl-25, 26, 27, 28-(ethylacetatoethoxy)calix[4]arene, 5, 11, 17, 23 tetra-*p-tert*-butyl, 25, 27- bis[aminoethoxy], 26, 28 dihydroxycalix[4]arene, 25, 27-dihydroxy-26-28-(dioxypargyl) *tert*-butylcalix[4]arene, 4-*tert*-butyl-azidocalix[4]arene, 25, 26, 27, 28-(diethylamino) ethoxycalix[4]arene), calix[4]pyrroles (*meso*-tetramethyl-tetrakis-(4-hydroxyphenyl ethyl) calix[4]pyrrole, *meso*-tetramethyl-tetrakis-(4-ethylacetatophenoxyethyl) calix[4]pyrrole), resorc[4]arene (C-pentyl-resorc[4]arene, C-pentylresorci[4]arene ester) and pyrogallol[4]arene (C-decyl pyrogallol[4]arene and C-4-aminophenyl pyrogallol[4]arene).

The solution properties (solubility and derived Gibbs energies of solution) for some drugs (sodium diclofenac and carbamazepine) have been investigated and the transfer Gibbs energies from a reference solvent (acetonitrile) to other solvents have been calculated in an attempt to obtain information regarding the differences in the solvation of these drugs in moving from one solvent to another. In the derivation of solution Gibbs energies particular attention was paid to the speciation present in solution. Thus sodium diclofenac was treated as a fully dissociated electrolyte in water and fully associated in solvents of low permittivity. Carbamazepine was considered to be fully associated in non-aqueous solvents. Partition coefficients were determined for diclofenac, chlorofibric acid and carbamazepine in the water-1-octanol solvent system at 298.15 K and the results were compared with literature data. For new receptors such as *meso*-tetramethyl-tetrakis-(4-hydroxyphenyl ethyl) calix[4]pyrrole and *meso*-tetramethyl-tetrakis-(4-ethylacetatophenoxyethyl) calix[4]pyrrole the solution properties showed that as for other calix[4]pyrrole derivatives these are not water soluble.

From all receptors synthesised, *per*-benzoylated cyclodextrin and calix[4]arene ester were selected for interaction with sodium diclofenac. The latter receptor was selected for interaction with sodium

diclofenac, due to the selectivity of the calix[4]arene ester derivative for the sodium cation. Given that this is a neutral receptor, cation and anion are taken simultaneously, to keep the neutrality of the system. Thermal analysis was the approach taken to assess the stability of the receptor, the drugs and the complex.

P-tert-butylcalix[4]arene amine CA-(NH₂)₂ was the receptor selected for further studies involving drugs (aspirin, clofibric acid, diclofenac, sodium diclofenac and ibuprofen). The 3-aminopropyl functionalised silica gel was used for the removal of aspirin from water.

Extraction experiments involving a solid phase (the free receptor) and the drug in aqueous medium were accomplished under different experimental conditions to determine the optimal conditions for the removal of the drug from water. It was found that the calix[4]arene ester was able to remove 0.2 mmol of the drug from aqueous solution per gram of receptor. As far as the modified cyclodextrin is concerned, the stability constant of the receptor-drug (sodium diclofenac) interaction was relatively low and the receptor have showed high hydrophobicity and the aggregation of the compound in the aqueous media prevent the progress with the extraction process. As far as clofibric acid, diclofenac, aspirin and ibuprofen are concerned, the presence of carboxylic groups in their structure led to the choice of the partially functionalised calix[4]arene amine derivative (5, 11, 17, 23 tetra-*p-tert*-butyl, 25, 27- bis[aminoethoxy], 26, 28 dihydroxycalix[4]arene) as a suitable receptor for these drugs. Several techniques were used to determine qualitatively and quantitatively the extent of interaction of these drugs with this receptor. Striking results were obtained. Thus the receptor was able to host two units of the drug per unit of receptor in the case of clofibric acid and diclofenac, while the capacity of the receptor was lower for aspirin, only a unit of this drug was taken up per unit of calix[4]arene amine. The selectivity behaviour of the calix[4]arene amine derivative for the drugs was demonstrated through the thermodynamics associated with protonation process.

.It is concluded that the receptor is able to recognise selectively these drugs in the following sequence based on the formation of host 1- complexes

Clofibric acid > Diclofenac > aspirin

Therefore this receptor has an enhanced capacity for clorofibric acid and diclofenac but in addition it fulfils the concept of selectivity, one of the main features of Supramolecular Chemistry. The application of this receptor for the removal of some drugs from water was investigated showing that 0.2 mmol of clofibric acid can be removed from water. Given that the removal of aspirin from water

by the calix[4]arene amine derivative was rather low, the 3-aminopropyl functionalised silica gel was used for the removal of aspirin from water. The optimal extraction conditions were determined.

For carbamazepine, the receptor found to interact with this drug was C-decylpyrogallol[4]arene and significant changes in the physico-chemical properties was observed.

For the novel calix[4]pyrrole receptor TTHCP affinity to complex with the fluoride and phosphate (tetrabutylammonium counter ion) and stable complexes were formed and high value for stability constant with phosphate was determined compared with fluoride.

Also the functionalisation of TTHCP with ester groups led to the production of a new receptor, TTECP, which shows a higher hosting affinity for the dihydrogen phosphate anion as well as a higher affinity for this anion relative to fluoride.

In real water samples, the materials need to be tested and some of the steps to be taken are briefly addressed (i) Sampling: sampling should be representative of the source of water under study. Several sampling methodologies have been reported in the literature, including frequency of sampling. Storage of samples needs to be considered and this would depend on the type of the analysis to be carried out (microbiological or physico-chemical analysis). Within the context of this work, physico-chemical analysis is the issue to address and it is important to emphasise that this type of analysis requires the availability of properly collected and stored samples otherwise the results are not meaningful. The amount of residual chlorine, pH and the turbidity should be determined immediately after sampling otherwise changes are found with time, (ii) Physico-chemical analysis: This process include: (a) Chlorine removal

Treatment with chlorine is the main disinfecting agent employed. Chlorine has low cost, it is efficient and easy to measure in the laboratory or “*in situ*”. Samples should be analysed for chlorine by the recommended methods

(b) pH measurements

Disinfection by chlorine requires a pH lower than 8, otherwise, disinfection is not effective. The pH can be measured ‘*in situ*’ with the appropriate electrodes

(c) Turbidity

Visual methods employing extinction are adequate

d. Analysis of samples

Analysis to test the presence of health pollutants such as heavy metals, fluoride as well as pesticides and pharmaceuticals should be carried out. For the determination of heavy metals, atomic absorption and ICP/ MS techniques can be used. Anions can be analysed by ion chromatography. For pesticides and pharmaceuticals, spectrophotometric techniques can be used. Interfering anions and cations may be removed. Materials reported in this thesis are to be tested for the removal of drugs from water under several experimental conditions discussed in this thesis (mass of the receptor, temperature, concentration of the pharmaceutical, pH, presence of interfering ionic and neutral species)

Suggestions for further work

Suggestions for further research include

A comprehensive study on calix[4] resorcarene derivatives covering interactions with neutral and ionic species in solution using NMR technique, electrochemical and thermal techniques. On the basis of fundamental studies attempts should be made to immobilise these receptors into solid supports and to proceed with an investigation of their extraction properties with the aim of obtaining easily recyclable materials for decontamination purposes as well as the use of these receptors for the design of ion selective electrodes. In this area significant advances have been already made with the use of calix[4] pyrrole derivatives as recently discussed by Danil de Namor and co-workers

Further research is required on the receptors discussed in this thesis, mainly on the calix[4]pyrrole derivatives and their interactions with cations particularly for those ligands for which preliminary work has demonstrated that cation-ligand interactions take place in solution

Expansion of this work by the use of Scanning Electron Microscopy to get insight on the surface characteristics of materials based on these receptors as well as Energy Dispersive X-ray Analysis to find the composition of membranes used for the design of ion selective electrodes. There is already work undergoing in the Thermochemistry Laboratory as well as in other Laboratories linked to Thermochemistry regarding the use of these techniques.

Testing these compounds under real situations is another issue which needs to be addressed

References

1. J. Steed and J. Atwood, *Supramolecular Chemistry*, John Wiley & Sons, **2009**
2. F. Davis and S. Higson, *Macrocycles: Construction, Chemistry and Nanotechnology Applications*, John Wiley & Sons, **2011**
3. P. Ehrlich, *Studies on Immunity*. Wiley: New York, **1906**.
4. A. Werner, *Chymia*, **1967**, 12, 221-232.
5. E. Fischer, *Ber. Deutsch. Chem. Ges.*, **1894**, 3, 2985-2993
6. C. J. Pedersen, *J. Am. Chem. Soc.*, **1967**, 89, 7017–7036.
7. C. J. Pederson, *J. Am. Chem. Soc.*, **1970**, 92, 386-391
8. J. M. Lehn, *J. Am. Chem. Soc.*, **1978**, 11(2), 49-57
9. J. M. Lehn, *Chem. Soc. Rev.*, **2007**, 36, 151–160
10. B. Dietrich, J.M. Lehn, J. Sauvage, *Tetrahedron*, **1973**, 29, 1647-1658
11. D. J. Cram, J. Cram, *Container Molecules and their Guests*, RSC, Cambridge, **1994**
12. D. J. Cram and J. M. Cram, *Science*, **1974**, 183, 803-809.
13. J. Szejtli, *Chem. Rev.*, **1998**, 98, 1743-1753.
14. Z. Pikramenou, J. Yu., R. Lessard, A. Ponce, P. Wong and D. Nocera, *Coord. Chem. Rev.*, **1994**, 132, 181-194
15. J. M. Lehn, *Angew. Chem., Int. Engl.*, **1988**, 27, 444-491.
16. P. Garratt, A. Ibbett, J. Ladbury, R. O'Brien, M. Hursthouse and K. Abdul Malik, *Tetrahedron*, **1998**, 54, 949-968
17. Y. Liu, B. Han, Ai-Di Qi and T. Rong, *Bioorg. Chem.*, **1997**, 25, 155–162.
18. R. Izatt, K. Pawlak and J. Bradshaw, *Chem. Rev.*, **1991**, 91, 1721-2085

-
19. J. M. Lehn, *Supramolecular Chemistry, Concepts and Perspectives*, Wiley-VCH: Weinheim, **1999**
20. A. F. Danil de Namor, L. Ghouseini, *J. Chem. Soc. Faraday Trans., I*, **1984**, 80, 2843-2849
21. A. F. Danil de Namor, L. Ghouseini, W. Lee, *J. Chem. Soc. Faraday Trans.*, **1985**, 81, 2495-2502
22. A. F. Danil de Namor, L. Ghouseini, T. Hill, *J. Chem. Soc. Faraday Trans.*, **1986**, 82, 349-357
23. A. F. Danil de Namor, *J. Chem. Soc. Faraday Trans.*, **1988**, 84, 2441-2444
24. A. F. Danil de Namor, D. Kowalska, *J. Phys. Chem.*, **1997**, 101, 1643-1648
25. A. F. Danil de Namor, M. Tanco, M. Salomon, C. Ng, *J. Phys. Chem.*, **1994**, 98, 11796-11802
26. A. F. Danil de Namor, C. Ng, M. Tanco, M. Salomon, *J. Phys. Chem.*, **1996**, 100, 14485-14491
27. A. F. Danil de Namor, P. Blackett, M. Cabaleiro, J. Al-Rawi, *J. Chem. Soc., Faraday Trans.*, **1994**, 90, 845-847
28. W. Saenger, *Angew. Chem., Int. Ed. Engl.*, **1982**, 19, 344-362
29. L. Tan and Y. Yang, *J Incl Phenom Macrocycl Chem.*, **2015**, 81, 13-33
30. S. Gutokturk, E. Caliskan, R. Y. Talman, U. Var, *Sci. World. J.*, **2012**, 1, 1-12
31. M. Albelda, J. Frías, E. García, H. Schneider, *Chem. Soc. Rev.*, **2012**, 41, 3859-3877
32. A. F. Danil de Namor and M. Shehab; *J. Phys. Chem. B*, **2005**, 109, 17440-17444
33. Q. Guo, H. Qian, and Y. Liu, *Eur. J. Org. Chem.* **2012**, 3962-3971
34. C. Daughton, T. Ternes, *Environ. Health Perspect.* **1999**, 107, 907-938
35. B. Sorenson, S. Nielsen, P. Lanzky, F. Ingerslev, H. Lützhof, S. Jorgensen, *Chemosphere*, **1998**, 36, 357-393

-
36. T. Ternes, M. Stumpf, J. Mueller, K. Haberer, M. Servos, R. Wilken, *J. Sci. Total Environ.*, **1999**, 225(1-2), 81-90.
37. T. Heberer, *Toxicol. Lett.*, **2002**, 131, 5-17.
38. M. Winkler, J. Lawrence and T. Neu, *Wat. Res.*, **2001**, 35, 3197-3205.
39. M. Stump, T. Ternes, R. Wilken, S. Rodrigues, W. Baumann, *J. Sci. Total Environ.*, **1999**, 225,135-141
40. J. Fick, R. Lindberg, M. Tysklind, D. Larsson, *Regul. Toxicol. Pharm.*, **2010**, 58, 516-523
41. C. Adams, Y. Wang, K. Loftin and M. Meyer, *J. Environ. Eng.*, **2002**, 253-260
42. T. Ternes, M. Meienheimer, D. McDowell, F. Sacher, H. Brauch, B. Guide, G. Preuss, U. Wilme and N. Seibert, *Environ. Sci. Technol.*, **2002**, 36, 3855-3863
43. M. Bueno, S. Ulses, M. Hernando, E. Davoli, A. Fernandez- Alba, *Water. Res.*, **2011**, 45, 2331-2341.
44. J-Q. Jiang, Z. Zhou, *Plos One*, **2013**, 8(2), e 55729, 1-10
45. Z. Zhou, J-Q. Jiang, *J. Pharm.Biomed. Anal.*, **2014**, July 1.
46. Z. Zhou, J-Q Jiang, *Chemosphere*, **2015**,119, S95-S100
47. H. Zhang, Lei Ye and K. Mosbach, *J. Mol. Recognit.* **2006**, 19, 248–259, (b) L. Andersson, R. Müller, G. Vlatakis, and K. Mosbach, *Proc. Natl. Acad. Sci. USA*, **1995**, 92, 7488-7492
48. J. Liu and G. Wulff, *Angew. Chem. Int. Ed.*, **2004**, 43, 1287-1287
49. G. Vasapollo, R. Del Sol, L. Mergola, M. Lazzoi, A. Scardino, S. Scorrano and G. Mele, *Int. J. Mol. Sci.*, **2011**, 12, 5908-5945
50. C. Dai, S. Geissen, Y. Zhang, Y. Zhang, X. Zhou, *Environ. Pollut.*, **2011**, 159, 1660-1666

-
51. C. Dai, J. Zhang, Y. Zhang, X. Zhou, Y. Duan, S. Liu, *Chem. Eng. J.*, **2012**, 211-212, 302-309
52. C. Cacho, E. Turiel, A. Esteban, C. Cond and C. Camara, *Anal Bioanal Chem.*, **2003**, 376, 491-496
53. J. Rane, P. Adhikar and R. Bakal, *AJPTI*, **2015**, 3(11), 75-91
54. A. Hargrove, S. Nieto, Tianzhi Zhang, J. Sessler, and E. Anslyn, *Chem. Rev.*, **2011**, 111, 6603–6782
55. (a) M. Ludlow¹, G. Luxton and T. Mathew, *Nephrol Dial Transplant*, **2007**, 22, 2763–2767
(b) C. Douglass and K. Joshipura, *Canc. Causes Cont.*, **2006**, 17, 481–482
56. J. Song, Y. Park, J. Hyun and J. Kim *Anticancer Res.*, **2005**, 25, 391-396
57. E. Everett, *J Dent Res.*, **2011**, 90(5), 552-560
58. B. Cox, H. Schneider, *Coordination and Transport Properties of Macrocyclic Compounds In Solution*, Elsevier, New York, **1992**
59. T. Loftsson, M. E. Brewster, *J. Pharm. Sci.*, **1996**, 85, 1017-1025
60. R. Breslow, S. Dong, *Chem. Rev.*, **1998**, 98, 1997-2011.
61. P. Liu, P. Neuhaus, D. Kondratuk, T. Balaban and H. Anderson, *Angew. Chem. Int. Ed.*, **2014**, 53, 7770-7773
62. M. Komiyama and H. Hirai, *Polymer J.*, **1981**, 13(2), 171-173
63. P. Fügedi, P. Nanasi, *Carbohydr. Res.*, **1988**, 175, 173-179
64. R. Breslow, *Pure & Appl. Chem.*, **1994**, 66, 1573-1582
65. A. Ueno, R. Breslow, *Tetrahedron Lett.*, **1982**, 23, 3451-3454
66. J. Iwai, N. Ogawa, H. Nagase, T. Endo, T. Loftsson and H. Ueda, *J. Pharm. Sci.*, **2007**,

- 96, 3140-3143.
67. K. Hirose, *J. Incl. Phenom. Macrocycl. Chem.*, **2001**, 39, 193–209
68. R. Singh, N. Bharti, J. Madan, S. Hiremath, *J. Pharm. Sci. and Technol.*, **2010**, 2, 171-183
69. O. Aslanoff, Y. Bleriot, R. Velty, M. Sollogoub, *Org. Biomol. Chem.*, **2010**, 8, 3437-3443
70. P. Shahgaldian and U. Pieleles, *J. Sensors* **2006**, 6, 593-615
71. H. Zhou, G. Su, P. Jiao and B. Yan, *Chem. Eur. J.*, **2012**, 18, 5501 – 5505
72. K. Kano and Y. Ishida, *Angew. Chem. Int. Ed.*, **2007**, 46, 727 –730
73. A. F. Danil de Namor, R. Traboulssi and D. Lewis, *J. Am. Chem. Soc.*, **1990**, 112, 8442-8447
74. H. Hammud, A. F. Danil de Namor, A. Falah, N. Yahfoufi, *Can. J. Chem. Eng. & Technol.*, **2011**, 2, 171-175.
75. Y Liu, B. Han, S. Sun, T. Wada and Y. Inoue, *J. Org. Chem.*, **1999**, 64, 1487-1493
76. K. Gong. H. Wang, X. Ren, Y. Wanga and J. Chen, *J. Green Chem.*, **2015**, 1-7
77. H. Yan, L. Zhu, X. Li, A. Kwok, X. Pan, Y. Zhao, *Asian J. Org. Chem.*, **2012**, 1, 314-318
78. Y. García, J. Zelenka, Y. Pabon, A. Iyer, M. Buděšínský, T. Kraus, C. Smith and A. Madder, *J. Org. Biomol. Chem.*, **2015**, 13, 5273-5278
79. C. J. Pederson, *J. Org. Chem.*, **1971**, 36, 254-257
80. G. Wu, W. Jiang, J. Lamb, J. Bradshaw and R. Izzat, *J. Am. Chem. Soc.*, **1991**, 113, 6538-6541
81. R. Izatt, K. Pawlak, and J. Bradshaw, *Chem. Rev.*, **1991**, 91, 1721-2085
82. E. Kyba, R. Helgeson, K. Madan, G. Gokel, T. Tarnowski, S. Moore, and D. Cram, *J. Am. Chem. Soc.*, **1977**, 99(8), 2564-2571
83. J. de Boer, D. Reinhoudt, S. Harkema, G. Hummekt and F. de Jongs, *J. Am. Chem. Soc.*, **1982**,

4075-4079

84. A. F. Danil de Namor and M. C. Ritt, *J. Chem. Soc. Faraday Trans.*, **1991**, 87, 3232-3239
85. Y. Ma, T. Marszalek, Z. Yuan, R. Stangenberg, W. Pisula, T. Chen and K. Müllen, *Chem. Asian J.*, **2015**, 10, 139-143
86. J. Zolgharnein, G. Shahmoradi, K. Zamani and S. Amani, *J Incl. Phenom. Macrocycl. Chem.*, **2007**, 59, 99-103
87. A. Blake, R. Donamaría, V. Lippolis, J. de-Luzuriaga, E. Manso, M. Monge, and M. Olmos, *J. Inorg. Chem.*, **2014**, 53, 10471-10484.
88. B. Dietrich, M. Hosseini, J. M. Lehn, and R. Sessions, *J. Am. Chem. Soc.*, **1981**, 103, 1282-1283
89. A. F. Danil de Namor and L. Ghousseini, *J. Chem. Soc. Faraday Trans I*, **1985**, 81, 781-791
90. B. Sui, X. Yue, M. Tichy, T. Liu, and K. Belfield, *Eur. J. Org. Chem.*, **2015**, 1189-1192
91. D. Cram and G. Lein, *J. Am. Chem. Soc.*, **1985**, 107(12), 3657-3668
92. R. Helgeson, B. Selle, I. Goldberg, C. Knobler and D. Cram, *J. Am. Chem. Soc.*, **1993**, 115, 11506-11511
93. D. J. Cram, J. Moran, E. Maverick, and K. Trueblood, *J. Chem. Soc. Chem. Commun.*, **1983**, 12, 645-646
94. T. Ogoshi, S. Kanai, S. Fuginami, T. Yamagishi, Y. Nakamoto, *J. Am. Chem. Soc.*, **2008**, 130, 5022-5023
95. T. Ogoshi and T. Yamagishi, *Eur. J. Org. Chem.* **2013**, 2961–2975
96. B. Gomez, V. Francisco, F. Nieto, L. Rio, M. Pastor, M. Paleo and F. Sardina, *Chem. Eur J.*, **2014**, 20, 12123-12132

-
97. Q. Wang, M. Cheng, Y. Zhao, L. Wu, J. Jiang, L. Wang and Y. Panb, *J. Chem. Soc. Chem. Commun.*, **2015**, 51, 3623-3626
98. R. Milev, A. Pacheco, I. Nierengarten, T. Trinh, M. Holler, R. Deschenaux and J. Nierengarten, *Eur. J. Org. Chem.*, **2015**, 479-485
99. H. Li, Q. Chen, C. Schönbeckab and B. Han, *RSC. Adv.*, **2015**, 5, 19041-19047
100. C. D. Gutsche, *Calixarenes an Introduction, Monographs in Supramolecular Chemistry*, 2nd Ed., J. Stoddart, *Royal Society of Chemistry*, London, **2008**.
101. *Calixarenes. A Versatile Class of Macrocyclic Compounds*, Eds. J. Vicens and V. Bohmer, Kluwer Academic, Dordrecht, **1991**
102. *Calixarenes 2001*, Z. Asfari, V. Böhmer, J. Harrowfield and J. Vicens, Kluwer Academic Publisher Dordrecht, **1994**
103. C. D. Gutsche, *J. Org. Chem.*, **1982**, 47, 2708-2712
104. A. F. Danil de Namor, R. Cleverly and M. Ormachea, *Chem. Rev.*, **1998**, 98, 2495-2525
105. L. Groenen, D. Loon, W. Werboom, S. Harkema, A. Casnati, R. Ungaro, F. Ugozzoli, D. Reinhoudt, *J. Am. Chem. Soc.*, **1991**, 113, 2385-2392
106. K. Iwamoto, K. Araki and S. Shinkai, *J. Org. Chem.*, **1991**, 56, 4955-4962
107. H. Kammerer, G. Happel and F. Caesar, *Makromol. Chem.*, **1972**, 162, 179
108. A. Arduini, A. Pochini, S. Reverberi and R. Ungaro, *J. Chem. Soc. Chem. Commun.*, **1984**, 981-982
109. C. D. Gutsche and J. Muthukrishnan, *J. Org. Chem.*, **1978**, 43, 4905-4906
110. L. Mandolini, R. Ungaro, "*Calixarenes in Action*", Imperial College Press, **2000**

-
111. J. Cornforth, P. Heart, G. Nicholas, R. Rees and J. Stock, *Brit. J. Pharmacol.*, **1955**, 10, 73-86
112. C. Jaime, J. de Mendoza, P. Prados, P. Nieto, and C. Shched, *J. Org. Chem.*, **1991**, 56, 3372-3376
113. M. McKervey, E. Seward, G. Ferguson, B. Ruhl and S. Harrisc, *J. Chem. Soc., Chem. Commun.*, **1985**, 388-390
114. F. Arnaud-Neu, E. Collins, M. Deasy, G. Ferguson, S. Harries, B. Kaitner, A. Lough, M. McKervey, E. Marques, *J. Am. Chem. Soc.*, **1989**, 3, 8681-8691
115. A. F. Danil de Namor, L. Salazar, M. Llosa Tanco, D. Kowalska, J. Villanueva Salas, R. Schulz, *J. Chem. Soc. Faraday Trans.*, **1998**, 94, 3111-3115
116. A. F. Danil de Namor, F. Sueros-Velarde, M. Cabaleiro, *J. Chem. Soc. Faraday Trans.*, **1996**, 92 (10), 1731-1737
117. A. F. Danil de Namor, S. Chahine, D. Kowalska, E. Castellano, and O. Piro, *J. Am. Chem. Soc.*, **2002**, 124, 12824-12836
118. A. F. Danil de Namor, M. ZapataOrmachea, O. Jafou and N. Al-Rawi, *J. Phys. Chem. B*, **1997**, 101, 6772-6779
119. A. Casnati; C. Fischer, M. Guardigli, A. Isernia, I. Manet, N. Sabbatini and R. Ungaro, *J. Chem. Soc. Perkin Trans.*, 2, **1996**, 395-399
120. J. Malone, D. Marrs, M. McKervey, P. O'Hagan, N. Thompson, A. Walker, F. Arnaud-Neu, O. Mauprivez, M. Weill, J. DozoI, H. Rouquettec and N. Simonc, *J. Chem. Soc., Chem. Commun.*, **1995**, 2151-2153
121. C. Tsai, I. Ho, J. Chu, L. Shen, S. Huang and W. Chung, *J. Org. Chem.*, **2012**, 77, 2254-2262

-
122. K. Daze, M. Ma, F. Pineux, and F. Hof, *Org. Lett.*, **2012**, 14, 1512-1514
123. J. van Loon, A. Arduini, L. Coppi, W. Verboom, A. Pochini, R. Ungaro, S. Harkema and D. Reinhoudt, *J. Am. Chem. Soc.*, **1990**, 55, 1539-1546
124. J. Rebek, *J. Chem. Soc. Chem. Comm.*, **2000**, 637-643
125. M. Brody, C. Schalley, D. Rudkevich, J. Rebek, *Angew. Chem. Int. Ed.*, **1999**, 38, 1640-1644
126. K. Wang, E. Yang, X. Zhao, H. Dou and Y. Liu, *J. Cryst. Growth & Des.*, **2014**, 14, 4631-4639
127. T. Clark, M. Makha, A. Sobolev, H. Rohrs, J. Atwood and C. Raston, *Chem., Eur. J.*, **2008**, 14, 3931-3938
128. Y. Lu, Y. Bi, Y. Bai and W. Liao, *J. Chem. Technol. Biotechnol.*, **2013**, 88, 1836-1840
129. Y. Wang, D. Guo, Y. Duan, Y. Wang & Yu Liu, *Drugs Sci. Rep.*, **2015**, 5: 9019, 1-7
130. D. Guo and Y. Liu, *J. Acc. Chem. Res.*, **2014**, 47, 1925-1934
131. C. D. Gutsche, M. Iqbal and I. Alam, *J. Am. Chem. Soc.*, **1987**, 107, 4314-4320
132. C. D. Gutsche and K. See, *J. Org. Chem.*, **1992**, 57, 4527-4539
133. D. Maity, R. Gupta, R. Gunupuru, D. Srivastava, P. Paul, *Sensors and Actuators B*, **2014**, 191, 757-764
134. R. Perrin, R. Lamartine and M. Perrin, *Pure & Appl. Chem.*, **1993**, 65, 1549-1559
135. *Calixarenes in the Nanoworld*, J Vicens, J Harrowfield, L Baklouti, Dordrecht: Springer **2007**
136. B. Mokhtari, K Pourabdoilan, S. Daiali, *J. Radianal. and Nucl. Chem.*, **2011**, 287, 921-934
137. K Kiegel, L Steczek, G. Zakrzewska- Trznadel, *J. Chem.*, **2013**, ID 76281
138. N. Toumi, F. Kajo, D. Fournier, F. Vocanson, R. Lamartine, I. Dumazet, *Mat. Sci & Eng. C*, **2008**, Issues 5-6, 645-652

-
139. A. Bayer, A; *Ber. Dtsch. Chem. Ges.*, **1886**, 19, 2184-2185
140. W. Allen, P. Gale, C. Brown, V. Lynch and J. Sessler, *J. Am. Chem. Soc.*, **1996**, 118, 12471-12472
141. S. Kim and J. Sessler, *Acc. Chem. Res.*, **2014**, 47, 2525–2536
142. Y. Wu, D. Wang, and J. Sessler, *J. Org. Chem.*, **2001**, 66, 3739-3746
143. C. Woods, S. Camiolo, M. Light, S. Coles, M. Hursthouse, M. King, P. Gale and J. Essex, *J. Am. Chem. Soc.*, **2002**, 124, 8644-8652
144. I. Saha, J. Lee and C. Lee, *Eur. J. Org. Chem.*, **2015**, 3859-3885
145. J. Blas, J. Bes, Marquez, J. Sessler, F. Luque and M. Orozco, *Chem. Eur. J.*, **2007**, 13, 1108–1116
146. P. Gale, J. Sessler, W. Ellen, N. Tvermoes, V. Lynch, *J. Chem. Soc. Chem. Commun.*, **1997**, 665-666
147. R. Nishiyabu and P. Anzenbacher, *J. Am. Chem. Soc.*, **2005**, 127, 8270-8271
148. A. Farinha, A. Tomé, J. Cavaleiro, *Tetrahedron Lett.*, **2010**, 51, 2184-2187
149. Y. Furusho, H. Kawasaki, S. Nakanishi, T. Aida, T. Takata, *Tetrahedron Lett.*, **1998**, 39, 3537-3540
150. A. F. Danil de Namor and M. Shehab; *J. Phys. Chem. A*, **2004**, 108, 7324-7330
151. A. F. Danil de Namor, I. Abbas and H. Hammud, *J. Phys. Chem. B*, **2007**, 111, 3098-3105
152. A. F. Danil de Namor and R. Khalife, *Phys. Chem. Chem. Phys.*, **2010**, 12, 753-760
153. D. Kim and J. Sessler, *Chem. Soc. Rev.*, **2015**, 44, 532 - 546
154. I. Park, J. Yoo, B. Kim, S. Adhikari, C-H. Lee, S. Kim, Y. Yeon, V. Lynch, J. Sessler, C.

- Hynes, J. Sutton, C. Tong and P. Gale, *Chem. Eur. J.*, **2012**, 18, 2514-2523, (b) S. Kim, V.
- Lynch, B. Hay, J. Kim and J. Sessler, *J. Chem. Sci.*, **2015**, 6, 1404–1413
155. W. More. *The Principles of Ion-Selective Electrodes and Membrane Transport* (Amsterdam-Oxford-New York **1981**)
156. P. Gale, J. Sessler, *J. Am. Chem. Soc.*, **1996**, 118, 5140-5141
157. P. Gale, J. Sessler, V. Kral, *J. Chem. Soc. Chem. Commun.*, **1998**, 1-8
158. J. Sessler, P. Gale, J. Genge, *Chem. Eur. J.*, **1998**, 4 (6), 1095-1099
159. E. Steinle, U. Schaller and M. Meyerhoff, *Analytical Sciences, JSAC*, **1998**, 14(1), 79-84
160. K. Park, S. Jung, S. Lee, and J. Kim, *Bull. Korean Chem. Soc.*, **2000**, 21, 909-912
161. A. F. Danil de Namor, A. El-Gamouz, S. AlHarthi, N. Al Hakawati and J. Varcoe, *J. Mater. Chem. A*, **2015**, 3, 13016–13030
162. J. Niederl, H. Vogel, *J. Am. Chem. Soc.*, **1940**, 62, 2512-2514.
163. H. Erdtman, S. Hogberg, S. Abarhamsson, B. Nilsson, *Tetrahedron Lett.*, **1968**, 1679-1682
164. L. MacGillivray and J. Atwood, *Nature*, **1997**, 389, 469-472
165. A. Högberg, *J. Am. Chem. Soc.*, **1980**, 102, 6046-6050.
166. A. Maerz, H. Thomas, N. Power, C. Deakyne and J. Atwood, *Chem. Commun.*, **2010**, 46, 1235–1237
167. L. McGillivaray and J. Atwood, *Nature (London)*, **1997**, 389, 469-472
168. A. Shivanyuk, J. Rebek, *J. Chem. Soc. Chem. Commun.*, **2001**, 2424-2425
169. A F. Danil de Namor, W. Aragon, N. Nwogu, A. El Gamouz, O. Piro, and E. Castellano, *J. Phys. Chem. B*, **2011**, 115, 6922–6934

-
170. D. J. Cram, S. Karbach, Y. Kim, L. Baczynskyj, G. Kallemeyn, *J. Am. Chem. Soc.*, **1985**, 107, 2575-2576
171. J. Sherman, *Tetrahedron*, **1995**, 51(12), 3395-3422
172. O. Berryman, A. Sather, A. Lled and J. Rebek, *Angew. Chem. Int. Ed.*, **2011**, 50, 9400–9403
173. A. F. Danil de Namor, J. Chaaban, O. Piro, E. Castelleno, *J. Phys. Chem. B*, **2006**, 110, 2442-2450
174. J. Atwood, L. Barbour, A. Jerga, B. Schottel, *J. Science*, **2002**, 298, 1000-1003
175. G. Liu, J. Liu, Yang Liu, and X. Tao, *J. Am. Chem. Soc.*, **2014**, 136, 590–593
176. R. Pal, M. Rddy, B. Dinesh, P. Balaram and T. Row, *J. Phys. Chem. A*, **2014**, 118, 9568- 9574
177. H. Kumari, L. Erra, A. Webb, P. Bhatt, C. Barnes, C. Deakyne, J. Adams, L. Barbour and J. Atwood, *J. Am. Chem. Soc.*, **2013**, 135, 16963–16967
178. R. Pfeiffer, D. Fowler and J. Atwood, *J. Cryst. Growth Des.*, **2014**, 14(8), 4205-4213
179. L. Avram, Y. Cohen, *J. Am. Chem. Soc.*, **2004**, 126, 11556-11563.
180. O. Webb; *Ph. D thesis*, University of Surrey, **2014**
181. R. Scott, *Separation Sciences Silica Gel and Bonded Phases (Their production, properties and use in LC)*, Wiley-Blackwell, **1993**
182. F. Plossi, M. Giera, F. Bracher, *J. Chromatographer A*, **2006**, 1135, 19-26
183. H. Weetall, *Covalent Coupling Methods for Inorganic Support Materials, Methods in Enzymology*, **1976**, 44, 134-148
184. J. Fan, Y. Qin, C. Ye, P. Peng and C. Wu, *J. Hazard. Mater.*, **2008**, 150, 343-350
185. A. F. Danil de Namor, J. Guerra, J. Salas, O. Piro, O. Webb, A. El Gamouz, W. Abou Hamdan,

- E. Castellano, *RSC Adv.*, **2015**, 5, 33524-33535.
186. L. Luo, X. Zhang, N. Feng, D. Tian, H. Deng & H. Li, *Scientific report*, **2015**, 5, 1-7
187. H. Kolb, M. Finn and K. Sharpless, *Angew. Chem. Int. Ed.*, **2001**, 40, 2004-2021
188. I. Jlalila, F. Meganim, J. Herscovici and C. Girard, *Molecules* **2009**, 14, 528-539
189. M. Meldal and C. Tornøe, *Chem. Rev.*, **2008**, 108, 2952-3015
190. W. D. Harkins, G. Jura; *J. Am. Chem. Soc.*, **1944**, 66 (8), 1366–1373
191. K. Walton and R. Snurr, *J. Am. Chem. Soc.* **2007**, 129, 8552-8556
192. A. Sallmann, “*The History of Diclofenac*” *Am. J. Med.*, **1986**, 80, 29-33.
193. S. C. Sweetman, W. Martindal, *The Complete Drug Reference*, 35th Edition, **2006**.
194. B. Furniss, A. Hannaford, P. Smith, A. Tatchel, *Vogel's-Practical Organic Chemistry*, 5th Ed.
195. D. Bax, de Ligny, A. Remijnse, *Recl. Trav. Chim. Pays-Bas*, **1972**, 91, 965
196. C. well, *J. Thermochemica Acta.*, **1988**, 132, 141-154
197. A. F. Danil de Namor, (*Thermodynamics of calixarene-ion interactions*), in *Calixarene* **2001**.
Eds. Z. Asfari, V. Bohmer, J. Harrowfield and J. Vacens, Chapter 19, 346-364
198. D. Skoog, F. Holler, *Principles of Instrumental Analysis*, 5th Ed., **1997**, 15-17
199. R. Scheytt, P. Mersman, R. Lindstadt, T. Heberer, *Water, Air Soil Poll.*, **2005**, 165, 3-11
200. J. Pawliszyn, “*Application of Solid Phase Microextraction*”, **1999**, 18-19
201. F. Guillo, B. Hamelin, L. Jullien, J. Canceill, J-M. Lehn, L. Robertis, H. Driguez, *Bull. Soc Chim.Fr.*, **1995**, 132, 857-866
202. S. Knoblauch, O. Falana, J. Nam, D. Roundhill, H. Hennig, K. Zeckert, *Inorg. Chim. Acta.*, **2000**, 300, 328–332

-
203. M. Shehab, *Ph.D. Thesis*, University of Surrey, Guildford, **2005**
204. J. Christensen, R. Izatt and L. Hansen, *Rev. Sci. Instrum.*, **1965**, 36, 779-783
205. Y. Liu, H. Wang, L. Wang, Z. Li, H. Zhang and Q. Zhang, *Tetrahedron*, **2003**, 59, 7967-7972
206. R. Ungaro, A. Arduini, A. Pochini, S. Reverberi, *J. Chem. Soc. Chem. Commun.*, **1984**, 981-982
207. R. Pathak, V. Hing, M. Mondal and C. Rao, *J. Org. Chem.*, **2011**, 76, 10039-10049.
208. R. Pathak, A.G. Dikundwar, T. Row, *J. Chem. Soc. Chem. Commun.* **2010**, 46, 4345-4347
209. J. Dyke, G. Levita, A. Morris and J. Ogden, *J. Phys. Chem. A*, **2004**, 10, 5299-5307
210. A. F. Danil de Namor, D. Tanaka, L. Regueira, I. Orellana, *J. Chem. Soc. Faraday Trans.*, **1992**, 88, 1665-1668
211. L. Bonomo, E. Solari, G. Toraman, R. Scopelliti, M. Laatrónico and C. Floriani, *J. Chem. Soc. Chem. Commun.*, **1999**, 2413-2414
212. A. Kalidkowski and A. Trochimczuk, *J. React. Func. Polym.*, **2006**, 66, 740-744
213. L. Tunstad, J. Tucker, E. Dalcanale, J. Weiser, J. Bryant, J. Sherman, R. Helgeson, C. Knobler, D. Cram, *J. Org. Chem.* **1989**, 54, 1305-1312.
214. P. Timmerman, W. Verboom, D. Reinhoudt, *Tetrahedron*, **1996**, 52, 2663-2704
215. T. Gerkenmeier, W. Iwanek, C. Agena, R. Fröhlich, S. Kotila, C. Näther, J. Mattay, *Eur. J. Org. Chem.*, **1999**, 2257-2262
216. L. Raff, *Principles of Physical Chemistry*, 1st Ed., Prentice-Hall International UK Limited, London, **2001**
217. G. Jones, C. Bradshaw, *J. Am. Chem. Soc.*, **1993**, 55, 1780-1800
218. J. Lind, J.J. Zwolenik, R. Fouss, *J. Phys. Chem.*, **1965**, 81, 1557-1559

-
219. K. Jansen, H. Buschman, E. Zliobaite, E. Schollmeyer, *Thermochem. Acta*, **2002**, 385, 177-184
220. Y. Liu and J. M. Sturtevant, *Protein Sci.*, **1995**, 4, 2559-2561
221. L. Briggner, I. Wadsö, *J. Biochem Biophys Methods*, **1991**, 22, 101-118
222. I. Wadsö and R. Goldberg, *Pure Appl. Chem.*, **2001**, 73, 1625–1639
223. B. Wunderlich “Thermal Analysis of Polymeric Materials”, **2005**, Springer-Verlag Berlin
224. L. Liu and S. Zhu, *J Pharm Biomed Anal*, **2006**, 40, 122-127
225. D. Giron, *J. Therm. Anal. Cal.*, **2002**, 68, 335-357
226. W. Acree, *J. Phys. Chem. Ref. Data*, **2014**, 43, 1-276
227. A. Llina`s, J. Burley, K. Box, R. Glen, and J. Goodman, *J. Med. Chem.*, **2007**, 50, 979-983
228. L. Zilnik, A. Jazbinsek, A. Hvala, F. Vrecer and A. Klamt, *J. Fluid Phase Equilibria*, **2007**, 261, 140-145
229. S. Habermann, K. Murphy, *Prot. Sci.*, **1996**, 5, 1229-1239
230. J. Dearden, *Environ. Health Perspect.*, **1985**, 61, 203-228
231. A. Grzesiak, M. Lang, K. Kim, A. Matzger, *J. Phar. Sci.*, **2003**, 92, 2260-2271
232. A.F. Danil de Namor, J. Guerra, V. Gracheve, W. Aragon, K. Fernandez and F. Velarde, *New J. Chem.*, **2005**, 29, 1072-1075
233. C. Ventura, I. Giannone, T. Musumeci, R. Pignatello, L. Ragni, C. Landolfi and C. Milanese, D. Paolino and G. Pugalisi, *Eur. J. Med. Chem.*, **2006**, 41, 233-240
234. V. Crupi, R. Ficarra, M. Guardo, D. Majolino, R. Stancanelli, V. Venuti, *J. Pharm. Biomed. Anal.*, **2007**, 44, 110-117
235. E. Valle, *Process Biochem.*, **2004**, 39, 1033-1046

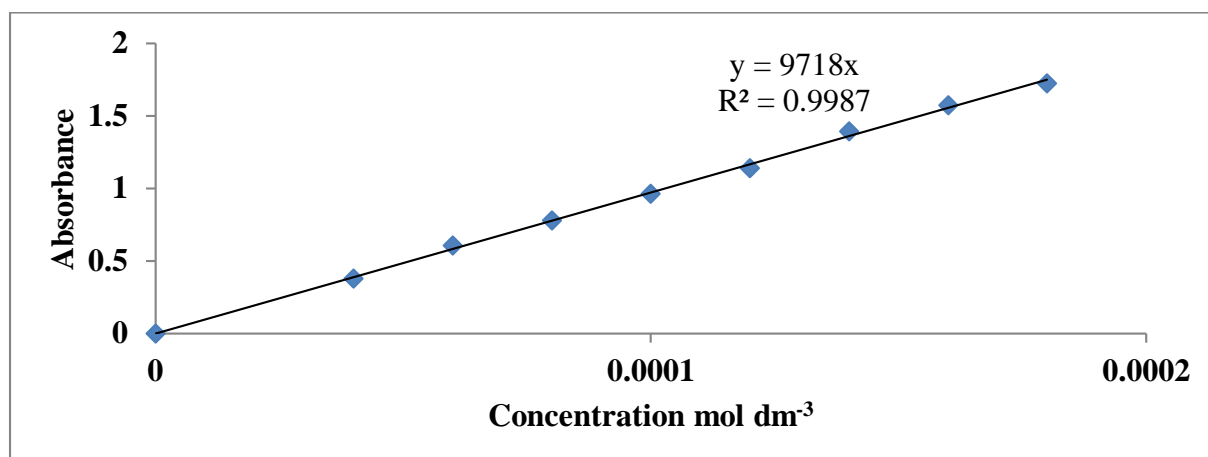
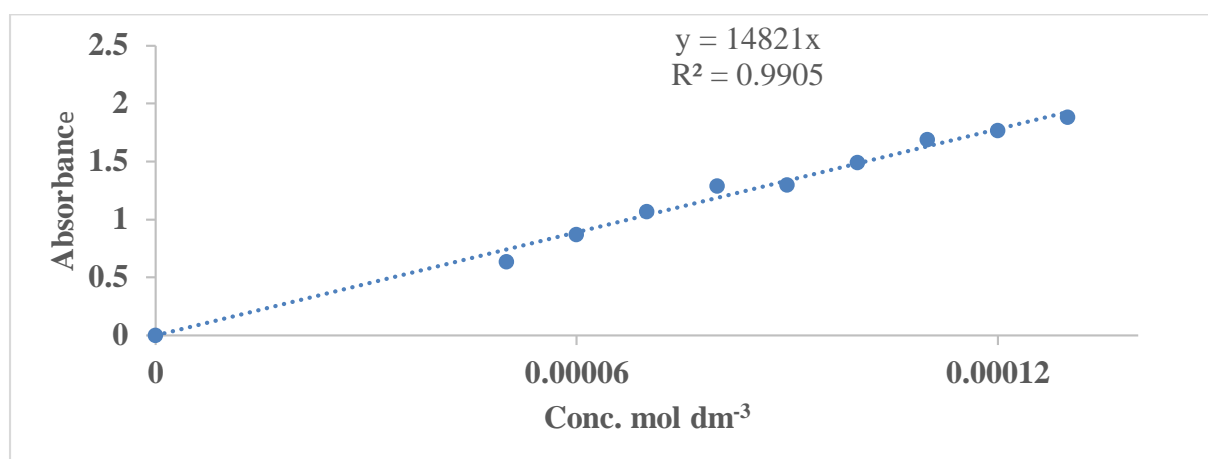
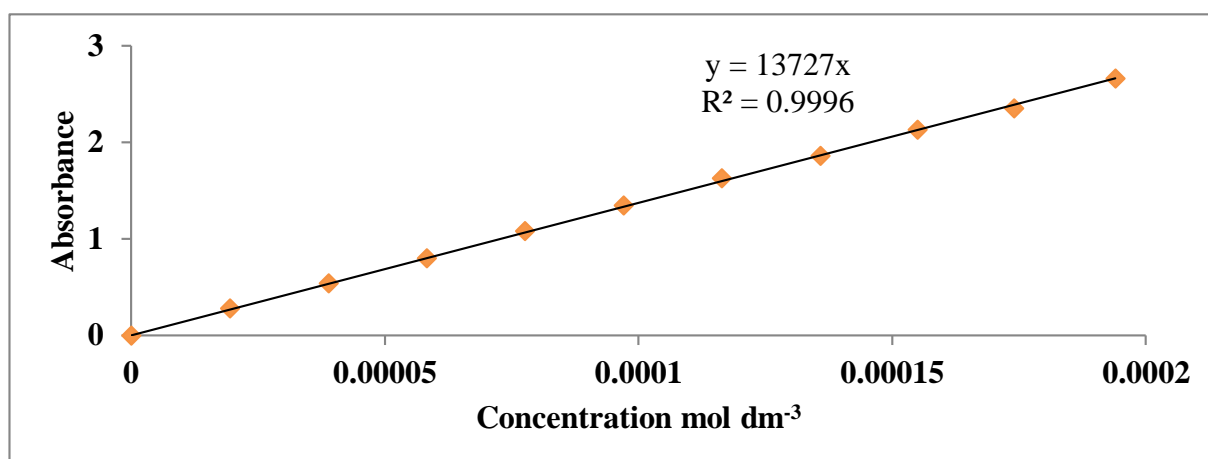
-
236. E. Kosower, *J. Am. Chem. Soc.*, **1958**, 80 (13), 3253-3260.
237. C. Reichardt “*Solvents and Solvent Effects in Organic Chemistry*”, 2003, 3rd Ed. Wiley-VCH
238. A. Vegilia and R. de Rossi, *Can. J. Chem.*, **2000**, 78, 233-237.
239. K. No and J. Koo, *J. Bull. Korean Chem. Soc.*, **1994**, 15,483- 488.
240. A. F. Danil de Namor, N. Sueros, M. McKervey, G. Barrett, F. Arnaud- Neuc and M. Weillc, *J. Chem. Soc. Chem. Commun.*, **1991**, 1546-1548.
241. M. Vihinin, *J. Protein Eng.*, **1987**, 1(6), 477-480.
242. P. Tudija, M. Khan, E. Mestrovic, M. Horvat and P. Golja, *Chem. Pharm. Bull.*, **2001**, 49 (10), 1245-1250.
243. M. Meloun, S. Bordovska´ and L. Galla, *J Pharm Biomed Anal.*, **2007**, 45, 552-564
244. Z. Yurtsever, B. Erman, E. Yurtsever, *Tur. J. Chem.*, **2012**, 36, 383-395
245. J. Yoo, M. Kim, S. Hong, J. Sessler, and C. Lee, *J. Org. Chem.*, **2009**, 74, 1065–106

Appendix

List of Appendix.....	Page
Fig. 1- A Calibration curve of sodium diclofenac in water at 298 K.....	218
Fig. 2-A Calibration curve of NaDF in methanol at 298 K.....	218
Fig. 3-A Calibration curve of NaDF in acetonitrile at 298 K.....	218
Fig. 4. A Calibration curve of NaDF in DMSO at 298 K.....	219
Fig. 5-A Calibration curve of NaDF in 1- Butanol at 298 K.....	219
Fig. 6-A Calibration curve of NaDF in ethylacetate at 298 K.....	219
Fig. 7-A Calibration curve of sodium diclofenac in DMF at 298 K.....	220
Fig. 8-A Calibration curve of sodium diclofenac in THF at 298 K.....	220
Fig. 9–A: Calibration curve of carbamazepine in water at 298 K.....	220
Fig. 10-A Calibration curve of carbamazepine in DCM at 298 K.....	221
Fig. 11-A Calibration curve of carbamazepine in acetonitrile at 298 K.....	221
Fig. 12-A Calibration curve of CBZ in DMSO at 298 K.....	221
Fig. 13-A Calibration curve of clofibric acid in water at 298 K.....	222
Fig. 14-A Calibration curve of carbamazepine in water at 298 K.....	222
Fig. 15-A Calibration of carbamazepine in DCM at 298 K.....	222
Fig. 15-A Calibration of carbamazepine in DCM at 298 K.....	223
Fig. 17-A Calibration curve of carbamazepine in DMSO at 298 K.....	223
Fig. 18-A Calibration curve of carbamazepine in DMF at 298 K.....	223
Fig. 1-B: ^1H NMR spectrum for monochlorinated β -cyclodextrine in DMSO-d_6 at 298 K.....	224
Fig. 2-B: ^{13}C NMR spectrum for mono chlorinated- β -cyclodextrine in DMSO-d_6 at 298 K.....	224
Fig. 3-B: ^1H NMR spectrum of per-benzoylated- β -cyclodextrine in DMSO-d_6 at 298 K.....	225
Fig. 4-B: ^1H NMR spectra for <i>p-tert</i> -buylcalix[4]arene tetraethylethanoate in CDCl_3 at 298 K.....	225

Fig. 5-B: ^1H NMR spectrum of 5, 11, 17, 23 tetra- <i>tert</i> -butyl, 25, 27 bis[2-cyanomethox] methoxy-26, 28 -dihydroxycalix[4]arene at 298 K.....	226
Fig. 6-B ^1H NMR spectrum of 5, 11, 17, 23 tetra- <i>tert</i> -butyl, 25, 27-bis[aminoethoxy]-26, 28-dihydroxycalix[4]arene at 298 K.....	226
Fig. 7-B ^1H NMR spectrum for 25, 26, 27, 28-tetrahydroxycalix[4]arene in CDCl_3 at 298 K.....	227
Fig. 8-B ^1H NMR spectrum of 5- <i>tert</i> -butyl-2-hydroxybenzaldehy.....	227
Fig. 9-B ^1H NMR spectrum of 5- <i>tert</i> -butyl-3-chloromethyl-hydroxybenzaldehy.....	228
Fig. 10-B ^1H NMR spectrum of 5- <i>tert</i> -butyl-3-azidomethyl-2-hydroxybenzaldehy in CDCl_3	228
Fig. 11-B ^1H NMR spectrum of 25, 27-dihydroxy-26-28-(dioxypargyl) <i>tert</i> -butylcalix[4]arene (ArCH) in CDCl_3 at 298 K.....	229
Fig. 12-B ^1H NMR spectrum of <i>p-tert</i> -butyl-azidocalix[4]arene in CDCl_3 at 298 K.....	229
Fig. 13-B ^1H NMR spectrum of 2-azidoacetamide in CDCl_3 at 298 K.....	230
Fig. 14-B ^1H NMR spectrum of 25, 26, 27, 28-(diethylamino) ethoxy calix[4]arene in CDCl_3 at 298 K.....	230
Fig. 15-B ^1H NMR spectrum of TTHCP in DMSO-d_6 at 298 K.....	231
Fig. 16-B ^{13}C NMR of TTHCP in DMSO at 298 K.....	231
Fig. 17-B ^1H NMR spectrum of TTECP in DMSO-d_6 at 298 K.....	232
Fig. 18-B ^1H NMR spectrum of calix[4]pyrrole derivative TTECP in CD_3CN at 298 K.....	232
Fig. 19-B Appendix H NMR spectrum of C-pentyl-resorcin[4]arene in CDCl_3	233
Fig. 20-B ^1H NMR spectrum of PG6 in cdCl_3 at 298 K.....	233
Fig. 21-B ^1H NMR spectrum of PG11 in CDCl_3 at 298 K.....	234
Table 3.1 ^1H NMR titration experiment and the chemical shift changes from the addition of increasing amounts of diclofenac to a fixed concentration of calix[4]arene amine in CD_3CN at 298 K.....	235

Table 3.2 Chemical shift changes for the receptor [(CA-(NH ₂) ₂] as a result from the addition of increasing concentrations of clofibric acid in CD ₃ CN at 298 K.....	236
Table 3.3 Conductance measurements for the diclofenac.....	237
Table 3.4 Conductivity values for the titration of clofibric acid solution in MeCN (1.96×10 ⁻³ mol dm ⁻³) with the CA-(NH ₂) ₂ receptor in MeCN (1.59×10 ⁻² mol dm ⁻³) at 298.15 K.....	238
Table 3.5 Conductometric titration of aspirin with CA-(NH ₂) ₂ in acetonitrile at 298.15 K.....	239
Table 3.6 Absorbance values change of diclofenac resulting from the addition of increasing concentration of CA-(NH ₂) ₂ in acetonitrile at 298 K.....	240
Table 3.7 Absorbance values change values of clofibric acid solution in acetonitrile as a result from the gradual addition of calix[4]arene amine solution in the same solvent.....	241
Table 3.8 Absorbance values change of aspirin solution in dry acetonitrile as a result from gradual addition of calix[4]arene amine at 298 K.....	242

A-Calibration Curves**Fig. 1- A** Calibration curve of sodium diclofenac in water**Fig. 2-A** Calibration curve of NaDF in methanol at 298 K**Fig. 3-A** Calibration curve of NaDF in acetonitrile at 298 K

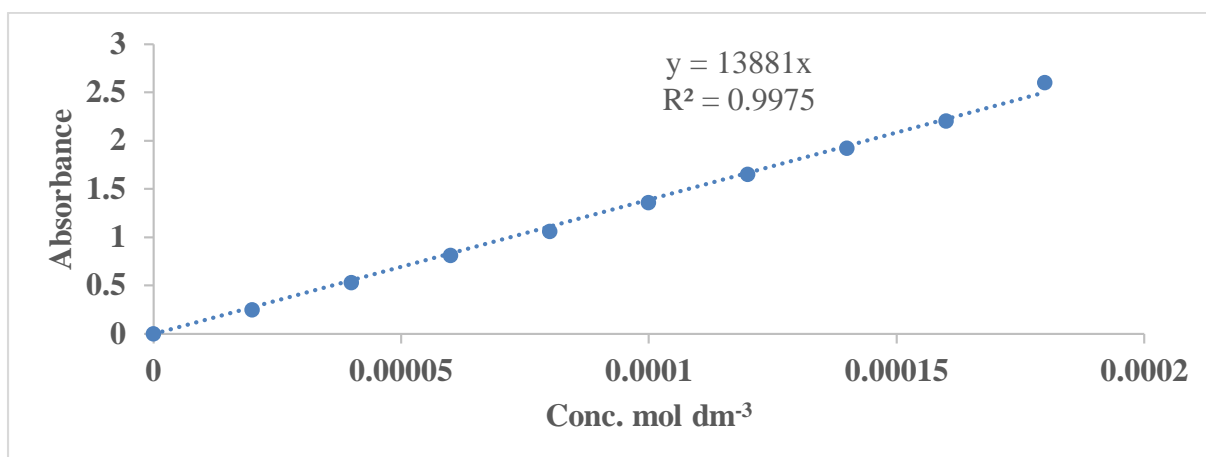


Fig. 4. A Calibration curve of NaDF in DMSO

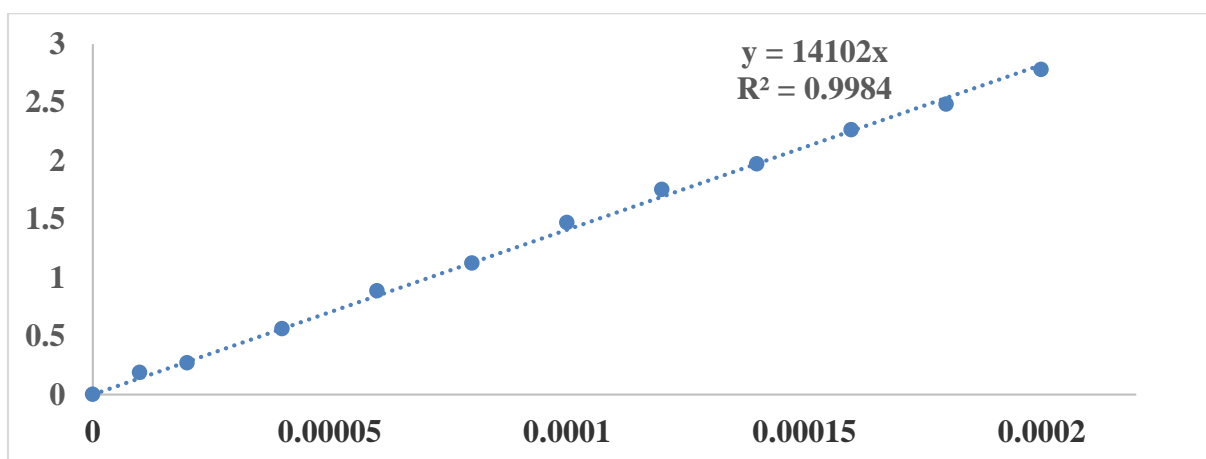


Fig. 5-A Calibration curve of NaDF in 1- Butanol at 298 K

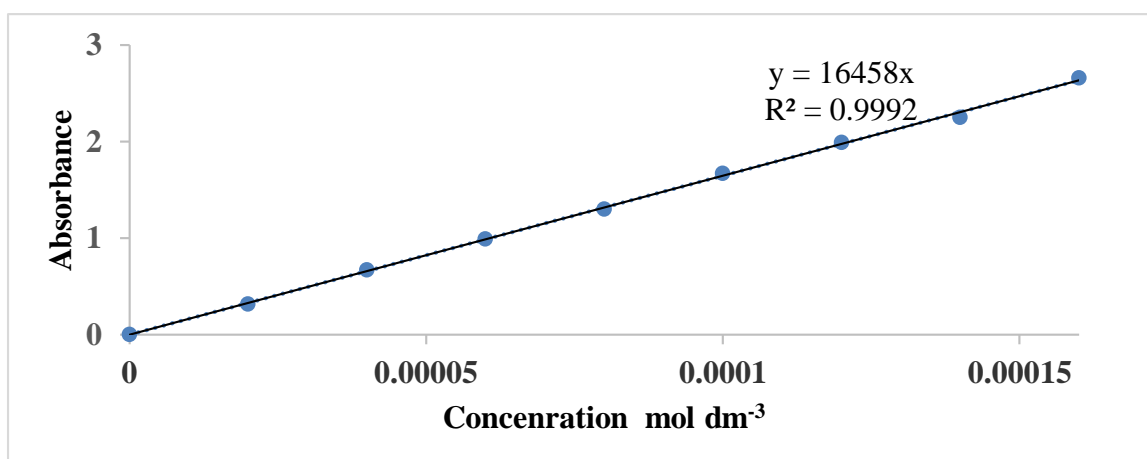


Fig. 6-A Calibration curve of NaDF in ethylacetate at 298 K

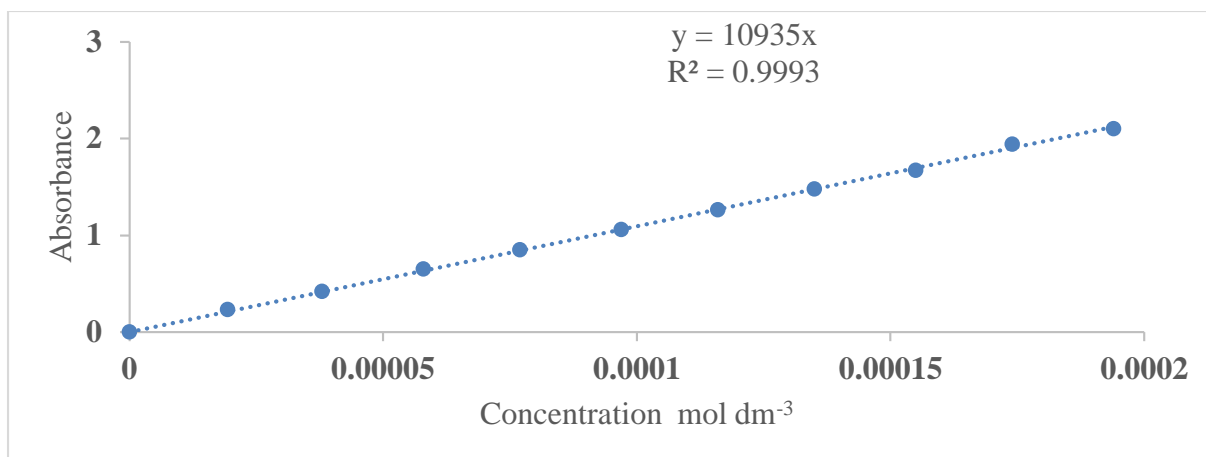


Fig. 7-A Calibration curve of sodium diclofenac in DMF

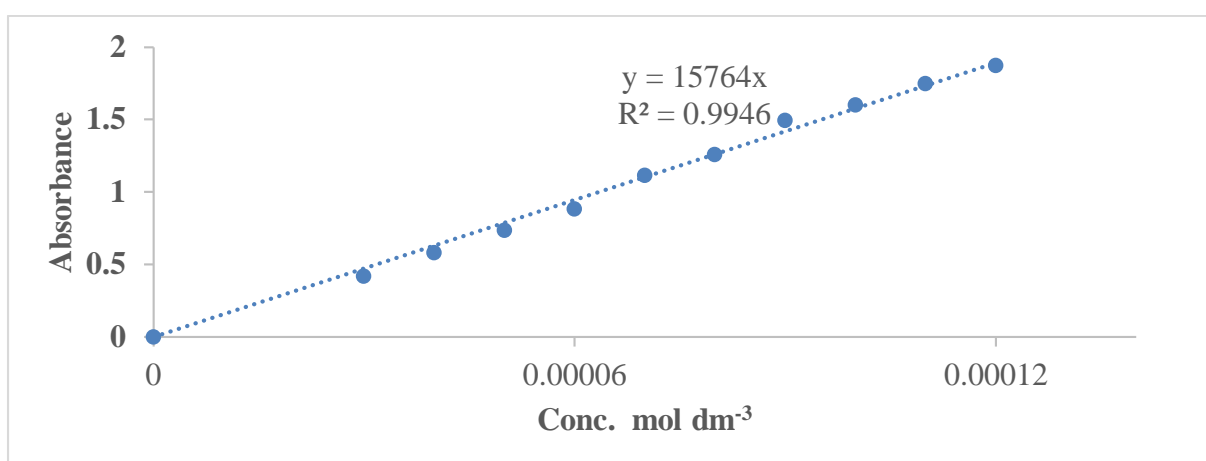


Fig. 8-A Calibration curve of sodium diclofenac in THF at 298 K

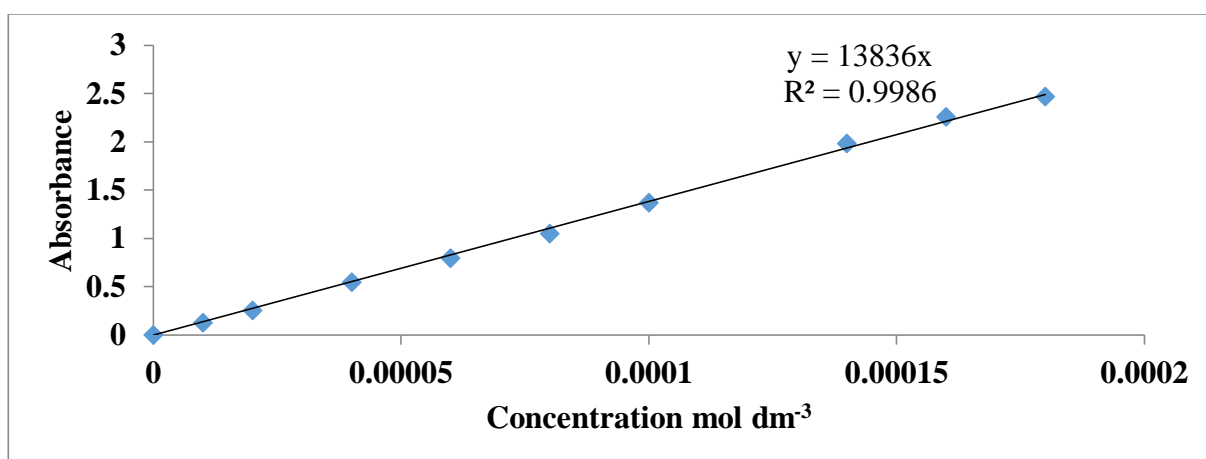


Fig. 9-A: Calibration curve of carbamazepine in water at 298 K

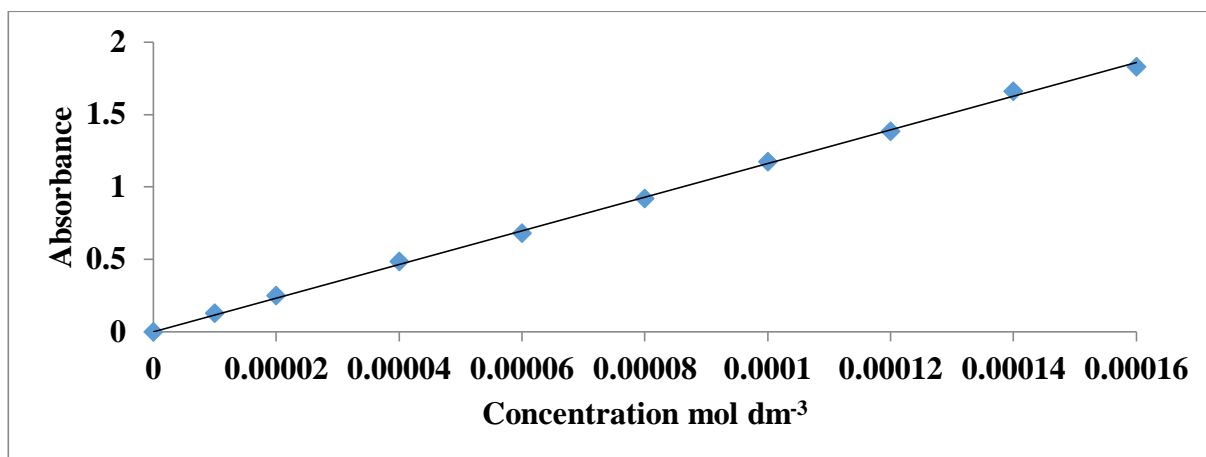


Fig. 10-A Calibration curve of carbamazepine in DCM at 298

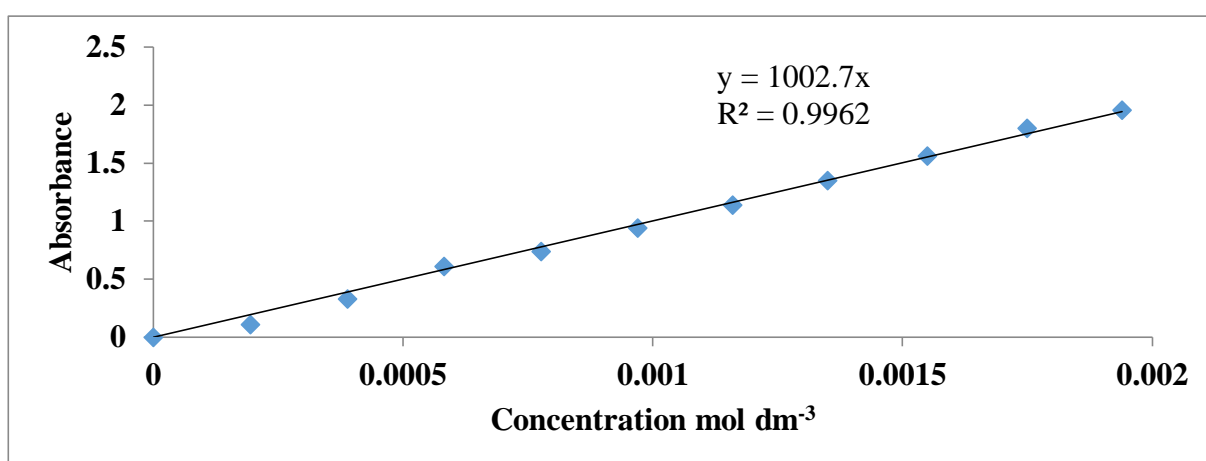


Fig. 11-A Calibration curve of carbamazepine in acetonitrile at 298 K

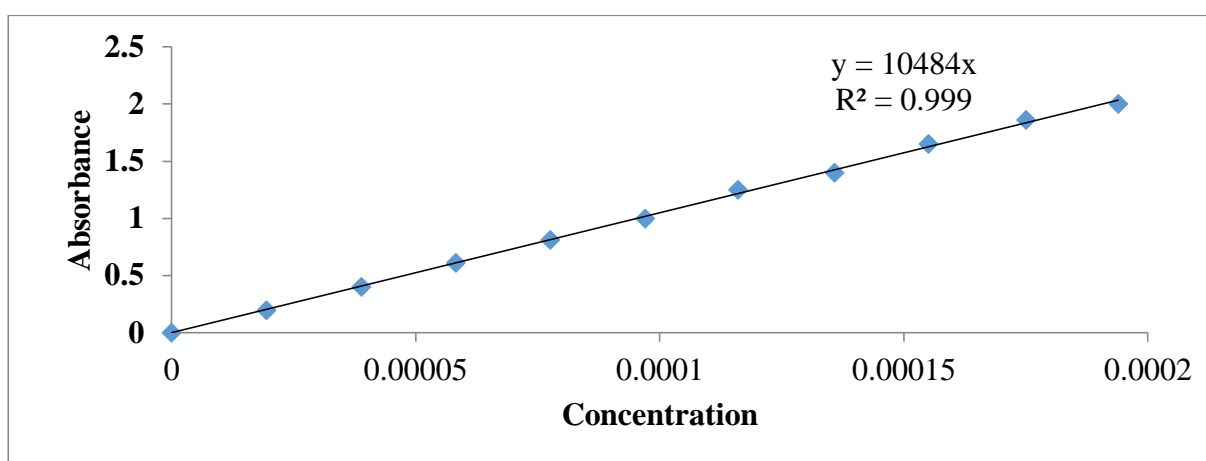


Fig. 12-A Calibration curve of CBZ in DMSO at 298 K

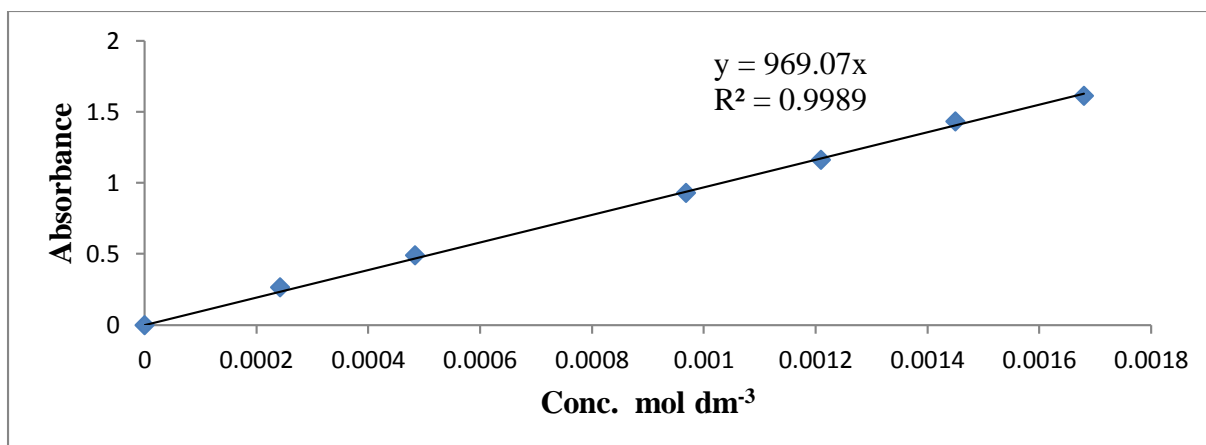


Fig. 13-A Calibration curve of clofibric acid in water

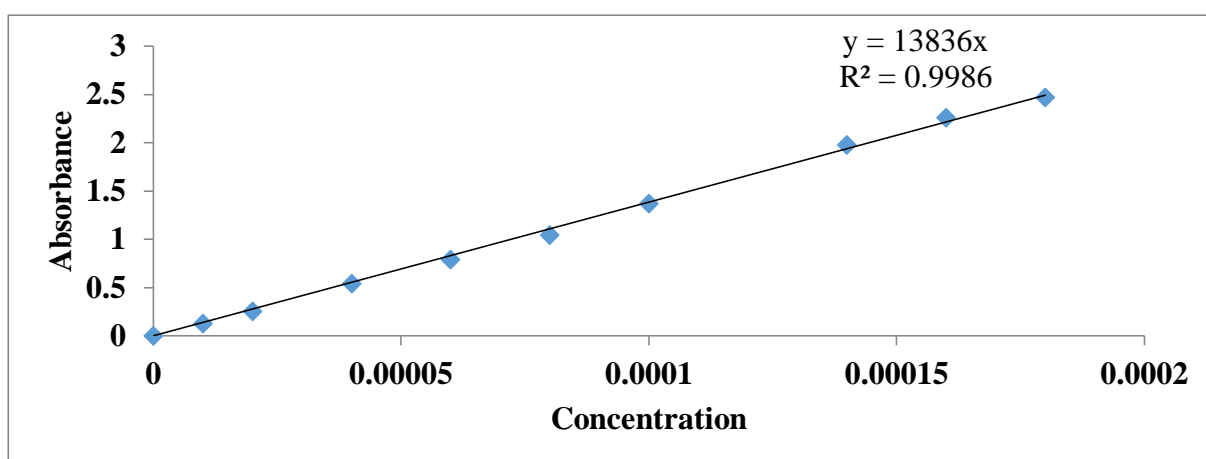


Fig. 14-A Calibration curve of carbamazepine in water

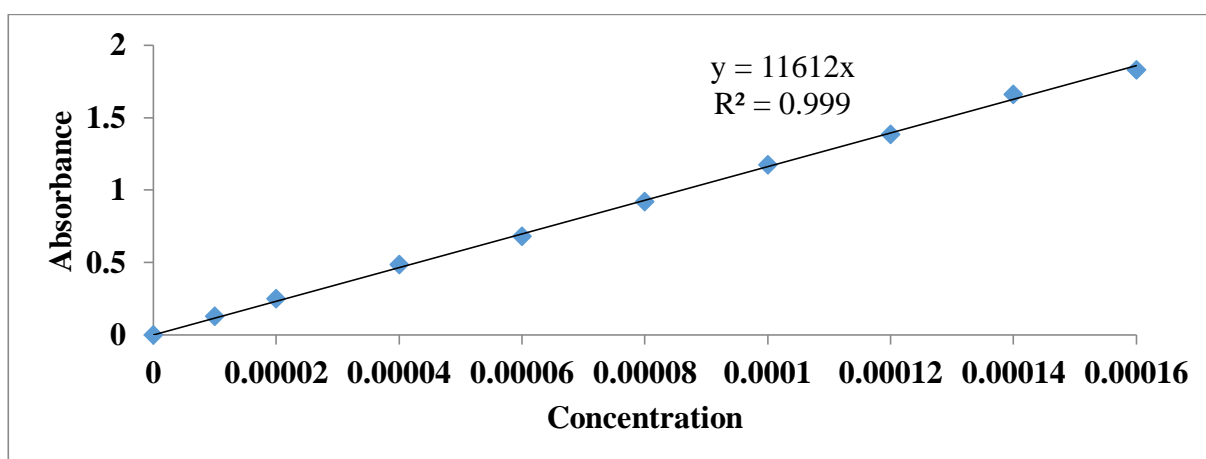


Fig. 15-A Calibration of carbamazepine in DCM at 298 K

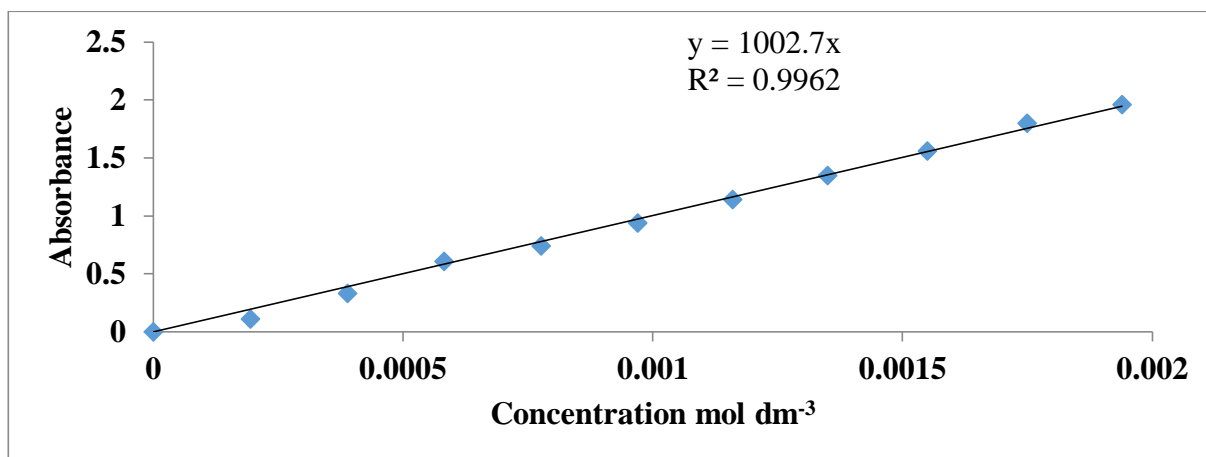


Fig. 16-A Calibration curve of carbamazepine in acetonitrile

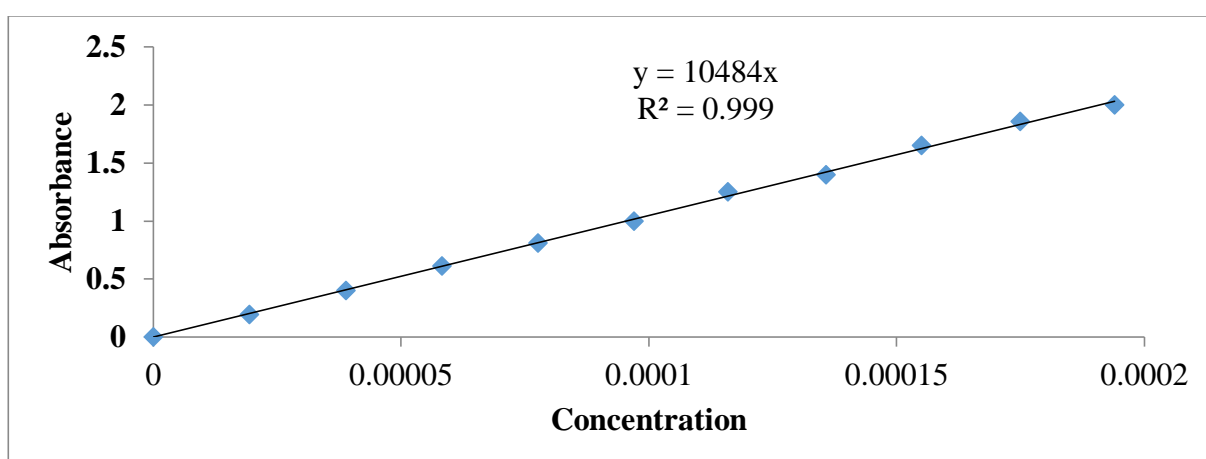


Fig. 17-A Calibration curve of carbamazepine in DMSO

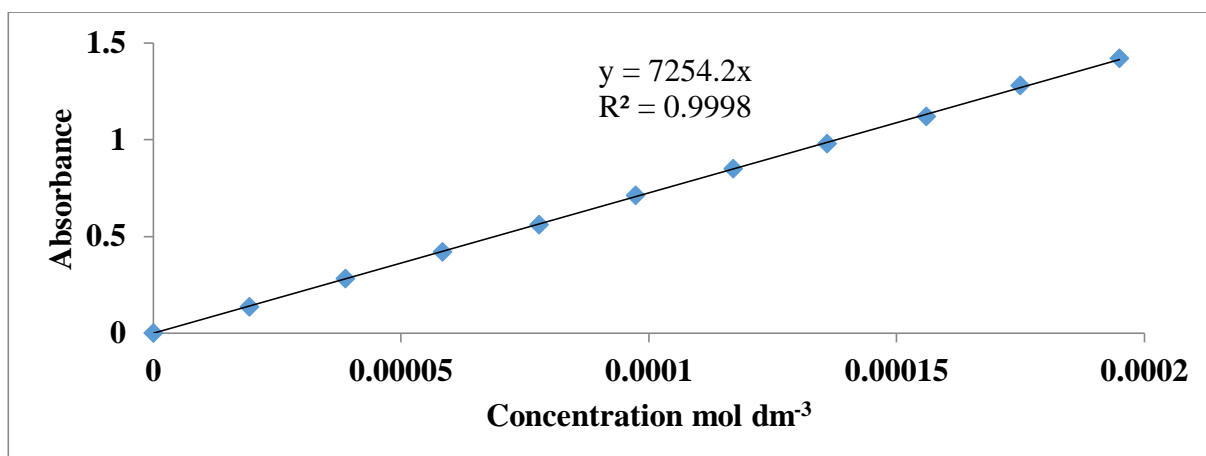
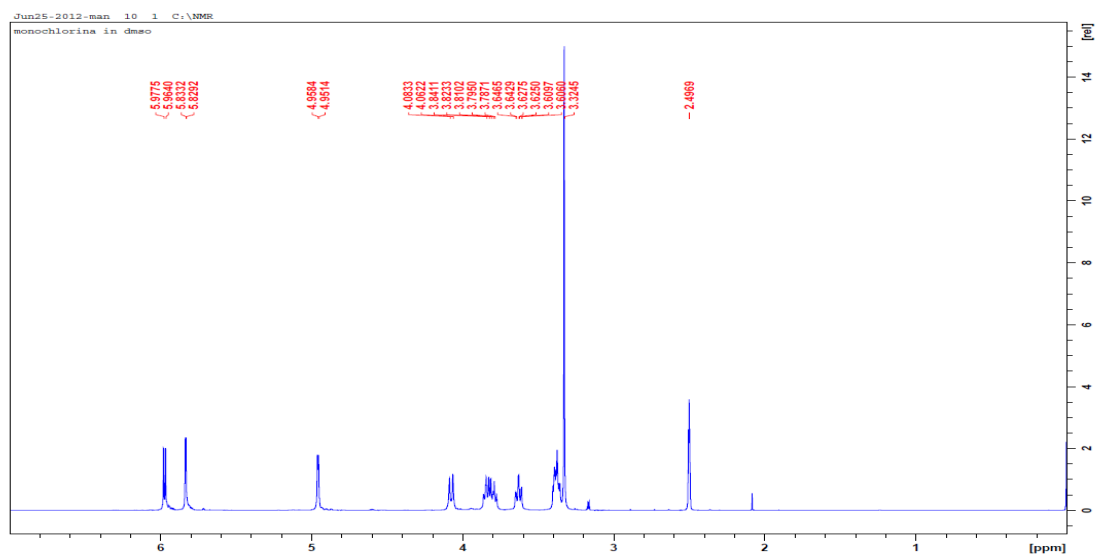
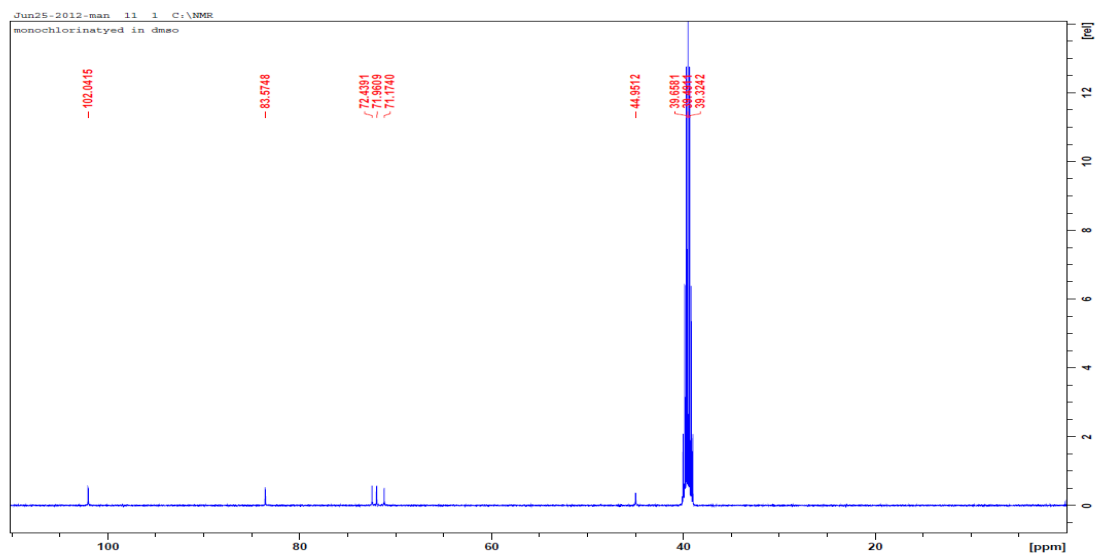
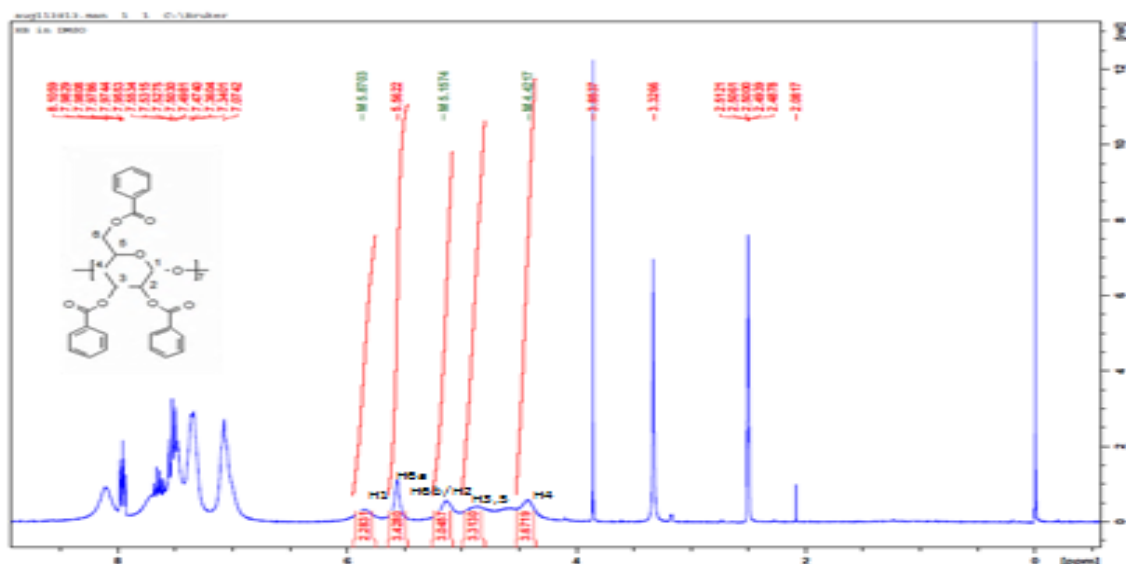


Fig. 18-A Calibration curve of carbamazepine in DMF

Appendix-B ^1H NMR SpectrumFig. 1-B: ^1H NMR spectrum for monochlorinated β -cyclodextrine in DMSO-d_6 Fig. 2-B: ^{13}C NMR spectrum for mono chlorinated- β -cyclodextrine in DMSO-d_6 at 298 K



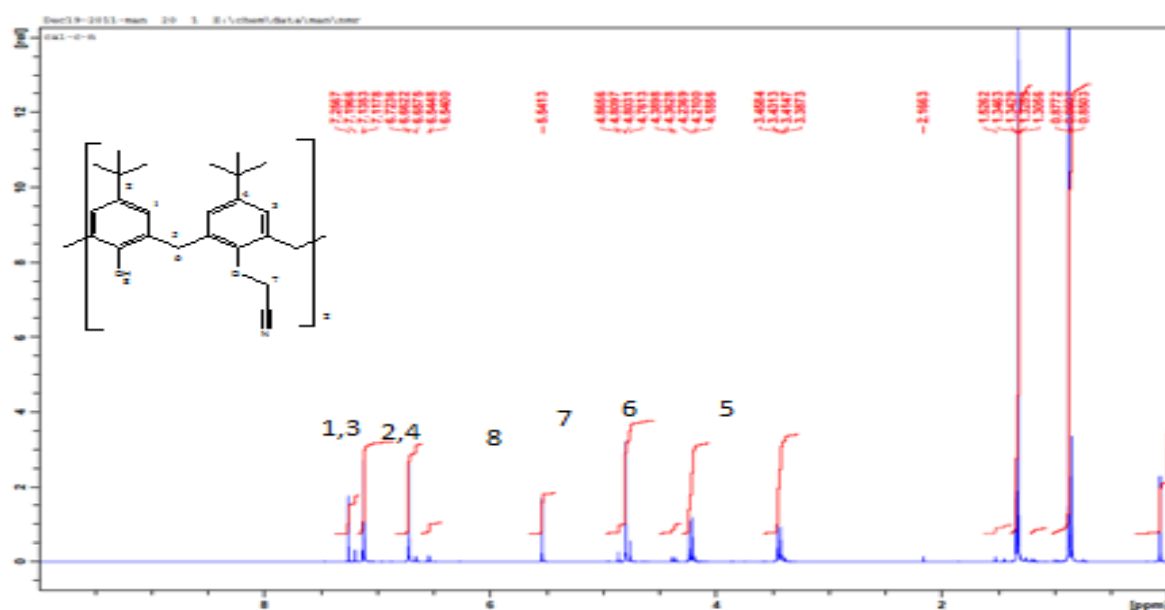


Fig. 5-B: ^1H NMR spectrum of 5, 11, 17, 23 tetra-*tert*-butyl, 25, 27 bis (2-cyanomethoxy) methoxy-26, 28 -dihydroxycalix[4]arene at 298 K

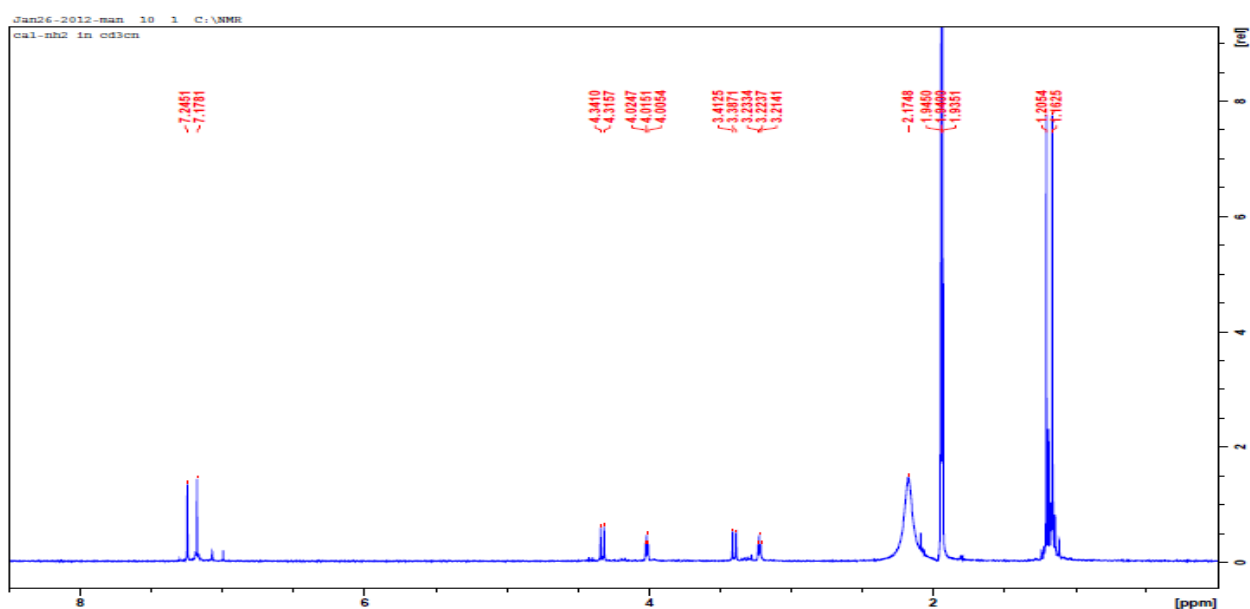


Fig. 6-B ^1H NMR spectrum of 5, 11, 17, 23 tetra-*tert*-butyl, 25, 27-bis (aminoethoxy)-26, 28 dihydroxycalix[4]arene at 298 K

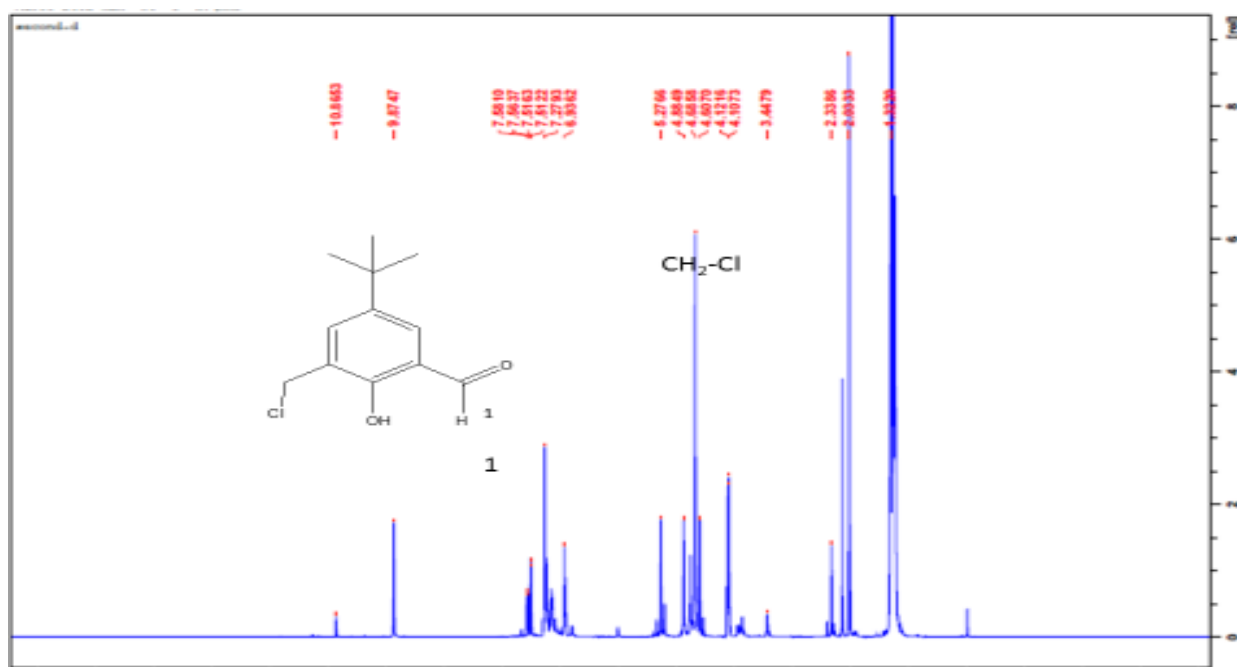


Fig. 9-B ^1H NMR spectra for 5-tert-butyl-3-chloromethyl-2-hydroxy benzaldehyde In CDCl_3 at 298 K

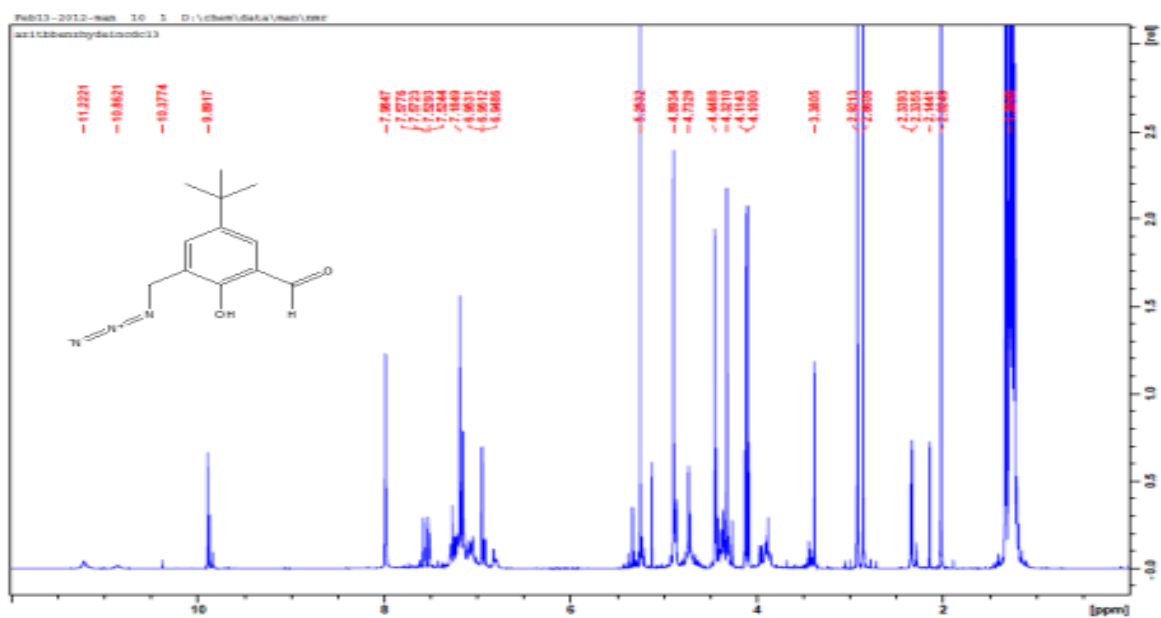


Fig. 10-B ^1H NMR spectroscopy for 5-tert-butyl-3-(azidomethyl)-2-hydroxyBenzaldehyde in CDCl_3 at 298 K

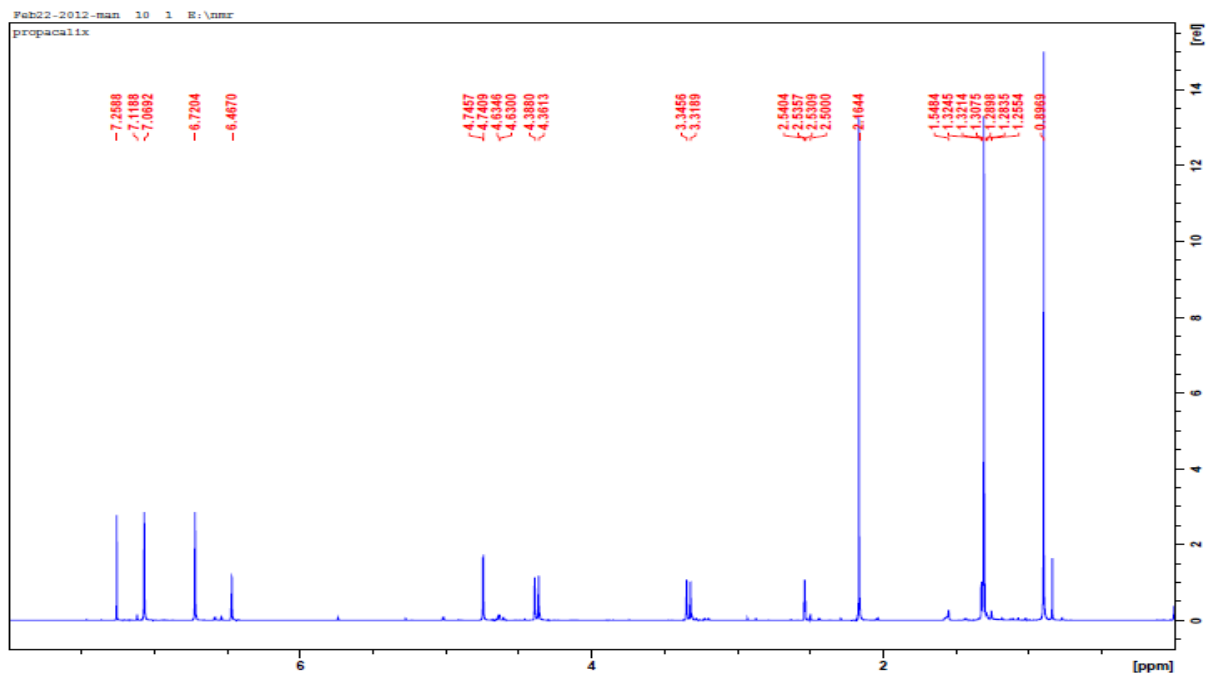


Fig. 11-B ^{13}C NMR spectrum of 25, 27-dihydroxy-26-28-(dioxypargyl) *tert*-butylcalix[4]arene (ArCH) in CDCl_3 at 298 K

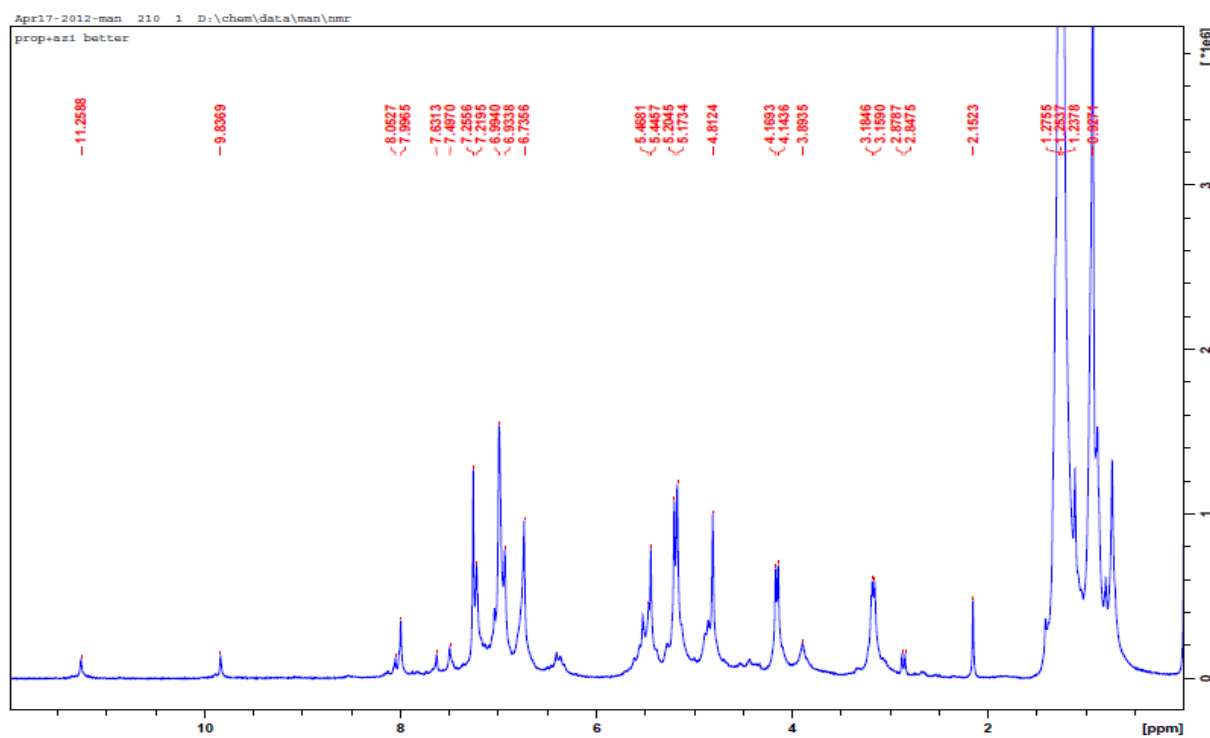


Fig. 12-B ^1H NMR spectrum of *p-tert*-butyl-azidocalix[4]arene in CDCl_3 298 K

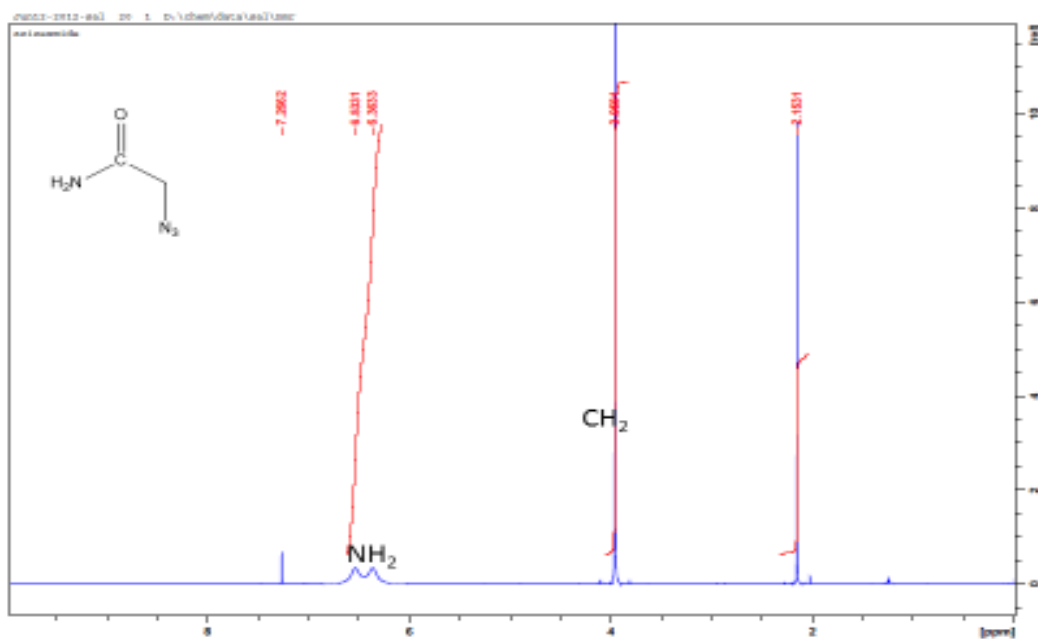


Fig. 13-B ^1H NMR spectrum of 2-azidoacetamide in CDCl_3 at 298 K

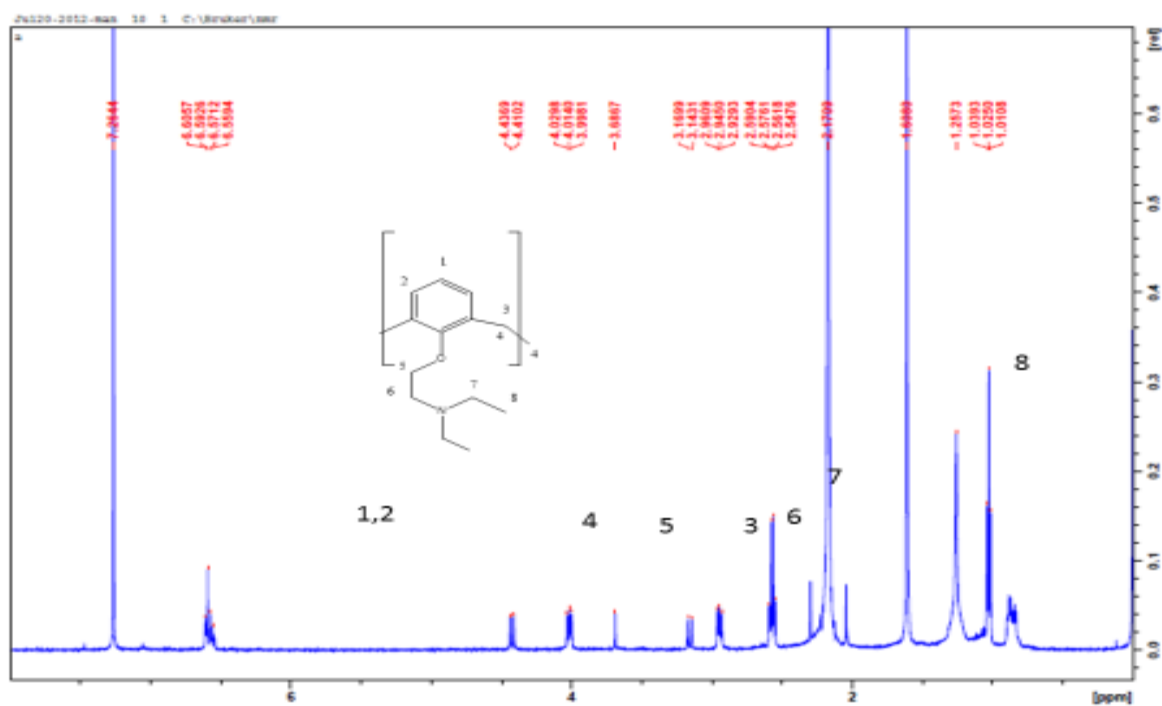


Fig. 14-B ^1H NMR spectrum of 25, 26, 27, 28-(diethylamino) ethoxy calix[4]arene in CDCl_3 at 298 K

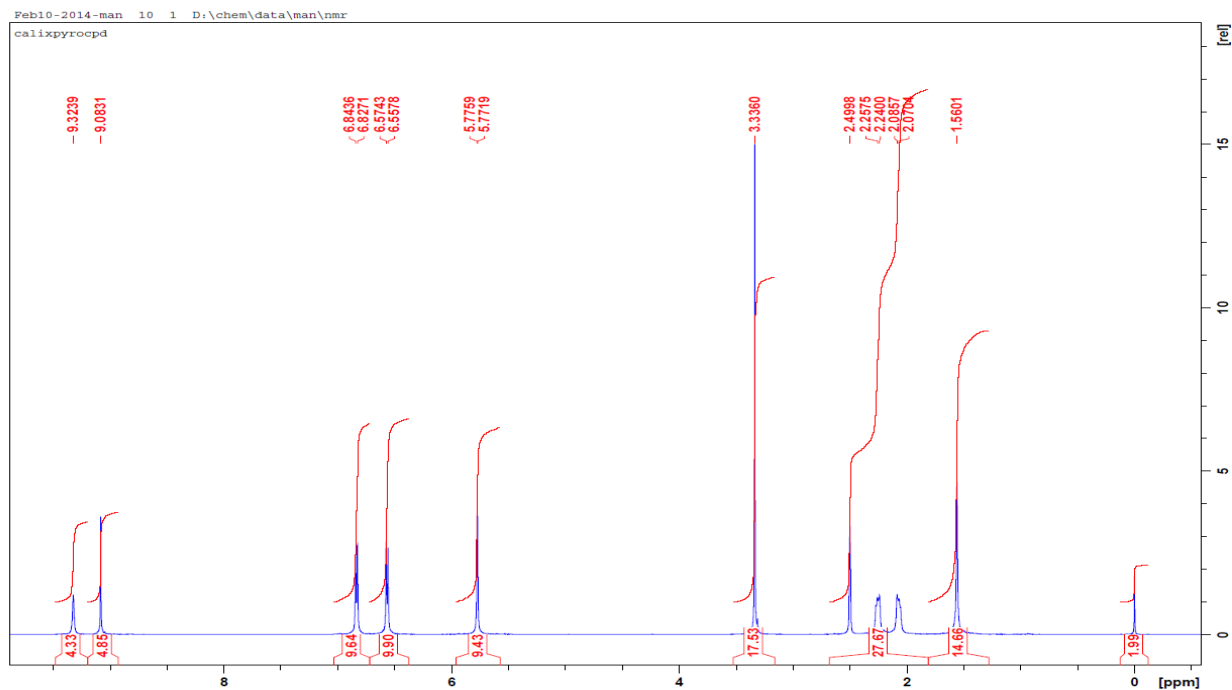


Fig. 15-B ^1H NMR spectrum of TTHCP in DMSO-d_6 at 298 K

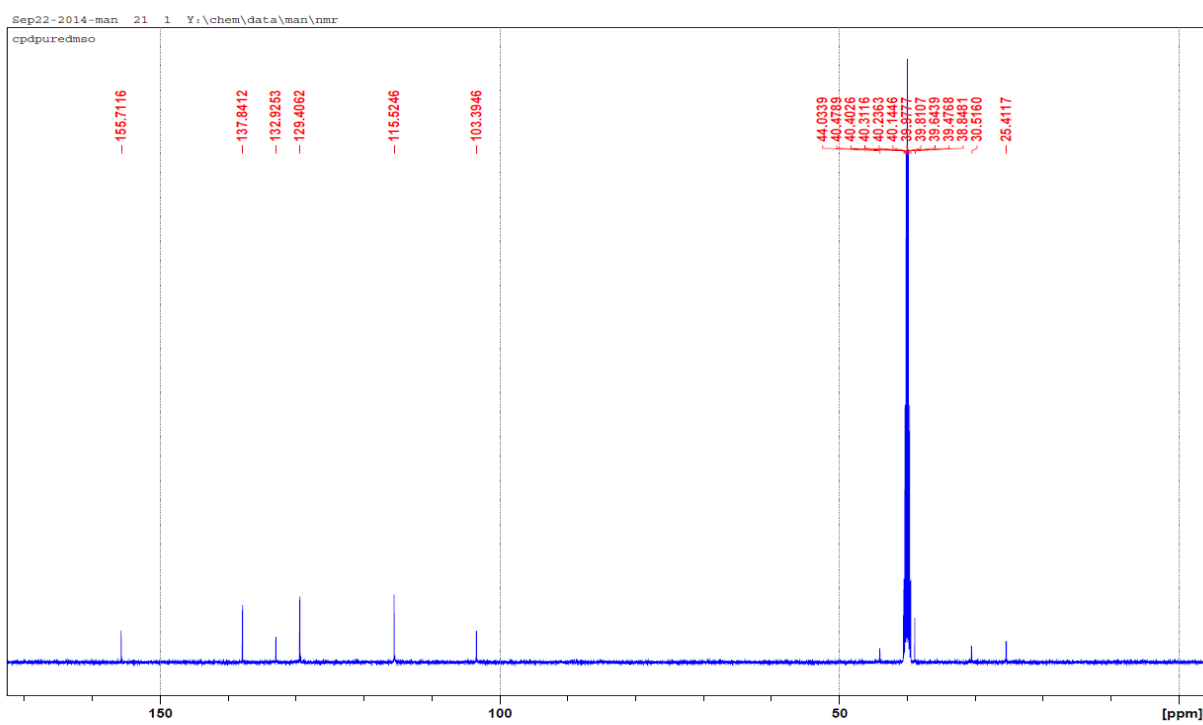


Fig. 16-B ^{13}C NMR of TTHCP in DMSO at 298 K

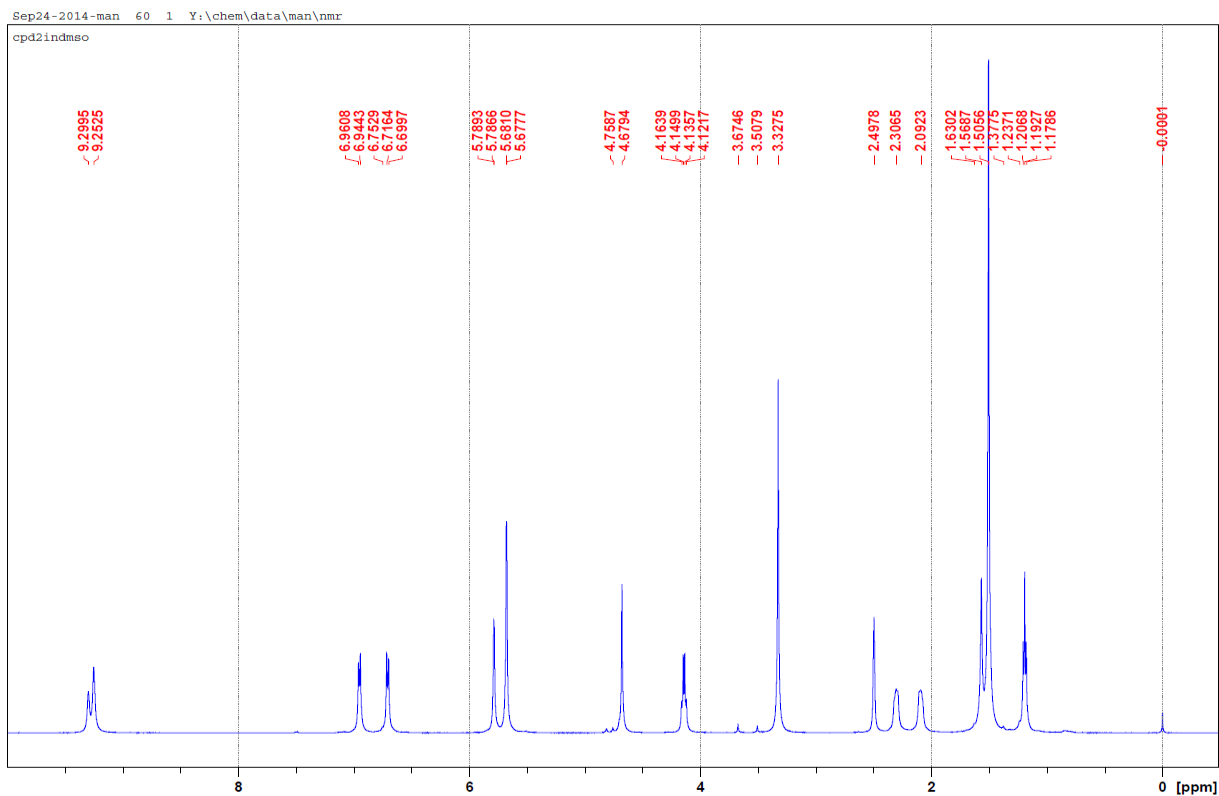


Fig. 17-B ^1H NMR spectrum of TTECP in DMSO-d_6 at 298 K

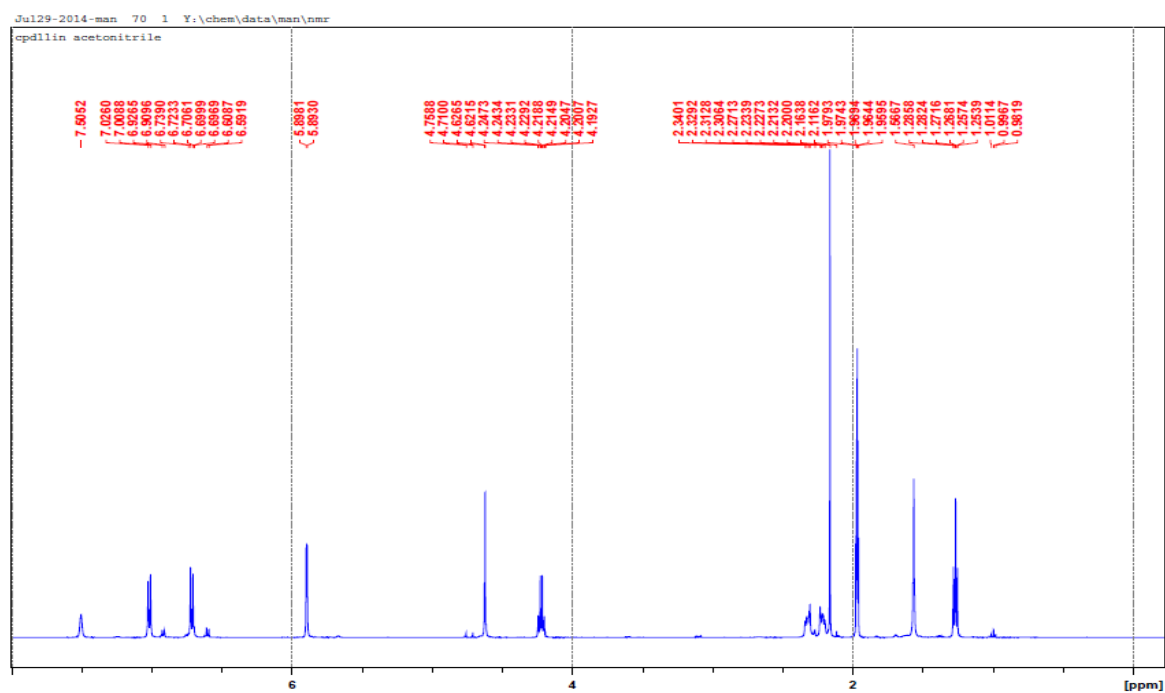


Fig. 18-B ^1H NMR spectrum of calix[4]pyrrole derivative TTECP in CD_3CN at 298 K

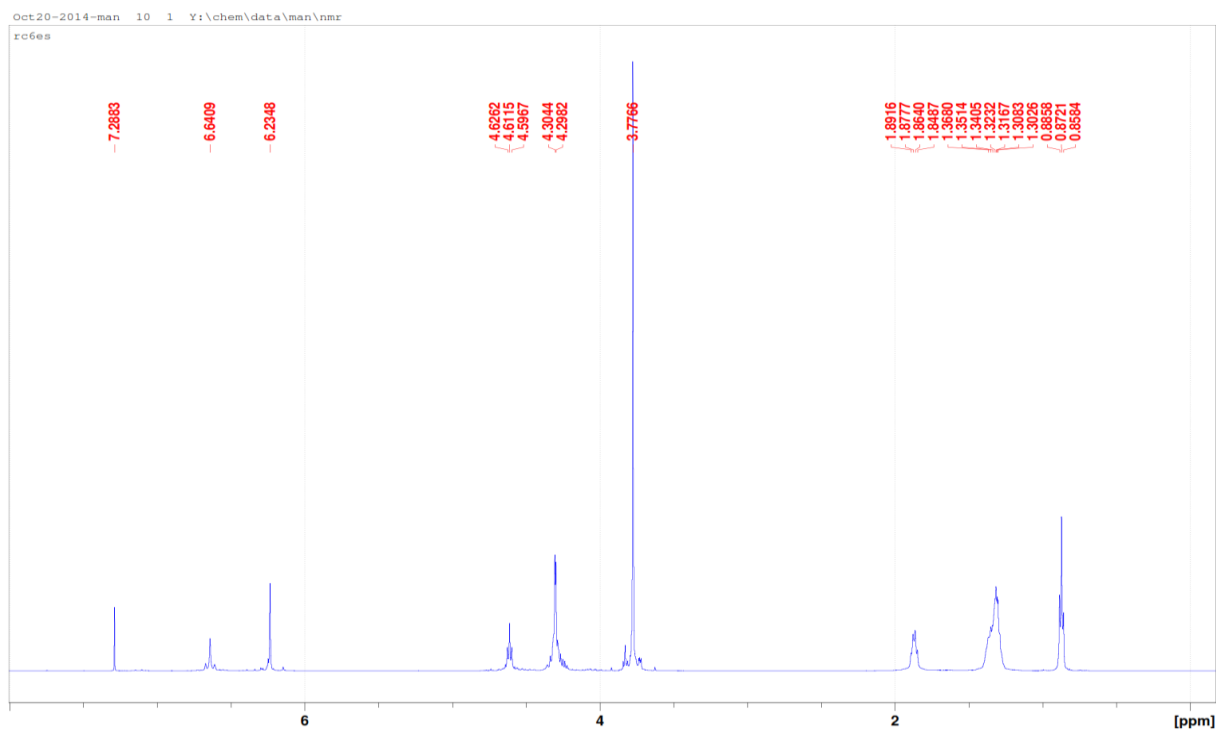


Fig. 19-B Appendix H NMR spectrum of C-pentyl-resorcin[4]arene in CDCl_3 at 298 K

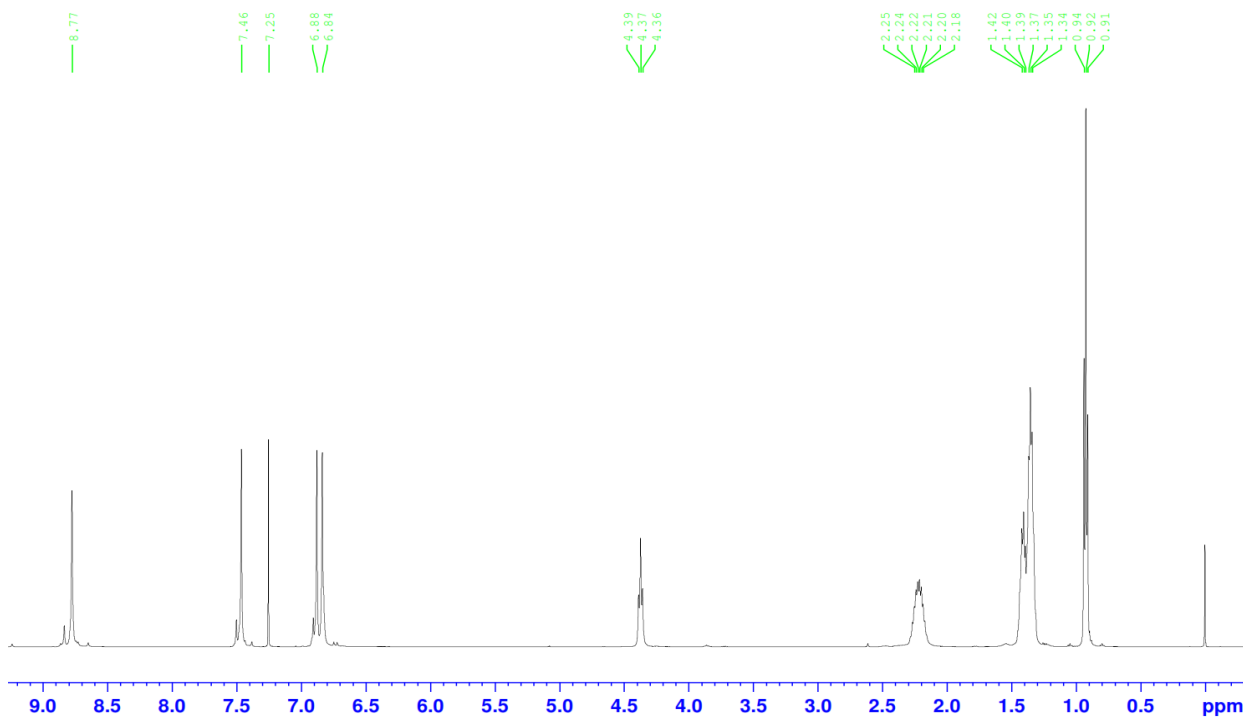


Fig. 20-B ^1H NMR spectrum of PG6 in cdCl_3 at 298 K

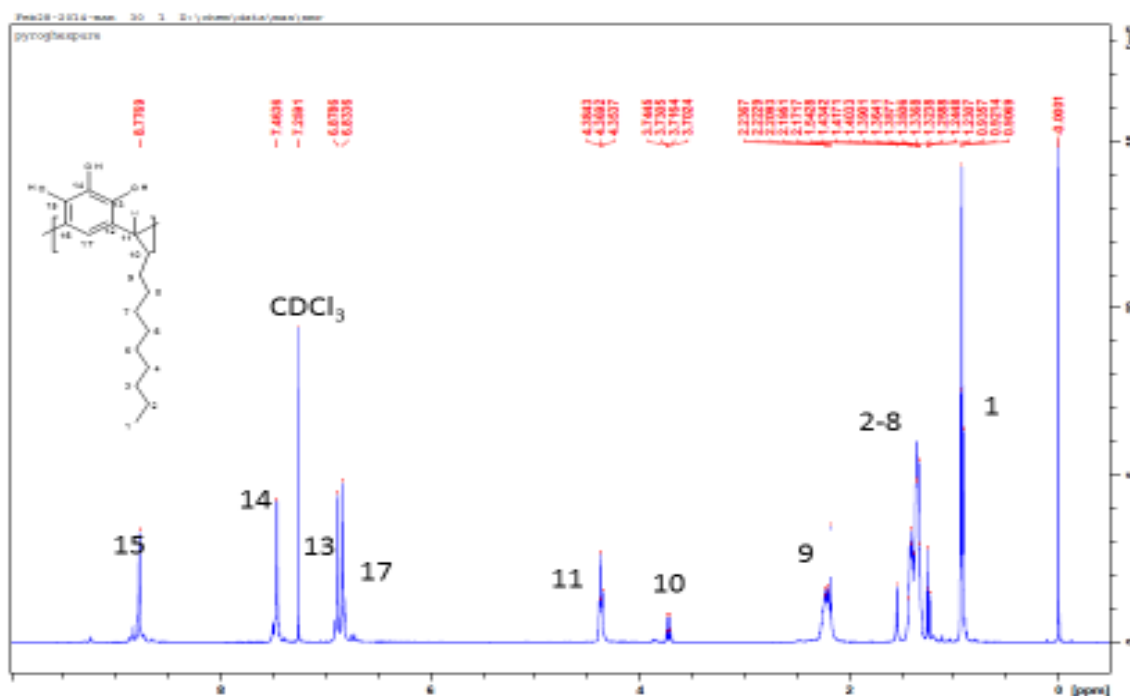


Fig. 21-B ^1H NMR spectrum of PG11 in CDCl_3 at 298 K

Table 3.1 ^1H NMR titration experiment and the chemical shift changes from the addition of increasing amounts of diclofenac to a fixed concentration of calix[4]arene amine in CD_3CN at 298 K.

DF/[$(\text{CANH}_2)_2$]	H1	H2	H3	H4	H5	H6	H7	H8	N-H 9
Free L	1.2	1.16	7.24	7.17	3.39	4.32	4.01	3.22	2.17
0.16	0.00	1.16	0.00	0.00	0.00	-0.01	0.01	0	0.14
0.32	0.00	1.16	0.00	0.00	0.00	-0.03	0.02	0.02	0.21
0.48	0.00	-0.01	-0.01	0.00	0.00	-0.05	0.04	0.04	0.24
0.64	0.00	-0.01	-0.01	-0.01	0.01	-0.08	0.06	0.06	0.26
0.8	0.01	-0.01	-0.01	-0.01	0.01	-0.1	0.07	0.07	0.27
0.96	0.01	-0.01	-0.01	-0.02	0.01	-0.12	0.08	0.09	0.27
1.12	0.01	-0.01	-0.01	-0.02	0.01	-0.14	0.09	0.1	0.27
1.28	-0.01	-0.01	-0.01	-0.01	0	-0.15	0.1	0.11	0.27
1.44	-0.01	-0.01	-0.01	-0.01	0.01	-0.16	0.11	0.12	0.26
1.6	-0.01	-0.01	-0.01	0.0	0.01	-0.17	0.12	0.12	0.25
1.76	-0.01	-0.01	-0.01	-0.01	0.01	-0.18	0.13	0.13	0.25
1.92	-0.01	-0.01	-0.01	0.00	0.01	-0.2	0.14	0.14	0.24
2.08	-0.01	-0.01	-0.01	0.00	0.00	-0.21	0.13	0.15	0.23
2.24	-0.01	-0.01	-0.01	0.00	0.01	-0.21	0.14	0.15	0.22
2.56	-0.01	-0.01	-0.01	0.00	0.01	-0.22	0.14	0.17	0.21

In Table 3.13 $[\text{CA}-(\text{NH}_2)_2]$ and $[\text{DF}]$ are the receptor and diclofenac concentrations in mol dm^{-3}
 $[\text{CAE}] = 2 \times 10^{-3} \text{ mol dm}^{-3}$, $[\text{DF}] = 4 \times 10^{-3} \text{ mol dm}^{-3}$, 0.04 cm^3 for each addition

Table 3.2 Chemical shift changes for the receptor [(CA-(NH₂)₂)] as a result from the addition of increasing concentrations of clofibric acid in CD₃CN at 298 K

[CLF]/[L]	H1	H2	H3	H4	H5	H6	H7	H8	N-H
Free L	1.2	1.16	7.24	7.14	3.37	4.32	4.01	3.21	2.17
0.16	-	-	-	7.14	0.02	-0.01	0.01	0.01	0.02
0.32	-	-	-	0.01	0.03	-0.02	0.03	0.03	0.12
0.48	-	-	-	0.01	0.03	-0.05	0.04	0.05	0.14
0.64	-	-	-	0.02	0.03	-0.07	0.06	0.06	0.18
0.8	-	-	-	0.02	0.04	-0.09	0.07	0.07	0.21
0.96	-	-	-	0.02	0.04	-0.11	0.08	0.09	0.23
1.12	-	-	-	0.02	0.04	-0.13	0.09	0.1	0.26
1.28	-	-	-	0.02	0.06	-0.15	0.1	0.12	0.26
1.44	-	-	-	0.02	0.05	-0.16	0.11	0.13	0.27
1.6	-	-	-	0.02	0.05	-0.17	0.12	0.13	0.29
1.76	-	-	-	0.02	0.05	-0.18	0.12	0.14	0.30
1.92	-	-	-	0.02	0.05	-0.20	0.12	0.14	0.30
2.08	-	-	-	0.02	0.06	-0.21	0.12	0.15	0.32
2.24	-	-	-	0.02	0.06	-0.22	0.12	0.16	0.32

In the table 3.14 [CA-NH₂)₂] and [CLF] are the receptor and clofibric acid concentrations in mol dm⁻³ units, [L] = 2 × 10⁻³ mol dm⁻³, [CLF] = 4 × 10⁻³ mol dm⁻³, 0.04 ml for each addition

Table 3.3 Conductance measurements for the Diclofenac

Volume added	Vol (acc)	[CA(NH ₂) ₂]	[Diclofenac]	[CA(NH ₂) ₂]/ [DF]	Λ_m
0.00	0.00	0.00	1.60×10^{-3}	0.00	1.20
0.25	0.25	1.59×10^{-4}	1.58×10^{-3}	0.10	2.10
0.25	0.50	3.15×10^{-4}	1.57×10^{-3}	0.20	3.07
0.25	0.75	4.68×10^{-4}	1.55×10^{-3}	0.30	3.88
0.25	1.00	6.18×10^{-4}	1.54×10^{-3}	0.40	4.55
0.25	1.25	7.65×10^{-4}	1.52×10^{-3}	0.50	5.20
0.25	1.50	9.09×10^{-4}	1.51×10^{-3}	0.60	5.87
0.25	1.75	1.05×10^{-3}	1.49×10^{-3}	0.70	6.37
0.25	2.00	1.19×10^{-3}	1.48×10^{-3}	0.80	6.93
0.25	2.25	1.33×10^{-3}	1.47×10^{-3}	0.90	7.47
0.25	2.50	1.46×10^{-3}	1.45×10^{-3}	1.00	8.00
0.25	2.75	1.59×10^{-3}	1.44×10^{-3}	1.10	8.60
0.25	3.00	1.72×10^{-3}	1.43×10^{-3}	1.20	9.11
0.25	3.25	1.85×10^{-3}	1.41×10^{-3}	1.31	9.55
0.25	3.50	1.97×10^{-3}	1.40×10^{-3}	1.41	10.27
0.25	3.75	2.09×10^{-3}	1.39×10^{-3}	1.51	10.82
0.25	4.00	2.21×10^{-3}	1.38×10^{-3}	1.61	11.40
0.25	4.25	2.33×10^{-3}	1.37×10^{-3}	1.71	12.03
0.25	4.50	2.45×10^{-3}	1.35×10^{-3}	1.81	12.49
0.25	4.75	2.56×10^{-3}	1.34×10^{-3}	1.91	13.11
0.25	5.00	2.67×10^{-3}	1.33×10^{-3}	2.01	13.64
0.25	5.25	2.78×10^{-3}	1.32×10^{-3}	2.11	14.30
0.25	5.50	2.89×10^{-3}	1.31×10^{-3}	2.21	15.03
0.25	5.75	3.00×10^{-3}	1.30×10^{-3}	2.31	15.71
0.25	6.00	3.10×10^{-3}	1.29×10^{-3}	2.41	16.63

Table 3.4 Conductivity values for the titration of clofibric acid solution in MeCN ($1.96 \times 10^{-3} \text{ mol dm}^{-3}$) with the CA-(NH₂)₂ receptor in MeCN ($1.59 \times 10^{-2} \text{ mol dm}^{-3}$) at 298.15 K

Volume _{added}	Volume _{accum}	CA-(NH ₂) ₂	[CLF]	CA-(NH ₂) ₂ / [CLF]	Λ_m
0.00	0.00	0.00	1.96×10^{-3}	0.00	1.52
0.25	0.25	1.59×10^{-4}	1.94×10^{-3}	0.08	2.29
0.25	0.50	3.15×10^{-4}	1.92×10^{-3}	0.16	3.07
0.25	0.75	4.68×10^{-4}	1.90×10^{-3}	0.25	3.77
0.25	1.00	6.18×10^{-4}	1.88×10^{-3}	0.33	4.32
0.25	1.25	7.65×10^{-4}	1.87×10^{-3}	0.41	4.85
0.25	1.50	9.09×10^{-4}	1.85×10^{-3}	0.49	5.32
0.25	1.75	1.05×10^{-3}	1.83×10^{-3}	0.57	5.84
0.25	2.00	1.19×10^{-3}	1.81×10^{-3}	0.66	6.15
0.25	2.25	1.33×10^{-3}	1.80×10^{-3}	0.74	6.54
0.25	2.50	1.46×10^{-3}	1.78×10^{-3}	0.82	6.93
0.25	2.75	1.59×10^{-3}	1.76×10^{-3}	0.90	7.31
0.25	3.00	1.72×10^{-3}	1.75×10^{-3}	0.98	7.70
0.25	3.25	1.85×10^{-3}	1.73×10^{-3}	1.07	8.06
0.25	3.50	1.97×10^{-3}	1.72×10^{-3}	1.15	8.49
0.25	3.75	2.09×10^{-3}	1.70×10^{-3}	1.23	8.88
0.25	4.00	2.21×10^{-3}	1.69×10^{-3}	1.31	9.30
0.25	4.25	2.33×10^{-3}	1.67×10^{-3}	1.39	9.76
0.25	4.50	2.45×10^{-3}	1.66×10^{-3}	1.48	10.18
0.25	4.75	2.56×10^{-3}	1.64×10^{-3}	1.56	10.54
0.25	5.00	2.67×10^{-3}	1.63×10^{-3}	1.64	11.06
0.25	5.25	2.78×10^{-3}	1.62×10^{-3}	1.72	11.47
0.25	5.50	2.89×10^{-3}	1.60×10^{-3}	1.80	11.94
0.25	5.75	3.00×10^{-3}	1.59×10^{-3}	1.88	12.45
0.25	6.00	3.10×10^{-3}	1.58×10^{-3}	1.97	13.09
0.25	6.25	3.21×10^{-3}	1.56×10^{-3}	2.05	13.46

Table 3.5 Conductometric titration of aspirin with CA-(NH₂)₂ in acetonitrile at 298.15 K

Vol(add)	Vol(acc)	CA-(NH ₂) ₂	[Aspirin]	CA-(NH ₂) ₂ /[Aspirin]	Λ_m
0.00	0.00	0.00	1.79×10^{-4}	0.00	2.84
0.200	0.20	1.44×10^{-5}	1.78×10^{-4}	0.08	5.78
0.200	0.40	2.85×10^{-5}	1.76×10^{-4}	0.16	9.13
0.200	0.60	4.24×10^{-5}	1.75×10^{-4}	0.24	12.48
0.200	0.80	5.61×10^{-5}	1.73×10^{-4}	0.32	15.63
0.200	1.00	6.95×10^{-5}	1.72×10^{-4}	0.40	18.89
0.200	1.20	8.28×10^{-5}	1.71×10^{-4}	0.48	22.29
0.200	1.40	9.58×10^{-5}	1.69×10^{-4}	0.57	25.40
0.200	1.60	1.09×10^{-4}	1.68×10^{-4}	0.65	28.58
0.200	1.80	1.21×10^{-4}	1.67×10^{-4}	0.73	31.86
0.200	2.00	1.34×10^{-4}	1.66×10^{-4}	0.81	34.86
0.200	2.20	1.46×10^{-4}	1.64×10^{-4}	0.89	38.37
0.200	2.40	1.58×10^{-4}	1.63×10^{-4}	0.97	42.43
0.200	2.60	1.70×10^{-4}	1.62×10^{-4}	1.05	45.68
0.200	2.80	1.82×10^{-4}	1.61×10^{-4}	1.13	48.66
0.200	3.00	1.94×10^{-4}	1.60×10^{-4}	1.21	51.87
0.200	3.20	2.05×10^{-4}	1.59×10^{-4}	1.29	55.66
0.200	3.40	2.16×10^{-4}	1.57×10^{-4}	1.37	59.37
0.200	3.60	2.27×10^{-4}	1.56×10^{-4}	1.45	64.84
0.200	3.80	2.38×10^{-4}	1.55×10^{-4}	1.54	67.2
0.200	4.00	2.49×10^{-4}	1.54×10^{-4}	1.62	71.32
0.200	4.20	2.60×10^{-4}	1.53×10^{-4}	1.70	76.85
0.200	4.40	2.70×10^{-4}	1.52×10^{-4}	1.78	79.44
0.200	4.60	2.81×10^{-4}	1.51×10^{-4}	1.86	82.04
0.200	4.80	2.91×10^{-4}	1.50×10^{-4}	1.94	85.85
0.200	5.00	3.01×10^{-4}	1.49×10^{-4}	2.02	88.69

Table 3. 6 Absorbance values change of diclofenac resulting from the addition of increasing concentration of CA-(NH₂)₂ in acetonitrile at 298 K

V _{add}	V _{acc}	V _t	[DCF]	[CA(NH ₂) ₂]	[CA(NH ₂) ₂]/[DCF]	Absorbance
0.00	0.00	0.00	1.12×10 ⁻⁴	0.000	0.000	0.112
0.05	0.05	1.05	1.07×10 ⁻⁴	5.00×10 ⁻⁵	0.469	0.387
0.05	0.10	1.10	1.02×10 ⁻⁴	9.55×10 ⁻⁵	0.938	0.600
0.05	0.15	1.15	9.74×10 ⁻⁵	1.37×10 ⁻⁴	1.406	0.731
0.05	0.20	1.20	9.33×10 ⁻⁵	1.75×10 ⁻⁴	1.875	0.780
0.05	0.25	1.25	8.96×10 ⁻⁵	2.1×10 ⁻⁴	2.340	0.850
0.05	0.30	1.30	8.62×10 ⁻⁵	2.42×10 ⁻⁴	2.800	0.879
0.05	0.35	1.35	8.30×10 ⁻⁵	2.72×10 ⁻⁴	3.20	

In Table 3.3 V_{add} is the volume of the receptor added into UV cell, V_t, is the total volum of the receptor and the drug accumulated in the UV cell, [D] and [L] is the drug and receptor concentration, the receptor concentration is 1.05 × 10⁻³ mol dm⁻³

Table 3.7 Absorbance values change values of clofibric acid solution in acetonitrile as a result from the gradual addition of calix[4]arene amine solution in the same solvent.

$[\text{CA}-(\text{NH}_2)_2] = 1 \times 10^{-3} \text{ mol dm}^{-3}$ Volume of the drug in the UV cell = 1ml

Amount added	Vacc	VT Acc	[Drug]	$[\text{CA}-(\text{NH}_2)_2]$	$[\text{CA}-(\text{NH}_2)_2]/[\text{Drug}]$	Abs
0.00	0.00	0.00	3.35×10^{-4}	0.000	0.000	0.36
0.05	0.05	1.05	3.19×10^{-4}	4.76×10^{-5}	0.149	0.51
0.05	0.10	1.10	3.05×10^{-4}	9.09×10^{-5}	0.299	0.69
0.05	0.15	1.15	2.91×10^{-4}	1.30×10^{-4}	0.448	0.80
0.05	0.20	1.20	2.79×10^{-4}	1.67×10^{-4}	0.597	0.92
0.05	0.25	1.25	2.68×10^{-4}	2.00×10^{-4}	0.746	1.03
0.05	0.30	1.30	2.58×10^{-4}	2.31×10^{-4}	0.896	1.10
0.05	0.35	1.35	2.48×10^{-4}	2.59×10^{-4}	1.045	1.15
0.05	0.40	1.40	2.39×10^{-4}	2.86×10^{-4}	1.194	1.19
0.05	0.45	1.45	2.31×10^{-4}	3.10×10^{-4}	1.343	1.23
0.05	0.50	1.50	2.23×10^{-4}	3.33×10^{-4}	1.493	1.24
0.05	0.55	1.55	2.16×10^{-4}	3.55×10^{-4}	1.642	1.24
0.05	0.60	1.60	2.09×10^{-4}	3.75×10^{-4}	1.791	1.27
0.05	0.65	1.65	2.03×10^{-4}	3.94×10^{-4}	1.940	1.28

Table 3.8 Absorbance values change of aspirin solution in dry acetonitrile as a result from gradual addition of calix[4]arene amine at 298 K

The concentration of the L [CA-(NH₂)₂] = 1.0×10^{-3} mol dm⁻³,

The initial volume of drug [D] in the UV cell = 1ml with the concentration 2.99×10^{-4}

Volume _{added}	V _{accumulated}	V _{total}	[D] mol dm ⁻³	[L]	[L]/[D]	Absorbance
0.0	0.0	0.0	2.99×10^{-4}	0	0	0.27
0.1	0.10	1.1	1.42×10^{-4}	4.76×10^{-5}	0.334	0.538
0.1	0.20	1.2	1.36×10^{-4}	9.09×10^{-5}	0.669	0.733
0.1	0.30	1.3	1.30×10^{-4}	1.30×10^{-4}	1.003	0.835
0.1	0.40	1.4	1.25×10^{-4}	1.67×10^{-4}	1.338	0.9
0.1	0.50	1.5	1.20×10^{-4}	2.00×10^{-4}	1.672	0.94
0.1	0.60	1.6	1.15×10^{-4}	2.31×10^{-4}	2.007	0.96
0.1	0.7	1.7	1.11×10^{-4}	2.59×10^{-4}	2.341	0.98
0.1	0.8	1.8	1.07×10^{-4}	2.86×10^{-4}	2.676	0.98
0.1	0.9	2.9	1.03×10^{-4}	3.10×10^{-4}	3.010	0.98